* Accompanied by 2 oversize plates. Ask at Special Collections.

GEOLOGY AND GENESIS OF THE MIDWAY SILVER-LEAD-ZINC DEPOSIT, NORTH-CENTRAL BRITISH COLUMBIA

by

JOHN ALLAN BRADFORD

B.A., The University of British Columbia, 1980

B.Sc., The University of British Columbia, 1985

A THESIS SUBMITTED IN PARTIAL FULFILLMENT OF
THE REQUIREMENTS FOR THE DEGREE OF
MASTER OF SCIENCE

in
THE FACULTY OF GRADUATE STUDIES
Department of Geological Sciences

We accept this thesis as conforming
to the required standard

THE UNIVERSITY OF BRITISH COLUMBIA
December, 1988

In presenting this thesis in partial fulfilment of the requirements for an advanced degree at the University of British Columbia, I agree that the Library shall make it freely available for reference and study. I further agree that permission for extensive copying of this thesis for scholarly purposes may be granted by the head of my department or by his or her representatives. It is understood that copying or publication of this thesis for financial gain shall not be allowed without my written permission.

Department of GEOLOGICAL SCIENCES

The University of British Columbia
Vancouver, Canada

Date DEC. 7, 1988

ABSTRACT

The Midway Ag-Pb-Zn manto deposit is hosted in Middle Devonian McDame Group limestones of the Cassiar Terrane, a displaced segment of the North American miogeocline. In the map area (1040/16), platformal carbonates and siliciclastics of Cambrian to Devonian age are unconformably overlain by Devono-Mississipian basinal sediments, including exhalites (Earn Group). These are structurally overlain, above a flat lying decollement, by Upper Paleozoic marginal basin sediments, basaltic volcanics, intrusives and ultramafites (Sylvester allochthon). The decollement represents the boundary between Cassiar Terrane and Slide Mountain Terrane in the map area.

Jurassic contraction of the North American margin and emplacement of the Sylvester allochthon produced southeasterly trending major and minor structures. Cretaceous - Tertiary extension, linked to transcurrent motion along the Kechika and related faults, produced the north trending high angle Tootsee River fault zone, which divides the map area.

Two intrusive suites, of mid-Cretaceous (100 Ma) and Late Cretaceous (70 Ma) ages, are documented by K-Ar dating. The Late Cretaceous episode is evidenced by large sericite - pyrite alteration zones southeast of Midway, but only a few felsic porphyry dykes are exposed at current erosion levels.

High angle faults in the Tootsee River fault zone confined intrusion driven hydrothermal fluid migration up plunge from an intrusive centre about 2 kilometres southeast of Midway. Fluids were ponded in a southeasterly plunging antiformal trap, and massive sulphides deposited in zones of pre-existing karst breccia porosity beneath a relatively impermeable shale cap. Fe and Cu rich pyrrhotitic assemblages occur at greater depth toward the intrusive centre, with sulphosalt rich pyritic assemblages at shallower depths to the north.

Immiscible aqueous - carbonic liquid and vapour were trapped in quartz deposited with sulphides at 300-340°C. Later lower temperature inclusions record the progressive loss of CH_4 and CO_2 from the system. Salinities were about 7-10 weight % NaCl equivalent. Sulphur isotopes of sulphides span a narrow range, indicating a well mixed reservoir and H_2S dominated environment. Both sedimentary and igneous sources are indicated. Oxygen isotopes of carbonates demonstrate large ^{18}O depletions due to extensive meteoric water interaction. In a regional context (Rancheria silver district), Midway lead isotopes suggest mixing of upper crustal lead from country rocks with intrusion derived lower crustal lead. Cassiar Terrane epigenetic deposits are distinguished from epigenetic deposits of Slide Mountain Terrane, which have significant mantle lead, consistent with derivation from oceanic and arc host rock assemblages.

TABLE OF CONTENTS

List of Tables

Page

List of Figures

Page

Page

Page

Page

Page

List of Plates

Acknowledgements

Financial support for this study was provided by the British Columbia Ministry of Energy, Mines and Petroleum Resources through the federal - provincial Mineral Development Agreement. Henrik Thallenhorst of Strathcona Mineral Services, Ltd. permitted access to the Midway property and granted the hospitality of the Midway camp during the 1986 and 1987 field seasons. Gord Hodge at the University of British Columbia helped with drafting and photography, and Yvonne Douma prepared thin and polished sections. Janet Gabites provided lead isotope analyses, and Dita Runkle and Joe Harakal performed the potassium - argon analyses. Roy Krouse and coworkers of the University of Calgary Stable Isotope Laboratory helped with the stable isotope analyses. T.J. Reynolds of Fluid, Inc. gave invaluable advice on fluid inclusion research, and provided useful comments on the results presented in section 4.6. The British Columbia Ministry of Energy, Mines and Petroleum Resources provided the heating - freezing stage, and Mike Fournier gave logistical support. Discussions with Hugh Gabrielse, Mike Orchard and Ken Dawson of the Geological Survey of Canada in Vancouver were helpful, and Dave Sinclair of the G.S.C. Ottawa contributed important ideas as well as microprobe and sulphur isotope data. Jim Hylands, formerly of Cordilleran Engineering, shared his extensive knowledge of Midway geology. Craig Leitch provided some useful comments on the sections on fluid inclusions and stable isotopes.

Colin Godwin suggested the topic of this thesis and allowed me to develop it in the directions which interested me, and contributed timely support and indefatigable editing. A special thanks to JoAnne Nelson for her friendship, encouragement, and ideas, and for teaching me the art and science of regional mapping.

1. Introduction

1.1. Location and Access

The Midway silver - lead - zinc deposit is approximately 8.5 kilometres south of the British Columbia - Yukon Territory border, about 80 kilometres west of Watson Lake, Yukon Territory, which is the main centre for exploration services in the region (Figure 1-1). The deposit is centred near latitutde 59o55' north, longitude 130o20' west. The property is accessible on an unpaved road from a turnoff at Mile 701 on the Alaska Highway, about 20 kilometres east of Rancheria. Good bridges spanning the Rancheria and Tootsee Rivers enable access to the property. South of the Tootsee River crossing the access road is susceptible to spring washouts, as occurred in 1987.

Topography in the area consists of rounded mountains and hills of the Stikine Ranges of the Cassiar Mountains, and broad, glaciated valleys. The deposit is situated at the northern base of Silvertip Mountain, which rises to 1,665 metres. The highest peak in the area is Whitehorn Mountain, two kilometres south of Silvertip Mountain, with an elevation just under 2,000 metres. Topography becomes increasingly rugged to the west where the area is underlain by the Cassiar batholith.

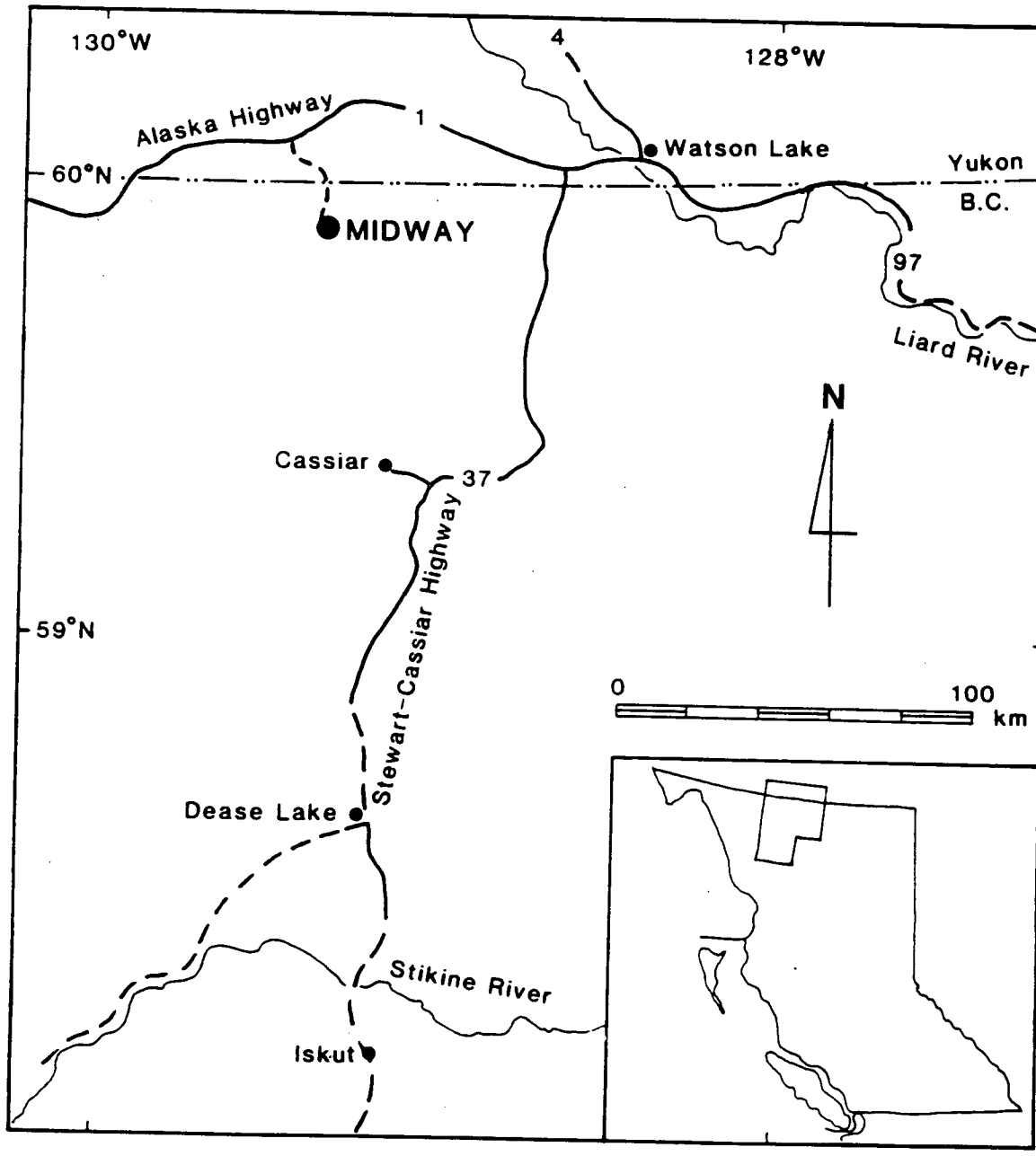

Figure 1-1: Location and access, Midway deposit, northern British Columbia (1040/16).

Tree line ranges between 1,300 and 1,500 metres. Ridge top exposures are generally good, but hillside exposures are commonly subjected to significant frost heaving and downslope creep. Valleys contain thick glacial till and outwash deposits, and are densely forested. Mean annual precipitation is about 50 centimetres, occurring mainly during winter months (Farley, 1979).

1.2. Exploration History and Evolution of Deposit Models

Silver - lead - zinc mineralization in the Midway area was first discovered in 1955 by prospectors on Silvertip Hill, about one kilometre southwest of the Midway deposit. The Silvertip claims were optioned in 1956 to Conwest Exploration Company Ltd., Toronto, Ontario, which drove two adits and undertook surface and underground diamond drilling. Mineralization on surface consisted of partly oxidized galena rich boulder trains suspected to have been derived from steeply dipping veins. Exploration proved the deposit to be highly oxidized to depths of over 150 metres (Brundland, 1958). Diamond drilling intersected several steep faults and breccia zones within the McDame Group carbonate host rocks. These breccias contained shale clasts derived from overlying clastic sediments. Failure to confirm continuity of the steep veins at depth led to a revision of the model, and the sulphides were believed to

represent semiconformable replacements (Brundland, 1958). One of the main faults (Camp Creek Fault) juxtaposed McDame Group on the west side with siliciclastic sediments (now Earn Group) on the east. It was suggested (Brundland, 1958; Gabrielse, 1969) that drilling on the east side of this fault might intersect unoxidized mineralization beneath the clastic sediment "cap" overlying McDame Group. Although sporadic drilling on Silvertip Hill continued through the 1960's (Holland, 1968), little exploration was done on the east side of the fault until the 1980's.

Regional Resources, Ltd., Vancouver, B.C. (now Toronto, Ontario), acquired 240 Yukon Territory and 881 British Columbia claim units in the Midway area in 1980. These were located on the basis of stream sediment geochemical anomalies. Exploration was keyed primarily to a sedimentary exhalative lead - zinc deposit model, due to exploration successes in the Selwyn Basin (MacMillan Pass) and Kechika Trough (Cirque) in similar siliciclastic sequences. Trenching near the present Midway portal exposed a 2 metre thick stratabound pyrite - sphalerite lens that was believed to be syngenetic in origin. Early accounts of Midway described the deposits as "exhalites", including the "Lower Zone", which was hosted in McDame Group carbonates at the contact with Earn Group (MacIntyre, 1982).

Diamond drilling eventually showed that the main sulphide deposits were in the McDame Group, not in the Earn Group as originally believed. The common association of mineralization with collapse or "trash" breccias led to comparisons with the "Mississippi Valley type" deposits of the East Tennessee lead - zinc district (Cordilleran Engineering, 1982, 1983). With this model in mind, diamond drilling was conducted on a square grid at 150 and later 75 metre intervals. Two deposits in the McDame Group, the Silver Creek and Discovery, were outlined from 1982 to 1984. Extrapolation of a laterally continuous orebody between drill intersections resulted in reserve estimates for the two deposits in excess of 6 million tonnes (Cordilleran Engineering, 1984).

By 1984, lead isotope modelling and mineralogical studies had made it fairly clear that the East Tennessee analogy did not hold, and that the basin dewatering models applicable to Mississipi Valley and related deposit types were not applicable to Midway. Rather, the Midway deposits had a tin - silver signature, and the lead isotope characteristics typical of young, intrusion related deposits in the northern Cordillera. More comparable deposit analogues were the Leadville deposit in Colorado, and "manto" type replacements of Mexico and Peru (Archambault, 1985; Sorenson, 1985). Subsequent underground exploration in 1985 and 1986, predicated on the initial large

tonnage projections, resolved the morphology of the mineralized structures, which were described as irregular, lenticular, "tube - like" bodies (Cordilleran Engineering, 1985). This led to a downward revision of tonnage estimates to the current 1.185 million tonnes, grading 410 grams/tonne silver, 9.7% zinc and 7.0% lead (Exploration in British Columbia, 1986). Following the completion of underground drilling in 1986, workings were allowed to flood, and subsequent exploration was regional in nature.

1.3. Previous Studies

Regional mapping of Jennings River map area (1040) was conducted by Gabrielse in 1965-7, and the results published in Gabrielse (1969). Poole (1956) had earlier described the geology of the adjoining Wolf Lake sheet (105B), which includes the Rancheria silver district, of which the Midway area is a part. Holland (1968) gave an account of the history and geology of the Silvertip showing. Subsequently, Mulligan (1975) published analyses of sulphides from Silvertip, which contained 0.25% tin, described as occurring in stannite. MacIntyre (1982, 1983) described the Midway deposit in the context of a sedimentary exhalative model, comparing its platformal setting to the basinal setting of other syngenetic deposts in northern British Columbia (Cirque, Windy Craggy). Geologists working for

Cordilleran Engineering (1981, 1982, 1983, 1984) gave thorough accounts of Midway geology and mineralization, and worked out a viable stratigraphy for the Earn Group (then Lower Sylvester Group). Later, Mundy (1984) made a detailed unpublished biostratigraphical study of the McDame Group. Abbott (1984) compared Midway with other epigenetic deposits of the Rancheria district, stressing their breccia features and relationship with regional transcurrent faults. Dawson et al. (1985) interpreted the lead isotope signature of Midway, which identified it as an epigenetic Cretaceous - Tertiary deposit. Archambault (1985) described sulphide mineralogy of the Silver Creek deposit, including the rare sulphosalt phases geocronite and franckeite. Sinclair (1986b) stressed Midway's probable association with A - type granites, and carried out K-Ar dating and microprobe analyses of sericite associated with the intrusive - hydrothermal system. Jonasson (written communication, 1986) performed sulphur isotope analyses on Discovery deposit and Earn Group hosted sulphides, confirming a lack of seawater sulphur origin. Nelson and Bradford (1987a, 1987b) conducted a 1:25,000 scale regional mapping program in the Midway area; results of K-Ar dating in this area were published in Bradford and Godwin (1988). Orchard and Irwin (1988) presented results of conodont studies of the McDame and Earn Groups in the Midway area.

1.4. Aims and Methods of the Present Study

The aims of the present study are:

(1) description of the regional geological setting of the Midway deposits. This is based on a three month field study in the Midway area in 1986, during which the northwest quarter of 1040/16 was mapped at a scale of 1:25,000 as part of a regional mapping program under J.L. Nelson (Nelson and Bradford, 1987b). Descriptions of geology and mineralization in the immediate vicinity of the deposits are based on surface mapping, examination of core and stockpiles from underground exploration, and thin and polished sections, as well as published and unpublished sources. Lack of access to underground exposures during field studies prevented more detailed descriptions of the orebodies.

(2) interpretation of galena lead isotopes of the Midway area within the context of the metallogenic evolution of the Cassiar Terrane and associated allochthonous terranes.

(3) investigation of the nature and evolution of the fluid system, source of some of its components, and pressure - temperature regime in which sulphides were deposited. This is based on microthermometric studies of fluid inclusions, sulphur isotope analyses of ore and gangue minerals, and oxygen and carbon isotope analyses of gangue and host rock.

2. Regional Geology and Lead Isotope Signatures of the Rancheria, Seagull and Cassiar Districts

2.1. Introduction

Galena lead isotope data from 28 mineral deposits in the Rancheria, Seagull and Cassiar districts (Figure 2-1) have been compiled in order to: (1) fingerprint deposit types, (2) compare and contrast the lead isotope signatures of different districts, and (3) relate contrasting isotopic signatures to the tectonic setting of different types of deposits. The data are presented in Table 2-1. Multiple analyses from single deposits are averaged, and the means and standard errors are presented in Table 2-2. Summary deposit and sample descriptions are compiled in Appendix A. The data are plotted on standard lead - lead plots in Figures 2-2, 2-3 and 2-4.

2.2. Regional Geology

The Rancheria, Seagull and Cassiar districts are situated west of the Tintina - Northern Rocky Mountain Trench fault system, and encompass three terranes: Cassiar, Slide Mountain and Dorsey (Figure 2-1). The Cassiar Terrane is a 600 kilometre long displaced terrane separated from ancestral North America by the Tintina - Northern Rocky Mountain Trench dextral

transcurrent fault (Wheeler et al., 1987; Figure 2-1). It has been interpreted as: (1) a segment of the Peace River Arch that was transported northwesterly over 600 kilometres by Cretaceous to Eocene transcurrent faulting (Gabrielse, 1985), and (2) a horst formed during Late Proterozoic or Early Cambrian rifting which has undergone about 450 kilometres of dextral transport (Roddick, 1964; Tempelman - Kluit, 1979; Mortenson, 1981). Its Upper Proterozoic to Upper Triassic stratigraphy is similar to that found in adjacent parts of the North American miogeocline.

The Cassiar Terrane is in structural contact with two accreted terranes, Slide Mountain and Dorsey (Wheeler et al., 1987), which have less obvious or unknown relationships to ancestral North America. These terranes lie between Cassiar Terrane and allochthonous Quesnellia and Cache Creek Terrane, and overlie Cassiar Terrane as scattered klippen (Figure 2-1). Slide Mountain Terrane, of Devonian to Upper Triassic age, includes oceanic marginal basin sediments and volcanics, arc volcanics, and plutonic and ultramafic rocks. The Dorsey Terrane is a subdivision of the Yukon Cataclastic Complex of Templeman - Kluit (1979) or the Yukon - Tanana Terrane (cf. Mortenson and Jilson, 1985). It consists of marginal basin chert and clastic sediments, and is similar to Slide Mountain Terrane but lacks ultramafics and includes coarse clastic units. It could

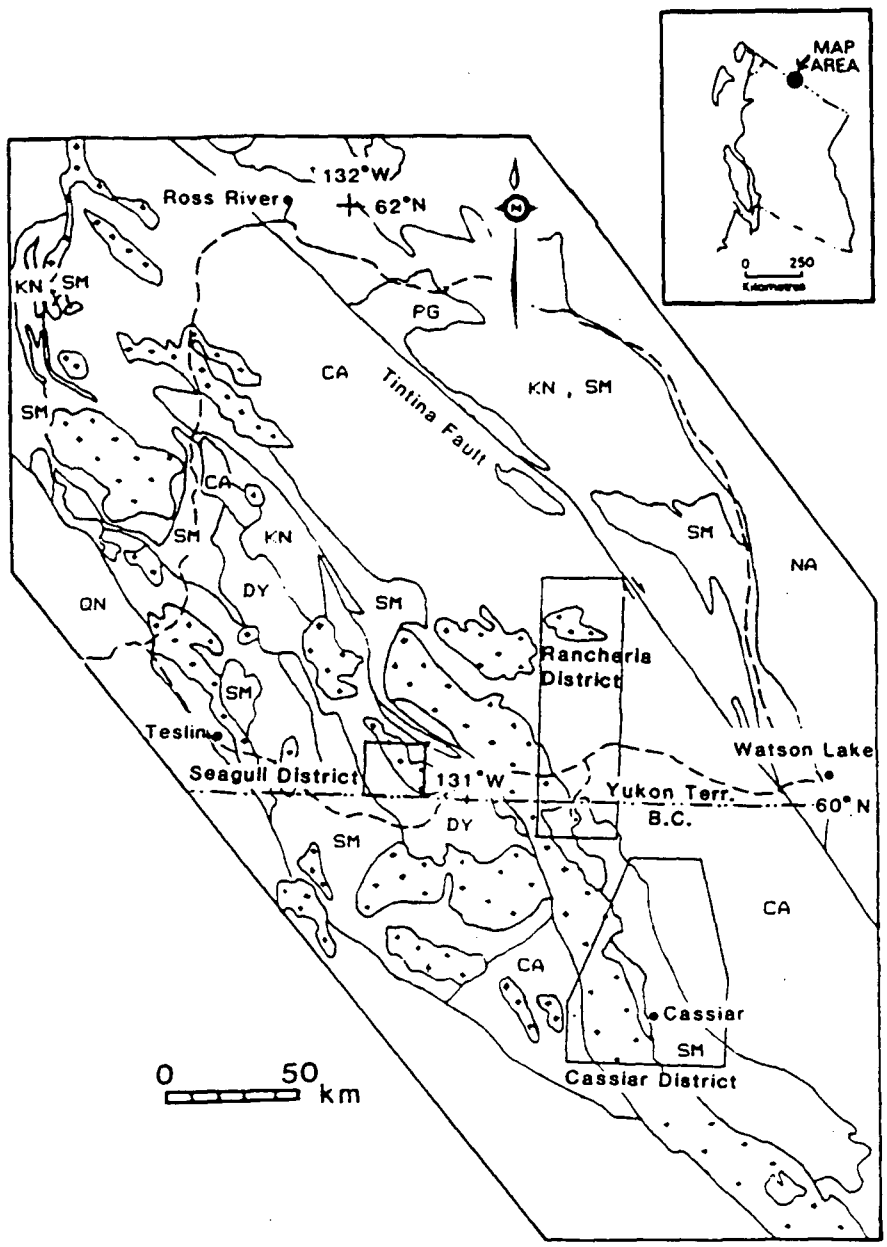

Figure 2-1: Regional geology of north-central British Columbia and south-central Yukon Territory, showing location of the Rancheria, Seagull and Cassiar districts. Abbreviations: CA - Cassiar Terrane, SM - Slide Mountain Terrane, KN - Kootenay (Nisutlin) Terrane, DY - Dorsey Terrane, QN - Quesnellia, NA - ancestral North America.

represent a facies of either Slide Mountain Terrane or Quesnellia (Wheeler et al., 1987).

Arc volcanics, intrusive rocks and clastic sediments of Quesnellia, and oceanic sediments and volcanics of Cache Creek Terrane lie to the southwest of the accreted assemblages adjacent to Cassiar Terrane (Figure 2-1). Suturing of these allochthonous terranes to the North American margin and obduction of intervening oceanic and marginal basin packages, such as Slide Mountain Terrane, occurred primarily in the Jurassic.

2.3. Characteristics of Lead Sources

The juxtaposition of miogeoclinal Cassiar Terrane with oceanic, marginal basin and arc packages suggests that isotopic contrasts between different mineral deposit types might reflect differences among their host terranes. These differences can be elucidated by reference to plumbotectonic models of mantle, lower crust, upper crust and orogene lead reservoirs (Doe and Zartman, 1979).

From Hadrynian to Upper Devonian time the Cassiar Terrane was the site of accumulation of thick shallow water carbonate and siliciclastic shelf sediments, while basinal shales

and cherts were deposited in the Selwyn Basin. The Paleozoic basinal succession overlapped onto Cassiar Terrane beginning in Late Devonian time, as extensive rifting, block faulting and subsidence occurred along the western margin of North America. Devono - Mississipian basinal successions and turbidites comprise the Earn Group, which consists of continental debris derived from relatively uplifted platformal blocks (Gordey et al., 1986).

Cassiar Terrane siliciclastic shelf sediments were ultimately derived from the North American craton. These sediments represent well - mixed, highly radiogenic upper crustal material which has been relatively isolated from significant mantle input since Early Hadrynian time. Devono - Mississipian siliciclastics are at least in part derived from a westerly source area, perhaps a rifted off segment of North America (Tempelman - Kluit, 1979). This represents a similar radiogenic upper crustal source.

Sediment hosted base metal ("sedex": Carne and Cathro, 1982) deposits in the Selwyn Basin, Kechika Trough and in the southern Cordillera were used by Godwin and Sinclair (1982) to define lead growth curves (shale curve) for upper crustal environments in the Canadian Cordillera. Applicability of this terrane specific model to sedex deposits in Cassiar Terrane has not been

documented, although it was anticipated that it would apply at least in part (Godwin and Sinclair, 1982).

Allochthonous terranes in structural contact with Cassiar Terrane include oceanic and marginal basin sediments, oceanic or back-arc volcanics, probable arc volcanics and intrusive correlatives and widespread ultramafites (e.g. Tempelman - Kluit, 1979; Mortenson and Jilson, 1985; Nelson et al., 1988). Lead derived from these assemblages is probably complex and heterogeneous. Some sediments are of continental provenance and might contain upper crustal lead similar to that defined by the shale curve. Oceanic and arc volcanics and intrusives probably have a significant mantle component.

Most epigenetic deposits in the Rancheria, Seagull and Cassiar districts are related to intrusions of mid-Cretaceous to Eocene age (Sinclair, 1986a). Depending on type of intrusion, derivation of melts and subsequent contamination, these could contribute lead with isotopic characteristics significantly different from country rocks hosting the deposits.

The principle Mezozoic and Cenozoic intrusive events in the northern Cordillera peaked in the mid-Cretaceous (100 Ma), Late Cretaceous - Paleocene (70 Ma), and Eocene (50 Ma) (Sinclair, 1986a; Armstrong, 1988). All three intrusive suites are

characterized by initial strontium ratios of 0.712 or greater (Armstrong, 1988), indicating that they are derived from old continental crust, or have undergone significant crustal contamination. According to Anderson (1985), the mid-Cretaceous intrusions resemble S - type granites, reflecting partial melting of thickened continental crust. The Late Cretaceous to Paleocene and Eocene suites are analogous to A - type granites, which are commonly described as remelts of depleted lower crust from which earlier, more voluminous intrusions have been derived (Whalen et al., 1987; Collins et al., 1982).

2.4. Lead Isotope Data

Data reported in Table 2-1 are mainly new, high precision analyses obtained by J. Gabites using a single rhenium filament, silica gel - phosphoric acid technique (Godwin et al., 1988). These have been supplemented by analyses by G.L. Cumming, at the University of Alberta, for the Geological Survey of Canada. If more than one analysis was obtained on the same sample these are usually reported as averages (suffix "A"). In some cases, if one run was judged of better quality than the other only the better analysis is reported. The Geological Survey of Canada data includes several deposits not included in the University of British Columbia data base. These are: YP, Erickson (Cusac), Erickson (Vollaug), Erickson (Maura-Allison), Cottonwood, Lang

Table 2-1: Galena lead isotope data for mineral deposits of the Rancheria, Cassiar and Seagull districts, northern British Columbia and southern Yukon Territory.

SAMPLE NO	DEPOSIT &/or SAMPLE NAME	NTS & GOVT REF	LAT N	LONG W	ANL	RUN:NORM DATE	RN	QUAL:TEMP:BLK	MT	PB6/4	%6/4	PB7/4	%7/4	PB8/4	%8/4	PB7/6	PB8/6
c 10102-001	LOGTUNG (DARVA VEIN)	105/B/04/E:SW-030	60.02	131.63	JG	08/02/85:06/26/85	1	GOOD: 1150:09	GL	19.123	0.03	15.682	0.03	39.035	0.03	0.82009	2.04137
c 10134-001	MC RIDGE (K3)	105/B/04/W:SW-045	60.18	131.76	JG	08/02/85:06/26/85	1	GOOD: 1150:08	GL	18.533	0.01	15.612	0.01	38.378	0.01	0.84240	2.07087
c 10134-001R	MC RIDGE (K3)	105/B/04/W:SW-045	60.18	131.76	JG	10/24/85:06/26/85	2	GOOD: 1150:08	GL	18.547	0.02	15.630	0.02	38.433	0.02	0.84279	2.07236
c 10134-001A	MC RIDGE (K3) (N=2)	105/B/04/W:SW-045	60.18	131.76	JG				GL	18.540	0.02	15.621	0.02	38.406	0.02	0.84259	2.07162
c 10134-002	MC RIDGE (K1)	105/B/04/W:SW-045	60.18	131.76	JG	08/02/85:06/26/85	1	GOOD: 1150:07	GL	19.162	0.02	15.689	0.02	39.109	0.02	0.81880	2.04111
c 10145-001	BLACK ROCK (ALAN)	105/B/02/E:SE-012	60.01	130.77	JG	12/03/84:06/26/85	1	GOOD: 1150:08	GL	19.490	0.02	15.702	0.02	39.667	0.02	0.80564	2.03523
c 10145-001R	BLACK ROCK (ALAN)	105/B/02/E:SE-012	60.01	130.77	JG	03/07/85:06/26/85	2	FAIR: 1150:12	GL	19.494	0.03	15.715	0.01	39.715	0.03	0.80612	2.03732
c 10145-001A	BLACK ROCK (ALAN, N=2)	105/B/02/E:SE-012	60.01	130.77	JG			GOOD/FAIR	GL	19.492	0.03	15.709	0.02	39.691	0.03	0.80588	2.03605
c 10154-002	MEISTER	105/B/08/W:SE-016	60.28	130.40	JG	12/03/84:06/26/85	1	GOOD: 1150:09	GL	18.571	0.03	15.665	0.02	38.068	0.03	0.84352	2.04986
c 10154-002D	MEISTER	105/B/08/W:SE-016	60.28	130.40	JG	06/05/85:06/26/85	1	GOOD: 1150:07	GL	18.557	0.03	15.662	0.02	38.044	0.03	0.84402	2.05012
c 10154-002A	MEISTER	105/B/08/W:SE-016	60.28	130.40	JG		1	GOOD:	GL	18.564	0.03	15.664	0.02	38.056	0.03	0.84377	2.05004
c 10155-001D	WOLF	105/B/09/E:NE-074	60.55	130.03	JG	02/01/88:11/09/87	1	good: 1150:13	GL	19.524	0.00	15.747	0.00	39.813	0.00	0.80655	2.03922
o 10166-501	YP (MS)	105/B/01/W:SE-	60.05	130.38	GSC		1	GOOD	GL	19.671	0.00	15.770	0.00	39.874	0.00	0.80169	2.02705
o 10166-502	YP (MS)	105/B/01/W:SE-	60.05	130.38	GSC		1	GOOD	GL	19.633	0.00	15.744	0.00	39.795	0.00	0.80192	2.02695
o 10166-503	YP (MS)	105/B/01/W:SE-	60.05	130.38	GSC		1	GOOD	GL	19.568	0.00	15.730	0.00	39.827	0.00	0.80387	2.03532
o 10166-504	YP (MS)	105/B/01/W:SE-	60.05	130.38	GSC		1	GOOD	GL	19.635	0.00	15.746	0.00	39.833	0.00	0.80194	2.02868
o 10166-505	YP (MS)	105/B/01/W:SE-	60.05	130.38	GSC		1	GOOD	GL	19.643	0.00	15.763	0.00	39.865	0.00	0.80248	2.02948
o 10166-506	YP (MS)	105/B/01/W:SE-	60.05	130.38	GSC		1	GOOD	GL	19.667	0.00	15.765	0.00	39.871	0.00	0.80160	2.02731
o 10166-AVG	YP (MS)	105/B/01/W:SE-	60.05	130.38	GSC			GOOD	GL	19.636	0.00	15.753	0.00	39.844	0.00	0.80225	2.02913
c 10168-001	LOLA	105/B/01/W:SE-006	60.01	130.47	JG	12/03/84:06/26/85	1	GOOD: 1150:08	GL	19.431	0.02	15.708	0.01	39.642	0.02	0.80841	2.04010
c 10168-001R	LOLA	105/B/01/W:SE-006	60.01	130.47	JG	03/21/84:06/26/85	2	GOOD: 1150:10	GL	19.344	0.03	15.699	0.01	39.747	0.04	0.81158	2.05474
c 10168-001A	LOLA (N=2)	105/B/01/W:SE-006	60.01	130.47	JG			GOOD:	GL	19.388	0.03	15.704	0.01	39.695	0.03	0.80999	2.04530
c 10168-002	LOLA	105/B/01/W:SE-006	60.01	130.47	JG	12/21/84:06/26/85	1	GOOD: 1150:07	GL	19.330	0.05	15.701	0.02	39.776	0.07	0.81227	2.05780
c 10168-003	LOLA	105/B/01/W:SE-006	60.01	130.47	JG	12/21/84:06/26/85	1	GOOD: 1150:08	GL	19.434	0.04	15.711	0.02	39.678	0.05	0.80844	2.04172
o 10168-501	LOLA	105/B/01/W:SE-	60.01	130.47	GSC		1	GOOD	GL	19.443	0.00	15.719	0.00	39.699	0.00	0.80847	2.04182
c 10177-101	FIDDLER (GREISEN)	105/B/01/W:SE-004	60.15	130.45	JG	11/18/85:06/26/85	1	GOOD: 1150:10	GL	19.672	0.01	15.755	0.00	39.837	0.01	0.80091	2.02515
c 10177-102	FIDDLER (SKARN)	105/B/01/W:SE-004	60.15	130.45	JG	11/18/85:06/26/85	1	GOOD: 1150:12	GL	19.668	0.01	15.753	0.01	39.826	0.01	0.80099	2.02505
c 10177-AVG	FIDDLER (N=2)	105/B/01/W:SE-004	60.15	130.40	JG			GOOD:	GL	19.670	0.01	15.754	0.01	39.832	0.01	0.80095	2.02510
c 10186-001	SILVER HART (METEORITE)	105/B/07/E:SE-	60.33	130.72	JG	04/30/87:06/26/85	1	good: 1200:09	GL	19.554	0.00	15.730	0.00	39.742	0.00	0.80444	2.03245
c 10186-101	SILVER HART (METEORITE)	105/B/07/E:SE-	60.33	130.72	JG	09/29/86:06/26/85	1	good: 1150:08	GL	19.494	0.00	15.756	0.01	39.777	0.00	0.80822	2.04044
c 10186-102	SILVER HART (BRECCIA)	105/B/07/E:SE-	60.33	130.72	JG	12/08/86:06/26/85	1	good: 1150:10	GL	19.565	0.00	15.729	0.01	39.727	0.00	0.80393	2.03055
c 30022-001	AXE	104/P/12/W:NW-	59.74	129.91	JG	01/29/88:11/09/87	1	good: 1150:11	GL	19.142	0.00	15.678	0.00	39.785	0.00	0.81986	2.07840
c 30023-001	REGGIE	104/P/12/E:NW-	59.53	129.52	JG	01/29/88:11/09/87	1	good: 1150:05	GL	18.525	0.00	15.660	0.00	38.529	0.00	0.84532	2.07983
c 30023-001R	REGGIE	104/P/12/E:NW-	59.53	129.52	JG	02/26/88:11/09/87	2	good: 1150:14	GL	18.506	0.01	15.644	0.00	38.480	0.01	0.84531	2.07928
c 30023-001A	REGGIE	104/P/12/E:NW-	59.53	129.52	JG	02 /88:11/09/88		good:	GL	18.516	0.01	15.657	0.00	38.504	0.01	0.84532	2.07956
c 30383-002	MAGNO (SILVER QUEEN)	104/P/05/W:SW-006	59.26	129.82	JG	10/11/84:06/26/85	1	GOOD: 1150:08	GL	19.199	0.02	15.681	0.01	39.323	0.02	0.81679	2.04814
c 30383-002R	MAGNO (SILVER QUEEN)	104/P/05/E:SW-006	59.26	129.82	JG	10/18/84:06/26/85	2	GOOD: 1150:08	GL	19.196	0.02	15.686	0.00	39.331	0.02	0.81716	2.04894
c 30383-002A	MAGNO (SILVER QUEEN) (N=2)	104/P/05/W:SW-006	59.26	129.82	JG			GOOD:	GL	19.198	0.02	15.684	0.01	39.327	0.02	0.81697	2.04894
c 30383-004	MAGNO (SILVER QUEEN)	104/P/05/W:SW-006	59.26	129.82	JG	07/25/85:06/26/85	1	GOOD: 1150:09	GL	19.198	0.02	15.685	0.02	39.337	0.03	0.81701	2.04901
c 30383-101	MAGNO (WEST)	104/P/05/W:SW-006	59.26	129.82	JG	10/25/85:06/26/85	1	GOOD: 1120:07	GL	19.199	0.01	15.684	0.01	39.328	0.01	0.81693	2.04842
c 30383-AVG	MAGNO (N=3)	104/P/05/W:SW-006	59.26	129.82	JG			GOOD:	GL	19.198	0.02	15.684	0.01	39.331	0.02	0.81697	2.04866
c 30385-102	MARBLE BASIN (UPPER D)	104/P/05/W:SW-044	59.26	129.87	JG	07/26/85:06/26/85	1	GOOD: 1150:08	GL	19.198	0.01	15.687	0.01	39.320	0.01	0.81713	2.04819
c 30385-102R	MARBLE BASIN (UPPER D)	104/P/05/W:SW-044	59.26	129.87	JG	10/25/85:06/26/85	2	GOOD: 1110:07	GL	19.196	0.01	15.683	0.01	39.306	0.01	0.81699	2.04760
c 30385-102A	MARBLE BASIN (UPPER D) (N=2)	104/P/05/W:SW-044	59.26	129.87	JG			GOOD:	GL	19.197	0.01	15.685	0.01	39.313	0.01	0.81706	2.04790

o	30400-501	CUSAC	104/P/04/E:SW-	59.19	129.70	GSC			1	GOOD		GL	19.171	0.00	15.649	0.00	39.042	0.00	0.81629	2.03652
o	30400-502	CUSAC	104/P/04/E:SW-	59.19	129.70	GSC			1	GOOD		GL	19.183	0.00	15.677	0.00	39.162	0.00	0.81724	2.04149
o	30436-002	ERICKSON (VOLLAUG)	104/P/04/E:SW-019	59.22	129.65	AA	02/03/83:		1	GOOD		GL	19.036	0.03	15.685	0.03	38.932	0.04	0.82396	2.04518
o	30436-501	ERICKSON (MAURA-ALISON)	104/P/04/E:SW-	59.22	129.65	GSC			1	GOOD		GL	19.133	0.00	15.694	0.00	38.950	0.00	0.82026	2.03575
o	30436-502	ERICKSON (MAURA-ALISON)	104/P/04/E:SW-	59.22	129.65	GSC			1	GOOD		GL	19.143	0.00	15.707	0.00	38.995	0.00	0.82051	2.03704
o	30436-503	ERICKSON (TABLE MTN- VOLLAUG)	104/P/04/E:SW-	59.22	129.65	GSC			1	GOOD		GL	19.076	0.00	15.677	0.00	38.896	0.00	0.82182	2.03900
o	30436-504	ERICKSON (PLAZA-VOLLAUG)	104/P/04/E:SW-	59.22	129.65	GSC			1	GOOD		GL	19.057	0.00	15.676	0.00	38.932	0.00	0.82259	2.04293
c	30460-001	MIDWAY (LOWER)	104/O/16/W:NE-003	59.91	130.33	JG	09/07/84:06/26/85	1	GOOD:	1150:07		GL	19.347	0.02	15.695	0.01	39.747	0.02	0.81123	2.05442
c	30460-002	MIDWAY (DISCOVERY)	104/O/16/W:NE-038	59.91	130.33	JG	09/07/84:06/26/85	1	FAIR:	1150:08		GL	19.279	0.08	15.686	0.08	39.718	0.02	0.81362	2.06016
c	30460-002$	MIDWAY (DISCOVERY)	104/O/16/W:NE-038	59.91	130.33	JG	09/07/84:06/26/85	1	GOOD:	1150:08		GX	19.296	0.04	15.679	0.04	39.696	0.04	0.81257	2.05716
c	30460-004	MIDWAY (DISCOVERY)	104/O/16/W:NE-038	59.91	130.33	JG	09/09/84:06/26/85	1	GOOD:	1200:08		GL	19.310	0.01	15.694	0.01	39.731	0.01	0.81275	2.05755
c	30460-005	MIDWAY (LOWER)	104/O/16/W:NE-003	59.91	130.33	JG	09/09/84:06/26/85	1	GOOD:	1150:07		GL	19.346	0.02	15.703	0.01	39.811	0.03	0.81168	2.05786
c	30460-006	MIDWAY (DISCOVERY)	104/O/16/W:NE-038	59.91	130.33	JG	09/20/84:06/26/85	1	GOOD:	1150:07		GL	19.326	0.03	15.695	0.03	39.766	0.04	0.81210	2.05763
c	30460-007G	MIDWAY (DISCOVERY)	104/O/16/W:NE-038	59.91	130.33	JG	09/20/84:06/26/85	1	FAIR:	1300:08		GL	19.290	0.10	15.677	0.10	39.710	0.10	0.81268	2.05856
c	30460-007GR	MIDWAY (DISCOVERY)	104/O/16/W:NE-038	59.91	130.33	JG	10/27/84:06/26/85	2	FAIR:	1300:08		GL	19.303	0.09	15.688	0.09	39.721	0.09	0.81269	2.05772
c	30460-007P	MIDWAY (DISCOVERY)	104/O/16/W:NE-038	59.91	130.33	JG	09/20/84:06/26/85	1	FAIR:	1300:09		PY	19.332	0.04	15.717	0.03	39.812	0.04	0.81298	2.05934
c	30460-007PR	MIDWAY (DISCOVERY)	104/O/16/W:NE-038	59.91	130.33	JG	11/21/84:06/26/85	2	GOOD:	1150:08		PY	19.324	0.00	15.708	0.01	39.783	0.02	0.81285	2.05869
c	30460-007PA	MIDWAY (DISCOVERY, N=2)	104/O/16/W:NW-038	59.91	130.33	JG			FAIR /GOOD			PY	19.329	0.02	15.713	0.02	39.798	0.03	0.81291	2.05901
c	30460-007GA	MIDWAY (DISCOVERY, N=2)	104/O/16/W:NE-038	59.91	130.33	JG			FAIR:			GL	19.297	0.10	15.683	0.10	39.716	0.10	0.81268	2.05814
c	30460-008R	MIDWAY (DISCOVERY)	104/O/16/W:NE-038	59.91	130.33	JG	10/26/84:06/26/85	3	FAIR:	1200:11		GL	19.307	0.08	15.694	0.08	39.763	0.08	0.81288	2.05948
c	30460-008R	MIDWAY (DISCOVERY)	104/O/16/W:NE-038	59.91	130.33	JG	10/01/84:06/26/85	2	GOOD:	1150:09		GL	19.331	0.03	15.708	0.03	39.803	0.04	0.81259	2.05903
c	30460-008A	MIDWAY (DISCOVERY) (N=2)	104/O/16/W:NE-038	59.91	130.33	JG			GOOD /FAIR			GL	19.319	0.06	15.701	0.06	39.783	0.06	0.81274	2.05925
c	30460-009!	MIDWAY (DISCOVERY)	104/O/16/W:NE-038	59.91	130.33	JG	09/20/84:06/26/85	1	POOR:	1350:09		GL	19.207	0.24	15.662	0.24	39.573	0.24	0.81541	2.06032
c	30460-009R	MIDWAY (DISCOVERY)	104/O/16/W:NE-038	59.91	130.33	JG	10/11/84:06/26/85	2	GOOD:	1220:13		GL	19.317	0.06	15.711	0.06	39.795	0.07	0.81332	2.06016
c	30460-010	MIDWAY	104/O/16/W:NE-003	59.91	130.33	JG	09/20/84:06/26/85	1	GOOD:	1150:08		GL	19.359	0.01	15.699	0.01	39.757	0.02	0.81035	2.05367
c	30460-011	MIDWAY	104/O/16/W:NE-003	59.91	130.33	JG	09/20/84:06/26/85	1	GOOD:	1200:08		GL	19.338	0.01	15.696	0.01	39.753	0.02	0.81169	2.05572
c	30460-012	MIDWAY (SILVERTIP)	104/O/16/W:NE-003	59.91	130.33	JG	12/13/84:06/26/85	1	FAIR:	1100:09		GL	19.345	0.02	15.706	0.01	39.818	0.03	0.81189	2.05825
c	30460-012R	MIDWAY (SILVERTIP)	104/O/16/W:NE-003	59.91	130.33	JG	12/28/84:06/26/85	2	GOOD:	1150:08		GL	19.325	0.04	15.699	0.03	39.747	0.05	0.81237	2.05672
c	30460-012A	MIDWAY (SILVERTIP, N=2)	104/O/16/W:NE-003	59.91	130.33	JG			FAIR /GOOD			GL	19.335	0.03	15.703	0.02	39.783	0.04	0.81213	2.05748
c	30460-013	MIDWAY	104/O/16/W:NE-003	59.91	130.33	JG	05/29/87:06/26/85	1	good:	1200:09		GL	19.321	0.00	15.702	0.01	39.771	0.00	0.81270	2.05845
o	30460-501	MIDWAY (SILVERTIP)	104/O/16/W:NE-	59.91	130.33	GSC		1	POOR			GL	19.303	0.00	15.689	0.00	39.765	0.00	0.81278	2.06005
o	30460-502	MIDWAY (DISCOVERY ZONE)	104/O/16/W:SE-	59.91	130.33	GSC		1	GOOD			GL	19.348	0.11	15.696	0.16	39.782	0.22	0.81125	2.05613
o	30460-503A	MIDWAY (DISCOVERY ZONE) (N=2)	104/O/16/W:NE-	59.91	130.33	GSC						GL	19.345	0.00	15.692	0.00	39.765	0.00	0.81117	2.05557
o	30460-504	MIDWAY (LOWER ZONE)	104/O/16/W:NE-	59.91	130.33	GSC		1	GOOD			GL	19.348	0.11	15.683	0.16	39.719	0.22	0.81058	2.05287
o	30460-505	MIDWAY (DISCOVERY ZONE)	104/O/16/W:NE-	59.91	130.33	GSC		1	GOOD			GL	19.309	0.11	15.683	0.16	39.746	0.22	0.81222	2.05842
o	30460-506	MIDWAY (DISCOVERY ZONE)	104/O/16/W:NE-	59.91	130.33	GSC		1	GOOD			GL	19.384	0.11	15.727	0.16	39.871	0.22	0.81134	2.05691
o	30460-507	MIDWAY (SILVERTIP)	104/O/16/W:NE-	59.91	130.33	GSC		1	GOOD			GL	19.340	0.11	15.700	0.16	39.795	0.22	0.81179	2.05766
o	30460-508	MIDWAY (SILVERTIP)	104/O/16/W:NE-	59.91	130.33	GSC		1	GOOD			GL	19.334	0.11	15.697	0.16	39.806	0.22	0.81189	2.05886
o	30460-509	MIDWAY (UPPER ZONE)	104/O/16/W:NE-	59.91	130.33	GSC		1	GOOD			GL	19.305	0.11	15.683	0.16	39.749	0.22	0.81238	2.05900
o	30460-510	MIDWAY (UPPER ZONE: O)	104/O/16/W:NE-	59.91	130.33	GSC		1	GOOD			GL	19.318	0.11	15.691	0.16	39.782	0.22	0.81225	2.05932
o	30460-511	MIDWAY (LOWER ZONE)	104/O/16/W:NE-	59.91	130.33	GSC		1	GOOD			GL	19.345	0.00	15.690	0.00	39.771	0.00	0.81106	2.05588
c	30461-001	BLUE (ICE LAKE)	104/P/12/W:NW-	59.53	129.99	JG	09/07/84:06/26/85	1	GOOD:	1200:08		GL	18.513	0.07	15.649	0.04	38.595	0.08	0.84529	2.08473
c	30461-001R	BLUE (ICE LAKE)	104/P/12/W:NW-	59.53	129.99	JG	09/09/84:06/26/85	2	GOOD:	1150:06		GL	18.544	0.03	15.670	0.03	38.648	0.03	0.84506	2.08416
c	30461-001A	BLUE (ICE LAKE) (N=2)	104/P/12/W:NW-	59.53	129.99	JG			GOOD:			GL	18.529	0.05	15.660	0.04	38.622	0.06	0.84517	2.08445
c	30552-001	AMY (MARBACO)	104/O/16/W:NE-004	59.92	130.48	JG	12/21/84:06/26/85	1	GOOD:	1150:07		GL	19.406	0.02	15.708	0.01	39.649	0.05	0.80945	2.04313
c	30552-002	AMY (MARBACO)	104/O/16/W:NW-004	59.92	130.48	JG	04/13/87:06/26/85	1	good:	1150:07		GL	19.315	0.00	15.705	0.00	39.773	0.00	0.81311	2.05919
c	30552-003	AMY (MARBACO)	104/O/16/W:NW-004	59.92	130.48	JG	04/13/87:06/26/85	1	fair:	1200:16		GL	19.324	0.00	15.711	0.01	39.773	0.00	0.81302	2.05815
c	30552-004	AMY (MARBACO)	104/O/16/W:NW-004	59.92	130.48	JG	04/17/87:06/26/85	1	good:	1200:07		GL	19.321	0.00	15.709	0.03	39.762	0.00	0.81302	2.05792

c 30680-001	LUCK GROUP	104/O/16/E:NE-033	59.99	130.45	JG	05/01/87:06/26/85	1	good:	1200:08	GL	19.563	0.00	15.728	0.01	39.810	0.00	0.80397	2.03495
c 30682-001	MT HASKIN	104/P/06/W:SW-020	59.34	129.49	JG	01/29/88:11/09/87	1	good:	1150:10	GL	19.108	0.00	15.696	0.00	39.573	0.00	0.82146	2.07102
c 30682-003	MT HASKIN	104/P/06/W:SW-020	59.35	129.51	JG	01/29/88:11/09/87	1	fair:	1150:07	GL	19.089	0.01	15.675	0.00	39.498	0.01	0.82118	2.06909
c 30682-003D	MT HASKIN	104/P/06/W:SW-020	59.35	129.51	JG	02/26/88:11/09/87	1	good:	1150	GL	19.091	0.00	15.677	0.00	39.511	0.01	0.82115	2.06957
c 30682-003A	MT HASKIN	104/P/06/W:SW-020	59.35	129.51	JG	02/ /88:11/09/87		good:		GL	19.090	0.01	15.676	0.00	39.504	0.01	0.82116	2.06933
c 30682-101	MT HASKIN (SE SKARN)	104/P/06/W:SW-020	59.34	129.49	JG	07/25/85:06/26/85	1	FAIR:	1200:10	GL	19.218	0.03	15.730	0.01	39.296	0.03	0.81849	2.04473
c 30682-101R	MT HASKIN (SE SKARN)	104/P/06/W:SW-020	59.34	129.49	JG	08/02/85:06/26/85	2	GOOD:	1100:07	GL	19.217	0.01	15.735	0.01	39.315	0.01	0.81882	2.04582
c 30682-101A	MT HASKIN (SE SKARN, N=2)	104/P/06/W:SW-020	59.34	129.49	JG			FAIR /GOOD		GL	19.218	0.00	15.733	0.00	39.306	0.00	0.81865	2.04527
c 30682-102	MT HASKIN (NW SKARN)	104/P/05/E:SW-020	59.35	129.51	JG	07/25/85:06/26/85	1	GOOD:	1150:08	GL	19.326	0.01	15.712	0.01	39.680	0.01	0.81300	2.05322
c 30682-102D	MT HASKIN (NW SKARN)	104/P/05/E:SW-020	59.35	129.51	JG	01/29/88:11/09/87	1	good:	1150:06	GL	19.309	0.01	15.699	0.00	39.636	0.01	0.81307	2.05274
o 30742-501	LANG CREEK	104/P/04/W:	59.23	129.77	GSC		1	GOOD		GL	19.137	0.00	15.672	0.00	38.085	0.00	0.81894	1.99012
o 30743-501	BAD BEAR (MCDAME BELLE)	104/P/06/W:	59.27	129.37	GSC		1	GOOD		GL	19.348	0.00	15.742	0.00	39.833	0.00	0.81363	2.05877
o 30744-501	COTTONWOOD	104/O/08/W:SE-	59.34	130.27	GSC	00/00/84	1	GOOD		GL	18.334	0.00	15.638	0.00	38.020	0.00	0.85295	2.07375
c 30872-101	NEEDLEPOINT SILVER	104/P/04/W:SW-	59.14	129.78	JG	07/26/85:06/26/85	1	GOOD:	1150:07	GL	19.348	0.02	15.695	0.02	39.530	0.02	0.81122	2.04314
c 30873-101	BILL-CARLICK (TRENCH 1)	104/P/03/E:SW-	59.22	129.22	JG	07/26/85:06/26/85	1	GOOD:	1150:06	GL	18.257	0.01	15.620	0.01	38.276	0.01	0.85555	2.09645
c 30873-102	BILL-CARLICK (TRENCH 2)	104/P/03/E:SW-	59.22	129.22	JG	07/26/85:06/26/85	1	GOOD:	1150:07	GL	18.153	0.01	15.607	0.00	38.200	0.01	0.85974	2.10429
c 30873-AVG	BILL-CARLICK (N=2)	104/P/03/E:SW-	59.22	129.22	JG			GOOD:		GL	18.205	0.01	15.614	0.01	38.238	0.01	0.85797	2.10036
c 30876-002	SILVER KNIFE	104/O/16/W:NE-	59.93	130.36	JG	09/03/87:11/09/87	1	good:	1200:11	GL	19.459	0.00	15.698	0.00	39.717	0.00	0.80673	2.04104
c 30876-003	SILVER KNIFE	104/O/16/W:NE-	59.93	130.36	JG	09/03/87:11/09/87	1	good:	1200:07	GL	19.442	0.00	15.707	0.00	39.719	0.00	0.80789	2.04289
c 30876-004	SILVER KNIFE	104/O/16/W:NE-	59.93	130.36	JG	09/03/87:11/09/87	1	good:	1200:06	GL	19.476	0.00	15.707	0.00	39.751	0.00	0.80646	2.04098
c 30876-101	SILVER KNIFE	104/O/16/W:NE-	59.93	130.36	JG	08/19/85:06/26/85	1	GOOD:	1150:13	GL	19.462	0.01	15.716	0.01	39.744	0.01	0.80755	2.04219
c 30888-001!	TOOTSIE STAR	104/O/16/W:NE-039	59.90	130.30	JG	04/30/87:06/26/85	1	fair:	1200:18	GL	19.350	0.01	15.738	0.06	39.900	0.01	0.81335	2.06202
c 30888-001D	TOOTSIE STAR	104/O/16/W:NE-039	59.90	130.30	JG	02/01/88:11/09/87	1	good:	1150:06	GL	19.291	0.00	15.692	0.00	39.760	0.00	0.81342	2.06103
c 30970-001	GUM MOUNTAIN	104/O/16/E:NE-	59.88	130.27	JG	05/01/87:06/26/85	1	good:	1200:08	GL	19.357	0.00	15.720	0.02	39.890	0.00	0.81211	2.06075

Notes: (1) Column 1 gives data status and normalization factors where: c = current normalization factor; o = other normalization factors, variable reliability (normalization factors are in Godwin et al., 1988, Table 5.1).

(2) Suffix codes: ! = analysis suspected to be poor; $ = analysis renormalized; A = average of repeats and duplicates for sample; D = duplicate analysis of sample using new chemical dissolution; R = analysis repeated from same shemical dissolution of sample.

(3) RN = run number.

(4) RUN:NORM = rundate, normalization date.

(5) QL:T:B = run quality: temperature (degrees C): number of data blocks.

(6) MT = material analyzed (PY = pyrite; GN = galena).

(7) Errors listed after analyses are expressed as % standard deviation.

Table 2-2: Mean lead isotope compositions, with standard deviations, Rancheria, Cassiar and Seagull districts, northern British Columbia and southern Yukon Territory.

DEPOSIT	206/204	207/204	208/204	207/206	208/206
A. Rancheria District					
Amy	19.342	15.708	39.739	.81215	2.05460
(n=4)	(.037)	(.002)	(.052)	(.0016)	(.00664)
Midway (McDame)	19.341	15.696	39.769	.81152	2.05627
(n=11)	(.009)	(.006)	(.027)	(.00058)	(.00190)
Midway (Earn)	19.313	15.693	39.757	.81248	2.05857
(n=10)	(.011)	(.011)	(.032)	(.00049)	(.00090)
Silverknife	19.460	15.707	39.732	.80716	2.04177
(n=4)	(.012)	(.006)	(.015)	(.00058)	(.00080)
Lucky	19.563	15.728	39.810	.803967	2.03495
Tootsee Star	19.291	15.692	39.760	.81342	2.06103
Gum Mountain	19.357	15.720	39.890	.81211	2.06075
Lola	19.398	15.709	39.712	.80979	2.04683
(n=4)	(.045)	(.007)	(.038)	(.0016)	(.00648)
Fiddler	19.670	15.754	39.832	.80095	2.02510
YP	19.636	15.753	39.844	.80225	2.04683
(n=6)	(.034)	(.014)	(.029)	(.00077)	(.00292)
Meister	18.564	15.664	38.056	.84377	2.05004
Alan	19.492	15.709	39.691	.80588	2.03605
Silverhart	19.538	15.738	39.749	.80553	2.03448
(n=3)	(.031)	(.012)	(.021)	(.00191)	(.00429)
Wolf	19.524	15.747	39.813	.806547	2.03922
B. Seagull District					
Logtung (Darva)	19.132	15.682	39.035	.82009	2.04137
MC (K-3)	18.540	15.621	38.406	.84259	2.07162
MC (K-1)	19.162	15.689	39.102	.81880	2.04111
C. Cassiar District					
Cottonwood	18.334	15.638	38.020	.85295	2.07375
Bill	18.205	15.614	38.238	.85765	2.10037
(n=2)	(.052)	(.007)	(.038)	(.00210)	(.00392)
Needlepoint	19.348	15.695	39.530	.81122	2.04314
Lang Creek	19.137	15.672	38.085	.81894	1.99013
Erickson (Maura)	19.138	15.701	38.973	.82039	2.03640
(n=2)	(.005)	(.007)	(.023)	(.00013)	(.00065)
Erickson (Vollaug)	19.056	15.679	38.920	.82279	2.04237
(n=3)	(.016)	(.004)	(.017)	(.00089)	(.00255)
Erickson (Cusac)	19.177	15.663	39.102	.81676	2.03900
(n=2)	(.006)	(.014)	(.060)	(.00048)	(.00249)
Marble Basin	19.198	15.685	39.326	.81699	2.04857
(n=4)	(.001)	(.001)	(.009)	(.00005)	(.00045)
Mount Haskin	19.184	15.703	39.512	.81857	2.05971
(n=4)	(.092)	(.020)	(.130)	(.00338)	(.01094)
McDame Belle	19.348	15.742	39.833	.81362	2.05877
Axe	19.142	15.678	39.785	.81906	2.07840
Blue	18.529	15.660	38.622	.84517	2.08445
Reggie	18.516	15.652	38.505	.84532	2.07955

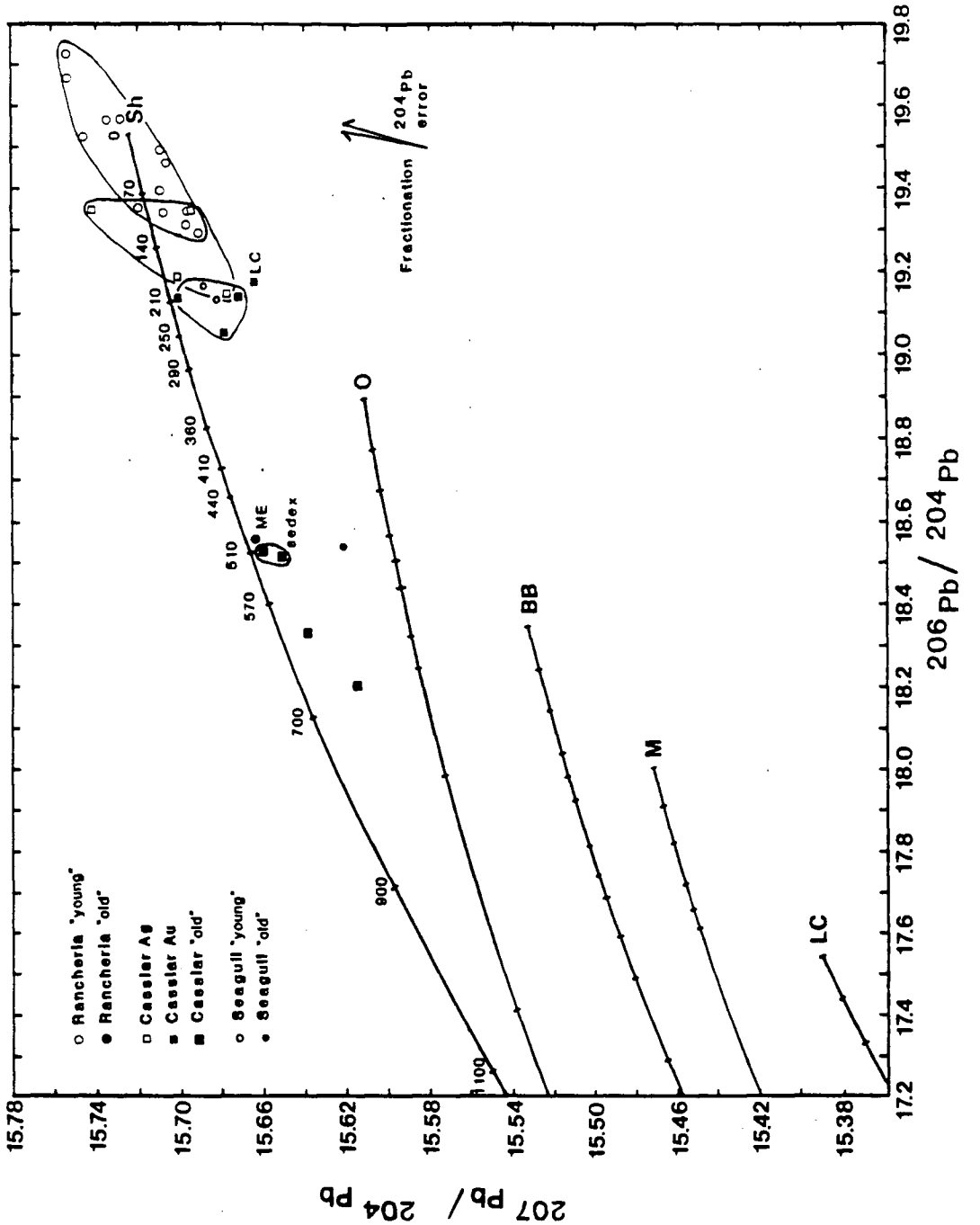

Figure 2-2: Lead isotope ratio diagram for mineral deposits of the Rancheria, Seagull and Cassiar districts. Lead growth curves are: Sh - shale (Godwin and Sinclair, 1982); M - mantle, LC - lower crust (Doe and Zartman, 1979); BB - Bluebell (Andrew et al., 1984). LC - Lang Creek deposit, Cassiar district.

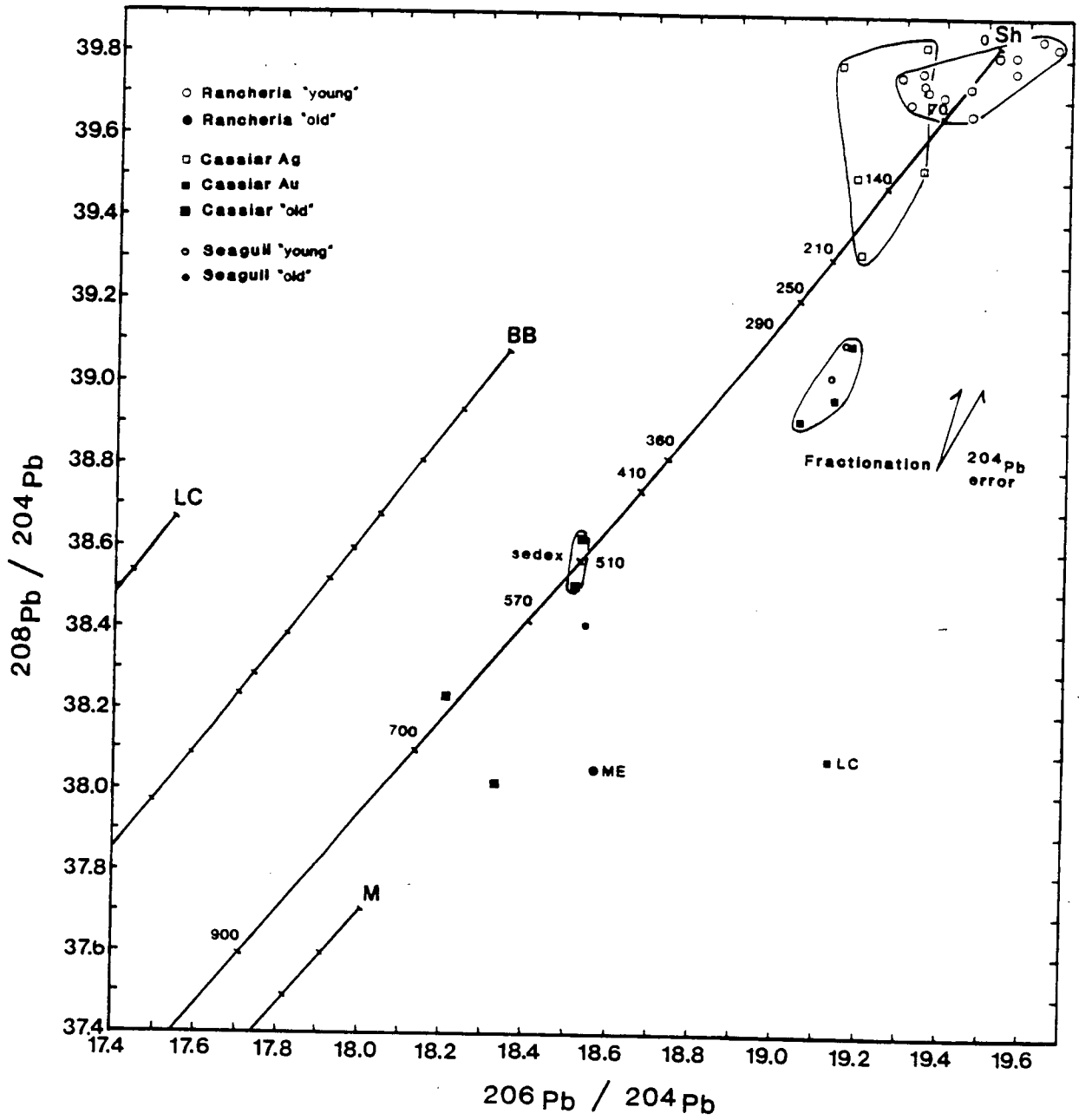

Figure 2-3: Lead isotope ratio diagram for mineral deposits of the Rancheria, Seagull and Cassiar districts. Abbreviations as in Figure 2-2.

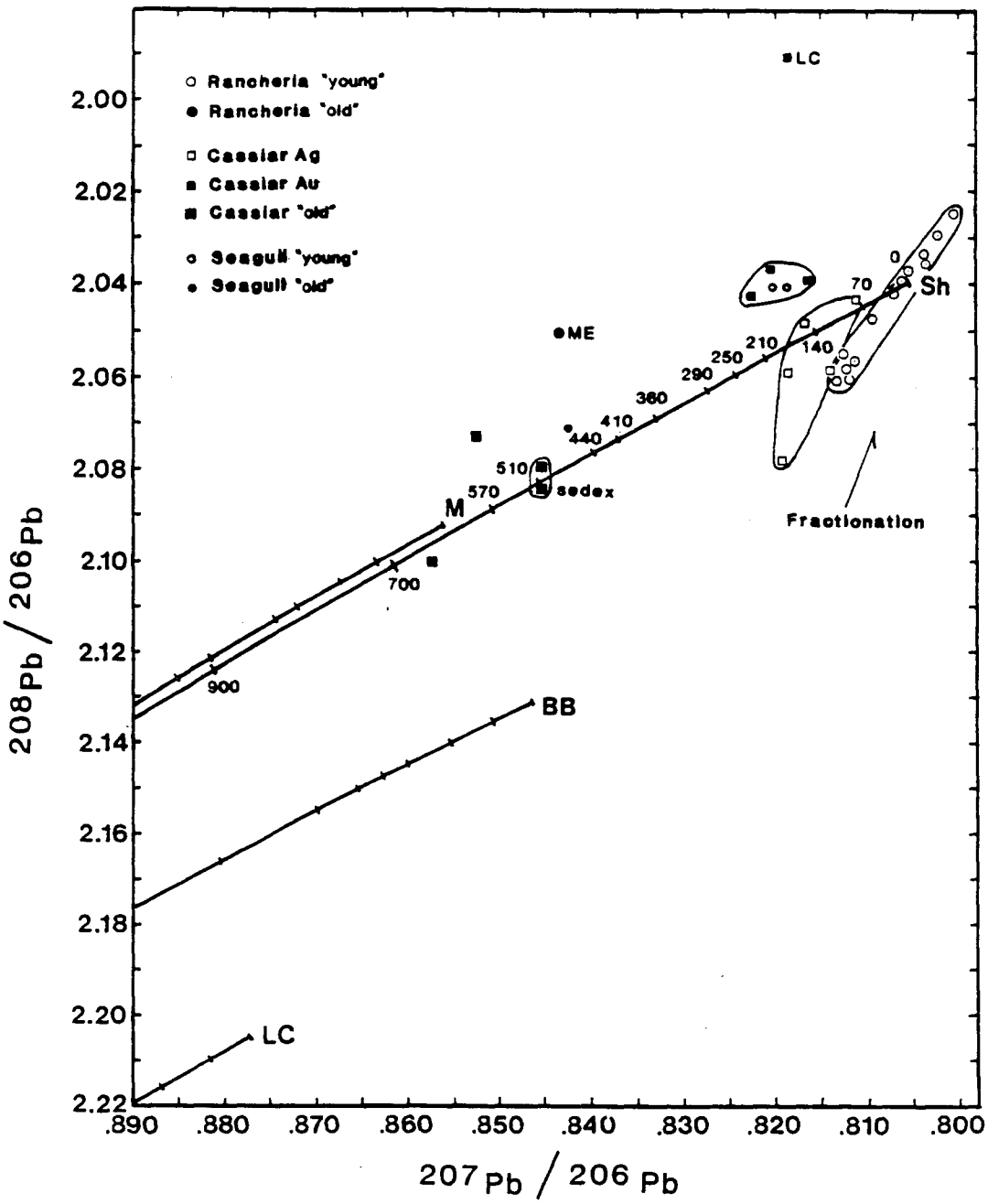

Figure 2-4: Lead isotope ratio diagram for mineral deposits of the Rancheria, Seagull and Cassiar districts. Abbreviations as in Figure 2-2.

Creek and McDame Belle showings. All deposits are located on Figures 2-5, 2-6 and 2-7.

For plotting purposes, suites of samples from single showings have been averaged. Most of the variability within deposits tends to lie along fractionation and/or ^{204}Pb error slopes. Averaging analyses therefore tends to remove some of the analytical noise and facilitates interpretation of the data.

2.5. Interpretation

Lead isotope plots (Figures 2-2, 2-3, and 2-4) show a separation of data into several deposit groups. The two main groups are: (a) "old" lead, plotting to the left of and below the 350 Ma point on the shale curve, and (b) "young" lead, plotting to the right of the 250 Ma point on the shale curve. One deposit, Lang Creek (LC), is a special case.

2.5.1. "Old" Deposits

The "old" deposits include two subgroups:

(1) Early Mississipian sediment hosted base metal deposits, hosted in Earn Group, Cassiar district (e.g. Blue, Reggie). These deposits plot at about 510 Ma (Cambro - Ordovician) on the

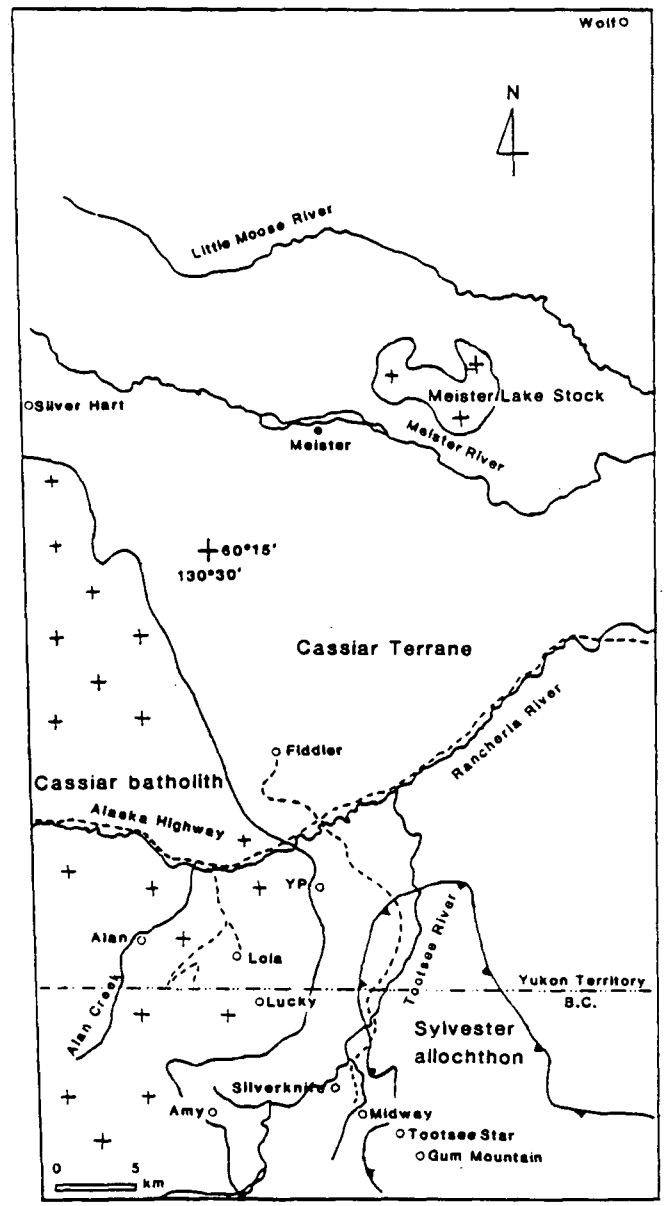

Figure 2-5: Location of mineral deposits of the Rancheria district, north-central British Columbia and south-central Yukon Territory.

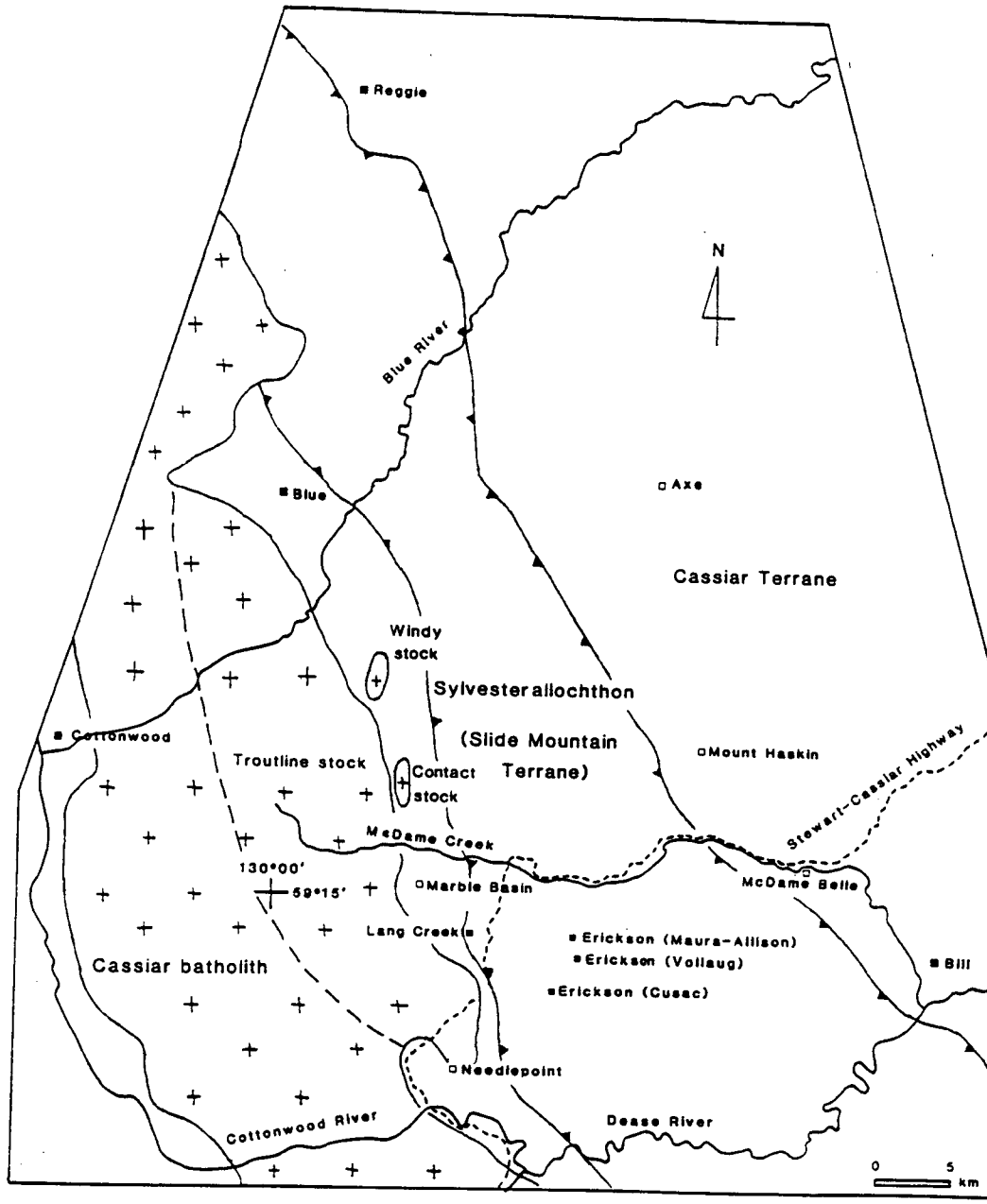

Figure 2-6: Location of mineral deposits of the Cassiar district, north-central British Columbia.

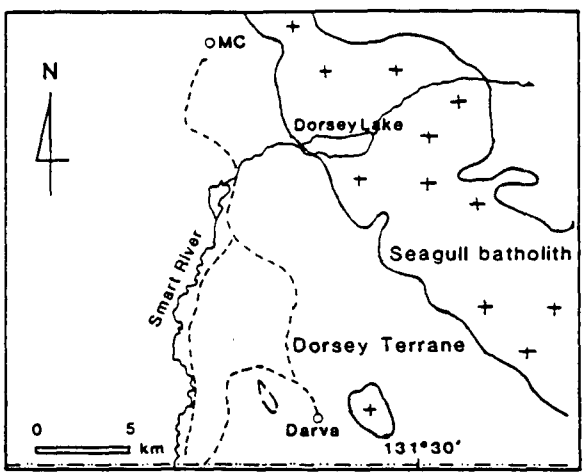

Figure 2-7: Location of mineral deposits of the Seagull district, south-central Yukon Territory.

shale curve on all plots. Lead in this group is less radiogenic than lead in to Devono - Mississipian shale hosted or "sedex" deposits in the Selwyn Basin (Godwin and Sinclair, 1982); hence the shale curve model age is older than the host rock age.

(2) Carbonate hosted galena - barite, Cassiar district (e.g. Cottonwood and Bill or Carlick). These two deposits have the least radiogenic lead reported here, with a Late Proterozoic shale curve model age. This again is older than the host rock ages (Lower Cambrian Atan Group for the Bill showing, and Carboniferous Oblique Creek Formation for the Cottonwood).

Two other showings, Meister and MC, do not fall into the above categories. Meister is hosted in Lower Cambrian or earlier metasediments and shows significantly lower values of ^{208}Pb (Figure 2-3). MC was believed to be a mid-Cretaceous skarn related to the Seagull batholith (Mato et al., 1983). One sample plots in the Seagull epigenetic group (see below), while the other sample plots in the old deposit group, with a lead model age of about 530 Ma. The latter therefore might represent a thermally metamorphosed Paleozoic deposit, spatially associated with a mid-Cretaceous skarn.

The distinctly less radiogenic lead isotope signature of the

"old" group of deposits has considerable exploration utility, since the younger deposits commonly have higher precious metal values, and currently are more important exploration targets. Field relations do not always distinguish the two groups. For example, the Reggie showing consists of crosscutting galena veins and was initially thought to be related to a young intrusion (Nelson et al., 1988). Lead isotopes are similar to those of a nearby sedex deposit (Blue), indicating a probable Mississipian age. Another example in which lead isotopes helped to change geological interpretation and exploration models is the Midway deposit, originally thought to be a Paleozoic sedex deposit (MacIntyre, 1982), and now known to be Late Cretaceous (Bradford and Godwin, 1988).

The data also show that the shale curve is not useful in dating these deposits, as model ages are significantly greater than host rock ages. A more primitive (lower mu and kappa) lead source is required for the sedex deposits in Earn Group overlying Cassiar Terrane (section 2.5.2.1.).

2.5.2. "Young" Deposits

This group of deposits can be divided into subgroups, according to the district in which they occur (Rancheria, Cassiar and Seagull). The Cassiar area deposits are further

subdivided on the basis of host terrane, with the "Cassiar gold" group hosted in Slide Mountain Terrane, and "Cassiar silver" group in Cassiar Terrane. The Seagull and Cassiar gold groups have similar lead isotope characteristics, which are very different from those of epigenetic deposits hosted in Cassiar Terrane (Rancheria and Cassiar silver groups).

2.5.2.1. Rancheria District

Rancheria district epigenetic deposits are mainly silver-lead-zinc veins and replacements in granitic and Cassiar Terrane carbonate host rocks (Abbott, 1984). They commonly have a significant tin component, suggestive of a genetic relationship with S or A - type granites. Data for this group form elongate clusters in Figures 2-2 and 2-3, and a well defined linear trend in Figure 2-4. The slope of a line drawn between the Midway and Fiddler deposits (Figure 2-2), at the extremes of the data cluster, is 0.176. This value is appropriate for a mixing line, being steeper than growth curves and isochrons, and shallower than fractionation and ^{204}Pb error lines. According to Dawson et al. (1985) these trends represent mixing lines between lead which evolved in a highly radiogenic upper crustal environment defined by the shale curve, and lead derived from a uranium depleted, thorium enriched (relative to mantle) lower crustal reservoir. The diffuse nature of the

elongate trend on Figure 2-2 could be due to ^{204}Pb error, as a tighter linear trend is observed when ^{204}Pb is removed (Figure 2-4).

There are two main problems with this interpretation. First, the median age for these deposits is about 70 Ma, whereas the proposed mixing line crosses the shale curve between 50 and 0 Ma. This is a relatively trivial objection, since the error involved in lead isotope model ages is commonly at least 50 Ma.

More importantly, the radiogenic end member lies well above and to the right of the shale curve at t = 0 Ma. This indicates that the shale curve only approximates one of the end member components of the mixing system. An upper crustal end member which intersects the radiogenic end of the mixing line at t = 70 Ma would require a mu value of 13.00, compared to the shale curve's 12.16, given the same starting point (Table 2-3).

Alternatively, a terrane specific growth curve applicable to Cassiar Terrane hosted deposits can be generated by choosing a different starting point from that used for the shale curve, and by balancing mu values calculated through $^{206}Pb/^{204}Pb$ and $^{207}Pb/^{204}Pb$ equations (cf. Godwin et al., 1988). Table 2-3 lists mu values for possible Cassiar Terrane growth curves, using various starting points and deposits of known age as reference

Table 2-3: Mu values of growth curves for Cassiar Terrane mineral deposits. Values are calculated using the programs in Godwin et al., 1988. The first number listed is calculated from the $^{206}Pb/^{204}Pb$ equation, the second from the $^{207}Pb/^{204}Pb$ equation.

Starting point	Cassiar sedex [1]	Midway [2]	Fiddler [3]
Shale curve [4]	11.04, 11.35	12.00, 11.61	13.00, 13.11
Pericratonic curve [5]	10.94, 11.15	11.85, 11.40	12.78, 12.71
2.2 Ga [6]	10.80, 10.90	11.63, 11.11	12.46, 12.16

1. t_2 = 355 Ma; $^{206}Pb/^{204}Pb$ = 18.522; $^{207}Pb/^{204}Pb$ = 15.656; $^{208}Pb/^{204}Pb$ = 38.563; average of Blue and Reggie showings (Table 2-2).

2. t_2 = 70 Ma; $^{206}Pb/^{204}Pb$ = 19.341; $^{207}Pb/^{204}Pb$ = 15.696; $^{208}Pb/^{204}Pb$ = 39.769; average for McDame Group hosted mineralization (Table 2-2).

3. t_2 = 70 Ma; $^{206}Pb/^{204}Pb$ = 19.670; $^{207}Pb/^{204}Pb$ = 15.754; $^{208}Pb/^{204}Pb$ = 39.832 (Table 2-2).

4. t_1 = 1.887 Ga; $^{206}Pb/^{204}Pb$ = 15.391; $^{207}Pb/^{204}Pb$ = 15.246; $^{208}Pb/^{204}Pb$ = 35.026 (Godwin et al., 1988).

5. t_1 = 2.0 Ga; $^{206}Pb/^{204}Pb$ = 15.159; $^{207}Pb/^{204}Pb$ = 15.192; $^{208}Pb/^{204}Pb$ = 34.799 (Godwin et al., 1988).

6. $^{206}Pb/^{204}Pb$ = 14.739; $^{207}Pb/^{204}Pb$ = 15.079; $^{208}Pb/^{204}Pb$ = 34.394; calculated from Stacey-Kramers' second stage growth curve by linear interpolation (Stacey and Kramers, 1975).

points. Starting points lie on the Stacey - Kramers second stage average crustal growth curve (Stacey and Kramers, 1975), as in the shale curve model (Godwin and Sinclair, 1982) and the "pericratonic" model of Goutier (1986). A third starting point, at 2.2 Ga, is added in accordance with provenance ages of Cassiar Terrane detrital zircons (Erdmer and Baadsgaard, 1987), and therefore is a preferred basement source age for the Cassiar Terrane.

Table 2-3 shows that the mu value for a growth curve modelling the radiogenic end member of the Rancheria mixing line (12.46, using the $^{206}Pb/^{204}Pb$ equation) is closer to the shale curve value (12.16) if the 2.2 Ga basement age is used as the starting point, rather than the shale curve's 1.887 Ga. However, the mu values calculated from the $^{206}Pb/^{204}Pb$ and $^{207}Pb/^{204}Pb$ equations are most closely balanced if the starting point of the pericratonic curve of Goutier (1986) is used for t1. This gives an average mu value of 12.75, from a t1, or apparent source age of 2.0 Ga.

An alternative to the upper crustal - lower crustal mixing interpretation assumes that the least radiogenic end member of the data cluster lies on an upper crustal growth curve (specific to Cassiar Terrane) which has a lower mu value than the shale curve's. The linear spread of data to more radiogenic values

therefore would be a secondary isochron, analogous those described by Godwin et al. (1982). Such an isochron might be generated by preferential leaching of lead from uranium rich minerals in clastic sediments (e.g. zircons), causing an enrichment in radiogenic lead. This model fails, however, because the slope of the Rancheria data cluster (0.176) is greater than the slope of a secondary isochron through the least radiogenic end of the cluster and any reasonable starting point for the growth curve. For the 2.2 Ga starting point, a secondary isochron through the Midway average value has a slope of 0.134. The Rancheria data cluster therefore cannot be modelled in this way.

Table 2-3 also shows that the Rancheria and Cassiar sedex deposits cannot both be adequately modelled by the same growth curve. For example, using the 2.0 Ga starting point, a Cassiar Terrane growth curve accurately modelling Cassiar sedex lead (Blue and Reggie showings) at t_2 = 355 Ma has a mu value of 10.94 (using the $^{206}Pb/^{204}Pb$ equation), significantly lower than mu of the curve modelling the least radiogenic Rancheria lead. This value is relatively insensitive to starting point age (Table 2-3). This means that the Rancheria epigenetic deposits and Cassiar sedex deposits contain lead from different crustal reservoirs, with the sedex reservoir being more primitive than the epigenetic reservoir. This is surprising, since the clastic

component of the Earn Group (host to the sedex deposits) is in part recycled Cassiar Terrane material. The implication might be that the sedex deposits formed during an extensional event of crustal magnitude along the Cordilleran margin, which allowed the ore forming fluids to tap deeper, more primitive lead reservoirs, perhaps by deep circulation along basin margin faults. This probably reflects significant crustal thinning along the North American margin in the Late Devonian.

2.5.2.2. Cassiar Silver Deposits

Epigenetic deposits hosted in Cassiar Terrane in the Cassiar area include silver-lead-zinc veins and replacements in carbonate host rocks, and are associated with Eocene (Mount Haskin) and Late Cretaceous granites (Panteleyev, 1980; Cooke and Godwin, 1984). Data from these deposits show a large amount of isotopic variability parallel to fractionation trends (Figure 2-2). On average, the lead isotopes from Cassiar silver deposits plot near the least radiogenic end of the Rancheria data clusters, and are generally less uranogenic and thorogenic than Rancheria deposits.

2.5.2.3. Cassiar Gold and Seagull Deposits

The Cassiar gold camp (Diakow and Panteleyev, 1982) consists

of a number of mesothermal gold - quartz vein systems hosted in greenstones and argillites of the Slide Mountain Terrane (Sylvester allochthon). Lead isotope data from the Cassiar gold camp shows a remarkable similarity to data from deposits related to the Seagull batholith and hosted in Dorsey Terrane (Figures 2-2, 2-3, and 2-4). The latter deposits are tin bearing skarns and veins marginal to the high level, tourmaline rich Seagull batholith and Logjam stocks (Mato et al., 1983). The Cassiar gold camp veins have been dated by potassium - argon method at about 125 Ma (Sketchley et al., 1986), while the Seagull batholith is about 100 Ma (Mato et al., 1983). Deposits from these terranes have distinctly less radiogenic lead isotope signatures than deposits hosted in Cassiar Terrane. This is particularly emphasized on the plots with a thorogenic axis (Figures 2-3 and 2-4).

Since both the Dorsey and Slide Mountain Terranes are in part allochthonous marginal basin assemblages, and since lead isotope signatures of deposits hosted within them are similar, a significant fraction of the lead is probably derived from the allochthonous host rocks. This lead is significantly different from shale curve lead at 125-100 Ma, indicating that the lead in this group of deposits evolved in a distinct environment. This is consistent with derivation of the lead from the host allochthonous terranes.

As shown on the plots with a thorogenic axis, displacement of this group of deposits away from the shale curve is in the general direction of a uranium and thorium depleted environment relative to upper crust; i.e. toward the mantle curve of Doe and Zartman (1979). This is consistent with derivation of a significant fraction of the lead from the allochthonous assemblages, which contain oceanic and arc volcanics which characteristically have a large mantle component. This is further emphasized by the Lang Creek showing (LC), a volcanogenic massive sulphide lens hosted in Mississipian (K. Dawson, personal communication, 1988) Slide Mountain terrane, which shows marked ^{208}Pb depletion indicative of lead with mantle characteristics (Figure 2-3).

2.6. Conclusions

(1) Lead isotope signatures of deposits genetically related to Mesozoic - Cenozoic intrusions enable these deposits to be distinguished from older deposits. This has exploration utility in that the younger deposits are commonly enriched in precious metals, and are not always distinguishable from older deposits on the basis of field relations.

(2) Older deposits in Cassiar Terrane generally have older shale

curve model ages than their host rock ages. The sedex deposits, of Early Mississipian age according to host rock paleontological dating, have Cambro - Ordovician shale curve model ages. Therefore the shale curve model cannot be extended to shale hosted sedex deposits in Cassiar Terrane.

(3) Epigenetic deposits hosted in Cassiar Terrane in the Rancheria and Cassiar areas have different lead isotope signatures. The Cassiar deposts are generally less radiogenic than Rancheria deposits, and show a wide scatter of lead isotope values.

(4) Rancheria epigenetic deposits define quasi - linear clusters on lead - lead plots. This could be due to mixing between lead derived from upper and lower crustal reservoirs, with the upper crustal end member having an older starting point (about 2.0 Ga) and a higher mu value (about 12.75) than the shale curve's.

(5) Rancheria district epigenetic deposits and Cassiar sedex deposits have lead isotope compositions incompatible with lead evolution in the same homogeneous reservoir, assuming reasonable basement source ages. The more primitive reservoir indicated for the sedex deposits might have been tapped by deep fluid penetration along large scale marginal detachments during

Devono-Mississipian extension.

(6) Mesothermal gold - quartz veins of the Cassiar area and tin bearing skarns and veins of the Seagull district have similar lead isotope signatures which are distinctive from the signatures of epigenetic deposits hosted in Cassiar Terrane. This indicates that a significant fraction of the lead in these deposits is derived from allochthonous marginal basin and oceanic host terranes (Slide Mountain and Dorsey), which have similar mantle-related lead characteristics. It also adds isotopic evidence to support the terrane concept as applied to Cassiar Terrane and associated accreted terranes.

3. Regional Geological Setting of the Midway Deposit

3.1. Introduction

The Midway deposit is near the southern end of the Rancheria district, a belt of silver - lead - zinc and lesser tungsten - tin - molybdenum mineralization extending north into the Yukon Territory (Wolf Lake map sheet, 105B/1). Mineralization occurs primarily in Paleozoic miogeoclinal carbonates on the east side of the mid-Cretaceous Cassiar batholith, and is associated with mid-Cretaceous and younger intrusions (Figure 3-1).

Miogeoclinal strata of the Rancheria district are part of the Cassiar Terrane (Figure 3-1), a displaced segment of Proterozoic - Paleozoic siliciclastic - carbonate shelf outboard of the main North American miogeocline (Monger and Berg, 1984). Northwesterly displacement of at least 450 kilometres occurred along the dextral Tintina transcurrent fault system in Cretaceous - Tertiary time (Roddick, 1964; Tempelman - Kluit, 1977; Gabrielse, 1985). Miogeoclinal strata are overlain by a basinal onlap sequence of Devono - Mississipian age (Earn Group), which is in turn structurally overlain by the Sylvester allochthon (Figure 3-1). The Sylvester allochthon consists mainly of pelagic sediments, mixed volcanic and intrusive rocks, and ultramafites of Late Devonian to Triassic age (Harms, 1986),

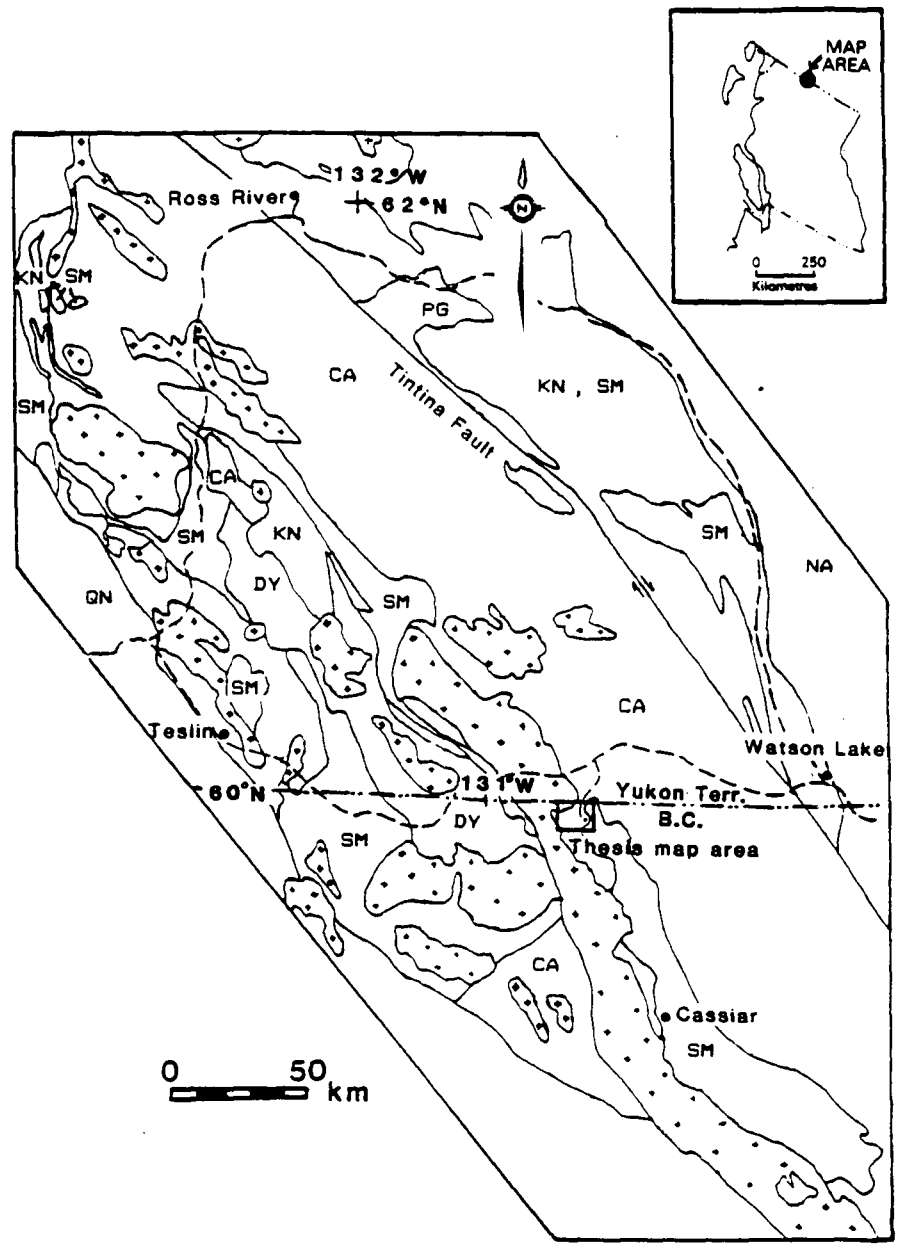

Figure 3-1: Location of the map area, and regional geological setting of the Midway deposit, northern British Columbia (1040/16).
Abbreviations: CA - Cassiar Terrane, SM - Slide Mountain Terrane, KN - Kootenay (Nisutlin) Terrane, DY - Dorsey Terrane, QN - Quesnellia, NA - ancestral North America.

and is part of the allochthonous Slide Mountain Terrane.

Several types of mineral deposits occur in the Rancheria district, representing Early Mississipian and mid-Cretaceous to Eocene metallogenic episodes. Late Devonian to Mississipian siliciclastic sediments of the Earn Group host stratiform barite and sphalerite exhalite horizons similar to those found in the MacMillan Pass and Gataga regions of the Yukon Territory and northern British Columbia (Carne and Cathro, 1982). Epigenetic silver - lead - zinc - tin veins and replacement deposits occur primarily in Lower Cambrian to Middle Devonian carbonates. These are associated with granitic stocks, dykes and batholiths of mid-Cretaceous to Eocene age. Some of the granitic rocks host silver and lead rich quartz veins and molybdenum bearing quartz stockworks, while tungsten - molybdenum skarns and breccias occur in their contact aureoles (Abbott, 1984).

The thesis map area discussed below is the northwest quarter of N.T.S. 104O/16 (Plate 1, in pocket). Reference is also made to adjacent parts of 104O/16 (Nelson and Bradford, 1987b), and to the map sheet to the north, 105B/1 (Lowey and Lowey, 1986). Key sections are lettered in Figure 3-2 for easy reference in the stratigraphic and structural descriptions. Table 3-1 is a table of formations, and Figure 3-3 is a stratigraphic column.

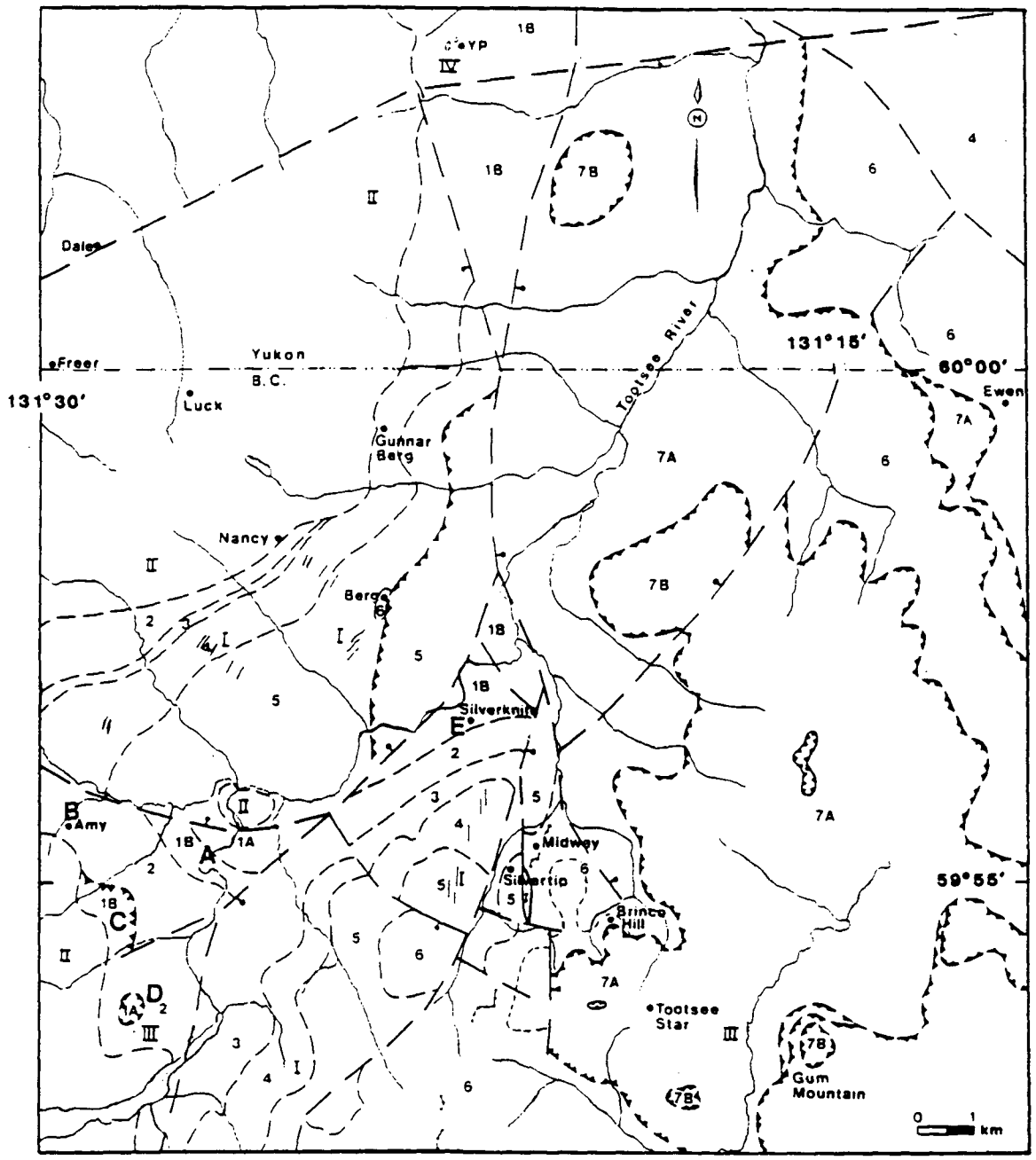

Figure 3-2: Generalized regional geology of the Midway area, including parts of 104O/16 and 105B/1, northern British Columbia and southern Yukon Territory. Geology in the Yukon Territory is modified after Lowey and Lowey (1986). Geology in British Columbia is based on Nelson and Bradford (1987b) and Plate 1 (in pocket). Lettered locations are sections referred to in the text. Lithological units are numbered as in Figure 3-3.

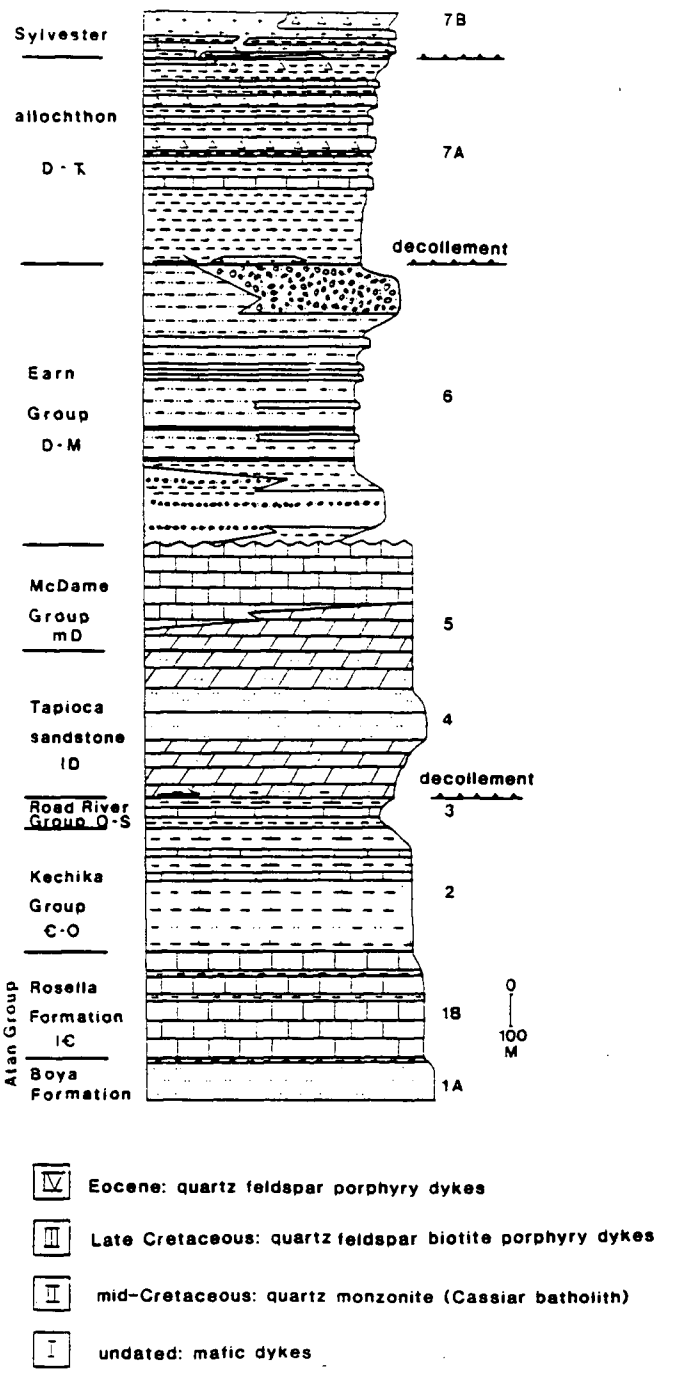

Figure 3-3: Stratigraphic column for the Midway area, northern British Columbia (1040/16).

Table 3-1: Table of formations, Midway area, north-central British Columbia (104O/16).

PERIOD	FORMATION AND THICKNESS	LITHOLOGIES
Tertiary?	Dykes	Mafic dykes
Late Cretaceous	Dykes	Quartz-feldspar-biotite-hornblende porphyry
Early Cretaceous	Cassiar batholith (Unit 8)	Quartz monzonite, granodiorite
	Intrusive contact	
Pennsylvanian?-Permian?	Sylvester allochthon (Division II) (Units 7C, 7D, 7E and 7F)	Basalt, basalt breccia, red and green chert, diabase, gabbro, serpentinite
	Thrust	
Mississipian - Permian?	Sylvester allochthon (Division I) (Units 7A, 7B) 700 metres	Argillite, chert, cherty phyllite, limestone, sandstone, tuff, mafic sills
	Decollement	
Mississipian	Earn Group (Unit 6D) 200 metres	Conglomerate, sandstone
Mississipian	Earn Group (Unit 6C) 640 metres	Slate, siltstone, sandstone, exhalite
Mississipian	Earn Group (Unit 6B) 250 metres	Sandstone, siltstone, conglomerate
Upper Devonian	Earn Group (Unit 6A) 45 metres	Silt shale, argillite
	Unconformity	
Middle Devonian	McDame Group (Unit 5) 350 metres	Limestone, dolostone, carbonate breccia
	Paraconformity	
Silurian - Lower Devonian	Tapioca sandstone (Unit 4) 450 metres	Dolostone, dolomitic quartz arenite, quartzite, dolomitic
	Disconformity, decollement	
Ordovician - Silurian	Road River Group (Unit 3) 200 metres	Calcareous graptolitic siltstone, argillaceous limestone
	Disconformity ?	
Cambrian - Ordovician	Kechika Group (Unit 2) 400 metres	Hornfels, marble, calcsilicate
	Conformable contact	
Lower Cambrian	Atan Group (Rosella Fmn) (Unit 1B) > 200 metres	Marble, phyllite
	Conformable contact	
Lower Cambrian	Atan Group (Boya Fmn) (Unit 1A)	Phyllite, schist, quartzite

3.2. Miogeoclinal Stratigraphy

3.2.1. Atan Group (Units 1A and 1B)

The Lower Cambrian Atan Group (units 1A and 1B) occurs in five sections in the map area (Figure 3-2): in a canyon on the Tootsee River (A), on two ridges southwest of the canyon (C and D), and north of Tricorn Mountain in the area of the Silverknife property (E). The four areas are discontinuous and isolated, and sequences are truncated by faults or intrusions. Stratigraphic control is therefore poor.

Atan Group consists of two formations (Fritz, 1980), the lower, predominantly siliciclastic Boya Formation, and the upper, carbonate dominated Rosella Formation. Both formations are present in the map area.

Boya Formation (unit 1A) occurs in sections A and D (Figure 3-2). In this area, structural complexities and a strong contact metamorphic overprint by the Cassiar batholith makes stratigraphic correlations difficult.

Boya Formation lithologies include quartzite and micaceous quartzite (sections A and D), black argillite (A and D), and black limestone (D). Elsewhere in 1040/16, coarser turbiditic

clastics, including quartz pebble conglomerates, are interbedded with black slates and siltstones (Nelson and Bradford, 1987a).

Boya Formation laminated pyritic black argillite is exposed at the north end of section A, and apparently underlies Rosella Formation carbonates and phyllites. The argillites have been uplifted and domed above an outlier of the Cassiar batholith (Figure 3-2).

Greenish to dark grey quartzite occurs with black argillite and black limestone in section D, overlying thin bedded pale Kechika Group calcsilicates and phyllitic hornfels. This is interpreted as a thrust sheet of Boya Formation. Contacts between lithologies within this thrust sheet are poorly exposed, and could represent thrusts as well.

Rosella Formation (unit 1B) occurs in sections A, C and E (Figure 3-2). The main lithology is a well foliated medium to coarse grained blue and white, locally platy marble with interfingering pinkish to orange weathering dolostone. In the Tootsee River canyon exposures (section A) and in diamond drill core from the Silverknife property (section E), the carbonate unit contains interbedded biotite - quartz phyllite and diopside - epidote - plagioclase - quartz calcsilicate hornfels. In section A, the phyllite - calcsilicate interbeds increase in

number and thickness upsection to the south. Similar transitions occur in the Silverknife core. In contrast, section C consists almost entirely of massive to thinly foliated marble, except at the northeast end of the ridge, where thin phyllite beds are exposed.

Atan Group rocks are characterized by a pronounced foliation in both carbonate and phyllite units. Tight to isoclinal folds are overprinted by a crenulation cleavage defining a lineation plunging 30 to 45 degrees south to southeast (section 3.7). In the map area, regional metamorphic effects are obscured by contact metamorphism due to the Cassiar batholith, resulting in marmorization and development of calcsilicate mineralogy.

3.2.2. Kechika Group (Unit 2)

Upper Cambrian to Ordovician Kechika Group sediments (unit 2; Table 3-1, Figure 3-3) outcrop on several ridges northwest and west of the Tootsee River adjacent to the Cassiar batholith (Plate 1) as well as in section B, which hosts the Amy silver - lead - zinc deposit (Figure 3-2). The base of the Kechika Group is nowhere exposed, while the top of the unit is apparently stratigraphically overlain by Ordovician - Silurian siltstones of the Road River Group. Maximum apparent thickness of about 400 metres occurs on a ridge about 3 kilometres north of the Amy

deposit; true thickness is unknown due to intense folding.

Kechika Group rocks on the ridges north of the Amy deposit consist of thin bedded green and brown calcsilicate and biotite hornfels with thin marble interbeds. Calcsilicate mineralogy consists of epidote, diopside and plagioclase. Quartzitic laminae are locally abundant, especially in biotitic sections. The progenitor to the contact metamorphosed Kechika Group seen in the map area has been described elsewhere as thin bedded calcareous shales and siltstones with minor thin limestone interbeds (Nelson and Bradford, 1987a).

Section B, below the upper adit at the Amy deposit (Figure 3-2), consists of phyllite, schist, quartzite and minor marble. The lower half of the section contains chlorite and biotite schist and phyllite, and about 15% interbedded quartzite. It is cut by several pegmatite and aplite dykes, and is probably underlain at a shallow depth by the Cassiar batholith. Metasediments contain up to 10% pyrite and pyrrhotite. Section B is atypical of Kechika Group in containing a significant proportion of quartzite. Kechika Group quartzite is not unknown; in the Gravel Creek map area (105B/10) a basal unit contains graphitic phyllite and quartzite beds up to 30 metres thick (D.C. Murphy, 1988). Section B probably contains the stratigraphically lowest Kechika Group in the map area.

Laminated grey and brown Kechika Group quartzites also occur at the south end of the Tootsee River canyon (section A) along with quartz - biotite - chlorite phyllites with rhomb - shaped biotitic porphyroblasts. This sequence is separated from the apparently underlying Rosella Formation to the north by a fault zone containing numerous quartz veins, quartz - iron carbonate alteration and sericitized biotite. The Kechika Group at the south end of section A projects to the northwest along strike to a position underlying section B. If sections A and B are interpreted as part of the same panel, then Kechika Group of section B overlies Kechika Group at the south end of section A, which is probably in fault contact with Rosella Formation of section A.

The part of section B overlying the marble - phyllite lens hosting the Amy deposit consists mainly of green and brown biotite - diopside calcsilicate. These strongly hornfelsed metasediments apparently underlie Rosella Formation (see section C, Figure 3-2). This means that Rosella Formation is thrust onto Kechika Group in section B.

Kechika Group rocks are everywhere tightly to isoclinally folded. These similar folds have thickened hinges and attenuated limbs. South to southeasterly trending crenulations deform a foliation defined by alignment of micas (section 3.7).

Transposition of bedding occurs locally in interbedded marble - phyllite units (Figure 3-4).

In the map area Kechika Group rocks occur within the contact metamorphic halo of the Cassiar batholith. Small, irregular metasomatic skarn zones are well developed in places, and are associated with quartz veins, pyrrhotite and scheelite. The mineralogy of these zones includes quartz, garnet, diopside, potassium feldspar, idocrase, calcite, muscovite, chlorite, actinolite and tremolite.

3.2.3. **Road River Group (Unit 3)**

The Ordovician to Silurian Road River Group (unit 3; Table 3-1, Figure 3-3) overlies Kechika Group strata northwest of the Tootsee River, and underlies Tapioca sandstone rocks southeast of the Tootsee River (Figure 3-2). Exposures weather recessively owing to the incompetence of Road River lithologies relative to overlying strata. Blue - grey to purplish, platy, calcareous to dolomitic siltstones, black argillaceous limestones, and pyritic black shales occur northwest of the river. Blue - grey to dark grey, laminated, usually platy calcareous to dolomitic siltstones occur southeast of the river. The upper part of the section is characterized by abundant graptolites (diplograptus), up to 10 centimetres long, of probable Silurian age.

Figure 3-4: Photograph of isoclinal folds and transposed bedding in Cambro - Ordovivian Kechika Group calcsilicate.

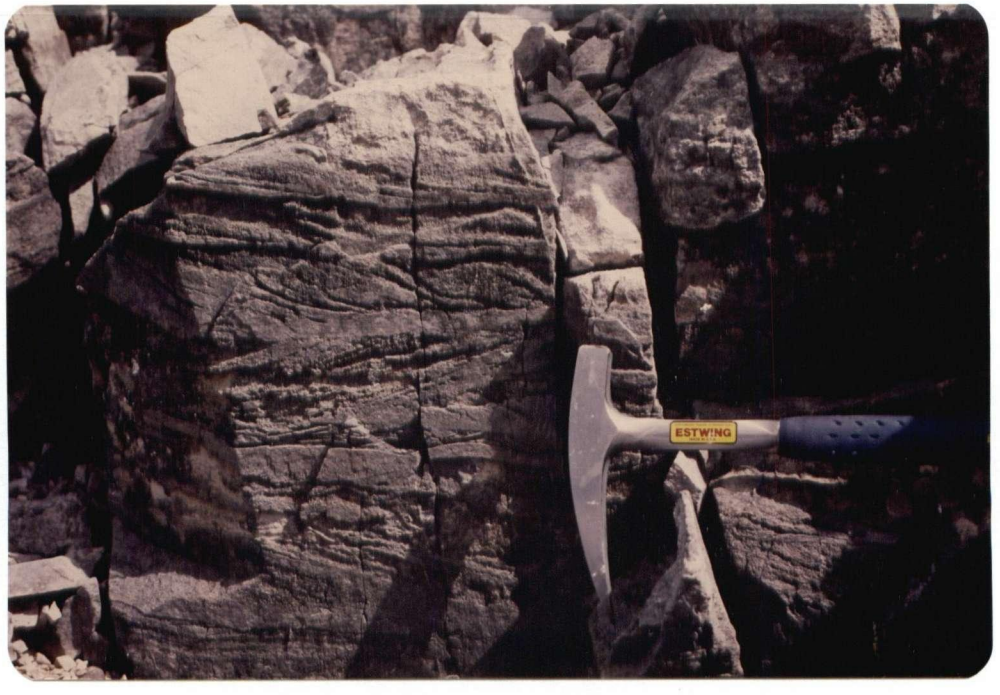

Figure 3-5: Photograph of cross bedding in Siluro - Devonian Tapioca sandstone dolomitic quartz arenite.

The maximum thickness of Road River strata exposed is about 200 metres, on the ridge north of the Amy deposit. Folding is apparently less intense than in underlying Kechika Group rocks, perhaps reflecting a damping effect due to thick, competent overlying strata. Road River strata therefore probably behaved as a decollement on which overlying strata moved during compressive deformation (Nelson and Bradford, 1987a). Further evidence for this includes panels of Tapioca sandstone and McDame Group thrust over Earn Group about 4 kilometres south of the map area on Table, Donegal and Weirami Mountains (Nelson and Bradford, 1987b).

Earlier accounts of the geology of the Jennings River area (1040) described an upper Kechika Group (in part) rather than Road River Group (Gabrielse, 1969). However, black shales, dark grey platy limestones, and dark grey to tan siltstones, which locally contain Silurian graptolites, are distinct from the generally lighter coloured silty shales and limestones of the Kechika Group (Gabrielse, 1981; Fritz, 1985). In Ware map area (west half of N.T.S. 94F), Road River strata are subdivided into an Ordovician black shale unit and a Silurian siltstone unit (Gabrielse, 1981). In the Gataga area (94E, F, K, L), the Silurian siltstone is overlain by black argillites, cherts and minor limestone, which is not seen in 1040/16 (McClay and Insley, 1986). In general, the Road River - Kechika Group

contact is diachronous. This could be due to a local basin and ridge topography, which caused nondeposition or erosion of Kechika Group strata in places (Gabrielse, 1981).

3.2.4. Tapioca Sandstone (Unit 4)

"Tapioca sandstone" (unit 4; Table 3-1, Figure 3-3) is an informal name proposed by Gabrielse (1969) for Upper Silurian (?) and Lower Devonian strata overlying Road River Group calcareous siltstones and underlying Middle Devonian McDame Group carbonates west of the Kechika Fault. In contrast to the Sandpile Group (Gabrielse, 1963), with which it is partly correlative, Tapioca sandstone is generally nonfossiliferous. Tapioca sandstone consists of buff, pale grey and white dolostone, dolomitic quartz arenite, and dolomitic siltstone and white, blue - grey, or black quartzite. Competent Tapioca sandstone strata form hills on ridges northwest of the Tootsee River, and thick sequences on Tricorn Mountain and the ridge east of Tootsee Lake. Thickness varies from 350 to 450 metres.

The lowermost Tapioca sandstone unit (unit 4A) is a bioturbated, pale grey, locally platy, buff weathering dolomitic siltstone up to 50 metres thick. Commonly overlying this is a white to buff, thin to thick bedded dolostone, which is succeeded by thin bedded to massive white, black, and blue -

grey dolomitic quartz arenite to quartzite with minor dolostone (unit 4B). The dolostone - quartzite sequences together range in thickness from 100 to 250 metres. White to buff interbedded dolostone and well laminated, commonly "ribby", cross-bedded dolomitic quartz arenite, 100 to 200 metres thick, overlies the quartzite (Figure 3-5). The typical "Tapioca sandstone" occurs in this section, with very well rounded and well sorted quartz grains floating in a dolomitic carbonate matrix. At the top of the sequence is a transitional unit of pale and dark grey, well bedded, locally well laminated dolostone in beds 0.5 to 2.5 metres thick, which grades upward into fetid dolostones of the lower McDame Group. During mapping of 1040/16, the Tapioca sandstone - McDame Group contact was placed at the top of the highest sandy bed in the gradational sequence (Nelson and Bradford, 1987a).

Tapioca sandstone strata are folded into broad open major folds, commonly with high angle faults of minor displacement cutting the hinge zone. Open to normal, northwest trending harmonic minor folds occur locally in sandy dolostone, where distinct competency contrasts between thin sandy and dolomitic beds exist. Competence of the unit is displayed by roughly north trending dyke swarms, which attest to brittle failure. East to northeast trending A-C joints are also well developed in quartzitic units (section 3.7).

Dolomitic facies are skarnified throughout the map area. Tremolite occurs as much as two kilometres away from the intrusive contact with the Cassiar batholith at surface. This indicates a shallow depth to contacts with the batholith.

3.2.5. McDame Group (Unit 5)

The Middle Devonian McDame Group (unit 5; Table 3-1, Figure 3-3) is exposed on ridges northwest of the Tootsee River and east of Tootsee Lake, and on Tricorn Mountain, Smoke Mountain, Silvertip Hill and Tour Ridge (Plate 1). A complete section is exposed on Tricorn Mountain where total thickness is about 350 metres. This unit is the host rock to the Midway silver - lead - zinc deposit.

McDame Group strata consist of fossiliferous, locally platy, blue - grey limestones, with lesser dark grey nonfossiliferous limestones and pale to dark grey, buff weathering fetid dolostones. Faunal assemblages exhibit little diversity even in intensely fossiliferous facies. Amphipora is the dominant genus (Figure 3-6), while other stromatoporoids, brachiopods (e.g. Stringocephalus), corals (Thamnopora), and rare gastropods and crinoids occur less widely. Shallowing upwards sequences are evidenced by cryptalgal laminites, stromatotacti, and locally, laterally linked, hemispherical stromatolites (Figure 3-7).

Figure 3-6: Photograph of Amphipora and other Stromotoporoids in Middle Devonian McDame Group limestone.

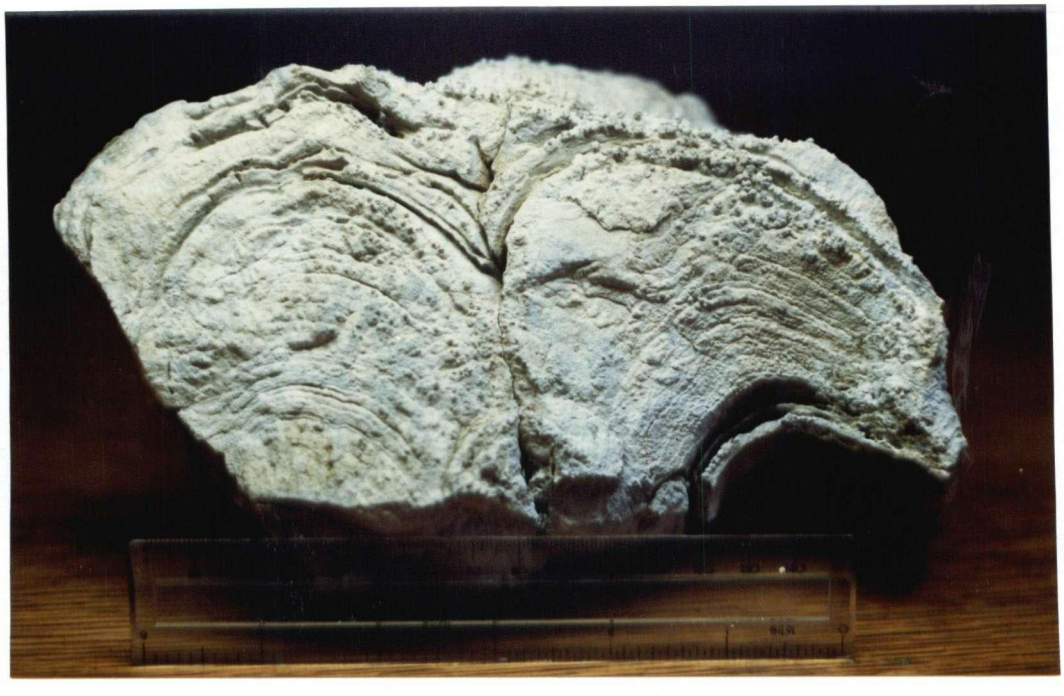

Figure 3-7: Photograph of stromatolites from Middle Devonian McDame Group limestone, Tricorn Mountain.

Biostratigraphic studies at Midway indicate that the Givetian guide fossil Stringocephalus is limited to the lower half of the McDame succession (Mundy, 1984).

The McDame Group comprises platformal carbonate facies deposited in a shallow sub-tidal lagoon or shelf flat. The McDame Group biota at Midway implies somewhat restricted conditions and deposition at some distance from the shelf edge (Mundy, 1984).

Calcite healed solution breccias are common throughout the McDame, and spar filled vugs are locally abundant. Solution features include stratabound and crosscutting crackle and mosaic breccias (Figure 3-8), mixed limestone (or dolostone) - shale breccias, shale - only breccias in a carbonate matrix, and lenticular or tubular paleocaves up to several metres across, which are filled with coarse blocky calcite, carbonate sand and, locally, iron - manganese oxides (Figure 3-9). Breccias involving shale fragments are found up to 100 metres below the top of the McDame Group, implying extensive and deep solution collapse. Both crenulated and noncrenulated shale fragments have been found, indicating karsting episodes both preceding and postdating Jurassic compressive deformation (cf. Chapter 4).

Subaerial exposure and karsting of the McDame is also

Figure 3-8: Photograph of crackle brecciated Middle Devonian McDame Group limestone.

Figure 3-9: Photograph of a karst cavity infilled with sparry calcite in Middle Devonian McDame Group limestone.

implied by a widespread erosional topography at the top of the carbonate sequence. In the Midway area, this erosional interval cuts through an estimated 165 metres of section (Mundy, 1984). At one location (Orchard and Irwin, 1988) dolomitic siltstones filling depressions along this unconformity have yielded Late Devonian conodonts of shallow water affinity. These are the youngest fossils found anywhere in the McDame, and could imply localized sedimentary infilling of karst sinkholes prior to large scale subsidence along the North American margin.

3.3. Earn Group (Unit 6)

Strata formerly called Lower Sylvester Group in the map area (Gabrielse, 1969) are now correlated with the Devono - Mississipian Earn Group (Gordey *et al.*, 1982; Gordey *et al.*, 1986). The name "Sylvester" is now reserved for para-allochthonous and allochthonous packages structurally overlying North American strata (Gabrielse and Mansy, 1980). Provenance of parts of the Sylvester allochthon, and the basis of the Earn Group - Sylvester distinction are controversial (Nelson *et al.*, 1988; Orchard and Irwin, 1988). Lowermost Earn Group strata in the Midway area have been dated as Early to Middle Famennian (Late Devonian) on the basis of conodont assemblages (Orchard and Irwin, 1988).

Earn Group (unit 6; Table 3-1, Figure 3-3) is exposed on Silvertip Mountain, Tour Ridge, Tricorn Mountain, Caribou Ridge, Smoke Mountain and locally northwest of the Tootsee River (Figure 3-2; Plate 1). Thicknesses of incomplete sections measured on Silvertip Mountain, Tour Peak and Caribou Ridge range from 550 to 750 metres. Therefore 650 metres is taken as the minimum thickness in the map area. Maximum thickness may be as much as one kilometre.

Earn Group strata consist of siliciclastic sediments ranging from shales to boulder conglomerates. In the Midway deposit area, two major coarsening upwards sequences have been designated E1 and E2 (Cordilleran Engineering, 1983). This is now considered the definitive Earn Group section in the Cassiar Mountains (Gordey et al., 1986). Units E1A, E1B, E2A and E2B of Cordilleran Engineering correspond to units 6A, 6B, 6C and 6D in Plate 1. South of Silvertip Mountain, on Caribou Ridge, Tricorn Mountain and Smoke Mountain, the thick coarse clastic intervals grade laterally into thinner coarse clastics with fine clastic interbeds.

Dark grey silt shale or argillite and thin bedded siltstone (unit 6A) usually overlies the McDame Group in the map area (Figure 3-3). This unit is variably graphitic, calcareous or siliceous. Thickness varies from 0 to 45 metres (Cordilleran

Engineering, 1983). Graphitic bedding parallel partings and slickensides are common, indicating local movement along the unconformity, probably during emplacement of the Sylvester allochthon (cf. section 3.6.2.).

The lowermost coarse clastic interval (unit 6B) overlies unit 6A in the Midway area (Figure 3-3). This unit is commonly 100 to 130 metres in thickness, but ranges up to 250 metres. It is characterized by medium to coarse grained, poorly sorted litharenite with lesser quartz - chert pebble conglomerate and siltstone. Reverse and normal graded bedding, ripups, scours, load structures and other indicators of turbiditic deposition are common. Rapid lateral thickness variations are consistent with deposition by channellized turbidite flows.

The second fine clastic sequence (unit 6C) abruptly overlies unit 6B in the Midway area (Figure 3-3). This contains exhalative beds of Lower to Middle Tournasian age (Orchard and Irwin, 1988) within 2 to 5 metres above the contact with unit 6B. Age of the Earn Group exhalative event in the Midway area is later than other parts of the Cordillera. In the MacMillan Pass (Abbott et al., 1987) and Gataga (McClay and Insley, 1986) regions, Frasnian or Fammenian (Late Devonian) exhalites are more common. Total thickness of unit 6C is commonly about 300 metres, but may range up to 640 metres (Cordilleran Engineering,

1984).

The lowermost beds in unit 6C consist of dark grey carbonaceous mudstone to siltstone. These are overlain by a section containing laterally continuous, well laminated siliceous or baritic, locally sulphide rich exhalites which range from 0.5 to 2.0 metres thick. These horizons extend discontinuously along a strike length of at least 10 kilometres in the Midway area, suggesting deposition into a basin from a string of exhalative centres.

Immediately overlying the lowermost exhalite zone in several places is a thin silty limestone to calcarenite unit, which is succeeded by mudstones, siltstones and fine grained sandstones. In mudstone, thin sandy beds with planar or graded contacts are common. The ratio of sand to silt increases upsection, and in the upper third of the sequence slumped and boudinaged sandy beds occur in less competent mudstone. Deformation and sub-greenschist (prehnite - pumpellyite) grade metamorphism has enhanced the bedding plane foliation, giving the finer clastics a slaty appearance.

Pebble to boulder conglomerate and lesser sandstone (unit 6D) abruptly overlies unit 6C on Silvertip Mountain and Tour Peak (Figures 3-2, 3-3). Exposed thickness of the unit ranges

from 150 to 200 metres. Pebbles are commonly stretched, with the long axis paralleling the regional southeasterly trending crenulation lineation. The conglomerate consists mainly of quartz, quartzite and chert pebbles in a silty - sandy matrix. Boulders consisting of miogeoclinal lithologies, including the McDame Group, occur on Tour Ridge (Figure 3-10).

Earn Group strata dip shallowly, and exhibit broad, open major folds and rare open to normal minor folds. A southeasterly trending crenulation lineation is locally well developed. This is locally deformed by later easterly trending chevron folds. Earn Group sandstones have undergone considerable pressure solution and exhibit flattened, recrystallized rhombic quartz grains with ragged fine grained pressure solution shadows. Fibrous quartz overgrowths on diagenetic pyrite are common. Ptygmatic folded quartz veinlets with fold axes parallel to bedding occur in units 6B and 6C; these are probably of diagenetic origin. East trending late folds are accompanied by en echelon quartz vein arrays, as well as by irregular quartz filled fractures subparallel to fold axes, which indicate transport of silica out of highly strained zones undergoing pressure solution.

3.4. Sylvester Allochthon (Unit 7)

The Sylvester allochthon (Unit 7) includes sediments, volcanics, and intrusive rocks of varied origin lying on Earn Group sediments above a bedding parallel, gently dipping decollement. Detailed studies in the Cry Lake map area (104I: Harms, 1984, 1985a, 1985b, 1986) have shown that ages of its component units range from Middle Devonian to Upper Triassic. In the map area, conodonts from various units range in age from Early - Middle Tournasian (Early Mississipian) to Late Namurian - Bashkirian (Early to early Middle Pennsylvanian) (Orchard and Irwin, 1988). Elsewhere in 104O/16, a zoned granodiorite - tonalite - gabbro complex is Permian by uranium - lead dating of zircons (J.L. Nelson, personal communication, 1988).

The basal decollement separating allochthonous and autochthonous units in the map area was not observed in outcrop, although its location can in places be constrained within 10 to 15 metres. Lithologically, the basal decollement represents a transition from coarse sandstones and pebble conglomerates to dark grey argillites with limestone and chert interbeds and locally basaltic to dacitic volcanics or sills.

Most of the Sylvester in the map area consists of thin pelagic sedimentary units traceable over several kilometres (unit 7A; Figure 3-3). This is equivalent to Division I of Nelson et al., (1988). The main lithological subdivisions

include:

(1) interbedded dark grey argillite and silty limestone to calcarenite, locally well laminated and cross-bedded, with irregular black chert interbeds (Figure 3-11),

(2) medium grey to dark grey argillite to phyllite and lesser intercalated grey chert and cherty phyllite,

(3) pale grey to green-grey ribbon chert with dark grey phyllite partings and intercalations (Figure 3-12). On the regional geology map (Plate 1) this has been mapped separately as unit 7B where it is thick enough. Recurring sequences of these units within the section might be structural repetitions, with each sequence underlain by a thrust. Thrusts, however, cannot be mapped definitively without more detailed paleontological control.

Medium grained quartz rich greywackes very similar to Earn Group sandstones occur near the top of the Sylvester sedimentary package in lenses up to several metres thick. These sediments contain zircon, detrital muscovite and tourmaline grains (J.L. Nelson, personal communication, 1986), indicating that part of the Sylvester package includes sediments of continental provinence. The presence of these Earn Group analogues within the Sylvester suggests that the allochthon has closer ties to North America than was previously realized (Nelson et al., 1988).

Figure 3-10: Photograph of a boulder of McDame Group limestone in Devono - Mississipian Earn Group conglomerate, Tour Ridge.

Figure 3-11: Photograph of limestone and black chert from unit 7A of the Sylvester allochthon (Mississipian?), north slope of Whitehorn Mountain.

The sedimentary package is structurally overlain by packages consisting mainly of resistant volcanic and intrusive lithologies on Whitehorn, Shambling and Sentinel Mountains (units 7C, 7D, 7E and 7F; Figure 3-3). These capping units overlie basal thrusts (Figure 3-13), and are internally imbricated. Basal and internal sheets or lenses of serpentinite (unit 7F) are common. These units are equivalent to Sylvester Division II of Nelson et al. (1988), and probably include Mississipian and Pennsylvanian - Permian packages.

Two main groups of lithologies comprise the capping units. Sentinel Mountain and a hill 2 kilometres southeast of Whitehorn Mountain consist of strongly altered basaltic flows and pyroclastics, with interfingering red and green chert (unit 7D). Pillow basalts are common, as are massive amygdaloidal flows. Pyroclastic breccias consist of lensoidal to wispy clasts, commonly in a strongly epidotized (Figure 3-14) or cherty matrix (Figure 3-15). Flow breccias and fine tuffs occur locally.

Most of Shambling Mountain and the cap on Whitehorn Mountain consist of subvolcanic mafic sills and dykes intruding cherty and fine grained, locally tuffaceous sediments (unit 7C). On the west side of Shambling Mountain, cherty sediments and diabase sills are imbricated with coarse grained, bastite bearing serpentinite. On Shambling Mountain (Plate 1) a serpentinite

Figure 3-12: Photograph of east trending kink folds in green grey chert of unit 7B of the Sylvester allochthon, north slope of Whitehorn Mountain.

Figure 3-13: Photograph of the west side of Shambling Mountain, showing a flat lying thrust fault separating Sylvester allochthon unit 7C (diabase, chert, basalt) and unit 7F (serpentinite) from underlying unit 7A (argillite, chert, limestone).

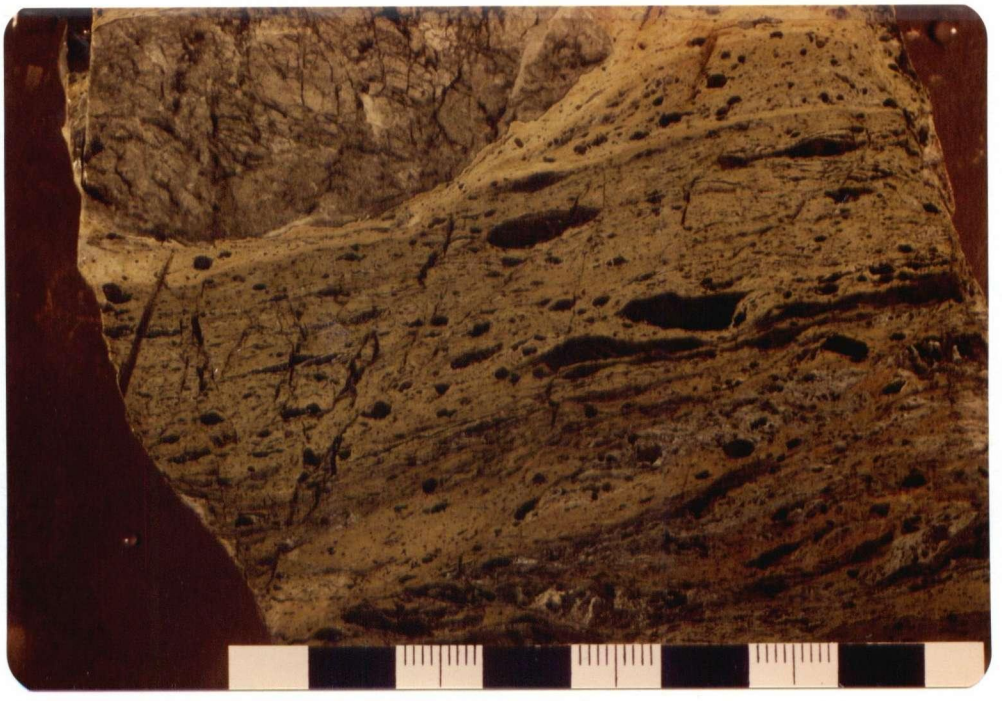

Figure 3-14: Photograph of Sylvester allochthon unit 7D lapilli tuff with strongly epidotized matrix, Sentinal Mountain.

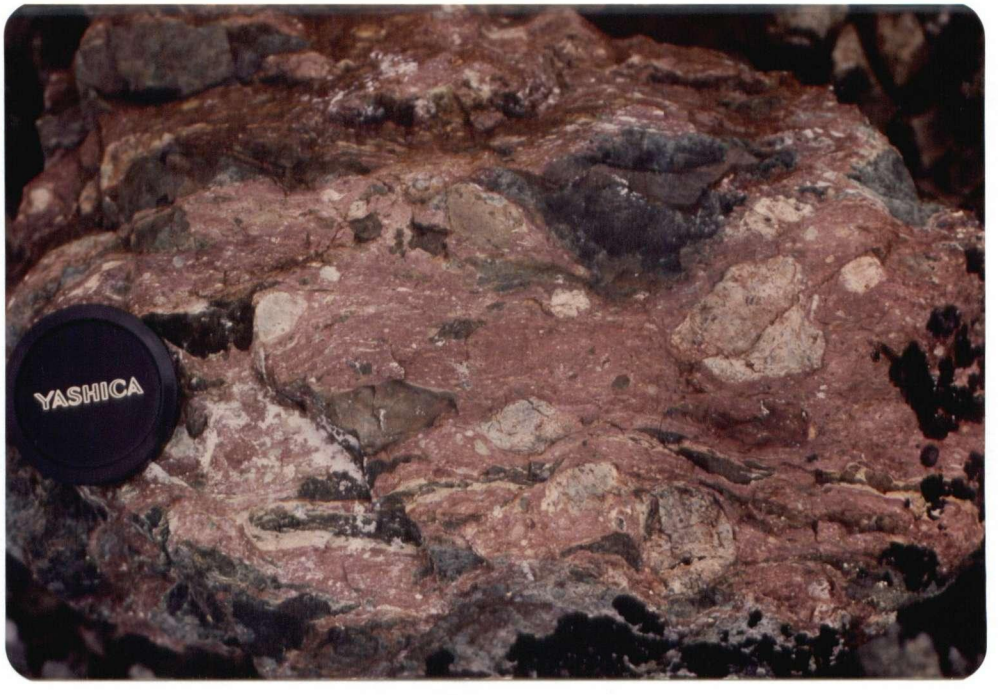

Figure 3-15: Photograph of Sylvester allochthon unit 7D pyroclastic breccia with mixed volcanic and chert clasts in red cherty matrix, Sentinal Mountain.

wedge separates two subvolcanic - sedimentary packages, with shearing in an intervening amygdaloidal metavolcanic unit increasing toward the wedge.

Very coarse grained pyroxene leucogabbro (unit 7E; Figure 3-16) occurs on the west side of Sentinal Mountain; contact relations with surrounding basalt flows are obscured by extensive talus. Similar gabbro bodies are found elsewhere in 1040/16 and throughout the Sylvester allochthon (Nelson and Bradford, 1987a; Nelson et al., 1988).

Altered dacitic(?) dykes or sills indigenous tc the Sylvester occur in several places in the map area, including the base of the sedimentary package north of Whitehorn Mountain, and on the east shoulder of Whitehorn, near the top of the package. These do not appear to cut strata underlying the Sylvester. Strong carbonate alteration obscures textures in these orange weathering bodies, although relict feldspar phenocrysts can be seen on weathered surfaces.

The lower Sylvester sediment package exhibits a style of deformation similar to that seen in the underlying Earn Group. Argillaceous sediments exhibit a weak to moderate bedding parallel foliation, and generally lack penetrative axial planar cleavage. A prominent crenulation cleavage commonly overprints

Figure 3-16: Photograph of Sylvester allochthon unit 7E pyroxene leucogabbro, Sentinal Mountain.

the bedding parallel foliation (section 3.7). Both southeast trending and later east trending minor folds occur in places. Locally, thin bedded cherts are tightly folded. Overlying volcanic packages are in places strongly sheared, and the presence of thin serpentinite wedges suggests that tectonic interleaving of lithologies is common.

3.5. Intrusive Rocks

3.5.1. Mafic Dykes

Mafic dyke swarms intrude miogeoclinal lithologies on Tricorn Mountain and on ridges northwest of the Tootsee River (Figure 3-2). The dykes are aphanitic to fine grained, equigranular to sub-porphyritic, and are generally intensely chloritized and carbonatized. They are usually recessive weathering, and occur as grassy linear features that can be traced by following weathered chips of dyke material.

On ridges northwest of the Tootsee River (Plate 1) the dykes trend northeasterly, subparallel to country rock foliation and to the Cassiar batholith intrusive contact. In some of these dykes an internal foliation parallel to the dyke margins is present. On Tricorn Mountain the dykes trend in a northerly direction.

Possibly correlative dykes occur in core from the Midway property, where intensely chlorite - sericite - pyrite altered, foliated pale green rocks cut McDame Group and Earn Group strata. Foliation is approximately flat lying, parallel to bedding in the country rocks. This in turn suggests that dyke emplacement preceded Jura-Cretaceous compressional deformation (section 3.7.2.). If this is so, then mafic dykes of probable Tertiary age hosted by the Cassiar batholith (Abbott, 1984; Lowey and Lowey, 1986) are unrelated.

Age of the mafic dyke suite is unknown. Evidence of pre - Jurassic foliation suggests that the age is constrained between the age of their youngest host rock (Early Mississipian) and Jurassic time. One possibility is that they are Early Mississipian dykes associated with crustal extension, anomalous heat flow and deposition of exhalites.

3.5.2. Cassiar Batholith (Unit 8)

The Cassiar batholith (Unit 8), of mid-Cretaceous age, lies along the western side of the map area (Figure 3-2). A large embayment of the batholith margin extends to the west of the map area into map sheet 1040/15. An outlier of the batholith lies at the mouth of the embayment, at a sharp bend of the Tootsee River. The batholith probably underlies the area of the

embayment at shallow depths. Lithologies include equigranular to sub-porphyritic biotite quartz monzonite, locally megacrystic potassium feldspar porphyritic quartz monzonite, and minor aplitic and pegmatitic intrusive phases. Locally, highly evolved phases such as a tourmaline bearing, equigranular muscovite granite near the Amy deposit occur as marginal phases or apophyses.

Margins of the batholith in the northwestern part of the map area crosscut foliation in the adjacent Kechika Group at a low angle, suggesting that foliation controlled emplacement to some extent. Country rock dips increase toward the intrusive contact.

3.5.3. Late Cretaceous Intrusions (inferred)

Late Cretaceous intrusions are inferred to occur in the map area on the basis of potassium - argon dating of alteration haloes (section 3.6). In addition, quartz - feldspar - biotite $\pm$ hornblende porphyry dykes occur sporadically in this area, where they are intensely altered. Possibly correlative porphyry dykes occur on a ridge north of the east end of Tootsee Lake. Coincident magnetic and gravity anomalies, roughly circular in plan view, occur about two kilometres southeast of Midway; they probably indicate a buried felsic stock at depth (J. Hylands, personal communication, 1986).

3.5.4. Eocene Intrusions

Quartz - feldspar porphyry stocks and dykes of Eocene age (Sinclair, 1987) outcrop near the YP (Butler Mountain) silver - lead - zinc - gold property, about 5.5 kilometres north of the British Columbia - Yukon Territory border (Figure 3-2). Coeval intrusions occur in the Cassiar area (Mount Haskin and Mount Reed; Christopher et al., 1972). Tungsten - molybdenum and silver - lead - zinc showings are associated with these intrusions. Correlative stocks have not been found in the map area.

Mafic dykes occurring within the Cassiar batholith have not been dated, but are post mid-Cretaceous, and could be Eocene. It is not clear whether dyke swarms on Tricorn Mountain and elsewhere belong to the same set, or whether some of them belong to an earlier intrusive episode.

3.6. Potassium - Argon Dating

Published and unpublished potassium - argon dates from the map area are compiled in Table 3-2. These record two separate intrusive and alteration events, of mid-Cretaceous (97-106 Ma) and Late Cretaceous (65-75 Ma) ages.

Table 3-2: Potassium - argon dating, Midway area, north-central British Columbia.

Sample Number	Location Latitude Longitude	Material	Date (Ma)
JN30-11 [1]	Gum Mountain 59o 53.5'N 130o 17'W	Sericite altered QFP dyke	67.1 ± 2.3
JB23-02 [1]	Brinco Hill 59o 54.5'N 130o 19'W	Sericite altered clastic sediments	65.4 ± 2.3
KG28-07 [1]	Lucky showing 59o 59.5'N 130o 28'W	Muscovite envelope around Qt-Gn vein	105 ± 4
JB26-12 [1]	Amy showing 59o 55.5'N 130o 29'W	Equigranular tourm. bearing muscovite granite	97.3 ± 3.4
SYA85-91 [2]	Midway; DDH B82-1 (284.2m) 59o 54.5'N 130o 20'W	Sericite altered clastic sediments	74.7 ± 2
DY 3077 [3]	Stock at bend in Tootsee R. 59o 55.8'N 130o 26'W	Biotite quartz monzonite	106 ± 4
DY 3090 [3]	Silverknife showing, DDH 85-5 (45.4 m) 59o 56.3'N 130o 21'W	Biotite hornfels	98.9 ± 3.5

1. Bradford and Godwin (1988).
2. W.D. Sinclair, written communication, 1986. Analysis by Geological Survey of Canada, Geochronology Section, Ottawa.
3. K. Dawson, written communication, 1987. Analysis by The University of British Columbia Geochronology Laboratory.

The mid-Cretaceous episode is associated with the Cassiar batholith. The unaltered biotite quartz monzonite outlier of the main batholith at a prominent bend in the Tootsee River (Figure 3-2) has an age of 106 Ma (Table 3-2: sample DY 3077). Muscovite vein envelopes at the Lucky Ag-Pb-Zn vein showing were dated at 105 Ma (sample KG28-07). Kechika Group biotite hornfels from a diamond drill intersection at the Silverknife property was dated at 98.9 Ma (sample DY 3090), and therefore appears to indicate the presence of an unexposed outlier of the Cassiar batholith south of that showing. This is consistent with observation of tremolite in carbonates up to two kilometres from Cassiar batholith exposures, indicating that the batholith underlies much of the western half of the map area. It is unclear whether this hornfelsing is genetically related to mineralization at the Silverknife showing. A tourmaline bearing equigranular muscovite granite at the Amy property was dated at 97.3 Ma (sample JB26-12). This body might therefore be a late volatile enriched phase of the Cassiar batholith, and its proximity to mineralization suggests that it is genetically related to the deposit.

Late Cretaceous ages were obtained from altered sediments (Table 3-2: samples JB23-02 and SYA85-91) and a dyke (sample JN30-11) southeast of the Midway deposit. These samples were

obtained from a large alteration zone extending almost five kilometres southeasterly from Silvertip Hill (Plate 1). This alteration is believed to have been caused by the hydrothermal system which deposited massive sulphides in McDame Group limestones at Midway. The hydrothermal cell was probably driven by an unexposed stock underlying Brinco Hill, about two kilometres southeast of Midway (Chapter 4). Coeval stocks occur in the Cassiar area (map sheet 104P/4,5: Panteleyev, 1985), and near the southeastern corner of 105B/1 (Hot claims tungsten prospect; W.D. Sinclair, written communication, 1986).

3.7. Structural Geology

3.7.1. Structural Divisions

The map area is subdivided into three structural blocks: (1) main block, east of the Tootsee River, (2) northwest block, northwest of the Tootsee River, and (3) southwest block, west of the Tootsee River in the southwest corner of the map area (Figure 3-2). Each block is separated by abrupt discontinuities interpreted as high angle extensional faults. These faults form part of a broad zone of anastomosing faults called the Tootsee River fault zone (Nelson and Bradford, 1987a). The three blocks are rotated with respect to one another by faulting and intrusion of the Cassiar batholith.

Deformation in the main block is characterized by broad northwesterly trending major folds with an amplitude of 1-2 kilometres, rare open northwesterly trending minor folds (Figure 3-17C), and a prominent northwest trending crenulation lineation (Figure 3-17B). Major folds are subtle warps in relatively flat lying strata. Crenulations are best developed in fine clastic sediments. Two northwest trending crenulation lineations diverging at a low angle are common, possibly due to progressive or episodic rotation of the regional stress field. A stretching lineation parallel to the crenulation lineation occurs in Earn Group pebble conglomerates, which exhibit highly strained elongate cylindrical pebble shapes. Pencil cleavage locally defines a northwest trending lineation in fine clastics (Figure 3-19). A penetrative axial plane cleavage is rarely observed. An irregular spaced cleavage dipping moderately to the northeast or southwest occurs locally (Figure 3-17D). A-C joints perpendicular to the northwesterly linear trends are common in competant units (Figure 3-17E). The northwesterly trending structures are locally deformed by later east trending minor kink and chevron folds (Figures 3-17C, 3-21).

The northwest block (Figure 3-2) is an east to south dipping panel which steepens toward the Cassiar batholith. Strike of bedding progressively rotates from a northerly

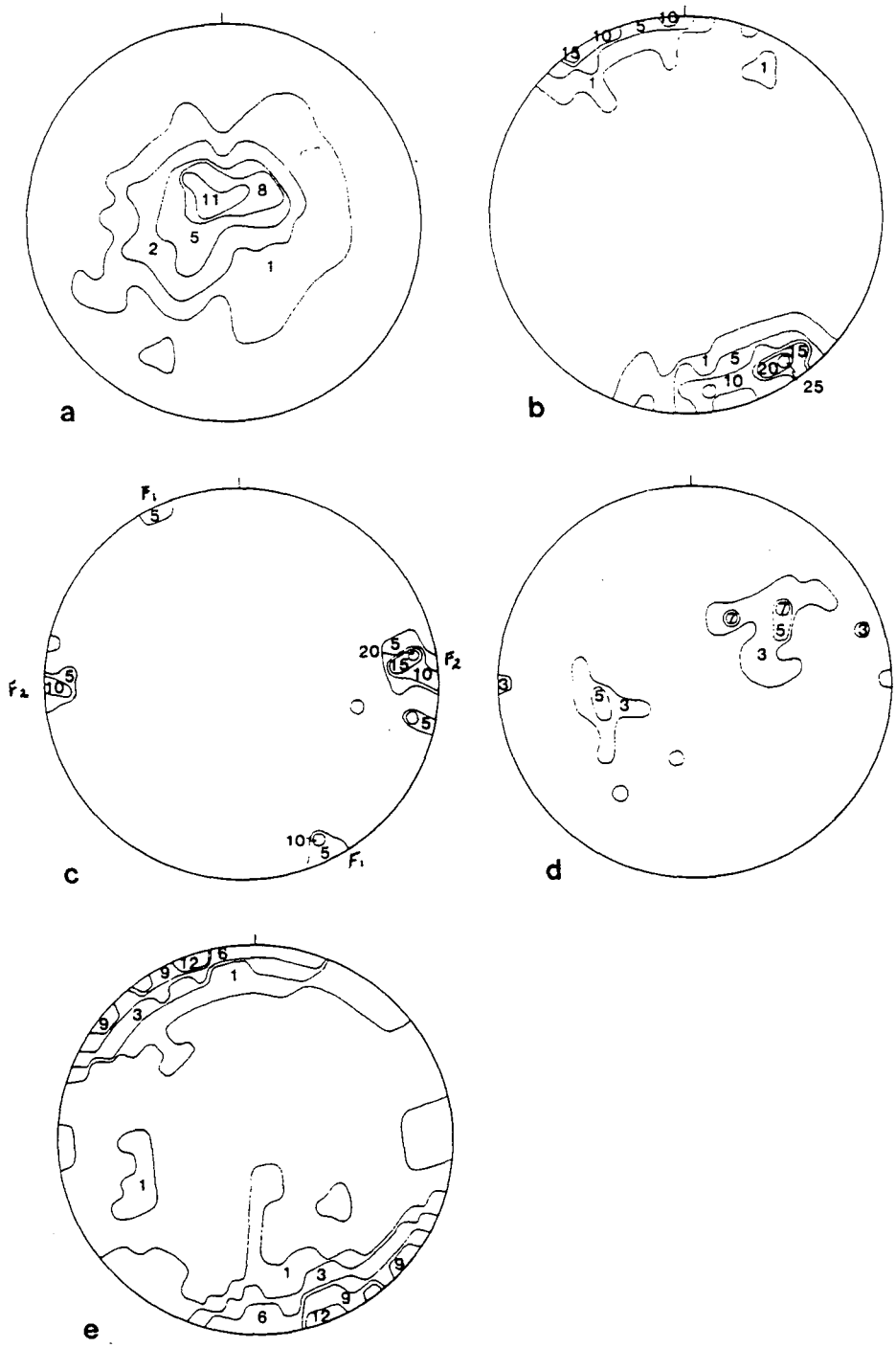

Figure 3-17: Equal area stereonet plots of structural data, main structural block. (A): poles to bedding (435 data points); (B): lineations (167 points); (C): minor fold axes, F1 and F2 (30 points); (D) poles to cleavage (54 points); (E) poles to joints and veins (137 points). Contours are in % per 1% area.

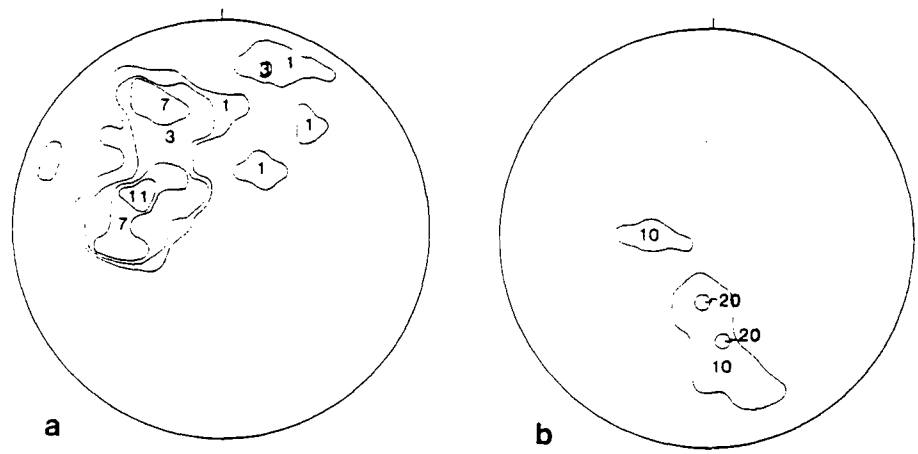

Figure 3-18: Equal area stereonet plots of structural data, northwest structural block. (A) poles to foliation (59 points), (B) lineations and minor fold axes (11 points). Contours are in % per 1% area.

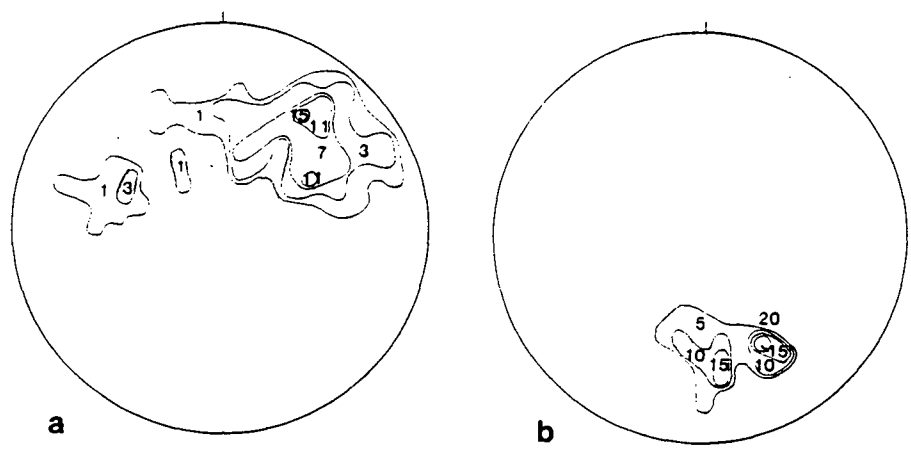

Figure 3-19: Equal area stereonet plots of structural data, southwest structural block. (A) poles to foliation (55 points), (B) lineations and minor fold axes (23 points). Contours are in % per 1% area.

orientation on the northernmost ridge, to an easterly orientation on the ridge at the western edge of the map area, north of the Amy deposit (Figure 3-18A; Plate 1). This change in orientation is paralleled by the curvature of the intrusive contact of the Cassiar batholith. Steepening of dips and the change in bedding orientations were caused by intrusion of the batholith, which rotated the lineations into steeper, southerly plunges (Figure 3-18B).

The southwest block (Figure 3-2) is a southwesterly dipping panel which is uplifted relative to the rest of the map area, probably due to intrusion of the Cassiar batholith. As a result, only units below the Road River decollement are exposed. Dips in this block are generally steeper than in the rest of the map area (Figure 3-19A). Units below the Road River decollement have undergone intense ductile deformation and are isoclinally folded. Crenulation lineations deforming the southwesterly dipping foliation have been rotated into steeper, more southerly plunging orientations by intrusion and faulting (Figure 3-19B).

3.7.2. Jurassic Deformation

Structural data in the map area support two major episodes of deformation. The prominent northwesterly trending structural fabric over most of the map area was generated by northeasterly

Figure 3-20: Photograph of pencil cleavage in Earn Group slate.

Figure 3-21: Photograph of east trending late chevron folds in Earn Group slate, south side of Silvertip Hill.

compression which occurred primarily during the Jurassic. This was followed by high angle faulting during the mid-Cretaceous to Tertiary (section 3.7.3).

Evidence for the Jurassic compressional episode includes both folding and thrust faulting. Major folds are generally northwest trending, consistent with northeasterly tectonic transport. Major folds are subtle features, as almost all shortening was taken up along decollements at the base of the Sylvester allochthon and within the Road River Group. Major fold axes trend across the base of the Sylvester allochthon, indicating that this folding was a late feature, post - dating emplacement of the allochthon. Intense strain occurred in units beneath the decollements, as shown by stretched pebbles and a well developed bedding parallel foliation in the Earn Group, and by isoclinal folds in the Kechika and Atan Groups.

A major series of thrusts in the miogeoclinal package occurs 3-4 kilometres south of the map area on Weirami, Donegal and Table Mountains (Nelson and Bradford, 1987b). These northeasterly verging thrusts cut upsection from Road River to McDame Groups, bringing Road River to McDame Group over Earn Group. Other thrusts in the Southwest block of the map area put Boya Formation on Kechika Group, and Rosella Formation on Kechika Group (Plate 1). These also verge northeasterly. A

thrust west of the Tootsee River in the Northwest block puts McDame Group on Earn Group in the vicinity of the Berg showing (Figure 3-2). This juxtaposition of units is not well constrained by exposures, and its interpretation as a thrust is tentative. Cryptic thrusts occur in the Midway area, bringing Earn Group unit 6B over unit 6C, and intercalating McDame Group and Earn Group strata (based on diamond drill hole data). Vergence of these thrusts is unknown. Other thrusts probably occur within the Earn Group and Sylvester allochthon, but are unrecognized due to lack of prominent markers and faunal control.

The basal decollement underlying the Sylvester, according to Harms (1985b, 1986), is the roof thrust to a duplex structure within the miogeocline whose sole fault is the Road River decollement. Emplacement of the allochthon was achieved partly by transport along the basal decollement, involving a series of imbrications of miogeoclinal strata beneath this horizon. Shortening in sub - Sylvester strata above the Road River decollement does not need to balance the amount of transport along the basal Sylvester thrust. Additional shortening occurred in sub - Road River strata, as evidenced by isoclinal folding and thrust imbrication of Atan and Kechika Groups in the southwest block.

Timing of compressional deformation is loosely constrained between the age of the youngest units in the Sylvester allochthon (Triassic) and the 100 Ma age of the Cassiar batholith, which cuts the Sylvester allochthon in the McDame map area (104P; cf. Nelson et al., 1988). Telescoping of the continental margins occurred as outboard arc terranes (Stikinia and Quesnellia) converged and accreted during that time. Intervening oceanic and marginal basin material was internally imbricated and in part obducted onto the North American margin as a result. Internal imbrication of the Sylvester occurred in part prior to its emplacement onto the continental shelf, as documented for the Cry Lake map area by Harms (1985a). Undoubtedly, compression was complex and episodic, as is indicated for example by diverging sets of crenulations (section 3.7.1) that suggest a rotation of the regional stress field.

3.7.3. Cretaceous - Tertiary Deformation

Deformation post - dating emplacement of the Sylvester allochthon is manifested primarily in high angle normal faults that cut both autochthonous and allochthonous strata. The main fault trend is north - south, compatible with subhorizontal easterly trending extension. Easterly trending minor chevron folds and kink bands with associated east trending en echelon quartz veins overprint northwesterly linear structures and are

consistent with a north trending principle compressive stress.

The Tootsee River fault zone, a complex, northerly trending fault system, divides the map area. Both north to northeasterly trending (Figure 3-22) and east trending (Figure 3-23) faults occur within this zone. Just south of the Yukon Territory - British Columbia border (Figure 3-2) this fault juxtaposes McDame Group carbonates and Sylvester cherts and argillites, indicating a minimum stratigraphic throw of 600 metres, east side down. Just north of the Midway deposit (Figure 3-2), Rosella Formation and Sylvester allochthon are juxtaposed across a narrow zone, indicating a minimum throw on the order of 1.5 kilometres. Three kilometres north of the Yukon Territory border (Figure 3-2), a downdropped block of Sylvester volcanics is juxtaposed against Rosella Formation, east side down again (Lowey and Lowey, 1986). A northeasterly trending fault east of Sentinel Mountain juxtaposes the upper Sylvester volcanic - chert package and Sylvester sediments, indicating a possible 300 metre displacement, northwest side down.

The Tootsee River fault zone is dominated by normal displacement with downdropped blocks on the east side. As a result, higher stratigraphic levels, including the Sylvester allochthon, are exposed in the east half of the map area (Figure 3-2). This structural exposure of the Sylvester was thought by

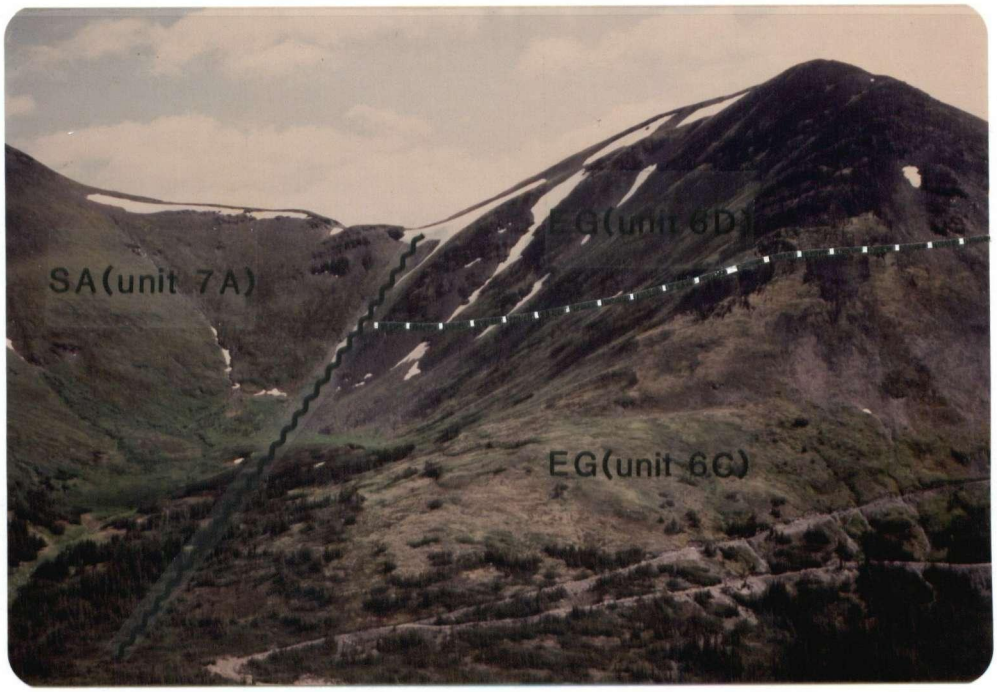

Figure 3-22: Photograph of a north trending high angle normal fault between Whitehorn Mountain and Tour Ridge, downdropped on the east side. SA: Sylvester allochthon; EG: Earn Group.

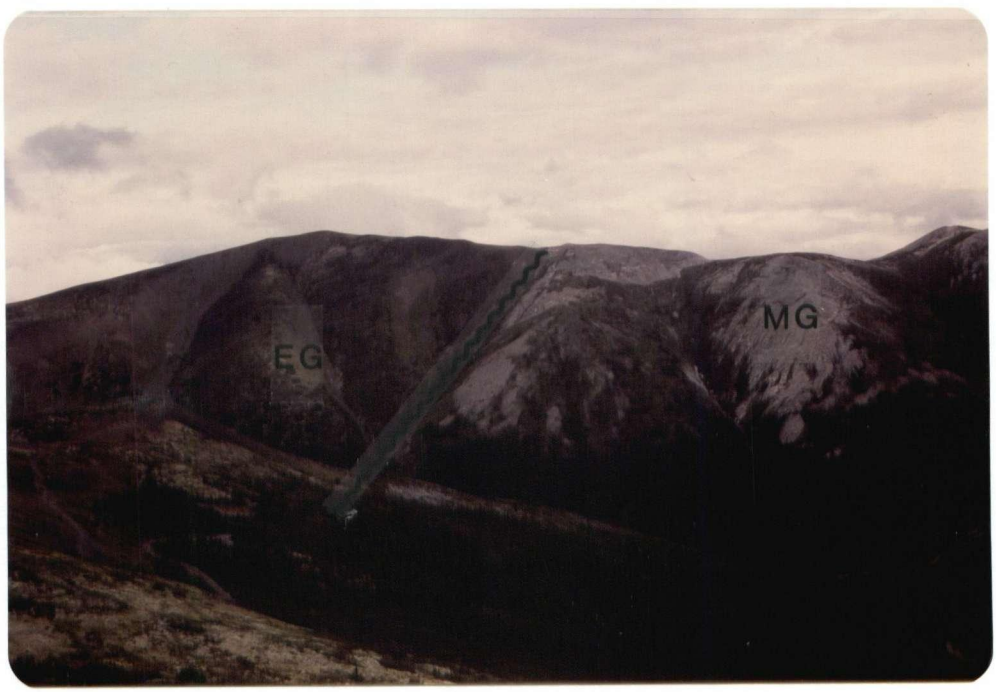

Figure 3-23: Photograph of an east trending high angle normal fault on Tricorn Mountain, downdropped on the south side. MG: McDame Group; EG: Earn Group.

Gabrielse (1963) to represent a northwesterly trending synclinorium (McDame Synclinorium). The southwest "limb" of the McDame Synclinorium in the map area therefore might more accurately be represented as a series of downdropped fault blocks.

The Tootsee River fault zone apparently splits into a number of anastomosing faults north of the Midway deposit (Plate 1, cross sections A-A' and B-B'). South of the deposit the zone dies out in a broad zone of faults with displacements generally 50 metres or less. To the north, in Wolf Lake map area (105B/1) the Tootsee River fault zone joins a northwest trending fault strand that could be an extension of the Kechika Fault system (Lowey and Lowey, 1986). This appears to die out near the northwestern corner of the Wolf Lake sheet, at which point dextral displacement is apparently transferred to the west to the Cassiar Fault, which follows the western edge of the Cassiar batholith (Figure 3-1).

Minor structures indicative of extensional deformation are common, especially in Earn Group and Sylvester sediments. Easterly trending kink and chevron folds crosscut and deform pre-existing crenulations (Figure 3-21). The kinks occur commonly with en echelon quartz vein arrays. Undeformed easterly trending quartz veins also crosscut pre-existing

northwest trending crenulations at a high angle. These could be related to older A-C joints developed during Jurassic compression.

The north trending normal faults of the Tootsee River fault zone are consistent with the northerly trending compressive stress which produced widespread dextral movement on northwesterly trending transcurrent faults during the Late Cretaceous and Tertiary (Gabrielse, 1985). According to Abbott (1984) the regional stress field required to generate northwest trending dextral transcurrent faults such as the Kechika Fault and Northern Rocky Mountain Trench zone is consistent with development of north - northwesterly trending synthetic shears, east to northeast trending antithetic shears, and north trending extensional faults (Figure 3-24). In this model, the Tootsee River fault zone and related faults are secondary faults caused by a large scale shear couple associated with Cretacous - Tertiary transcurrent faulting, which in turn is related to oblique compression between North America and accreted terranes.

The localized district scale extension evident in the high angle normal faults of the map area could have overprinted and in part remobilized earlier extensional structures. Devono - Mississipian extension is well documented throughout the Cordillera. Evidence includes a peak of alkaline volcanic and

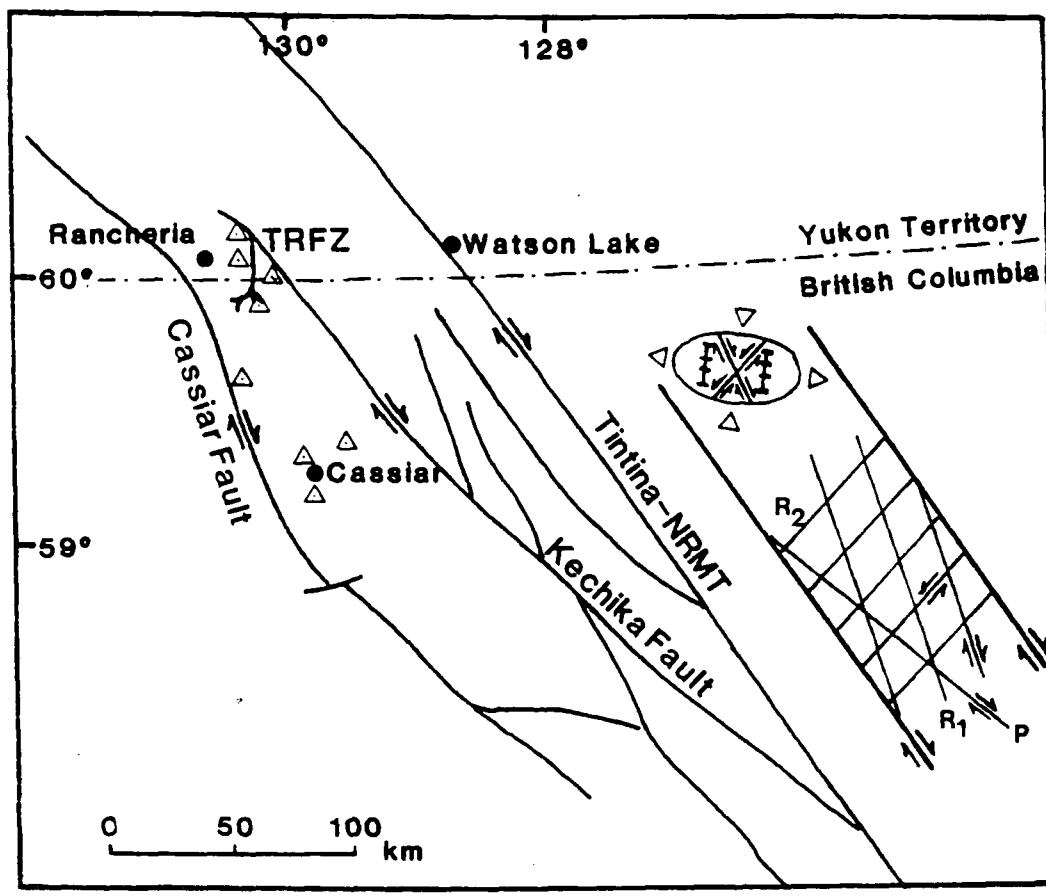

Figure 3-24: Map of northeastern British Columbia and southeastern Yukon Territory showing the distribution of major transcurrent faults and possible relationships to local fault systems (after Abbott, 1984). R1 and P: northwest trending synthetic shears; R2: easterly to northeasterly trending antithetic shears; EF: north trending extensional faults; TRFZ: Tootsee River fault zone; NRMT: Northern Rocky Mountain Trench. Triangles are Late Cretaceous to Eocene intrusions.

intrusive activity in the Early Mississipian (Pell, 1987), and the transition from a carbonate shelf in the Middle Devonian to basinal or off - shelf clastics in the Late Devonian. This transition is evident in the map area, and is indicative of widespread, rapid subsidence along the continental margin (Gordey et al., 1986). It was succeeded in the Early Mississipian by significant, district scale deposition of exhalites, which testify to continued extension and high geothermal gradients.

Models for exhalite deposition emphasize the important role played by second and third order faults (e.g. Carne and Cathro, 1982), and associated rapid vertical and lateral facies transitions. Such transitions are evident in the Midway area in the abrupt changes from fine to coarse clastic intervals, and their dramatic lateral thickness variations (cf. Chapter 4, Figure 4-3). The widespread nature of exhalite deposition and the significant time period between Late Devonian (Early Fammenian) subsidence (section 3.3) and Tournasian exhalite deposition (section 3.3) signify an intense and persistent extensional event in the Midway area. This event probably left a legacy of zones of structural weakness that were exploited by extensional faults generated during Cretaceous - Tertiary wrench faulting.

4. Deposit Geology, Alteration, Mineralization, Fluid Inclusions and Stable Isotopes

4.1. Introduction

The Midway deposit consists of irregular, pipe like, open space filling and replacement massive sulphide bodies in Middle Devonian McDame Group carbonates beneath a major unconformity. Reserves currently stand at 1.185 million tonnes grading 410 grams/tonne silver, 9.6% zinc, and 7.0% lead (Lefebure, 1987).

The deposit lies near the southern termination of the Tootsee River fault zone, a broad, northerly trending extensional fault system (Nelson and Bradford, 1987a). This zone intersects a 5 kilometre long, northwesterly trending belt of hydrothermal alteration just south of the deposit. Intense sericitic alteration and quartz veining in Devono - Mississipian Earn Group sediments, and coincident geophysical anomalies indicate that a buried intrusive body underlies Brinco Hill, about 2 kilometres southeast of the Midway deposit. Deposit chemistry, sulphide mineralogy, isotopic signatures, and fluid inclusion data show that Midway is an epigenetic manto deposit. Potassium - argon dates and lead isotope model ages support a Late Cretaceous age of mineralization.

The following discussion of the stratigraphy and structural geology of the Midway deposit draws on material presented in Chapter 3, and some redundancy is unavoidable. The deposit geology focuses on the area of Figure 4-1, and on the immediate area of the Midway deposit (Figure 4-2). Since only strata above the Road River decollement occur in Figure 4-2, these strata are renumbered. Units 1, 2, 3 and 4 (Figure 4-2) correspond to units 4, 5, 6 and 7 in section 3 (Table 3-1, Figure 3-2, Plate 1), and subunits 6A, 6B, 6C and 6D become 3A, 3B, 3C and 3D. Only units 2 (McDame Group) and 3 (Earn Group) are described in detail in section 4.2.1 below.

Descriptions of lithologies and mineralization are based primarily on examination of diamond drill core at the Midway property. In the following discussion, diamond drill intersections -- e.g. MW 204 (5.2) -- give the deposit prefix, drill hole number, and metreage (in brackets). Drill hole numbers up to 101 were collared at surface; numbers from 102 to 270 were collared underground. A map of the first 101 surface diamond drill holes is shown in Figure 4-4.

4.2. Deposit Geology

4.2.1. Stratigraphy

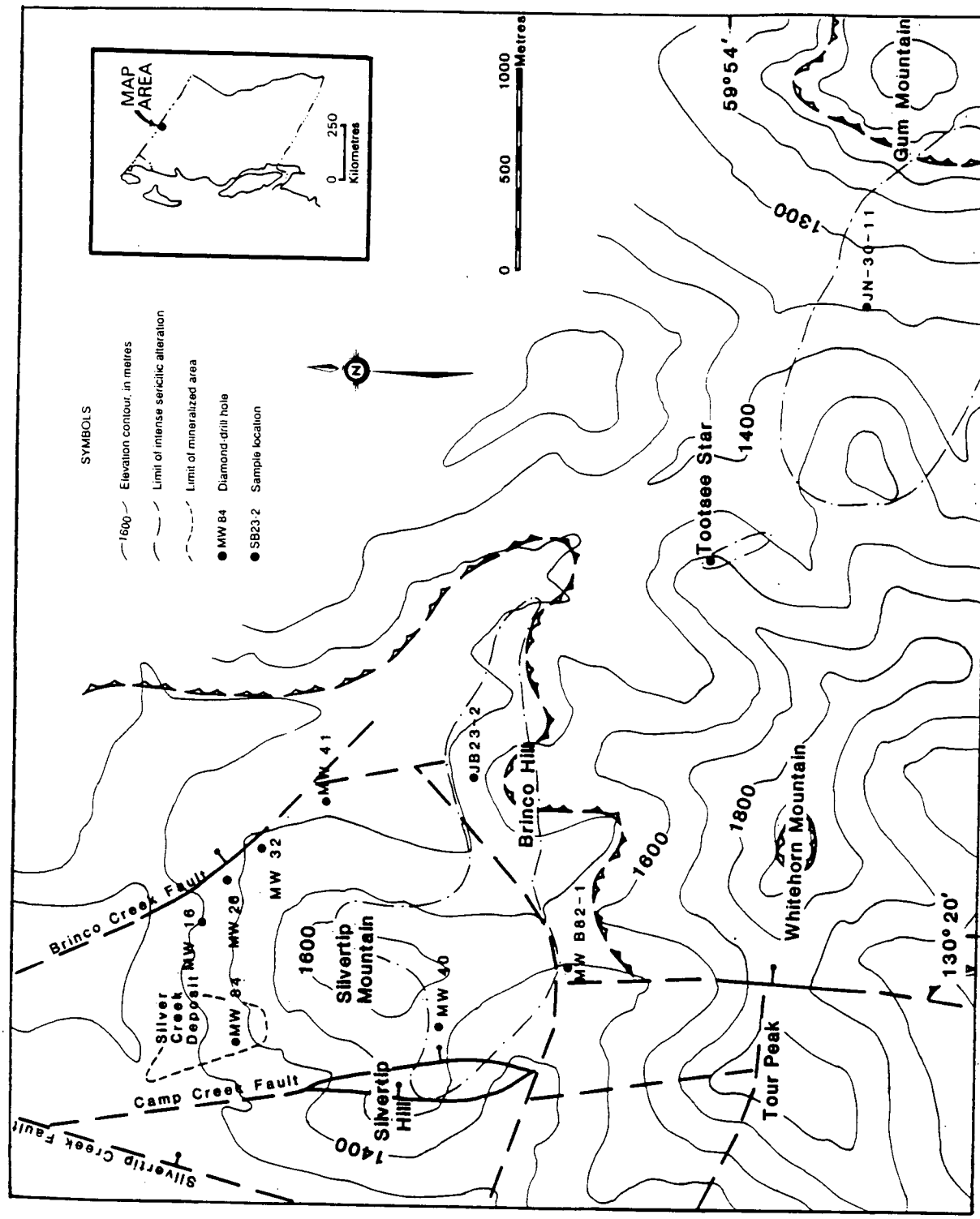

Figure 4-1: Map of the Midway area showing distribution of major faults, alteration zones, the Silver Creek deposit, and diamond drill holes and locations referred to in the text.

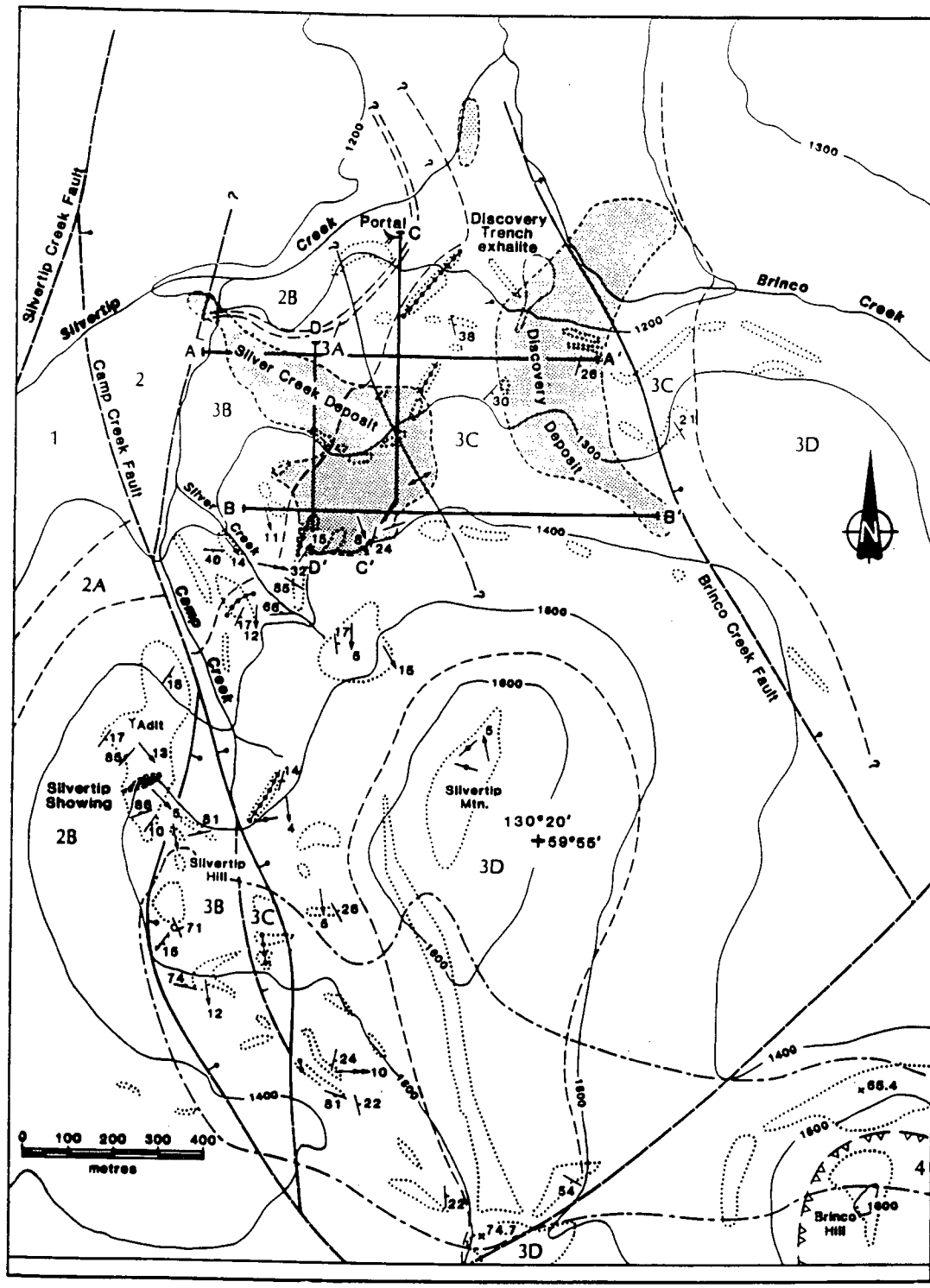

Figure 4-2: (A) Geology of Silvertip Mountain, including the Midway area.

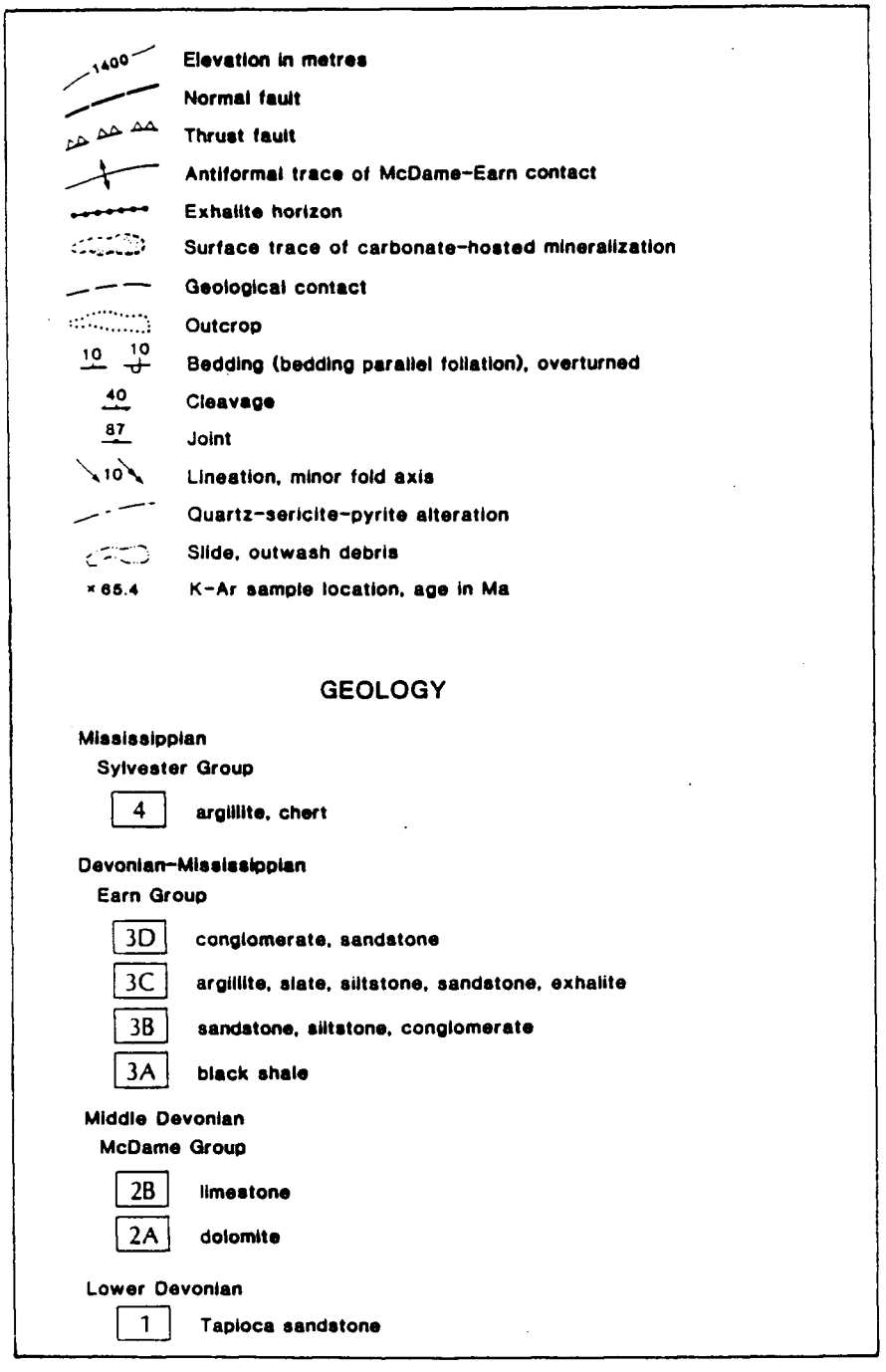

Figure 4-2: (B) Legend and symbols, geology of Silvertip Mountain, including the Midway area.

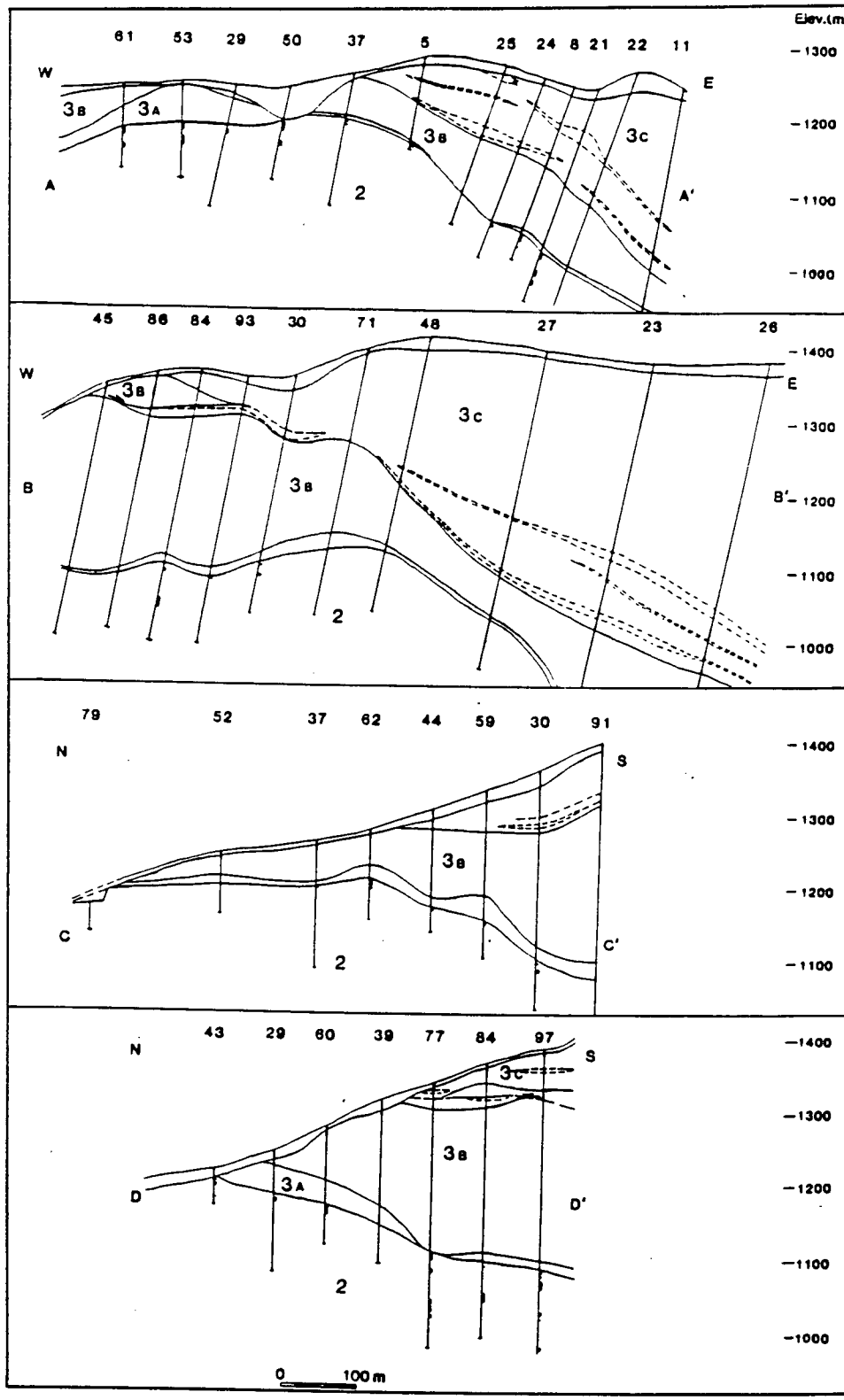

Figure 4-3: Cross sections of the Midway deposit area; units are as in Figure 4-2.

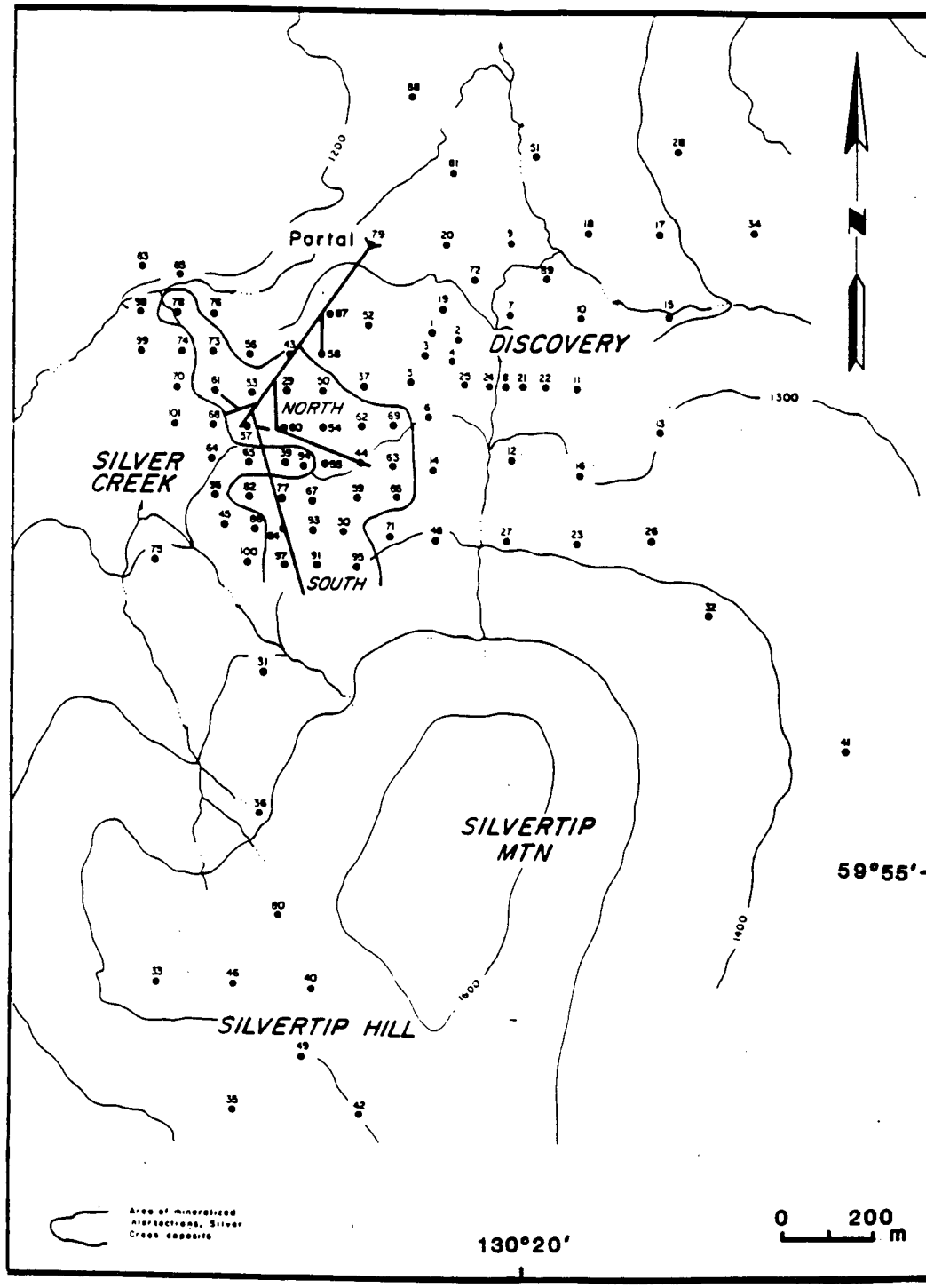

Figure 4-4: Location map of surface diamond drill holes.

Strata exposed east of Silvertip Creek in the vicinity of Midway range from Silurian to Mississipian in age (Figure 4-2). Miogeoclinal carbonates of Silurian to Middle Devonian age are unconformably overlain by Devono - Mississipian (mid - Fammenian to mid - Tournasian: Orchard and Irwin, 1988) basinal shales and turbidites of the Earn Group. The latter is structurally overlain by oceanic sediments and volcanic and intrusive rocks of the Sylvester allochthon.

4.2.1.1. Tapioca sandstone

Siluro - Devonian dolostones and sandy dolostones, informally termed "Tapioca sandstone", are exposed at lower elevations on the west side of Silvertip Hill (unit 1, Figure 4-1). These are well bedded, locally cross - bedded, very mature carbonate - siliciclastic shelf sediments. Tapioca sandstone attains a thickness in excess of 450 metres elsewhere in 1040/16 (cf. section 3.2.4.).

4.2.1.2. McDame Group

McDame Group carbonates, of Middle Devonian age, paraconformably overlie Tapioca sandstone, outcropping on Silvertip Hill west of Camp Creek Fault, on the south side of Silvertip Creek in the Midway portal area, and on the north end

of Tour Peak, south of Silvertip Hill (unit 2, Figure 4-2; cf. section 3.2.5). Non - fetid dolostones and interbedded dolomitic quartz arenite of the upper Tapioca sandstone grades up into alternating dark and pale grey well laminated, fetid dolostones at the base of the McDame Group.

Total thickness of the McDame Group in the Midway area is about 350 metres. Dolomitic facies dominate the lower third of the section (Figure 4-2, unit 2A), and consist of dark grey, fetid cryptalgal laminites and interbedded massive dolostone. The upper two - thirds of the section consists of fossiliferous, fetid rudstones, floatstones, wackestones and packstones, with interbedded micritic limestones. Faunal assemblages, of low diversity, consist primarily of stromatoporoids, with local accumulations of brachiopods, corals, crinoids and bivalves (Mundy, 1984).

The upper McDame contact is a regional unconformity marked by topographic relief of 165 metres (Mundy, 1984). Erosional irregularities along the contact are observable from hand specimen to map scale. The unconformity indicates that uplift and subaerial exposure of the McDame Group occurred prior to deposition of overlying clastic sediments of the Earn Group. Detailed biostratigraphic correlations suggest that uplift may have been accompanied by local block faulting (Mundy, 1984).

Widespread karsting is manifested by spar - healed breccias and vugs, and by coarse spar - filled paleocaverns up to several metres across. The breccias commonly include shale clasts derived from Earn Group. Breccia types are described in greater detail in section 4.4.3. Locally, well bedded mudstones and siltstones occur within compacted shale and limestone breccias in cavities 30 metres or more below the top of the McDame, indicating that some cavities were open to the ocean floor during deposition of the Earn Group (e.g. MW 95 (332 - 341)).

At one location in 1040/16, dolomitic siltstone containing conodonts of Late Devonian age (Frasnian to Fammenian) fills hollows at the unconformity. This could represent an early shallow water fauna deposited during the initial stages of subsidence, prior to deposition of overlying deep basinal sediments (J.L. Nelson, personal communication, 1987; Orchard and Irwin, 1988).

4.2.1.3. Earn Group

Devono - Mississipian Earn Group has been subdivided into four informal formations in the Midway area: units 3A, 3B, 3C and 3D (Figure 4-2). (These units correspond to units E1A, E1B, E2A and E2B of Cordilleran Engineering, 1983).

The lowermost Earn Group unit (3A) consists of carbonaceous, locally calcareous or siliceous, black silt shales up to 40 metres thick (Figure 4-2). This euxinic basin facies contains a rich conodont fauna of mid-Fammenian age (Orchard and Irwin, 1988). Thickness is variable over short distances, while in places the unit is missing entirely, perhaps due to depositional control by McDame paleotopography. Particularly thick sections overlying mineralized zones may represent filling of karstic depressions produced by solution collapse (Figure 4-3, section A-A'). Graphitic slickensides are common, indicating that the unit served as a detachment surface between the McDame Group and overlying thick, coarse siliciclastic sediments. Some thickening and thinning, therefore, might be structural in nature. Contacts between limestone and calcareous shale facies are commonly marked by numerous closely spaced stylolites. Shales in places consist of disrupted and rotated clasts along the contact, giving further evidence of detachment (e.g. MW 72 (167.5)).

A thick (up to 250 metres) succession of coarse sandstone, mudstone, and pebble conglomerate, unit 3B (Figure 4-2), overlies the black shale unit. Facies changes within this unit are rapid, and classic turbidite features such as normal and reverse graded bedding, load and flame structures, rip - ups, mud drapes, and sole marks are ubiquitous. Thickness changes are

abrupt; for example, in section B-B' (Figure 4-2) thickness tapers from 250 to 75 metres over less than 400 metres. The sandstones are litharenites, consisting mainly of quartz, chert and shale grains. According to Gordey et al. (1986), the development of this and overlying turbidite successions occurred as a result of local uplift and erosion of miogeoclinal blocks during early Mississipian extension.

A thick succession of argillite, slate, siltstone, calcarenite and sandstone containing several exhalative horizons, unit 3C (Figure 4-2), overlies coarse turbidites of unit 3B. Conodonts from unit 3C give early Mississipian (early to mid - Tournasian) ages (Orchard and Irwin, 1988). This unit is also of widely variable thickness, ranging from 200 to at least 600 metres. The upper half of this unit contains sandy beds exhibiting boudinage structures in zones of intense strain, while mudstone interbeds have a well developed bedding - parallel foliation and slaty appearance.

The lowermost exhalative horizon, Discovery zone, or "Discovery trench exhalite" (Figure 4-2), occurs above a carbonaceous mudstone unit which overlies unit 3B sandstones. Exhalite horizons exposed at surface consist of orange weathering laminated silica, barite, pyrite and locally, sphalerite. They rarely attain thicknesses of over 1 metre.

Laminated zinc rich exhalites occur in the Discovery zone in the vicinity of the Midway carbonate hosted deposits. (Note that "Discovery zone" is not the same as "Discovery deposit", which is carbonate hosted manto mineralization; the manto deposits were collectively referred to as "Lower Zone" in earlier nomenclature, e.g. Cordilleran Engineering, 1983). This zone grades laterally into baritic and siliceous exhalite (Figure 4-5). Sphalerite in the Discovery Zone is yellow to pale purple - brown, in contrast to the dark red - brown to black sphalerite of the carbonate hosted mineralization. Individual laminae are 0.2 to 3 millimetres thick, and are composed of alternating quartz and sphalerite (Figure 4-6). Grain size (40 to 80 microns) is on average almost an order of magnitude smaller than in manto mineralization. Sphalerite is speckled with clots of chalcopyrite grains 5 to 15 microns across. This accounts for the chalcanthite coatings on oxidized surface exposures of the zone. Galena is rare, other than in crosscutting veinlets related to later manto mineralization.

Discontinuous exhalites are exposed along a strike length of almost 10 kilometres south from Midway (Nelson and Bradford, 1987b). Exhalative barite also occurs about 9 kilometres northeast of Midway (the Ewen and Perry barite showings). The large lateral extent of these exhalites is probably related to a

Figure 4-5: Photograph of baritic exhalite showing soft sediment deformation, from about 500 metres southwest of the Silver Creek deposit.

Figure 4-6: Photograph of laminated sphalerite - quartz with minor pyrite, Discovery Zone exhalite.

major zone of rifting developed in the Midway area in the Late Devonian. Faulting along this rifted zone might have controlled later deposition of conglomeratic turbidite channel facies (unit 3D).

A sequence of pebble to boulder conglomerate and lesser sandstone (Figure 4-2, unit 3D) overlies exhalite bearing fine clastics on Silvertip Mountain and Tour Peak, where it attains thicknesses in excess of 150 metres. Pebbles are commonly stretched, with the long axis paralleling the regional northwesterly structural trend. The conglomerate contains a variety of clast lithologies, mainly derived from platformal units. On Tour Peak, a section of well - rounded boulder conglomerate contains clasts of: McDame limestone, Tapioca Sandstone quartzite and dolostone, possibly Lower Cambrian Boya Formation quartzite, and black massive chert of undetermined origin.

The transition from unit 3C to unit 3D might represent a turbidite feeder channel prograding over its distal lower fan. The channel deposits are confined to the Silvertip Mountain - Tour Peak areas (Figure 4-1), with no thick conglomerate occurring to the south or west. Instead, thinner lensoid conglomerates are interbedded with, and overlain by, fine clastics in the Caribou Ridge area south of Tour Peak (Figure

4-1), which suggests a lateral facies change.

4.2.1.4. Sylvester allochthon

A thick sequence of black argillite, limestone with black chert, and green thin bedded chert and cherty phyllite, unit 4, abruptly overlies unit 3D across a poorly exposed decollement (Figure 4-2). This sequence has been assigned to Division I of the Sylvester allochthon (Nelson et al., 1988). The base of unit 4 marks the structural boundary between Cassiar Terrane and Slide Mountain Terrane in the map area. Conodonts from unit 4 range from early Mississipian (Tournasian) to Pennsylvanian (Orchard and Irwin, 1988). The sediments are overlain by thrust packages of cherts with diabase sills, volcaniclastic rocks, basalt flows and gabbros. Serpentinite lenses occur locally along thrust contacts.

4.2.2. Structural Geology

The set of sulphide bodies which constitutes the Silver Creek deposit is near the axis of a shallowly southeasterly plunging open anticline (Figure 4-7). The east limb dips to the east at about 25 degrees, while the west limb is folded and cut by a strand of the Tootsee River fault zone (cf. section 3.7.3). The fold axis parallels southeasterly

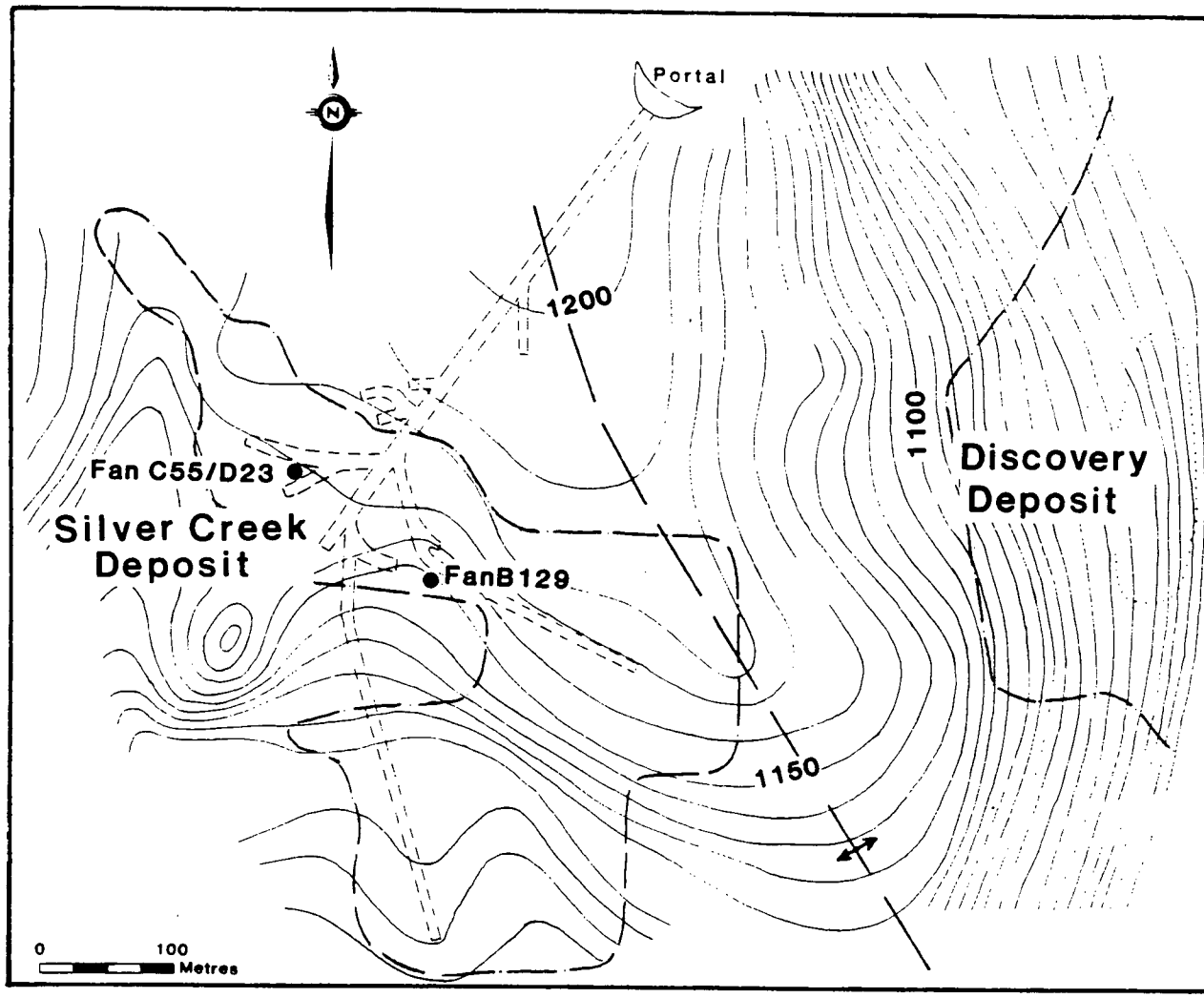

Figure 4-7: Contour map showing elevation of the McDame Group - Earn Group unconformity in the Midway area. Contour interval is 10 metres.

regional structural trends, manifested by intersection, crenulation, pebble elongation and pencil lineations, and by axes of broad, open folds. This trend is the result of Jura-Cretaceous compression and emplacement of the Sylvester allochthon (Nelson and Bradford, 1987a). Deformation was accompanied by sub-greenschist grade (prehnite - pumpellyite) metamorphism (J.L. Nelson, personal communication, 1986). Locally, a later east trending phase of folding deforms southeasterly trending structures. This phase is characterized by chevron and kink folds that are often accompanied by east trending en echelon quartz veins.

Thrust faulting can be inferred from diamond drilling in the Silver Creek and Silvertip areas, although mapping of thrusts within the Earn Group is inhibited by lack of marker beds and faunal control. In the southern part of the Silver Creek deposit (Figure 4-3, section B-B'), a wedge of unit 3B is imbricated with unit 3C above the lowermost exhalite horizon. On Silvertip Hill (MW 40) McDame Group limestone (unit 2B) is imbricated with unit 3A, which has undergone possible structural thickening. Thrusts putting Earn on Earn probably floor in unit 3A, which serves as a logical detachment horizon. Thrusts putting McDame on Earn may root within the McDame, or cut through the Siluro - Devonian massive carbonates and floor in the Road River Group, a decollement horizon of regional extent (Nelson and Bradford,

1987a).

The Silvertip area is cut by several strands of the Tootsee River fault zone, a northerly trending complex of anastomosing high angle faults extending from about 7 kilometres south of Midway to about 17 kilometres north of the British Columbia - Yukon Territory border (Lowey and Lowey, 1987). These include the Silvertip Creek, Camp Creek, and Brinco Creek faults (Figure 4-2). The strands converge to the north of the Midway deposit and form a narrow zone with large stratigraphic throw about 1.5 kilometres north of the deposit. Diamond drilling in an area about 0.5 to 0.75 kilometres north of the deposit encountered several fault zones expressed as thick gouge intersections (MW 275, 283). Inferred sense of motion on these faults is normal dip slip, but a strike slip component could be present.

The Silvertip Creek fault separates Silvertip Hill and Tricorn Mountain to the west (Figure 4-2). Rotation of large blocks juxtaposed a southerly dipping panel on Tricorn Mountain with easterly dipping strata on Silvertip Hill. On the west side of the fault, deeper structural levels are exposed to the north. East side strata are generally north striking, so stratigraphic throw increases to the north to a maximum of about 1.5 kilometres. Only minor offset occurs immediately west of Silvertip Hill.

The Camp Creek fault juxtaposes McDame Group and Earn Group on Silvertip Hill, where it diverges into two main strands with offsets of about 50 metres, east side down (Figure 4-2). Between fault strands, Earn Group strata are disrupted and locally overturned. The Silver Creek deposit and the Silvertip showing are both adjacent to this fault zone, which could have been a hydrothermal fluid guide.

The Brinco Creek fault offsets strata east of the Discovery deposit, with a displacement of about 100 metres, east side down. Other faults with smaller offsets might occur west of the Brinco Creek fault. The latter appears to die out to the southeast, as the base of the Sylvester allochthon east of Brinco Hill is not offset.

Late Cretaceous (Midway) and Eocene (Butler Mountain) intrusions (section 3.5) associated with silver-lead-zinc showings both occur within the Tootsee River fault zone and related splays. Overprinting of early Mississipian exhalative and Cretaceous - Eocene intrusive related mineralization within the zone suggests that it might represent a long lived, periodically remobilized zone of structural weakness and anomalous heat flow that was initiated in the Late Devonian during extension along the continental margin. Remobilization of

old structures during Late Cretaceous to Eocene dextral wrench faulting (Gabrielse, 1985) could have contributed to localization of post Cassiar batholith intrusions.

4.3. Alteration and Evidence of Intrusions

Intense sericitization of Earn Group and Sylvester sediments occurs in a northwesterly trending zone extending from Silvertip Hill southeast for about 5 kilometres to Gum Mountain (Figure 4-1). Alteration crosscuts the Earn Group - Sylvester allochthon contact, and therefore postdates emplacement of the Sylvester. Strong alteration is also evident at deeper levels in diamond drill holes in the southeasterly part of the Midway drill grid (near MW 16, 32, and 41; Figure 4-4) and south of Silvertip Mountain near DDH B82-1. Its strongest surface expression is on the north side of Brinco Hill, which coincides with magnetic and gravity anomalies interpreted as consistent with a buried intrusion at depth (J. Hylands, personal communication, 1986).

At Brinco Hill (Figure 4-8), Earn Group sandstones and conglomerates are altered to sericite, quartz, pyrite, rutile and rare carbonate, with both matrix and non - silica clasts being completely replaced. The altered sediments are cut by numerous vuggy, locally comb textured 1 to 10 centimetre thick quartz veins containing pyrite, chalcopyrite and rare galena

Figure 4-8: Photograph of Brinco Hill, with Whitehorn Mountain in the background, showing orange brown gossan.

blebs. Vugs contain sericite and jarosite.

Quartz - feldspar - biotite - hornblende porphyry dykes are exposed at surface west of Gum Mountain (Figure 4-1), where they intrude intensely sericitized and pyritized argillites and cherts of the Sylvester allochthon. The dykes contain 5 to 10 per cent partially resorbed quartz phenocrysts up to one centimetre across. Biotite and hornblende phenocrysts are pseudomorphed by fine grained sericite, carbonate and opaques, which are concentrated along crystallographic planes. The matrix consists of fine grained sericite and carbonate, with abundant relict feldspar laths.

Both altered sediments and altered dykes from the Brinco Hill - Gum Mountain area have been dated by potassium - argon methods. Three analyses give ages ranging from 65 to 75 Ma (cf. section 3.6., Table 3-2). These ages define an intrusive - hydrothermal event which post - dates potassium - argon ages on the Cassiar batholith by at least 30 Ma.

Alteration is associated with anomalous fluorine values near the hypothesized intrusive centre at Brinco Hill (Table 4-1; Figure 4-9). Grab samples indicate that felsic porphyry dykes near Gum Mountain contain up to 0.2% fluorine, while

Table 4-1: Microprobe analyses of fluorine in sericite, Midway deposit, northern British Columbia (1040/16).[1]

Sample Location [2]	Avg. % F (No. of analyses)	Range (% F)
DDH MW 32 (707.8 m)	0.29 (5)	0.13-0.42
DDH MW 41 (763.2 m)	0.40 (5)	0.35-0.47
DDH MW 41 (839.6 m)	0.70 (6)	0.64-1.10
SYA 86-40 (Brinco Hill)	1.11 (7)	0.65-1.24
DDH B82-1 (284.2 m)	2.19 (6)	1.14-3.34

1. Data is courtesy of W.D. Sinclair, written communication, 1986.
2. Diamond drill holes are located in Figure 4-4 and Figure 4-9.

sericitized conglomerates at Brinco Hill contain 0.08% fluorine (W.D. Sinclair, personal communication, 1987; Nelson et al., 1988b). Microprobe analyses of sericites from surface and drill core show averaged values for several probe sites per sample ranging from 0.29 to 2.19% fluorine (Table 4-1), with the highest values occurring in samples at depth near Brinco Hill (Figure 4-9). Fluorine content decreases with increasing distance from Brinco Hill, and with increasing elevation.

Although the evidence for fluorine zoning around Brinco Hill is not conclusive because of the small number of samples, the fluorine values are high, and typical of micas related to altered, highly evolved plutons. Substitution of fluorine for hydroxyl groups in alteration zone micas probably reflects the contribution of magmatic volatiles to the hydrothermal system centered on Brinco Hill.

Epizonal felsic intrusions, elevated fluorine in alteration minerals, and a geological setting within an extensional fault system adjacent to an older, voluminous intrusion (e.g. Cassiar batholith), are all features typical of A - type granites (W.D. Sinclair, written communication, 1986; Collins et al., 1982). The strong tin signature of Midway mineralization (cf. section 4.4) is also consistent with this interpretation. Intrusive

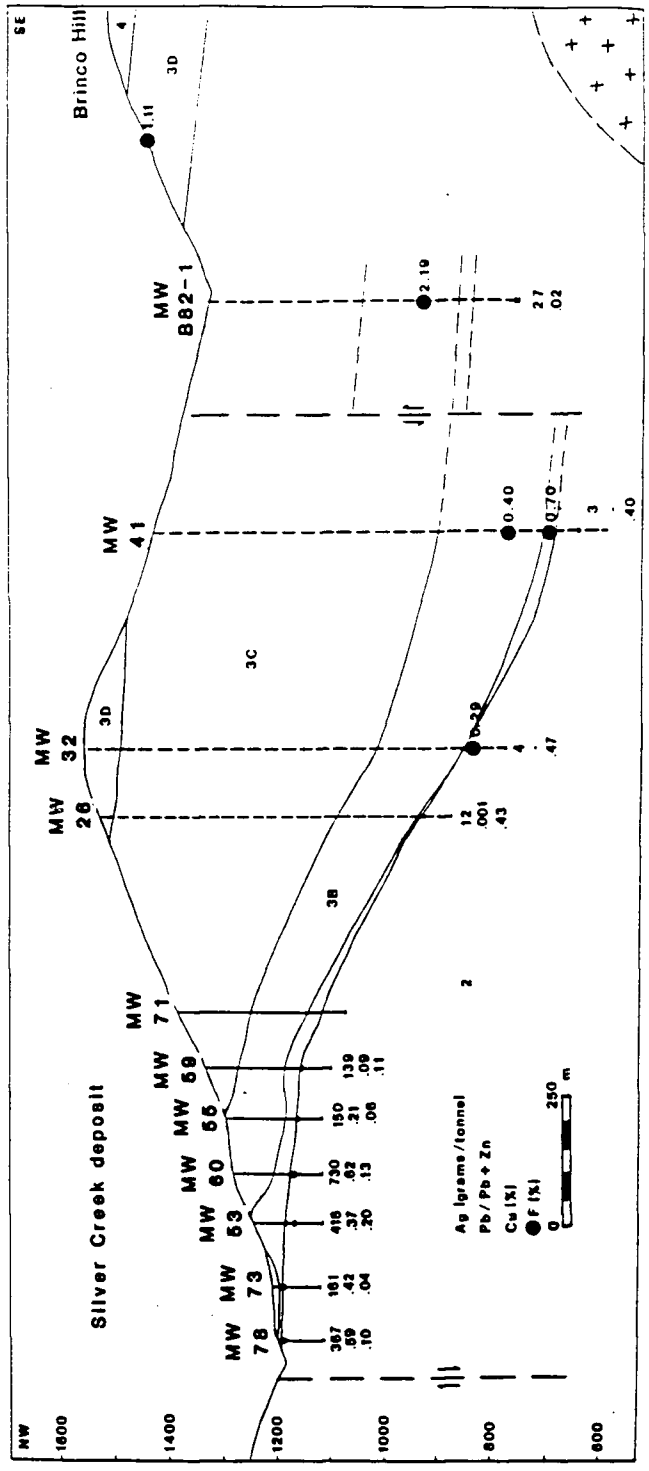

Figure 4-9: Northwest - southeast cross section from the Silver Creek deposit to Brinco Hill, showing metal zoning and fluorine analyses. Units are numbered as in Figure 4-2. Widened part of diamond drill holes are sulphide intersections, and metal grades are averaged over the intersection. Fluorine data is in Table 4-1. Dashed diamond drill holes are projected onto the section.

bodies coeval with the Midway system in the Cassiar Terrane include the Troutline, Kuhn and Windy stocks in the Cassiar area. Numerous polymetallic skarns and veins, fluorine stream anomalies, fluorite veins, and molybdenum - tungsten skarns and stockworks are associated with the 70 Ma Cassiar intrusions (Panteleyev, 1980; 1985). Trace element chemistry which would discriminate A - type granites (Whalen et al., 1987) is not yet available, although Rb-Sr data suggests that the Late Cretaceous suite represents a lower crustal anatectic melt which has undergone some upper crustal contamination (Cooke and Godwin, 1984).

4.4. Sulphide Mineralization

4.4.1. Distribution of Sulphide Bodies

Carbonate hosted sulphide bodies in the Midway area are irregularly distributed within three main deposits south of the junction of Silvertip Creek and Brinco Creek, north of Silvertip Mountain (Figure 4-2). This mineralized area extends almost one kilometre from north to south and an equal distance from east to west. Minor sulphides are sporadically distributed to the south of the main mineralized area. Depth of cover rocks makes surface diamond drilling prohibitively expensive south of currently explored mineralization. The three main deposits, Silver Creek,

Discovery, and Disco North, consist of irregular, stratabound and crosscutting massive sulphides with limited lateral continuity.

The Silver Creek deposit contains the largest known concentration of massive sulphide bodies with the highest grade precious metal values. Mineralization extends over about 500 metres north to south and 300 metres east to west. A crude elongation of sulphide distribution occurs along a northwesterly structural trend, paralleling the anticlinal fold axis. The core of the deposit contains massive sulphides over 12.5 metres thick, with grades of 730 grams/tonne silver, 1.96 grams/tonne gold, 15.34% lead, 9.23% zinc and 0.13% copper; tin averages about 0.75% (Cordilleran Engineering, 1984).

The Discovery deposit lies east of the Silver Creek deposit at deeper levels (Figure 4-2 and 4-3). Sulphides in this zone are distributed across 700 metres north to south and 300 metres east to west. Sulphide bodies discovered to date do not attain the thickness and grades encountered in the Silver Creek deposit. The thickest intersection is just over seven metres. Mineralization tends to be zinc rich and lead poor. The Discovery deposit has undergone only limited exploration due to depth of cover rocks.

The Disco North showing is about 300 metres northeast of the Silver Creek portal in a low lying area near the junction of Brinco Creek and Silvertip Creek (Figure 4-2). Two drill holes in this area have intersected significant mineralization (MW 81, 280).

The Silvertip deposit, the original silver rich discovery in the Midway area, lies about 750 metres southwest of the southernmost limit of explored mineralization in the Silver Creek deposit. Surface and underground workings traced galena rich mineralization which is largely oxidized to depths of over 150 metres (Holland, 1968).

4.4.2. Morphology of Sulphide Bodies

The morphology of sulphide bodies in the Silver Creek deposit has been partially delineated by underground exploration, which indicates an irregular network of subhorizontal pipes radiating outward from a high grade core zone near DDH MW 60 (J.Hylands, personal communication, 1987). Sulphide bodies tend to occur close to the McDame Group - Earn Group contact in the north part of the deposit, but occur at deeper levels below the contact to the south (Cordilleran Engineering, 1985). Sulphide bodies are massive and irregular in form, with sharp wallrock contacts. Both subhorizontal, pipe

like bodies and keel shaped chimneys occur (Figures 4-10 and 4-11). The two types do not have predictable compositional differences, as at some manto deposits (J.Hylands, personal communication, 1986; cf. Lovering et al., 1978).

Descriptions of features of sulphide bodies which follow are based on studies of drill core and rounds from underground exploration made during the 1986 and 1987 field seasons. Photographic documentation of underground exposures (W.D. Sinclair, D. MacIntyre, personal communications, 1987) was also considered.

4.4.3. Breccia Types

The Midway deposits are characterized by widespread breccias of numerous types. These include breccias interpreted as pre-mineral, syn-mineral, and post-mineral. In some cases, questions of genesis and timing cannot be resolved without detailed underground mapping. A descriptive classification of breccia types includes: (1) carbonate clast, calcite matrix breccias, (2) shale clast and mixed shale - limestone clast, calcite matrix breccias, (3) stylolitic breccias, (4) sulphide matrix breccias, (5) sulphide clast, calcite matrix breccias, and (6) tectonic breccias.

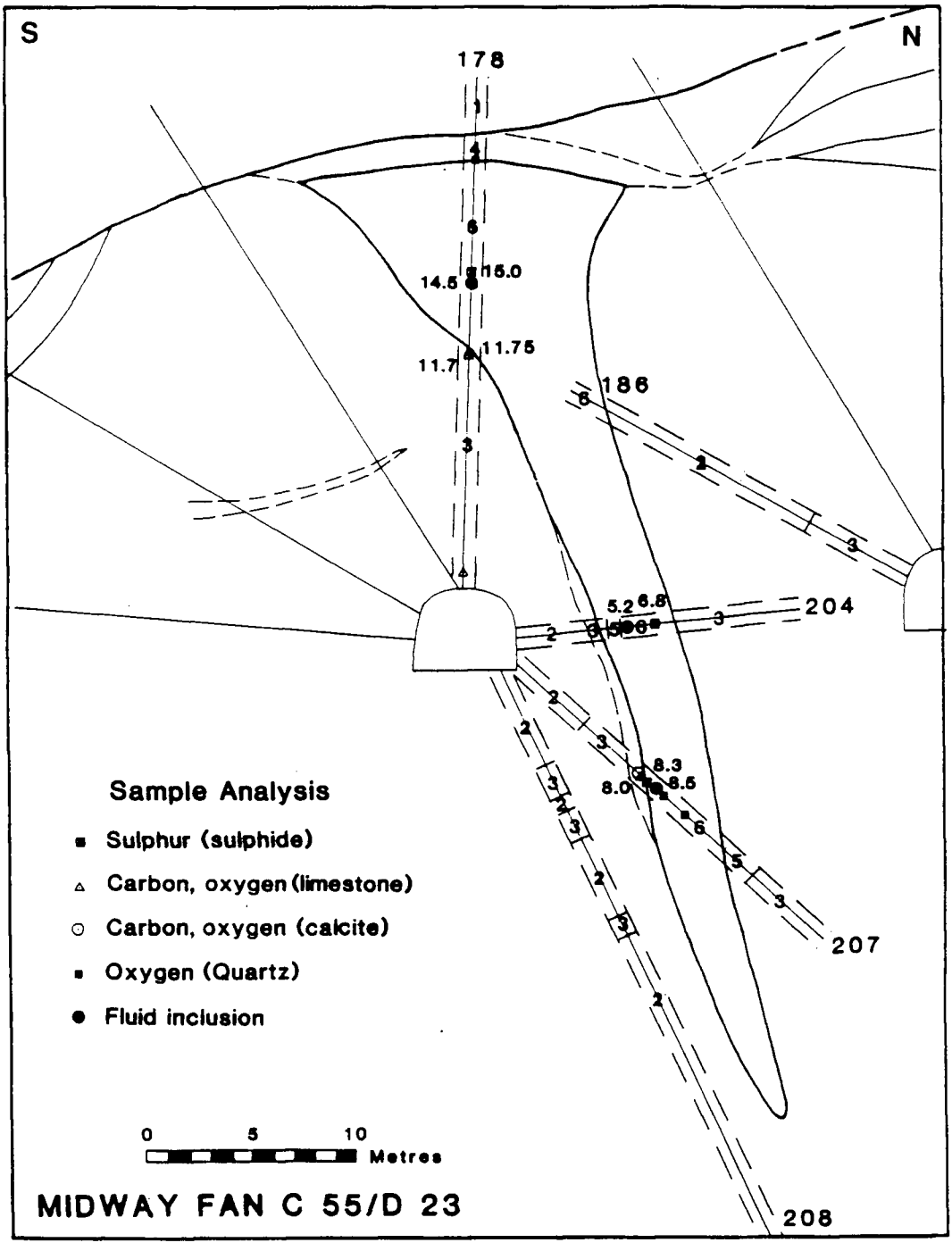

Figure 4-10: Cross section of massive sulphide pipe at underground drill station Fan C55/D23, showing drill hole numbers, sample locations, and lithology or breccia type. Symbols: 1 - Earn Group, 2 - McDame Group (unbrecciated), 3 - limestone crackle breccia, 4 - shale $\pm$ limestone matrix or disrupted breccia, may have sulphide clasts, calcite or quartz matrix, 5 - sulphide > shale $\pm$ limestone clast breccia, sulphide or carbonate matrix, 6 - massive sulphide or sulphide vein.

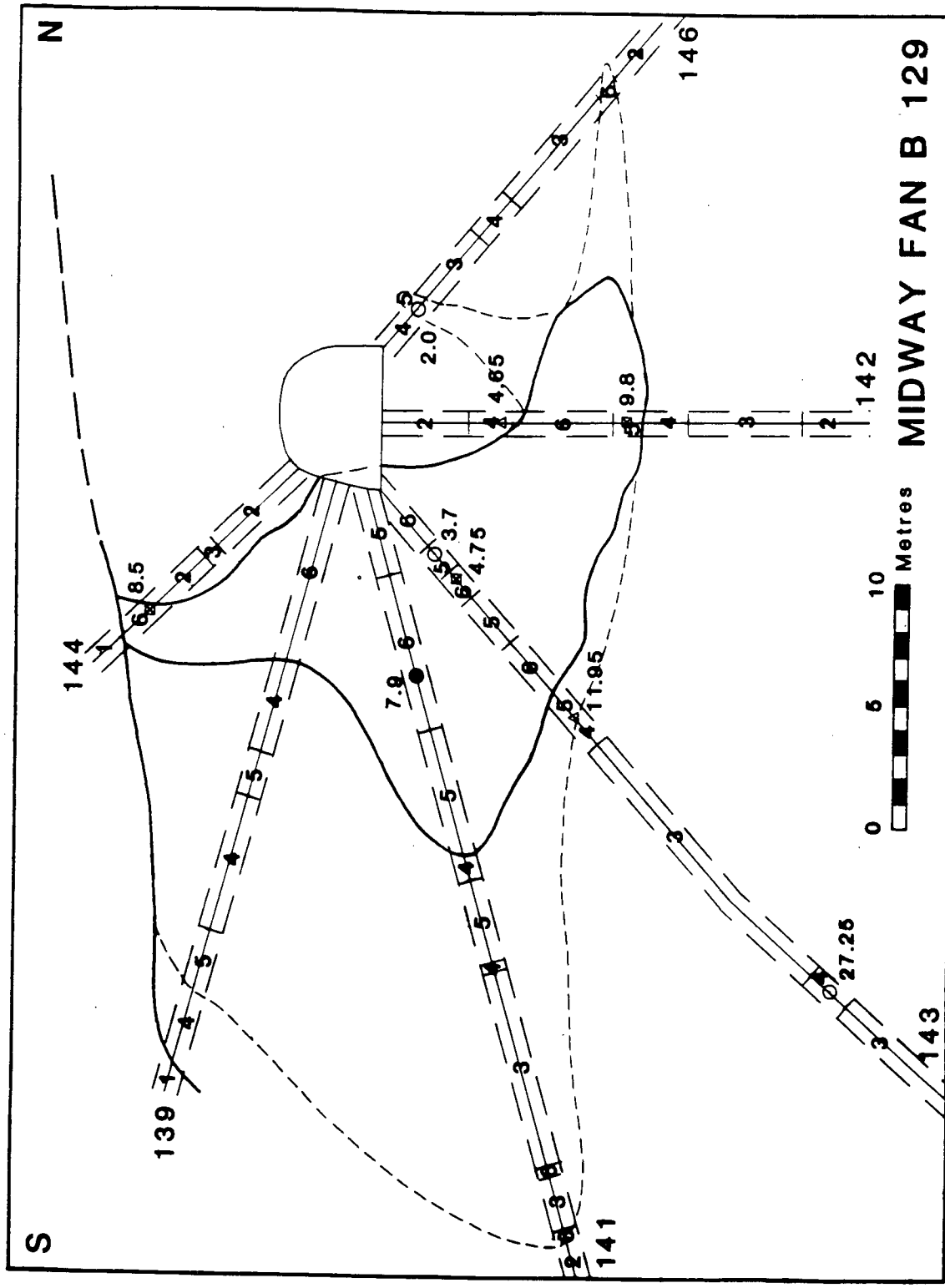

Figure 4-11: Cross section of massive sulphide pipe at underground drill station Fan B 129, showing drill hole numbers, sample locations, and lithology or breccia type. Symbols are as in Figure 4-10.

Carbonate clast, calcite matrix breccias occur throughout limestones of the McDame Group, and include stratabound and crosscutting zones of brecciation of varying intensity. They can be subdivided into: (a) crackle breccias, in which the limestone is cut by thin, irregular veinlets of calcite (Figure 3-8), (b) mosaic breccias, in which unrotated angular clasts of variable size are tightly supported by calcite matrix, and (c) disrupted breccias, in which angular rotated clasts, in some cases of mixed biofacies or lithology, are juxtaposed in a calcite matrix. Crackle breccias, widespread regionally, are characteristic of the McDame Group. Mosaic and disrupted breccias occur both adjacent to and within some sulphide bodies. Calcite veining parallel to margins of large calcite healed zones locally gives the limestone a "stoped" appearance (Figure 4-12). Transitions outward from pipe-like sulphide bodies grade from matrix dominated breccias, to mosaic, then crackle breccias (Figure 4-10). Calcite matrix and limestone clasts adjacent to these bodies are replaced by sulphide. Relict, unreplaced carbonate is commonly scattered throughout the sulphide (e.g. MW 77 (311.4)).

Shale and mixed shale - limestone clast, calcite matrix breccias contain shale clasts derived from Earn Group unit 3A. These breccias seem to occur mainly in the vicinity of the Midway deposits, although locally they occur away from

Figure 4-12: Photograph of disrupted limestone breccia with calcite matrix, taken underground near the Silver Creek deposit. Photograph is courtesy of W.D. Sinclair.

Figure 4-13: Photograph showing the sharp contact between an Earn Group shale breccia with calcite matrix, and bleached and brecciated McDame Group limestone (MW 59, 216-223 m). Note the limestone clasts within the shale breccia. The McDame Group - Earn Group contact is at 175 metres, 44 metres above the top of the shale breccia. A sulphide intersection 4.5 metres thick occurs at the contact.

mineralized areas. Some of these are demonstrably premineral, containing shale clasts lacking the Jurassic crenulation lineation which is pervasive in unit 3A, and which predates Late Cretaceous manto mineralization. Shale clast breccias within the McDame Group are commonly chaotic, containing very jumbled angular clasts commonly 1 to 10 centimetres across. Contacts between shale breccias and enclosing limestone or sulphide are commonly very sharp (Figure 4-13). Shale clasts occur as much as 90 metres below the McDame - Earn contact; e.g. MW 77 (314). Commonly, mixed clast breccias contain both shale and limestone clasts (Figure 4-14). In one version of this, small (1 centimetre and less) shale and limestone fragments are enclosed in pale grey, granular dolomitic matrix, which is in turn brecciated and infilled by multiple generations of calcite (Figure 4-15). Such multiple generation breccias are probably widespread. Some shale clast breccias are tabular in form. In some cases these contain manto type sulphide clasts and are therefore postmineral. Replacement of pre-existing calcite matrix and veining of shale clasts is common within sulphide bodies (Figure 4-16), giving evidence that the breccias are pre-mineral.

Stylolitic breccias are very common in the McDame Group. Stylolites are usually roughly bedding parallel, and are locally

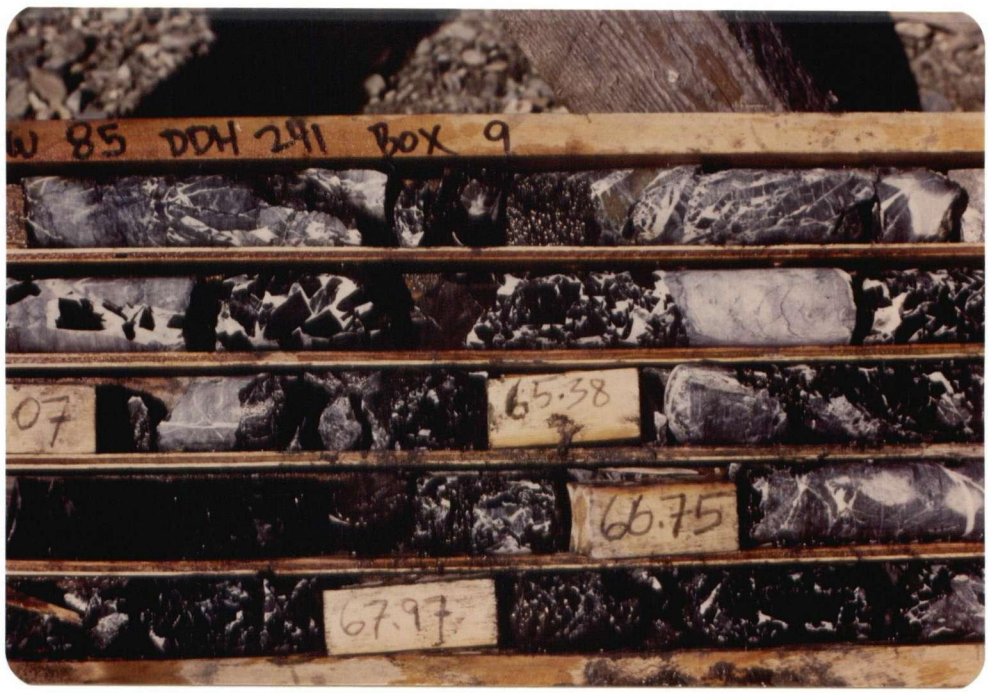

Figure 4-14: Photograph of a disrupted breccia containing Earn Group shale and bleached McDame Group limestone clasts in calcite matrix (MW 241, 64-68 m).

Figure 4-15: Photograph of a multi-episodic breccia, with angular Earn Group shale clasts in a lighter coloured dolomitic carbonate matrix, brecciated and rimmed by grey calcite, then filled by white calcite. Scale is in centimetres.

Figure 4-16: Photograph of relict calcite matrix of a shale breccia, partly replaced by sulphide at the base of a massive sulphide body, Silver Creek deposit. Photograph courtesy of W.D. Sinclair.

associated with extension gashes perpendicular to the stylolites, and thus parallel to the main compressive stress. These are of diagenetic origin, and are caused by pressure solution due to compactional overpressures (Nelson, 1985). Stylolites are also abundant in spar healed limestone breccias and mixed shale - carbonate breccias. One breccia with shale and limestone clasts (including fine limestone fragments) in a pale grey, calcareous mudstone matrix is crosscut by irregular stylolites along clast boundaries, indicating that stylolite formation postdated the brecciation event. These breccias are locally vuggy, and contain calcite crystal vug fillings. Disrupted stylolitic breccias commonly juxtapose stylolites at variable angles, suggesting a reorientation caused by later dissolution of intervening soluble material. The significance of these breccias is discussed in section 4.4.4.

Sulphide matrix breccias contain shale clasts, limestone clasts, sulphide clasts, and any combination of the three. Some can be interpreted as pre-existing calcite matrix breccias in which the original matrix has been completely or partially replaced by sulphide. Evidence for this includes the presence of uncrenulated shale clasts, and pre-existing unreplaced calcite matrix. In other cases, evidence of timing is equivocal. Some shale breccias are clearly synmineral, consisting of unrotated to rotated blocks and clasts which are veined and surrounded by

sulphides at the McDame - Earn contact (Figure 4-17). In these, the sulphide veining itself produced the breccia texture. These occur above massive sulphide bodies which are localized along the contact. Multiple mineralization episodes separated by brecciation events are indicated by sulphide matrix breccias containing sulphide and shale clasts (Figure 4-18). Locally, synmineral sulphide clast, sulphide matrix breccias exhibit contrasting clast and matrix mineralogy, reflecting changes in depositional conditions. An example is shown in Figure 4-19, where blocky pyrite clasts are cemented by pyrrhotite. Sulphide clast breccias are especially common in the southern part of the Silver Creek deposit.

Sulphide clast, calcite matrix breccias demonstrate that the latest phase of the hydrothermal system at Midway was carbonate dominated. Timing of this phase is indicated by calcite veins cutting sulphides, and by sulphide clast breccias cemented by calcite (Figure 4-20). These are generally matrix poor, and locally contain shale and limestone clasts as well, although only the presence of sulphide clasts differentiates these from premineral breccias.

Tectonic breccias occur locally, and postdate at least some of the mineralization. These contain intensely brecciated

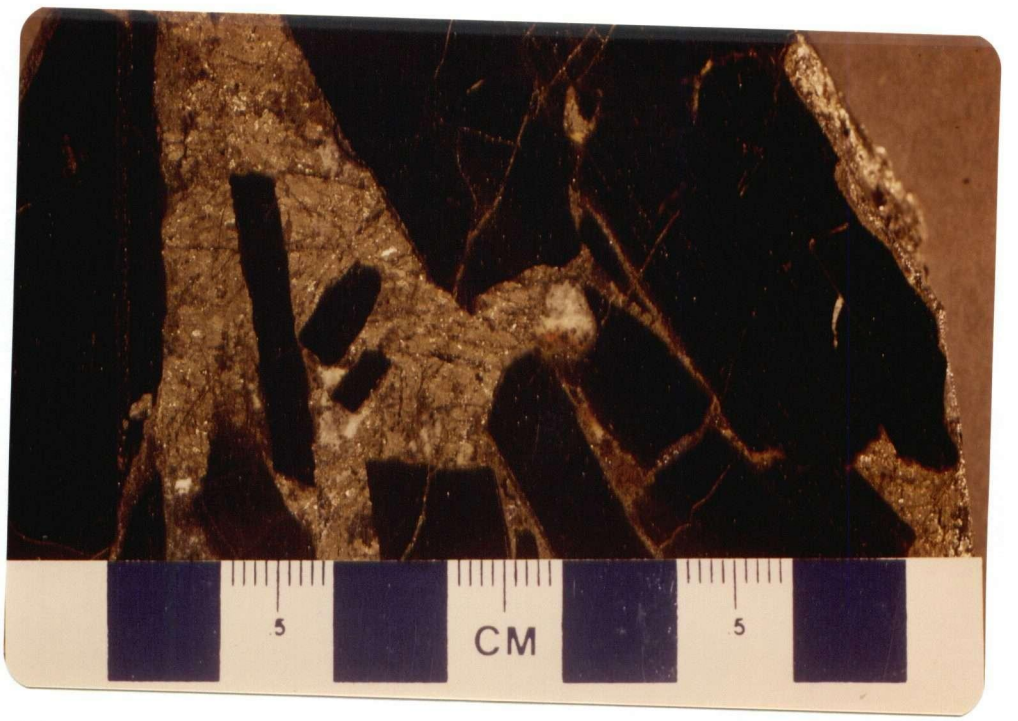

Figure 4-17: Photograph of Earn Group shale clasts veined by pyrite, in a pyrite - quartz matrix.

Figure 4-18: Photograph of mixed shale and sulphide clasts in a sulphide matrix synmineral breccia, Silver Creek deposit. Photograph courtesy of W.D. Sinclair.

Figure 4-19: Photograph of brecciated pyrite in a pyrrhotite rich matrix (MW 97, 317 m).

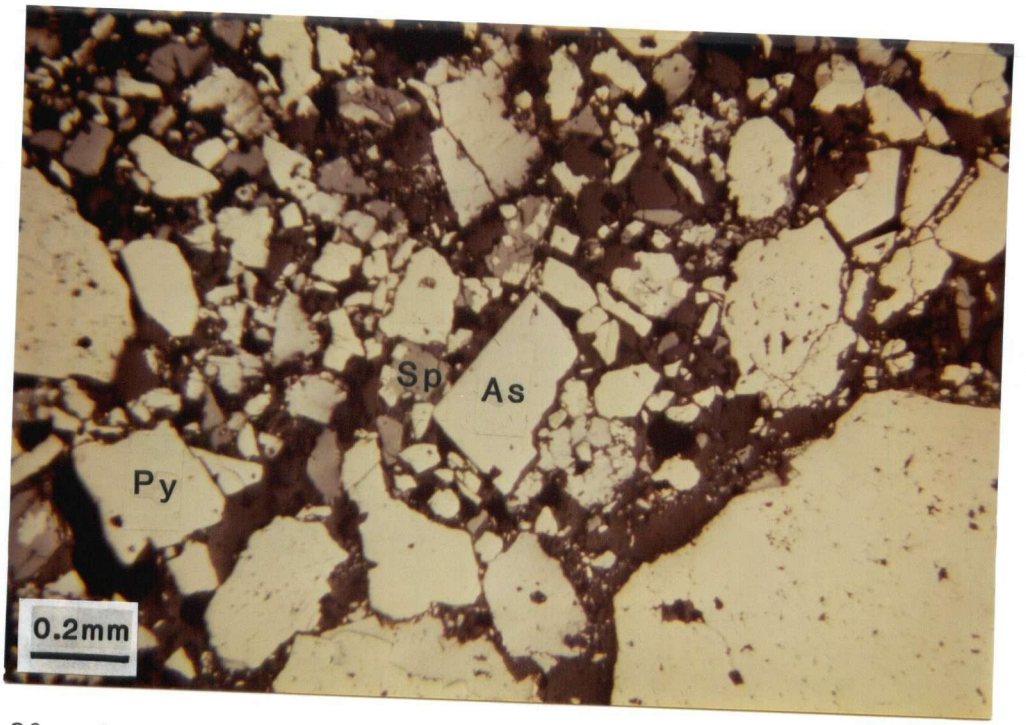

Figure 4-20: Photograph of brecciated sulphides and quartz in calcite matrix (MW 77, 233 m).

sulphides in which brittle shear bands crosscut both clasts and matrix. These breccias may be related to postmineral movement on Cretaceous - Tertiary block faults.

4.4.4. Significance and Timing of Breccias

Not only are breccias significant in constituting a large percentage of the sulphide deposits at Midway, they also provide clues to the genesis of the orebodies and to understanding controls on fluid migration and sulphide deposition. Although conclusive documentation of timing of brecciation events would benefit from detailed underground mapping, the evidence above permits some tentative conclusions.

Many features suggest that premineral breccias are related to karsting of the McDame Group and constitute an important ground preparation feature. The widespread nature of McDame breccias indicates that they are not caused primarily by the mineralizing system, but the intensity of their development near orebodies suggests that they influenced hydrothermal fluid migration and sulphide deposition. Evidence for pre-mineral origin includes: replacement textures and relict carbonate breccias within sulphide bodies, uncrenulated shale clasts in shale and mixed clast breccias, stylolites of diagenetic origin

within breccias (rather than within clasts only), the presence of bedded mudstones associated with shale breccias within McDame Group limestones, the presence of calcareous mud matrix "trash" (mixed clast) breccias within and at the base of some sulphide bodies, and the vertical extent of clast mixing within the McDame (at least 90 metres), which is difficult to explain by processes other than solution collapse as a result of karst development. In addition, the pipe and gallery morphology of the sulphide bodies and their association with calcite healed breccia haloes suggests that their emplacement was controlled by premineral breccia porosity of karst origin (Archambault, 1985).

Observation of breccia and other solution induced features, and timing of uplift and erosion of the McDame Group indicates that pre-mineral brecciation probably occurred during Late Devonian karsting, during which widespread vug to cave scale porosity was generated. Solution collapse, mixing Earn Group clasts into the upper McDame Group, probably occurred in the Late Devonian, since Earn Group clasts within McDame Group are limited to shale of unit 3A (Fammenian). Porosity filling with carbonate fragments, shale clasts, lime and organic rich mud occurred at this time, and later diagenetic pressures generated abundant stylolites in these zones.

Later brecciation occurred during mineralization, as multi-episodic mineralization caused mixing of earlier sulphide and country rock clasts in later sulphide matrix. Mixing of crenulated shale clasts into sulphide bodies along the unconformity suggests that significant porosity existed during mineralization, enabling collapse of shale clasts into limestone later filled and replaced by sulphides. Postmineral or late hydrothermal brecciation deposited calcite, cementing sulphide and other clasts.

Postmineral karsting could have been involved in creation of cavern scale porosity and carbonate and iron oxide sanding in the McDame Group. These zones were encountered by diamond drilling and underground exploration at Midway. Recent karsting is consistent with the high water flow levels encountered during underground exploration (Cordilleran Engineering, 1985). Alternatively some of these cavities might represent earlier karst features which were not accessed by hydrothermal solutions during mineralization.

4.4.5. Other Internal Features of Sulphide Bodies

Massive sulphide bodies commonly show highly contorted and irregular internal layering. Layering occurs inward from

wallrock contacts, outward from breccia clasts, and within non - layered sulphide. Scale of layering ranges from microscopic to several centimetres for individual layers. Grain size grading and gradational compositional layering (e.g. from pyritic to galena rich assemblages) are ubiquitous. Rarely, pyrite occurs in cross - laminated layers. At wallrock contacts it is common to see successive layers of galena, then sphalerite, then pyritic sulphides inward from limestone. Alternating layers of pyrite and quartz occur in addition to layering of different sulphide assemblages. Such crude layering features are common in manto type sulphide bodies, and indicate fluctuations in fluid chemistry during deposition.

Wallrock contacts adjacent to sulphide bodies can be strongly bleached outward for several metres (Figure 4-21), or can be apparently unaltered. Strongly silicified zones with faint outlines of relict limestone and stylolites are common adjacent to massive sulphide. Silicified zones can contain either white bull quartz or clearer grey quartz. Dolomitization of hydrothermal origin is distributed erratically, and does not appear to have played a role in ground preparation, as in some manto districts (e.g. Gilman and Leadville, Colorado: Lovering et al., 1978).

At contacts between limestone and sulphide bodies, sulphides commonly follow stylolites and stylolitic contacts outward, with thin (less than a millimetre thick) sulphide seams being deposited along the stylolite. This suggests a localized redox control on sulphide deposition. Stylolites also appear to play a role as small scale solution guides. In addition to juxtaposing different limestone facies, in places they also juxtapose silicified and unsilicified limestone, indicating that they provided local barriers to hydrothermal fluid flow (Figure 4-22).

4.4.6. Mineral Paragenesis

Sulphide paragenesis is based on optical study of 75 polished sections from two detailed cross-sections of large sulphide pipes in the Silver Creek deposit (Figures 4-10 and 4-11), from a north - south transect of the Silver Creek area with large vertical exposure in four diamond drill holes (cf. Archambault, 1985), and from several locations in the Discovery deposit and southernmost sulphide intersections. Identification of obscure phases is based on mineralographic and SEM - EDS studies in Archambault (1985).

Figure 4-21: Photograph of a contact between massive sulphide and McDame Group limestone, showing a halo of bleached limestone. Photograph is courtesy of W.D. Sinclair.

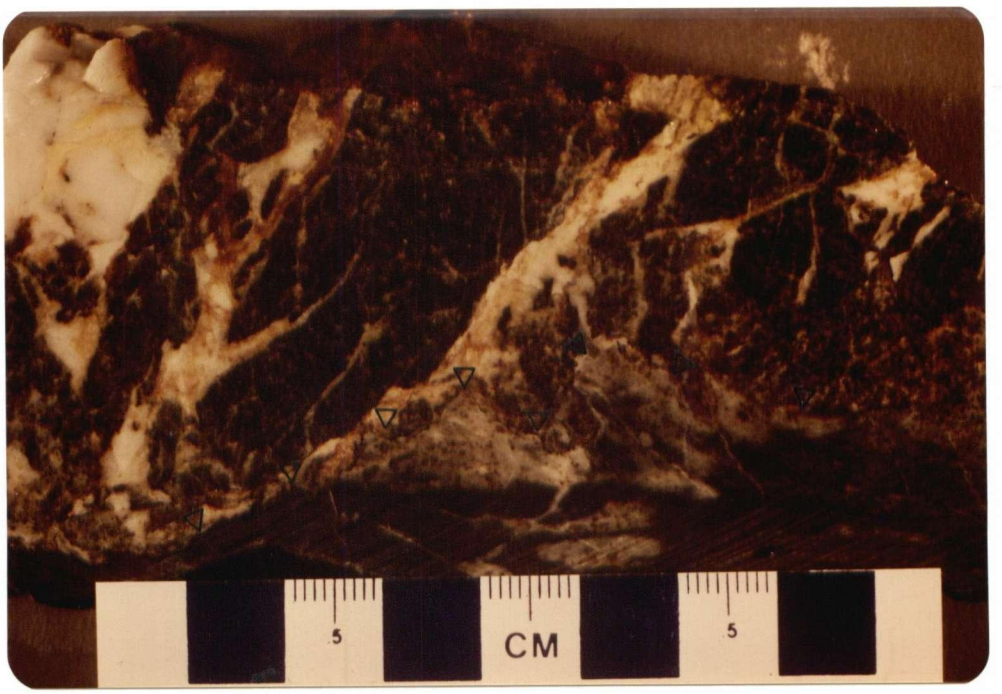

Figure 4-22: Photograph of a stylolitic contact between silicified limestone and white quartz, and unaltered limestone.

Detailed sulphide paragenesis is extremely complex and locally variable. The generalized evolution of the hydrothermal system can be represented in four stages: (1) early silica - pyrite, (2) main stage sulphide - silica, (3) sulphosalt - sulphide, and (4) carbonate (Table 4-2). Within this gross schema, more detailed paragenetic relations between individual minerals are described below.

Pyrite appears in a wide variety of habits, and appears to have accompanied all four depositional stages. Overall, pyrite probably represents about 70% of sulphides deposited, although this varies widely. Fine grained subhedral to euhedral pyrite - quartz intergrowths are crosscut and replaced by later main stage sulphides. Coarse grained euhedral growth zoned pyrite occurs in quartz with minor early sphalerite (Figure 4-23); the bulk of sphalerite deposition is accompanied by later fine grained pyrite. Pyrite commonly occurs as elongate grains in feathery or dendritic forms possibly due to rapid crystallization (Figures 4-24 and 4-25). This might be related to sudden pressure decreases associated with brecciation or major porosity increases. Similar forms have been ascribed elsewhere to replacement of an earlier iron bearing phase, such as hematite or marcasite (e.g., Craig and Vaughn, 1977). At Midway, however, there is no evidence of primary hematite or marcasite in any of the sulphide bodies, and therefore this

Table 4-2: Mineralogy and paragenetic sequence, Midway deposit, northern British Columbia (1040/16).

ASSEMBLAGE / MINERAL	SILICA - PYRITE	SULPHIDE - SILICA	SULPHIDE - SULPHOSALT	CARBONATE
Quartz	--------	----------	--------	
Pyrite	------	----------	---	---
Arsenopyrite	---	-----		
Pyrrhotite		----------		
Sphalerite		----------	---	
Chalcopyrite		----		
Stannite		----		
Galena		-------	-------	
Geocronite		----	----------	
Franckeite			--------	
Freibergite			--------	
Acanthite			--------	
Boulangerite			--------	
Pyrargyrite			--------	
Barite			? ---- ?	
Calcite				----
Gypsum				---
Marcasite				---
Cassiterite		?		

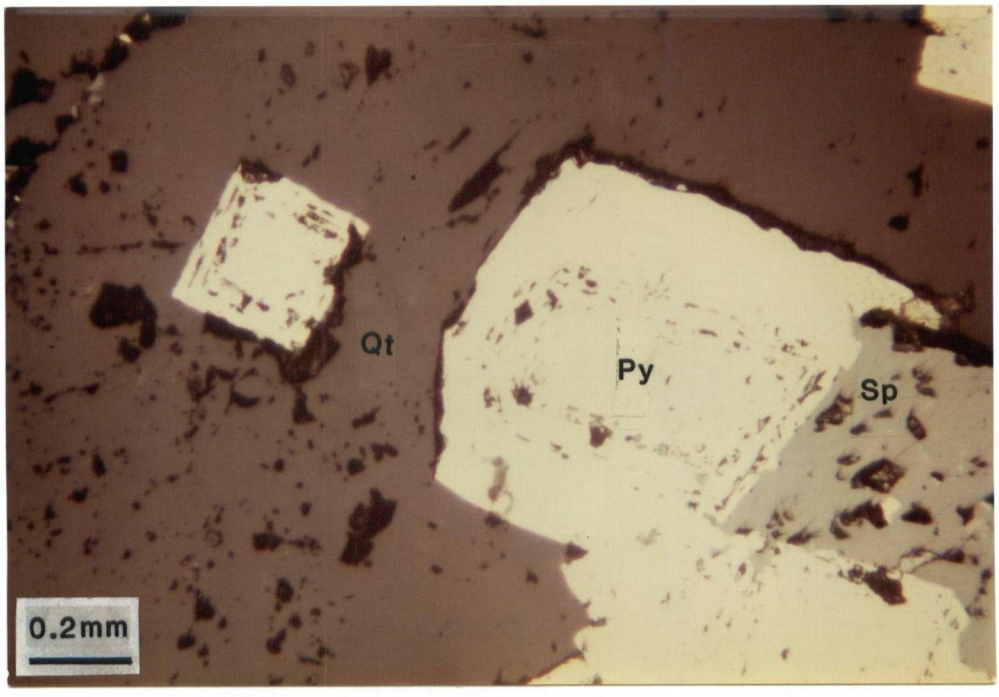

Figure 4-23: Photograph of growth zoned pyrite, with sphalerite in a quartz matrix (MW 207, 10.6 m).

Figure 4-24: Photograph of feathery pyrite interlayered with sphalerite - galena and quartz (MW 77, 303 m). Scale is in centimetres.

habit must be considered to be a primary feature of pyrite deposition. These dendritic forms locally have a preferred orientation with respect to layering and thus define a tops direction with respect to deposition. Other dendritic forms occur in hemispherical clusters. Galena and sphalerite, probably crystallizing slightly later than pyrite, are interstitial to the feathery aggregates. Locally, open space remains between close fitting pyrite grain clusters. Framboidal pyrite occurs in some shale breccias, with later interstitial galena and sphalerite. Some late euhedral pyrite occurs with galena, sphalerite, and quartz as vug fillings in pre-existing sulphide, and in late crosscutting calcite veinlets. Thus the range of pyrite deposition spans the entire evolution of the Midway hydrothermal system.

Arsenopyrite occurs as a main stage phase, overgrowing pyrite or sphalerite, and being overgrown by galena or galena - sulphosalt assemblages. Some arsenopyrite occurs in vugs on earlier sulphide, filled by later calcite or quartz (Figure 4-26).

Pyrrhotite is abundant in places at Midway, generally occurring with galena and sulphosalt - poor assemblages. Intergrowths with pyrite, sphalerite, and chalcopyrite are common (Figure 4-27). Locally, pyrrhotite occurs as a matrix to

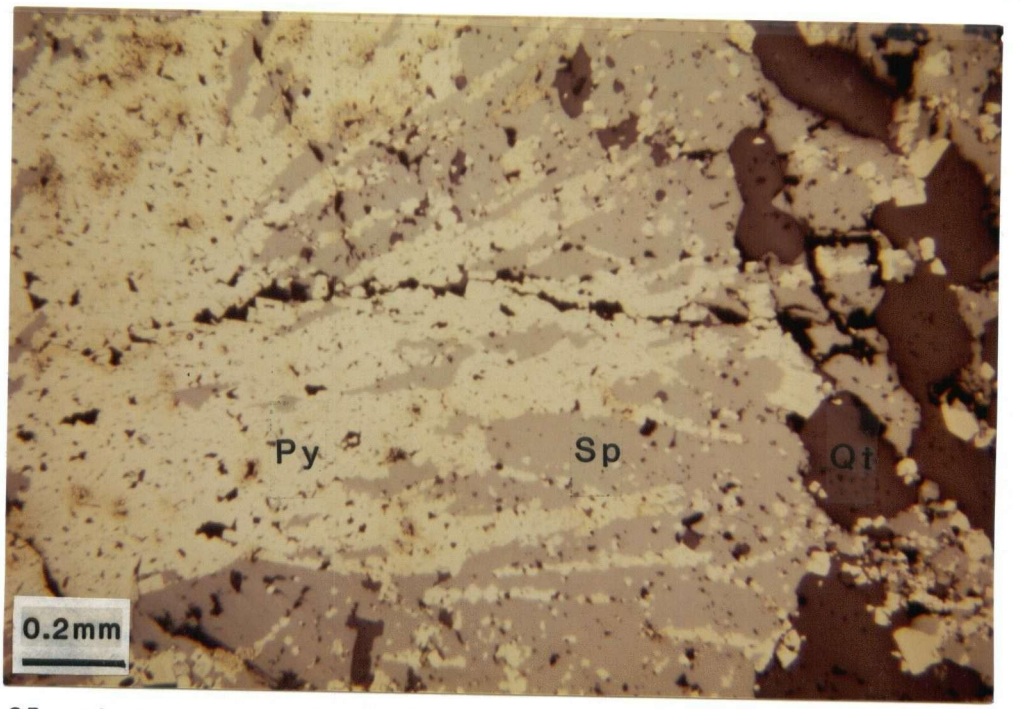

Figure 4-25: Photograph of feathery pyrite enclosed by sphalerite, with subhedral quartz (MW 178, 14.5 m).

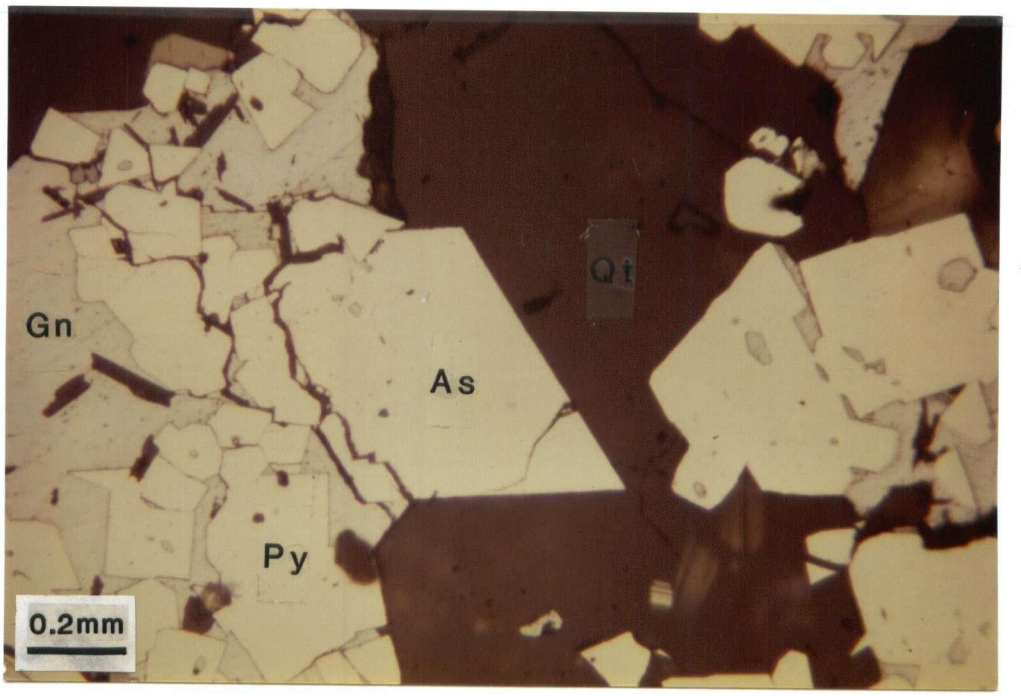

Figure 4-26: Photograph of arsenopyrite overgrowing pyrite and galena, and enclosed in quartz (MW 77, 305.5 m).

pyrite clasts, whereas in other places it is cut by later pyrite veinlets.

Sphalerite is the second most abundant sulphide, and occurs interstitially to and overgrows early pyrite, commonly intergrown with a later pyrite phase. Sphalerite occurs both as fine grained dense intergrowths with pyrite, and as interlocking pyrite free grains. Sphalerite and galena deposition are for the most part coeval, but in places earlier sphalerite - pyrite is crosscut by later sphalerite - galena. Fractured sphalerite locally occurs as mosaics in a pyrite matrix.

Stannite and chalcopyrite are commonly associated with sphalerite in copper and tin rich assemblages. Stannite ($Cu_2(Fe,Zn)SnS_4$) occurs as irregular blebs or fine exsolution intergrowths, and is often found along sphalerite - galena or sphalerite - pyrite grain boundaries (Figure 4-28). Chalcopyrite occurs as small blebs and crystallographic intergrowths (chalcopyrite "disease") in sphalerite, and as rims on pyrrhotite. In places transitions from sphalerite to stannite to chalcopyrite give evidence of zinc - copper gradients.

Galena overlaps sphalerite and pyrite in main stage sulphide deposition, but is also a major component of later sulphosalt rich assemblages. Complex intergrowths of galena,

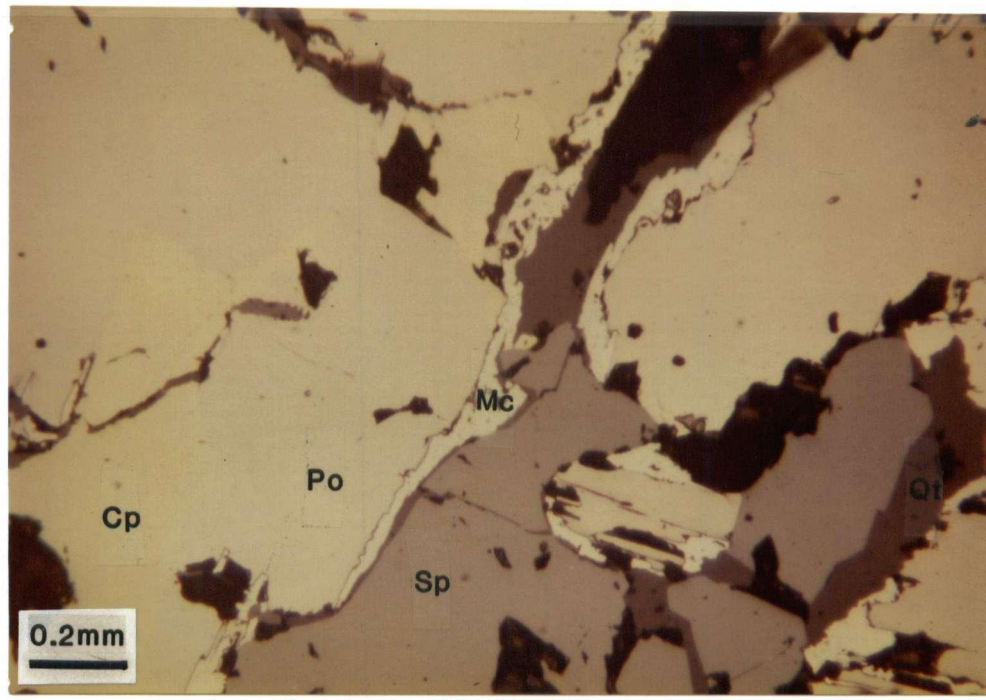

Figure 4-27: Photograph of intergrown pyrrhotite and chalcopyrite with sphalerite and quartz. Pyrrhotite is being replaced by marcasite along grain boundaries (MW 84, 317 m).

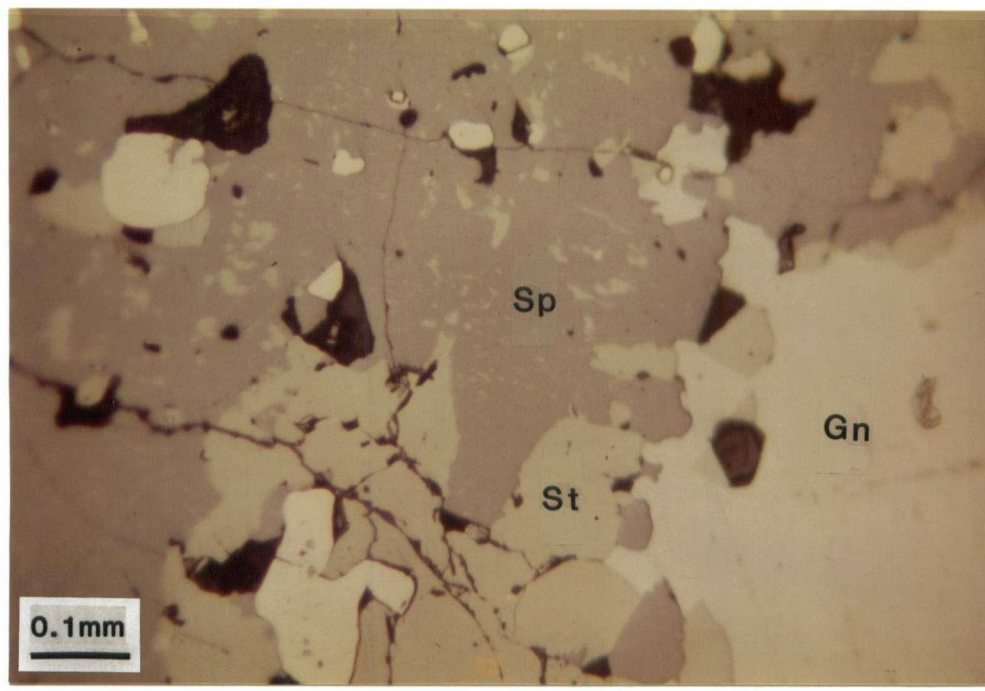

Figure 4-28: Photograph of intergrown stannite and sphalerite, with pyrite and galena (MW 77, 307 m).

geocronite (Pb_5SbAsS_8), franckeite ($Pb_5FeSn_3Sb_2S_{14}$), and tetrahedite crosscut, replace, and overgrow earlier (main stage) pyrite and sphalerite (Figures 4-29 and 4-30). Sulphosalts also crosscut earlier galena. Tetrahedrite (variation freibergite: Archambault, 1985) occurs within galena and along galena - sphalerite grain boundaries. Locally, densely intergrown galena and tetrahedrite occur in silver rich assemblages (Figure 4-31). Pyrargyrite ($Ag_{33}SbS_3$) locally accompanies the late sulphosalt - sulphide phase, occurring as minute blebs and stringers in galena.

Tin bearing sulphosalt assemblages (Figure 4-32) are known from tungsten - tin - silver deposits in Bolivia and Peru. Geocronite almost invariably occurs in carbonate hosted deposits (Birnie and Petersen, 1977). Franckeite occurs in minor amounts at the Renison Bell tin mine, Tasmania (Stillwell and Edwards, 1943). The Marion showing in the Coal River area, Yukon Territory (NTS map area 95E) contains a mineral assemblage almost identical to that of Midway (Evans, 1959). This showing is a sulphosalt bearing calcite vein in slate, and is probably associated with poorly exposed tourmaline rich stocks which have been dated at about 70 Ma.

Quartz, like pyrite, occurs throughout sulphide deposition, but is most abundant during early quartz - pyrite and main

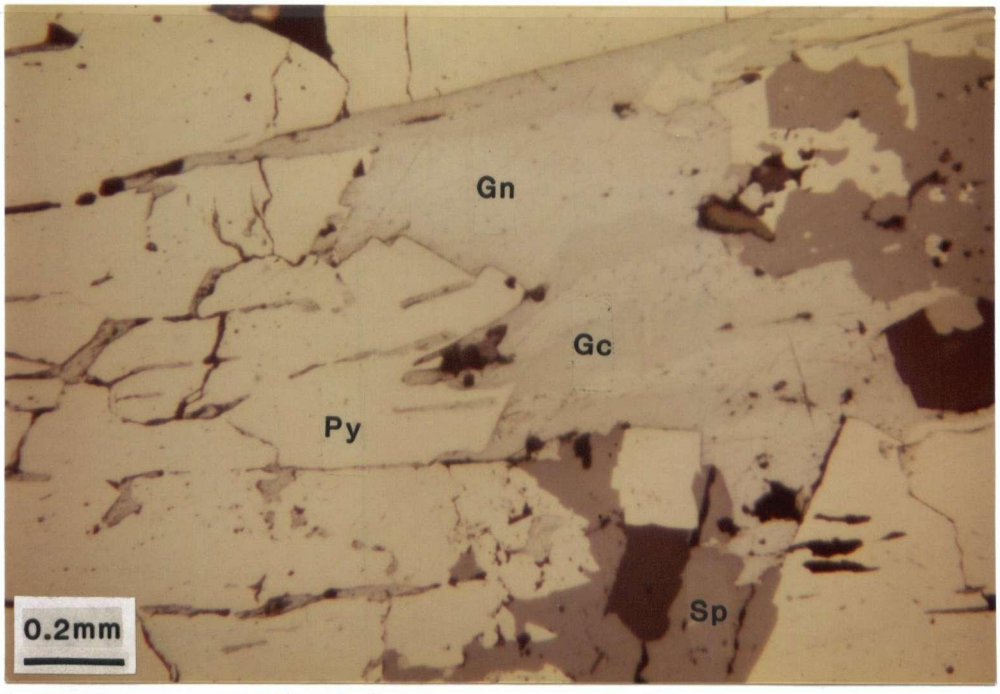

Figure 4-29: Photograph of intergrown galena, geocronite, and sphalerite replacing pyrite along fractures and grain boundaries (MW 143, 2.3 m).

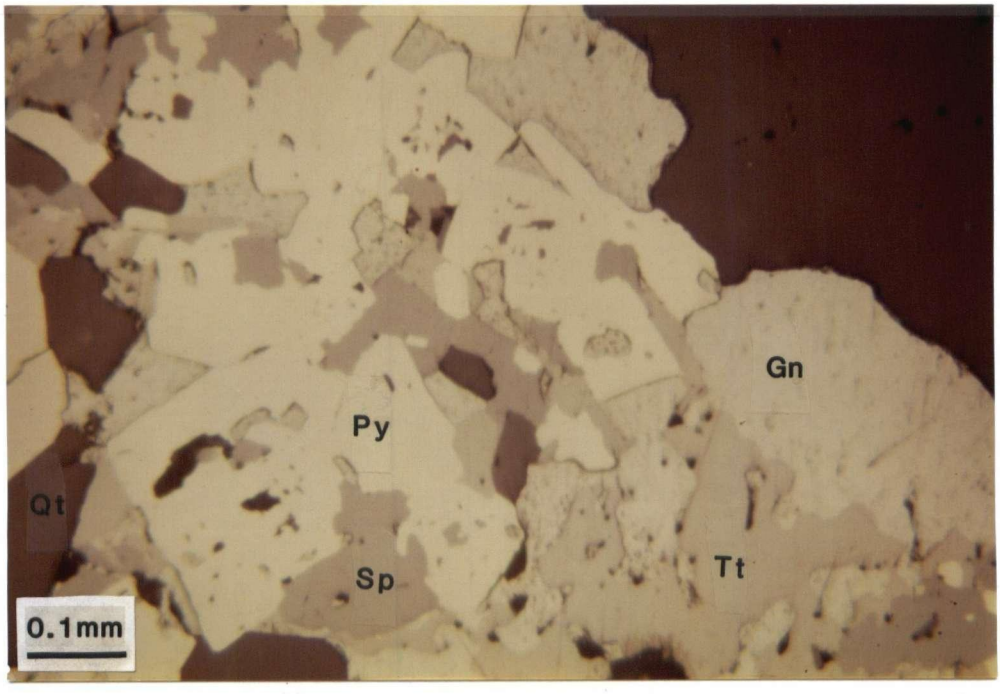

Figure 4-30: Photograph of geocronite - galena - tetrahedrite - sphalerite replacing pyrite (MW 204, 5.2 m).

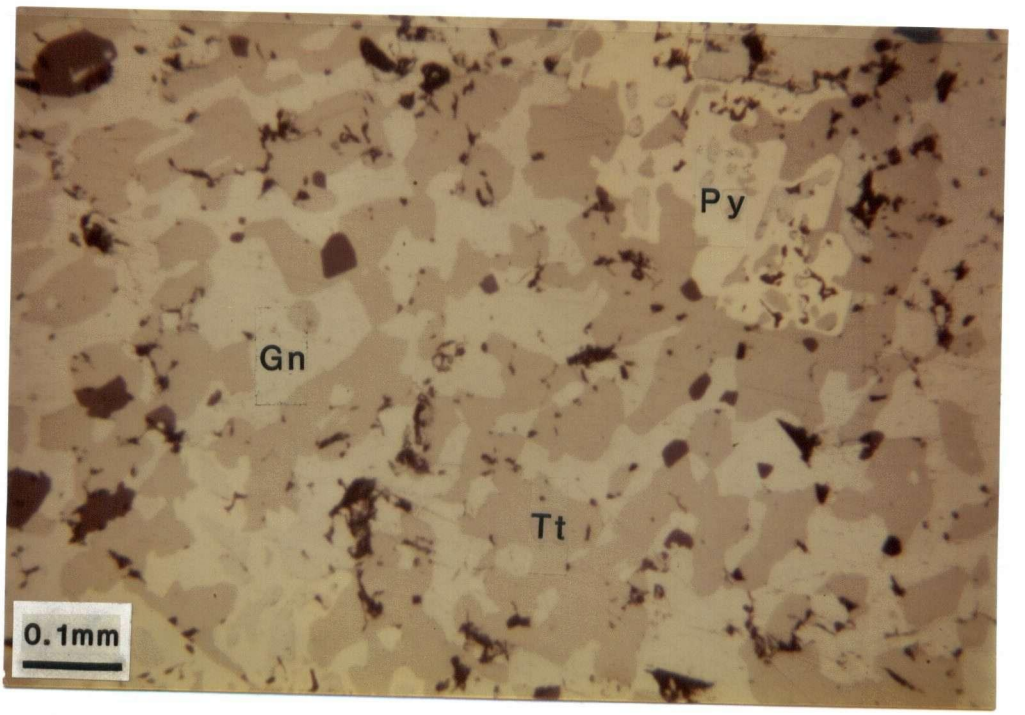

Figure 4-31: Photograph of "myrmekitic" galena - tetrahedrite, replacing pyrite (MW 204, 6.8 m).

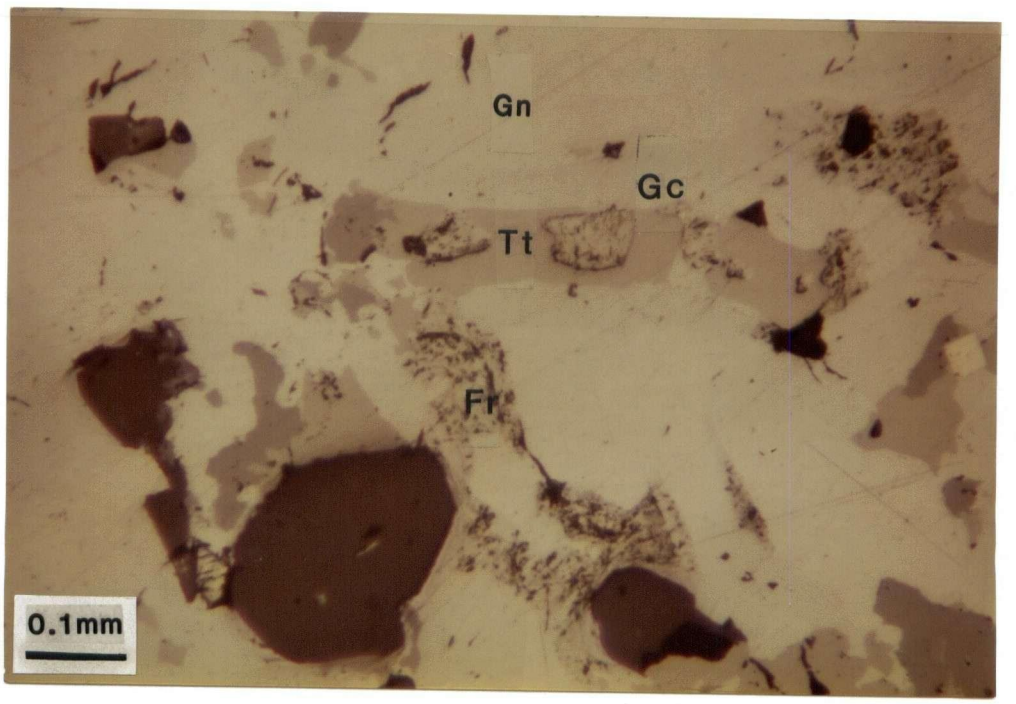

Figure 4-32: Photograph of intergrown galena - geocronite - tetrahedrite - franckeite - quartz (MW 143, 2.3 m).

sulphide stages. Quartz is the most abundant non - sulphide component of Midway mineralization, forming 5 to 50% of most assemblages. Aggregates of clear euhedral grains in sulphide are common, as are masses of white quartz in silicified haloes replacing carbonate adjacent to sulphide zones. Thin quartz rims occur around shale fragments in sulphide - matrix breccias, testifying to early silica deposition. Late veinlets crosscut sulphides locally, and beautiful late euhedral crystal clusters in vugs are common.

Barite occurs as coarse euhedral crystals both intergrown with sulphides and in vugs. Colour ranges from grey to yellow to pale green. Barite overlaps with latest deposition of sulphides, but is believed to be a late phase on the basis of its habit.

Calcite associated with sulphide bodies occurs invariably as a late phase, primarily as veinlets crosscutting all assemblages (Figure 4-33), and as matrix to sulphide - quartz breccias. Some coarse calcite spar occurs as sulphide overgrowths and vug fillings.

Marcasite occurs primarily as a postmineral replacement, probably associated with supergene meteoric water infiltration. Pyrrhotite is replaced by marcasite outward from fractures

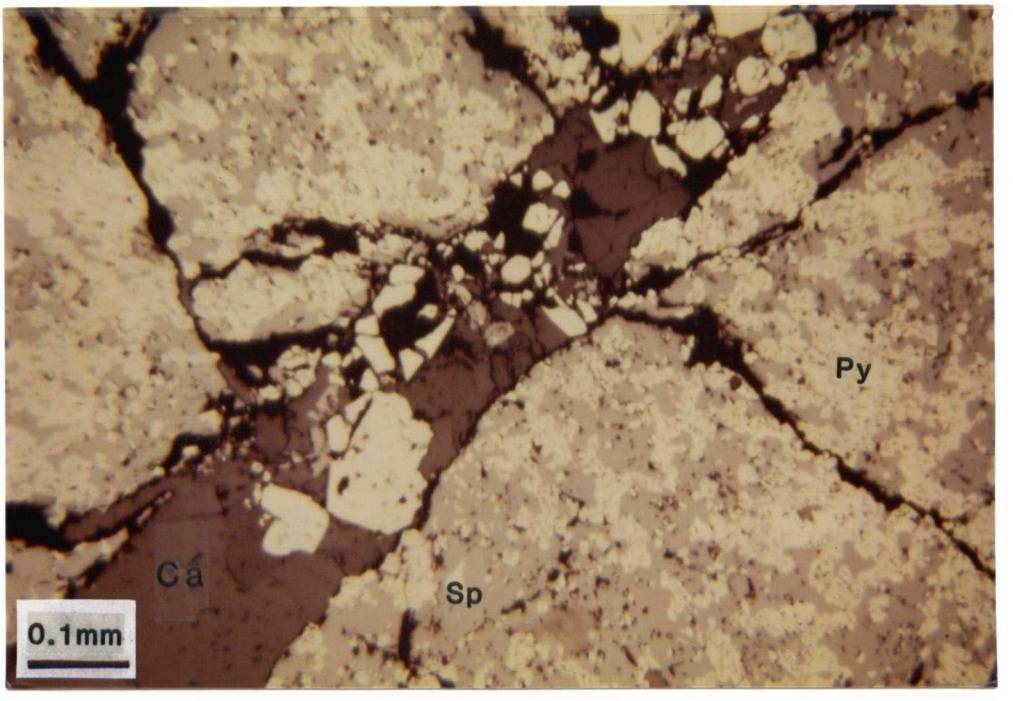

Figure 4-33: Photograph of a calcite veinlet with late pyrite crosscutting intergrown pyrite - sphalerite (MW 144, 8.5 m).

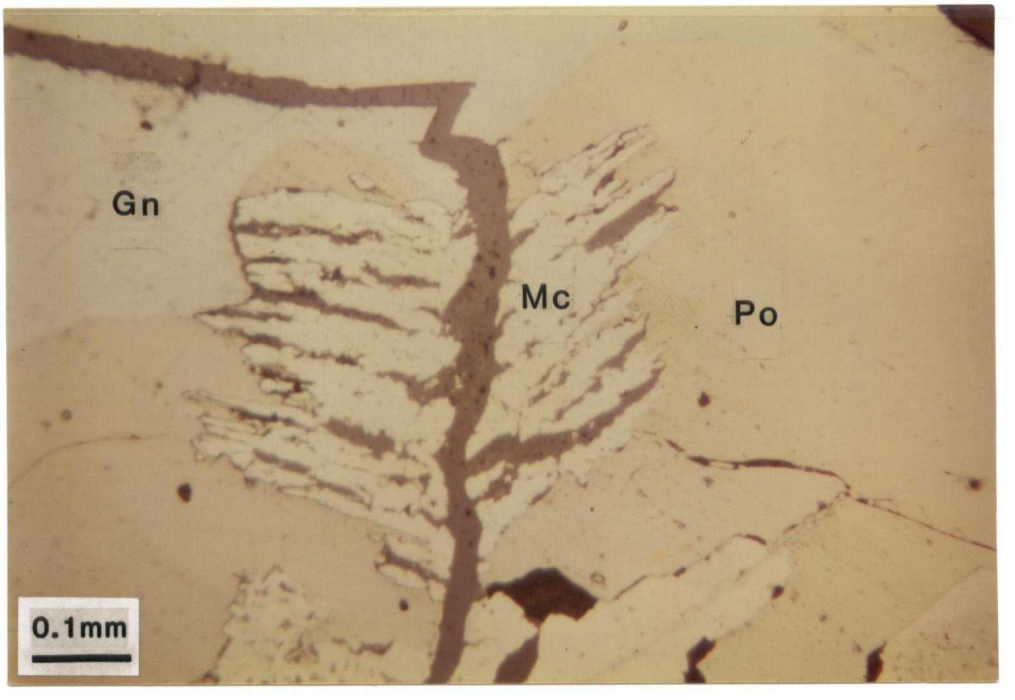

Figure 4-34: Photograph of marcasite replacing pyrrhotite outwards from a fracture. Note how the marcasite stops at the galena - pyrrhotite boundary (MW 84, 316 m).

(Figure 4-34). Locally pyrite - pyrrhotite intergrowths are pervasively altered to marcasite.

Gypsum, another postmineral phase, occurs as coarse, euhedral crystals in vugs. It may have been deposited from cool, sulphate rich vadose waters, which extracted calcium from surrounding carbonates.

4.4.7. Mineral and Metal Zoning

Manto deposits commonly show a district scale compositional or mineralogical zonation, reflecting temperature and chemical gradients with respect to the intrusive heat ± volatile source, and pressure gradients with respect to surface (e.g. Darwin, California: Hall and MacKevett, 1962; Zimapan, Mexico: Simons and Mapes, 1956). Exploration at Midway has been sufficient to indicate analogous zoning patterns. Within the Silver Creek deposit, a north - south transect (Figure 4-35) shows an apparent mineralogical shift which might be a function of distance from heat source and depth. The transition occurs over a distance of about 300 metres. In the northern part of the deposit, near DDH MW 60 and Fan B129 (Figure 4-4), sulphides have high lead sulphosalt contents, commonly up to 15%, and locally as high as 40%. Drill hole MW 77 (LZ 1) contains minor sulphosalts while deeper zones and zones to the south have very

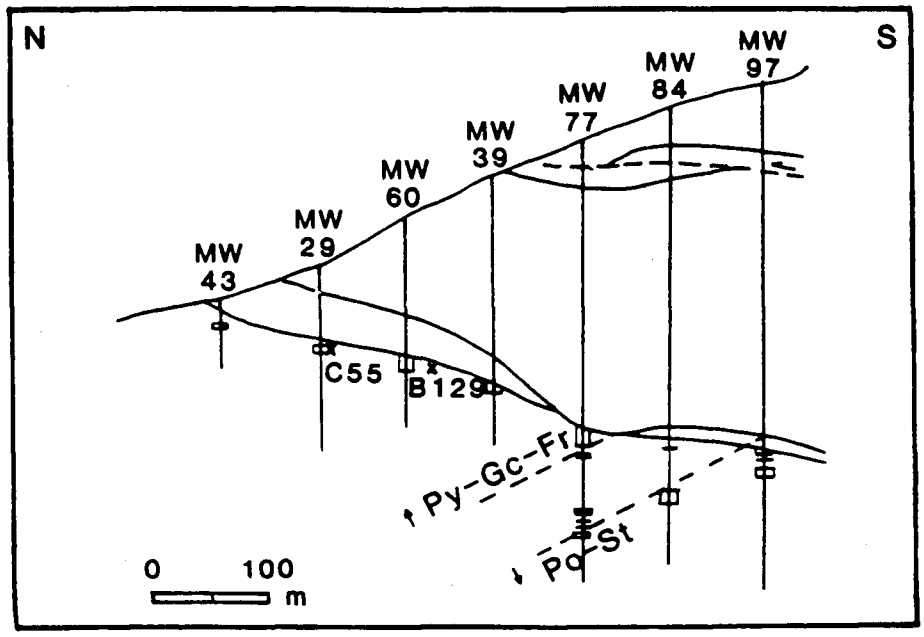

Figure 4-35: North - south cross section through the Silver Creek deposit showing the transition from pyritic assemblages with abundant geocronite and the tin sulphosalt franckeite to pyrrhotitic assemblages with rare sulphosalts and stannite as the main tin bearing mineral.

low sulphosalt contents*. High sulphosalt intersections coincide with high silver values. In high sulphosalt sections, Pb/(Pb+Zn) ranges from 0.35 to 0.60, which decreases in deeper zones to the south to 0.10 to 0.20 (Figure 4-9). Silver shows a correlative decline from 150 to 700 grams/tonne, to 100 to 150 grams/tonne.

In addition to indicating a possible zonation with respect to heat source and depth, such transitions could also be a function of pre - existing permeability, with high Pb/Zn and high Ag/Pb representing zones of high permeability (Birnie and Petersen, 1977).

Abundant pyrrhotite occurs in the southern part of the Silver Creek deposit (Figure 4-4: DDH MW 84 (LZ 2) and MW 97 (LZ 1, 2)). Pyrrhotite also occurs in the lowermost sulphide zone in MW 77 (LZ 9) (Figure 4-35). Pyrrhotitic assemblages predominate

---

* LZ refers to carbonate - hosted mineralized zones, which are numbered consecutively from highest to lowest. "Fan C55" refers to underground fan drilling stations, with metreage indicated from the beginning of the drifts, which are given letter designations.

in deeper sulphide intersections in the southern part of the Discovery deposit (Figure 4-4: MW 16, 26, 32 and 41), and in DDH B82-1, west of Brinco Hill. These intersections also contain abundant chalcopyite and negligible galena. Copper grades increase from 0.05 to 0.20% in the Silver Creek deposit, to greater than 0.40% in deeper intersections (Figure 4-9). These intersections also contain significant bismuth (up to 0.4%).

The change from galena - sulphosalt to pyrrhotite - chalcopyrite apparently defines a deposit - scale zonation pattern (Cordilleran Engineering, 1983). This provides evidence for relating the alteration zone centred on Brinco Hill to the sulphide pipes at Midway, since similar mineralogical transitions in better explored skarn - manto systems correlate with distance from intrusion, with Fe - Cu rich sulphides representing proximal/deeper, and Pb - As - Sb - rich zones distal/shallower mineralization (e.g. Simons and Mapes, 1956). In addition, deep holes closest to Brinco Hill (MW 26) contain calcsilicates intimately intermixed with pyrrhotite -- skarn mineralogy has not been found elsewhere in the Midway system.

Tin mineralogy is also zoned. Tin grades are high (> 0.1%) in two areas: (1) near DDH MW 60 (LZ 1) to MW77 (LZ 1), and (2) in DDH MW 97 (LZ 1, 3) (Figure 4-4). The two areas differ, in that Sn-Pb sulphosalts (franckeite) are the primary tin -

bearing minerals in the former case, whereas stannite is the only tin mineral in the latter, where it accompanies pyrrhotitic mineralization (Figure 4-35).

In manto - skarn systems elsewhere, distal, shallower sulphosalt rich zones are commonly silver rich, while proximal, deeper, iron - copper sulphide zones are commonly gold rich and silver poor. Therefore, in view of the limited exploration done in areas near Brinco Hill (due to depth of cover rocks), gold bearing mantos and veins in cover rocks could represent an interesting exploration target south of currently explored mineralization.

4.5. Summary of Geology and Mineralization

4.5.1. Sequence of Events

The following summarizes the sequence of geological events in the Midway area, based on the evidence discussed above. This sequence of events is similar to that discussed in Archambault (1985).

1. Middle Devonian: deposition and diagenesis, McDame Group.
2. Late Devonian: uplift of the carbonate platform, subaerial exposure, erosion, block faulting, and karsting of the upper

McDame Group, local solution collapse, generation of enhanced porosity.

3. Late Devonian: subsidence of the carbonate platform, to initial shallow levels, and local deposition of dolomitic siltstones.

4. Late Devonian (Fammenian): Major extension and subsidence of North American shelf margin, with deep water deposition of anoxic basin sediments of the lowermost Earn Group; solution collapse of karsted upper McDame and mixing of shale clasts into collapse breccias and healing of breccias by calcite.

5. Mississipian (Tournasian): deposition of the rest of the Earn Group, including exhalites.

6. Late Triassic to Early Cretaceous: contraction of continental margin due to convergence of suspect terranes, major compressional deformation, and emplacement of allochthonous off shelf and oceanic sediments, volcanics, etc. of Sylvester allochthon.

7. Mid-Cretaceous: continent scale transcurrent and district scale block faulting begins; emplacement of Cassiar batholith.

8. Late Cretaceous: emplacement of higher level felsic intrusions, generation of large scale hydrothermal systems, deposition of sulphide bodies in high porosity zones in the McDame Group and development of hydrothermal breccias.

9. Late Cretaceous: late stage oxidation of hydrothermal system,

calcite deposition and post mineral brecciation.
10. Tertiary: continuation of transcurrent and block faulting and local shearing of sulphide bodies.
11. Tertiary to Recent: erosion and exposure of Silvertip and exhalative mineralization, continued karsting of the McDame Group and generation of supergene assemblages.

4.5.2. Exploration Parameters and Mineralization Controls

The foregoing discussion suggests the importance of several controls on manto type mineralization which could have broader exploration significance. Regionally, localization of intrusive and associated hydrothermal systems along large scale, high angle fault systems is important. Many skarn - manto - vein systems in carbonates in Cassiar Terrane are associated with Late Cretaceous - Tertiary felsic intrusions. Although commonly recessive in outcrop, these tend to generate large alteration haloes in non - carbonate cover rocks, and are associated with F, Sn, W, Mo, Pb and Zn anomalies. Major element geochemistry of these intrusions is similar to that of S-type granites, and trace element signatures of A type granites are likely (W.D. Sinclair, written communication, 1986). Strongly fractionated (volatile enriched) late phases of older intrusions can also be mineralizers.

At the deposit scale, fault control of fluid pathways could be significant in areas with coeval or overlapping intrusion and faulting. At Midway, known sulphides are largely distributed between the Camp Creek and Brinco Creek faults, while no mineralization has been found west of the Silvertip Creek Fault. These faults converge north of Midway; the coincidence of this fault convergence with an antiformal structure above which lies a shale cap of low permeability probably contributed to focussing of hydrothermal fluid migration in the vicinity of the Silver Creek deposit. The southeasterly plunge of this antiform controlled upward and outward migration of fluids from the intrusive center to the trapping structure.

Stratigraphically, both a strongly brecciated, karsted carbonate sequence with enhanced permeability, and less permeable capping sequences are significant controls on sulphide deposition.

Deposit scale mineral zoning can be useful in defining intrusive centres and their spatial relationship to ore bodies. At Midway, sporadic sulphides are found throughout the area bounded by the Camp Creek and Brinco Creek faults in veins in cover rocks as well as in limestone. By comparison with skarn - manto systems elsewhere, major sulphide bodies are probably not limited to the relatively distal unskarned environment of the Silver Creek deposit; mineralization of a different tenor

(e.g. enhanced in copper, gold and bismuth) would be expected closer to the intrusive core of the system.

4.6. Fluid Inclusions

4.6.1. Introduction

Microthermometric studies on fluid inclusions determined some of the characteristics of the hydrothermal fluid from which sulphides at Midway were deposited. Inclusion studies defined the major components of the hydrothermal fluid, and the temperature and pressure under which sulphide deposition occurred. As well, the evolution of fluid composition and temperature over time was constrained. Fluid inclusions were found in quartz intergrown with, and probably coeval with, sulphides. Attempts to use inclusions in sphalerite failed due to the opacity of this phase.

4.6.2. Analytical Procedures

Fluid inclusions in quartz from mineralized zones in the Midway deposit were analyzed using standard microthermometric techniques. Data were obtained with a Fluid Inc. - adapted U.S.G.S. gas - flow heating / freezing system and a Nikon Optiphet microscope with 15x oculars and 4x, 10x and 32x

objectives. Temperatures were monitored with a chromel - constantan thermocouple attached to a Doric Digital Trendicator (Model 410A). The Trendicator thermocouple accuracy was determined to be better than ± 0.4°C from -56.6°C to +660.4°C (Fluid Inc. company data). Gradients within the heating / freezing stage were < 1°C at temperatures < 290°C. Ice and clathrate melting temperatures were generally repeatable to ± 0.2°C. Accuracy of homogenization temperatures varied depending on the type of inclusion, from ± 3°C for relatively low temperature, liquid - rich inclusions to ± 10°C or more for some vapour - rich inclusions. Heating and freezing measurements were obtained using standard "cycling" techniques.

Data were obtained on inclusions from groups exhibiting roughly consistent liquid to vapour ratios in order to minimize effects of necking (cf. Bodnar et al., 1985). Verification of the visual estimate of consistency is shown by consistent (± 10° C) homogenization temperatures within the groups. In some cases a wider range of homogenization temperatures was tolerated if most of the inclusions homogenized within a narrow range. Some groups with extremely variable liquid to vapour ratios were homogenized to determine if the variability were real or due to varying inclusion orientations. These groups gave homogenization temperatures from 100 to over 450° C, which were omitted from the data compilations.

Examples of the types of inclusion groups from which valid temperature determinations were made are shown in Figures 4-36 and 4-37.

4.6.3. Fluid Inclusion Petrography

Valuable information was obtained from inclusion petrography prior to making microthermometric measurements. In many cases, these were the only data obtainable from a sample, because suitable inclusions for heating / freezing measurements did not exist. Useful microthermometric data were obtained from ten doubly polished plates. Of these, five were from two massive sulphide bodies in the Silver Creek deposit: Fan B129 (MW 141 (7.9)), and Fan C55/D23 (MW 204 (5.6), 207 (8.5), 178 (14.5) and 178 (15.0)) (Figures 4-10, 4-11). Two plates were from a quartz - calcite - sulphide vein near the Silver Creek deposit (MW 73 (38.5 and 39.0)), two were from the Discovery deposit (MW 11 (317.65), and 16 (385.8)), and one was from Brinco Hill, about 2 kilometres southeast of Midway (Figure 4-1). No heating / freezing data was obtained from ten other plates, although useful petrographic information was obtained. Of these, seven were from the Silver Creek deposit, two from exhalative sulphides in the Earn Group, and one from the Discovery deposit. In cases where no microthermometric data were obtained, either

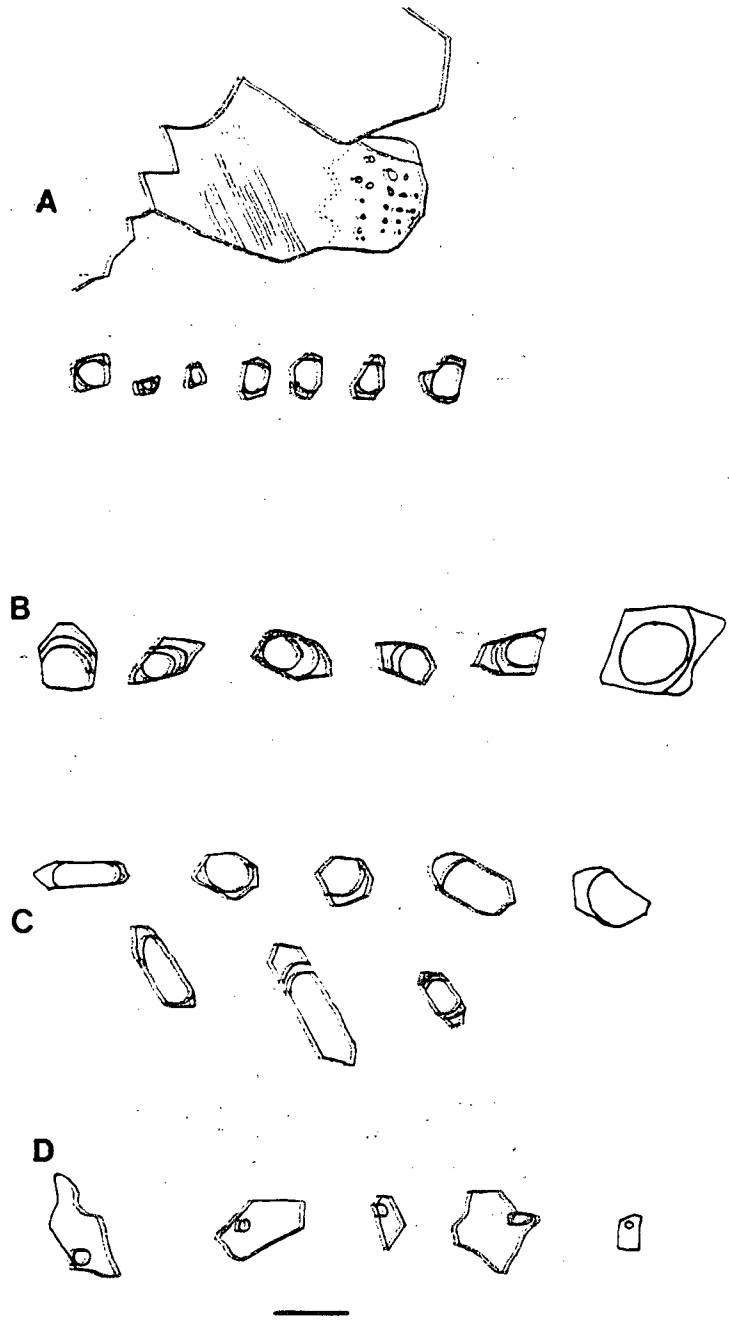

Figure 4-36: Line drawings of fluid inclusion groups: (A) type 1 primary inclusions from quartz grain surrounded by sphalerite and quartz, showing size gradation of type 1 inclusions, picket fence growth zone, and subparallel secondary planes (MW 204, 5.2 m); (B) type 2 inclusions with CO_2 densities varying from 0.26 to 0.6 g/cc; not drawn are associated type 1 and type 3a inclusions (MW 207, 8.5 m); (C) type 1 and 2 inclusions (MW 204, 5.2 m); (D) type 4 inclusions (MW 204, 5.2 m). Scale bar is 10 microns long.

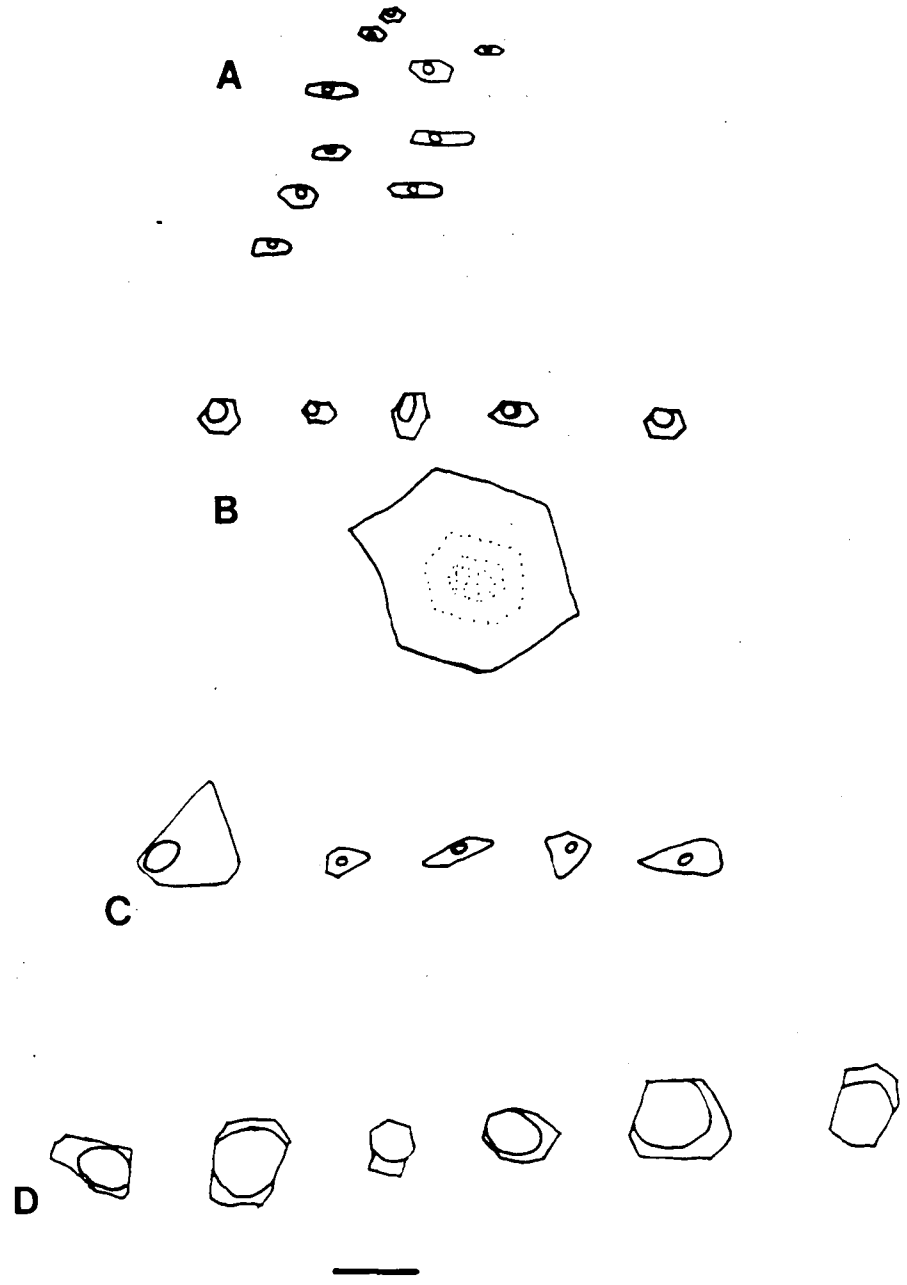

Figure 4-37: Line drawings of fluid inclusion groups: (A) type 3b secondaries; plane of inclusions dips to the right (MW 141, 7.9 m); (B) type 3a inclusions from euhedral growth zoned grain about 0.35 mm across; inclusions are from the inclusion rich core (MW 73, 39.0 m); (C) type 3b inclusions (MW 73, 39.0 m); (D) type 1 inclusions (MW 178, 14.5 m). Scale bar is 10 microns long.

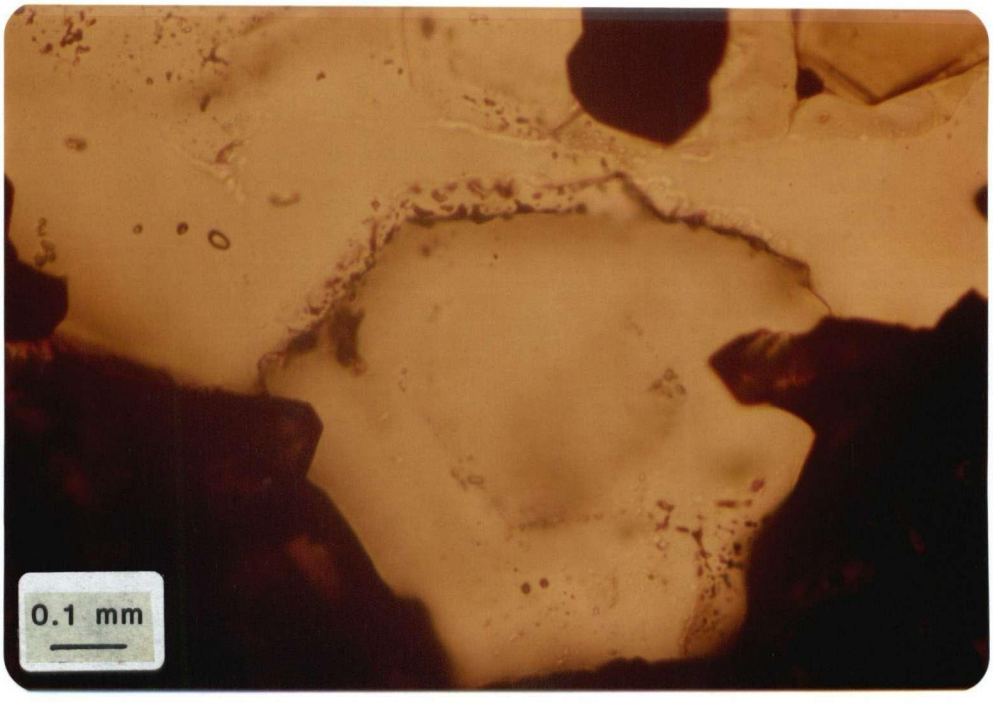

Figure 4-38: Photograph of growth zoned quartz with type 3a inclusions defining the growth zone and type 1 inclusions along the grain boundary (MW 204, 5.6 m).

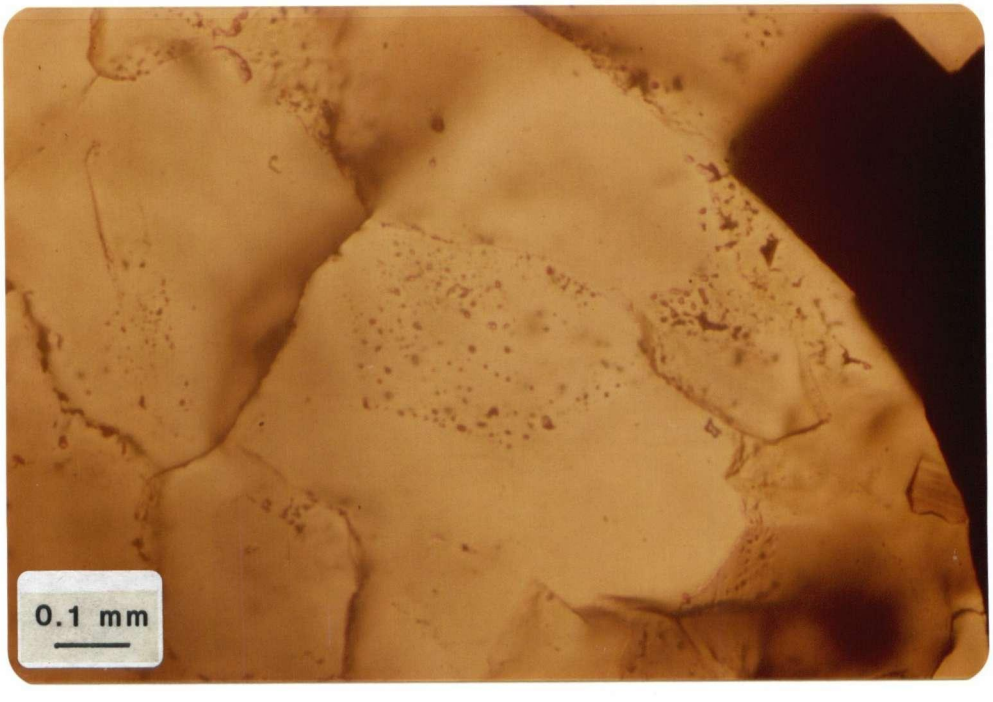

Figure 4-39: Photograph of type 3a and type 1 primaries in an inclusion rich quartz core overgrown by inclusion free quartz (MW 204, 5.6 m).

no inclusions were visible or the inclusions exhibited highly variable liquid to vapour ratios.

Inclusions typical of both primary and secondary origin are abundant, as are inclusions for which there is no conclusive evidence of origin. Primary inclusions occur along crystallographically - oriented growth zones in quartz (Figure 4-38) as well as in hexagonal quartz crystal cores overgrown by relatively inclusion-free quartz (Figures 4-39, 4-40). Commonly, these core inclusions are densely packed and have extremely variable liquid to vapour ratios (Figure 4-41). Vapour rich inclusions are abundant in these groups. Primary inclusions locally show a size gradation from core outward, generally from larger to smaller. Growth zoning is in some cases multi-episodic (Figure 4-42). Inclusions trapped along growth zones are commonly small (< 5 microns), irregular and exhibit variable liquid to vapour ratios, and consequently are unsuitable for heating measurements.

Secondary inclusions occur along flat or curviplanar healed microfractures (Figure 4-43), both crosscutting grain boundaries and terminating within the grain. The latter are called pseudo - secondaries if inclusions of the same type, composition and homogenization temperature occur also as primaries. As such, "pseudo - secondary" is not a purely textural distinction.

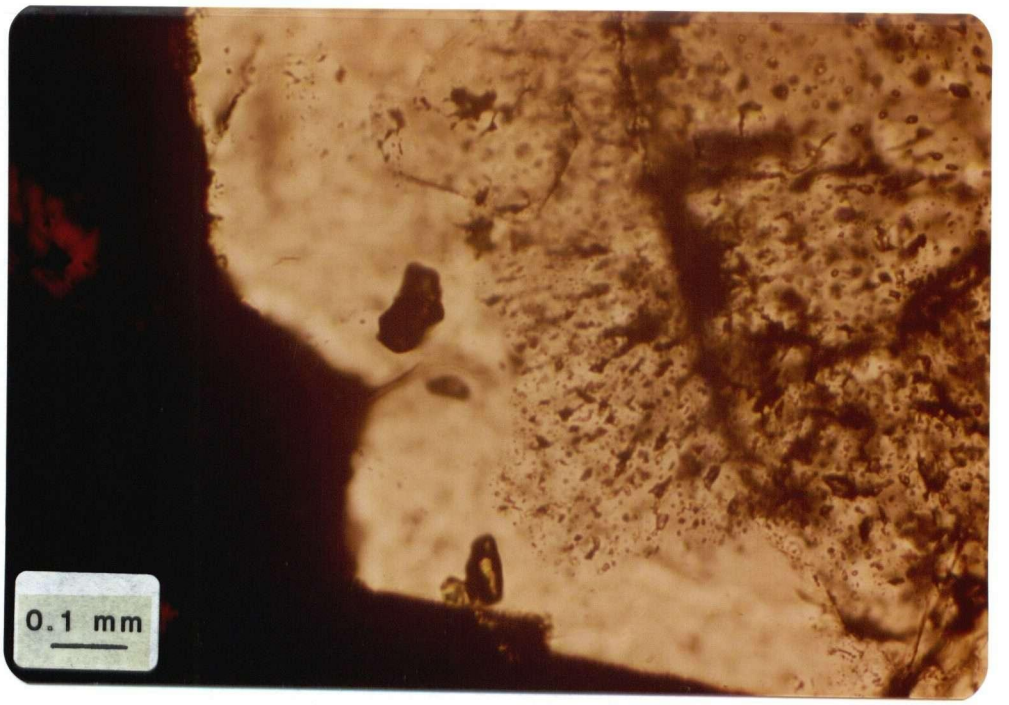

Figure 4-40: Photograph of an inclusion rich quartz core containing mainly type 1 inclusions, overgrown by inclusion free quartz (MW 204, 5.6 m).

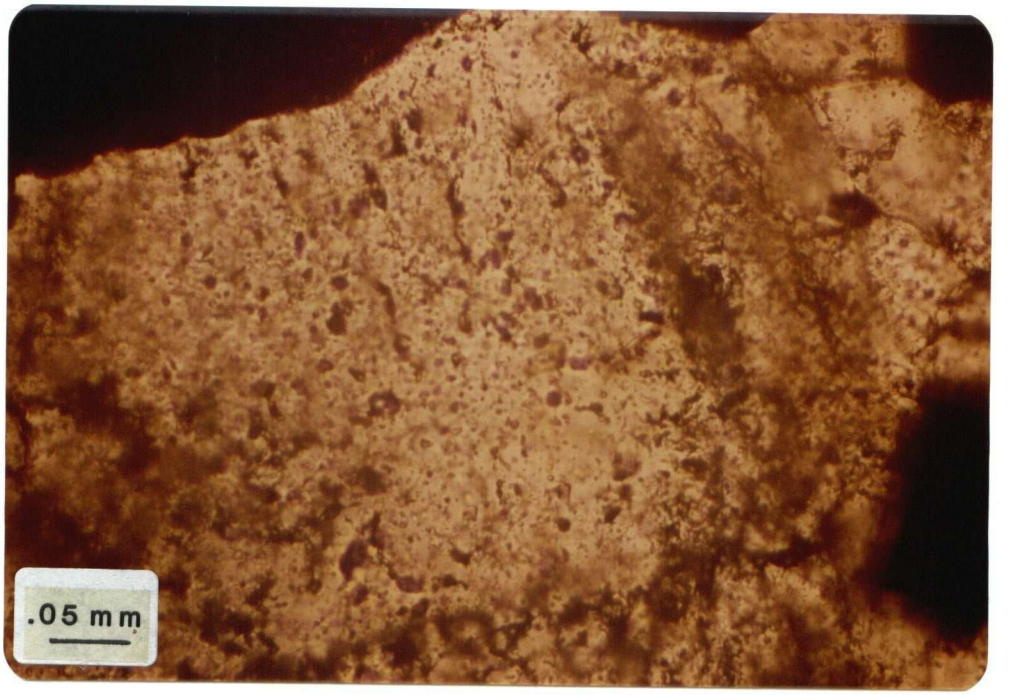

Figure 4-41: Photograph of inclusion rich quartz containing mainly type 1 inclusions.

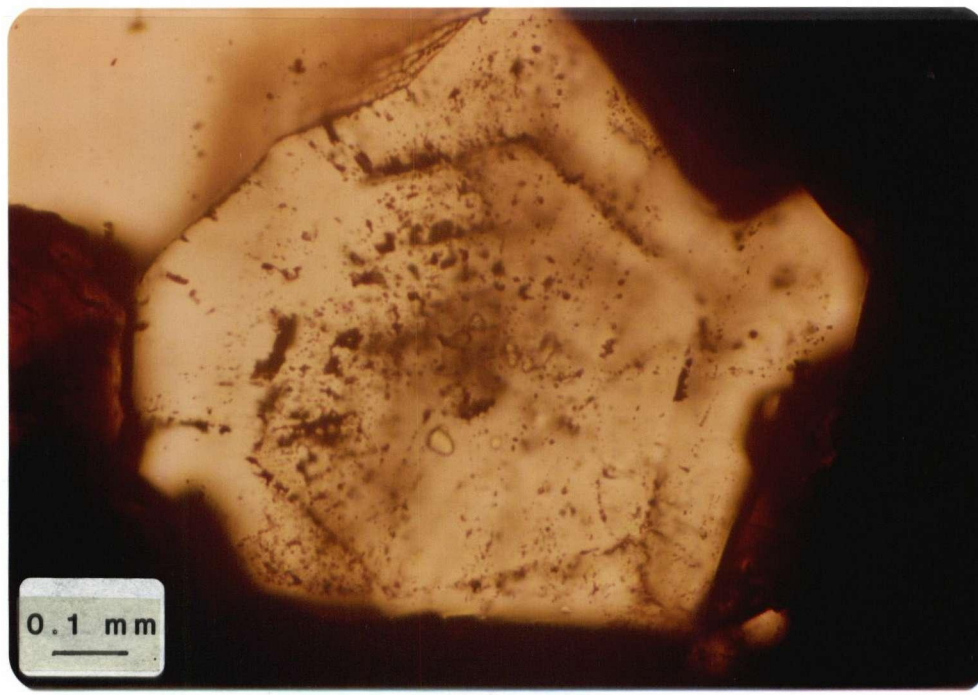

Figure 4-42: Photograph of multi - episodic growth zoning in quartz dominated by type 1 inclusions.

Figure 4-43: Photograph of cross-cutting type 3a secondary inclusion planes (MW 73, 39.0 m).

Texturally distinguished pseudo - secondary inclusions are identifiable only if the healed microfracture terminates against a primary crystallographic feature (e.g. growth zone) within the grain. These were rarely identified. Secondary inclusions provide evidence for multi - episode microfracturing and healing after deposition of quartz and associated sulphides. Commonly the microfractures have a subparallel orientation which is consistent from grain to grain within a sample. In other cases they crisscross, with no dominant orientation (Figure 4-43).

Two features of secondary inclusions indicate that mineralization occurred at a depth greater than that characteristic of epithermal deposits. One is the presence of "wispy" textures caused by swarms of crosscutting microfractures defined by very small inclusions (Figure 4-44). This texture commonly occurs in quartz less than a millimetre away from clear quartz with few or no microfractures. These two different types of quartz probably represent two temporally separate phases, but textural evidence for this is equivocal. The other feature is the presence of abundant three - phase (H_2O liquid, CO_2 liquid and CO_2 vapour) inclusions. These two features taken together are not known in the epithermal environment, but are common in both porphyry systems and so - called "mesothermal" quartz veins (T.J. Reynolds, personal communication, 1987).

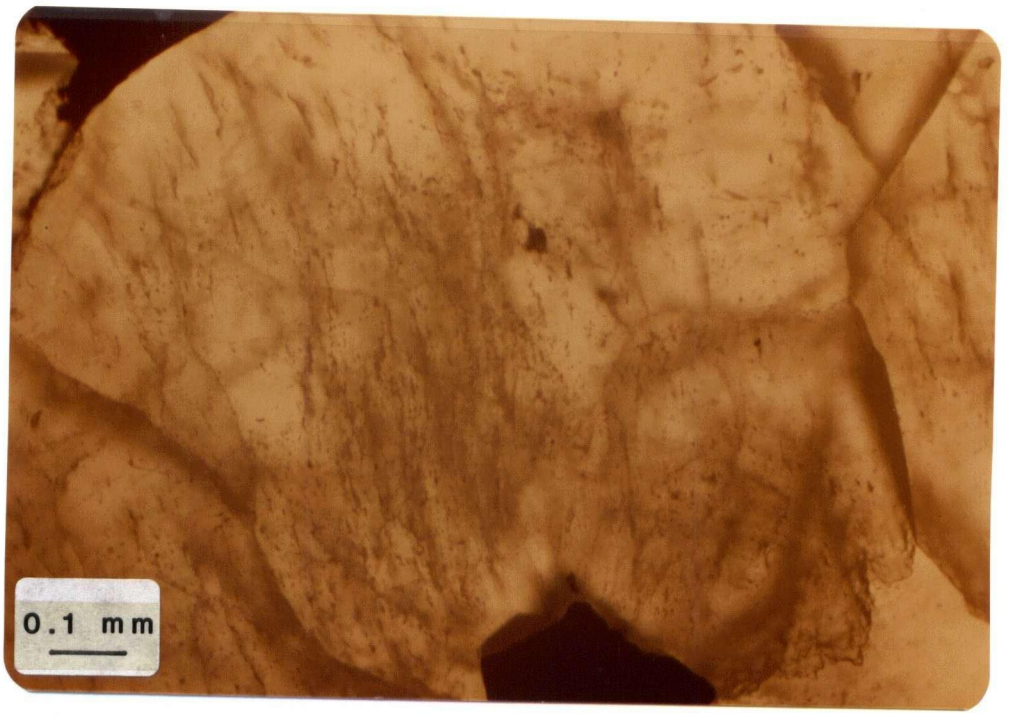

Figure 4-44: Photograph of "wispy" textured quartz produced by myriad irregular planes of minute secondary inclusions (MW 178, 14.5 m).

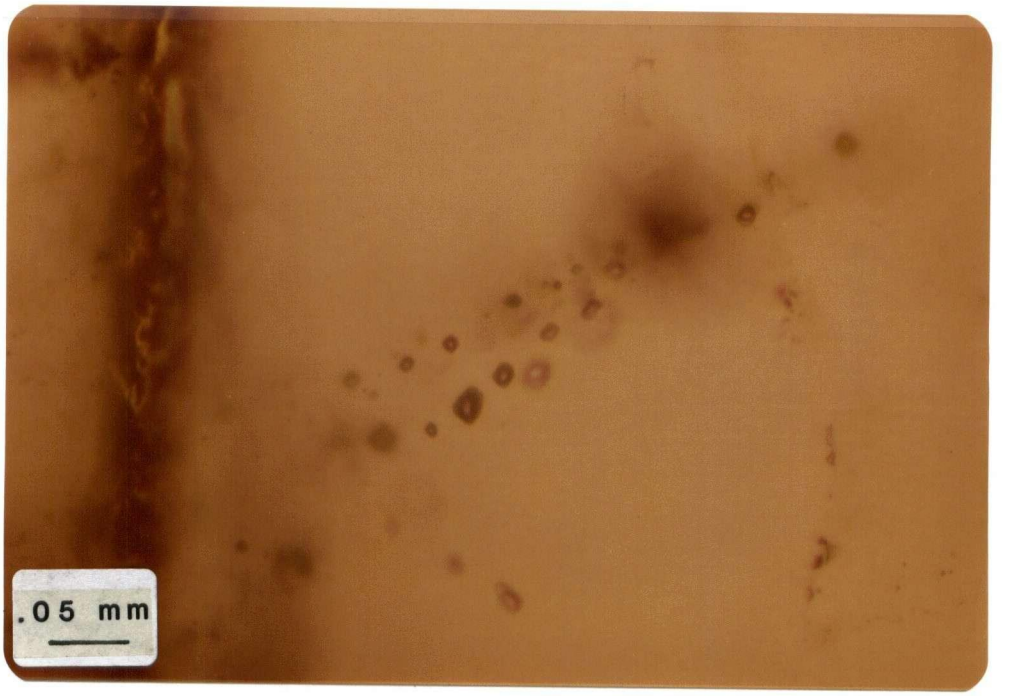

Figure 4-45: Photograph of a plane of type 1 pseudosecondary inclusions (MW 178, 14.5 m).

Figure 4-46: Photograph of equant type 3a secondary inclusions. (MW 73, 39.0 m).

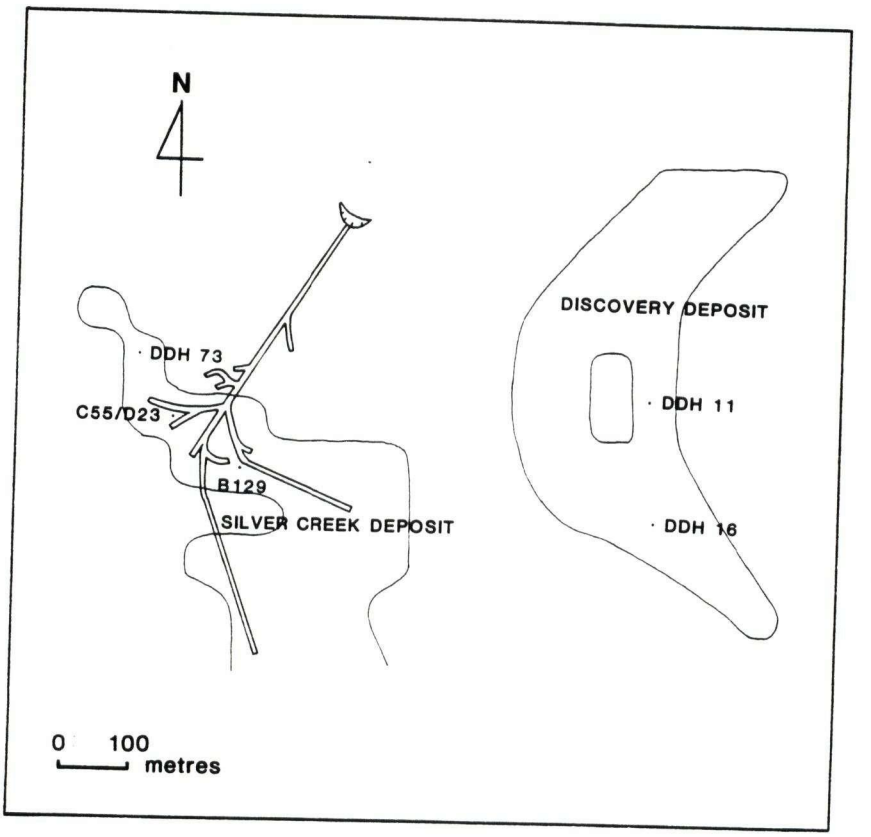

Figure 4-47: Map of fluid inclusion sample locations.

Quartz used in microthermometric studies is intimately intergrown with sulphides, and commonly contains sulphide inclusions. The presence of intergrown quartz, sphalerite and galena in the samples studied from the Silver Creek deposit suggests that the quartz was deposited with main stage sulphides (section 4.4.6). Temperature determinations therefore apply to the fluids involved in this stage of sulphide deposition, as well as in later microfracturing events. Timing of microfracturing is not constrained relative to the sulphosalt - sulphide and late carbonate paragenetic episodes.

4.6.4. Inclusion Types and Data

Microthermometric data are summarized in Table 4-3, and a comprehensive compilation of observations and data is contained in Appendix B. Histograms of data, arranged according to inclusion type, are in Figures 4-48, 4-49, 4-50 and 4-51. Homogenization temperatures span a wide range, from about 120°C to 340°C. Because all of this data were obtained from groups which exhibit fairly consistent liquid to vapour ratios and which homogenize commonly within a range of 25°C, these are all valid temperatures. The temperature range is therefore real for the most part, and not a product of post - trapping modification.

Table 4-3: Fluid inclusion data, summarized by inclusion type, Midway area, north-central British Columbia (1040/16). Dash indicates that no data is available. All temperatures are in degrees Celsius.

Inclusion type[1]	1	2	3a	3b	4
T_h	279-340	272-330	267-330	182-213	122-176
T_mCO_2	-57.1 to -61.8	-56.8 to -58.7	-56.6 to -57.2	-56.6	-
T_e	-	-21 to -40	-	-	-
T_mice	-	-	-14.4 to -17.4[2]	-4.3 to -6.7	-6.4 to -7.1
$T_mclathrate$	9.8-12.6	9.2-11.6	6.9-8.8	6.0-6.8	-
T_hCO_2	-	21.0 to 31.2	-	-	-
Tdecrep.	> 400	350-400	-	-	-

1. Type 1 = vapour rich.
   Type 2 = three phase (CO_2 liquid, CO_2 vapour, H_2O liquid).
   Type 3a = liquid rich, high T_h, CO_2 bearing.
   Type 3b = liquid rich, moderate T_h, CO_2 bearing.
   Type 4 = liquid rich, low T_h, no CO_2.

2. Atypical inclusions only, with liquid/vapour = 0.5; can homogenize to vapour or liquid, but included in type 3a because of T_mCO_2 (=-56.6°C).

Most inclusions are CO_2 bearing, and most of these have CO_2 melting temperatures less than -56.6°C, indicating the presence of another volatile phase. In addition, clathrate formation is common, but clathrate melting temperatures are generally greater than 10°C. Both of these observations imply the presence of methane (Burruss, 1981). Methane as an additional volatile phase is also consistent with the circulation of fluids in organic rich carbonates (McDame Group), and with the presence of reduced carbon in the form of pyrobitumen in veins in the Midway area. It is also consistent with a high sulphide/sulphate ratio in the fluid system, based on sulphide assemblages and sulphur isotope variability (section 4.7.3).

Inclusions observed in Midway quartz can be classified into five main types (Table 4-3). In addition to these types, one phase inclusions and two inclusions with daughter minerals were noted.

Type 1 (vapour rich, H_2O-CO_2-CH_4+NaCl) inclusions (Table 4-3, Figure 4-48) are vapour rich inclusions which homogenize to vapour or, less commonly, by critical phase change (see below). They are very common in parts of the deposit, and are conspicuous, with glossy black bubbles which appear to occupy from 60 to 100% of the inclusion volume (Figure 4-36, A and C; Figure 4-37D). They occur in groups of mixed inclusion types

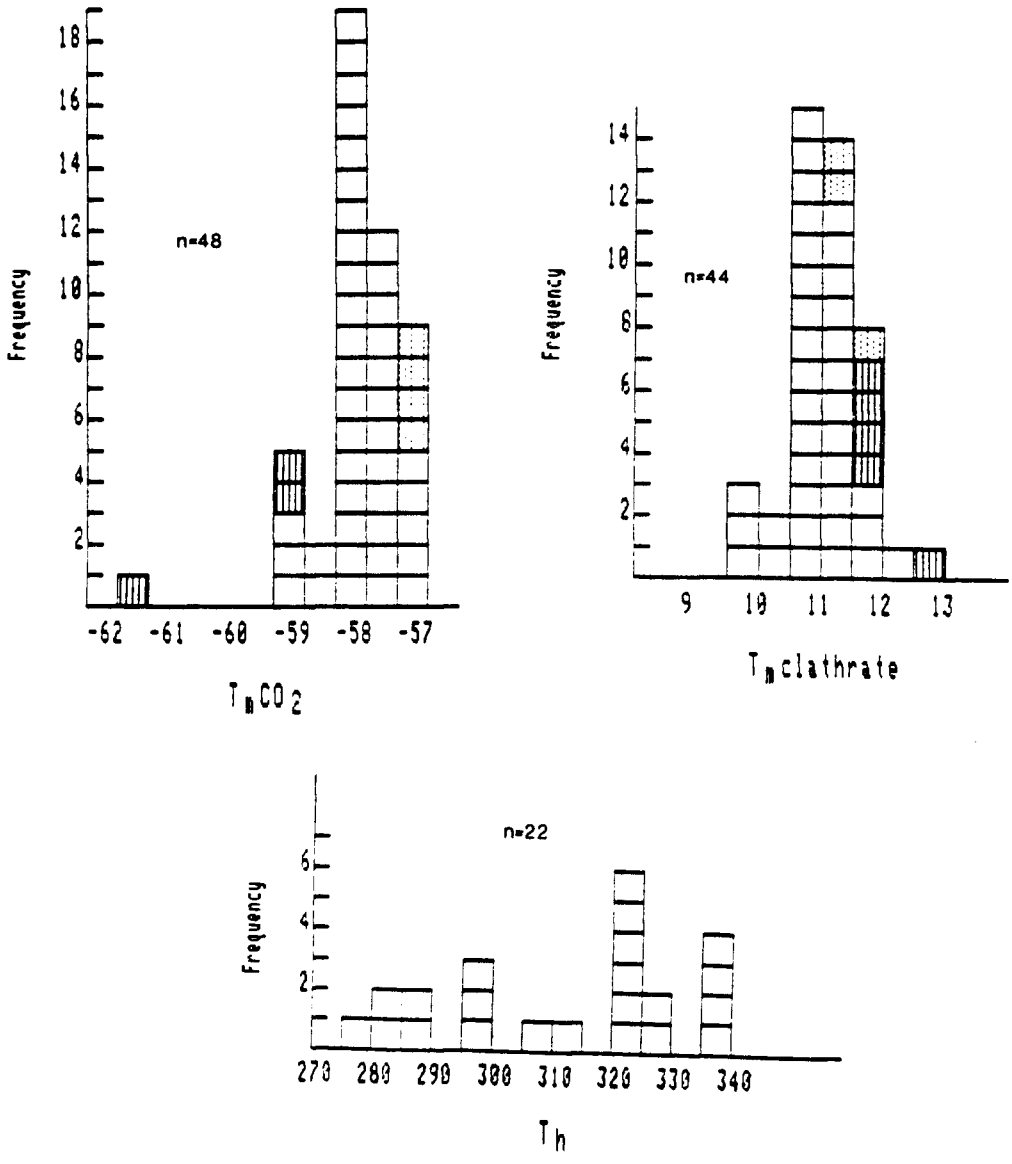

Figure 4-48: Histograms of data, type 1 inclusions. Legend is in Figure 4-49.

with a primary inclusion habit, as pseudosecondaries, with some liquid rich inclusions, and as pseudosecondaries with no liquid rich inclusions (Figure 4-45). Some quartz cores contain type 1 inclusions almost exclusively. Pseudosecondary vapour rich inclusions are commonly equant. These are useable for microthermometric studies if no or few liquid rich inclusions are present (i.e. necking is not a possible mode of origin).

Some type 1 inclusions homogenize by critical phase change, that is, "meniscus fading". Instead of homogenization by expansion of the vapour phase until the inclusion is vapour filled, the liquid - vapour boundary gradually fades away at the homogenization temperature. These inclusions can occur with others that homogenize to vapour. Phase changes in both types of vapour rich inclusions are observable only if there is sufficient liquid to keep the phase boundary away from the inclusion wall; this generally is not the case.

Type 1 inclusions, including those of primary and pseudosecondary origin, are H_2O-CO_2-CH_4±NaCl mixtures. Salinities of the liquid phase are unknown due to the lack of observable ice melting. Clathrate melting, observed in most cases, invariably occurs at temperatures of 10.0-12.5°C. The presence of methane makes salinity determinations by the method of Collins (1979) impossible, because the Collins method

requires a three component system. CO_2 melting occurs over a few degrees , with final melting occurring between -57.1 and -61.8°C. Separate CO_2 liquid and gas phases are rarely observable, indicating a low vapour phase density. Homogenization temperatures range from 279-340°C, with a mode of 322.5°C. These temperatures have an accuracy of $\pm$ 10°C at best, due to the difficulty of observing final homogenization of the liquid phase.

Type 2 (three phase (L,L,V), H_2O-CO_2-CH_4-NaCl) inclusions (Table 4-3, Figure 4-49) contain three phases at room temperature (20°C), water rich liquid, CO_2 rich liquid, and CO_2 rich gas. These inclusions are abundant, and occur in both primary and secondary habits. Most occur in groups of mixed inclusion types; only rarely are type 2 inclusions the dominant type.

Type 2 inclusions are H_2O-CO_2-CH_4-NaCl mixtures. The presence of methane is indicated by CO_2 melting temperatures of -56.8 to -58.7°C. No ice melting was observed, but clathrate melting in some cases occurred below 10°C. The lower range of clathrate melting (to about 9°C) suggests salinities of 1 to 2 weight percent NaCl equivalent, but since the lowering of clathrate melting is offset by the presence of CH_4 (Collins, 1979), actual salinities are slightly higher (2 to 3 weight

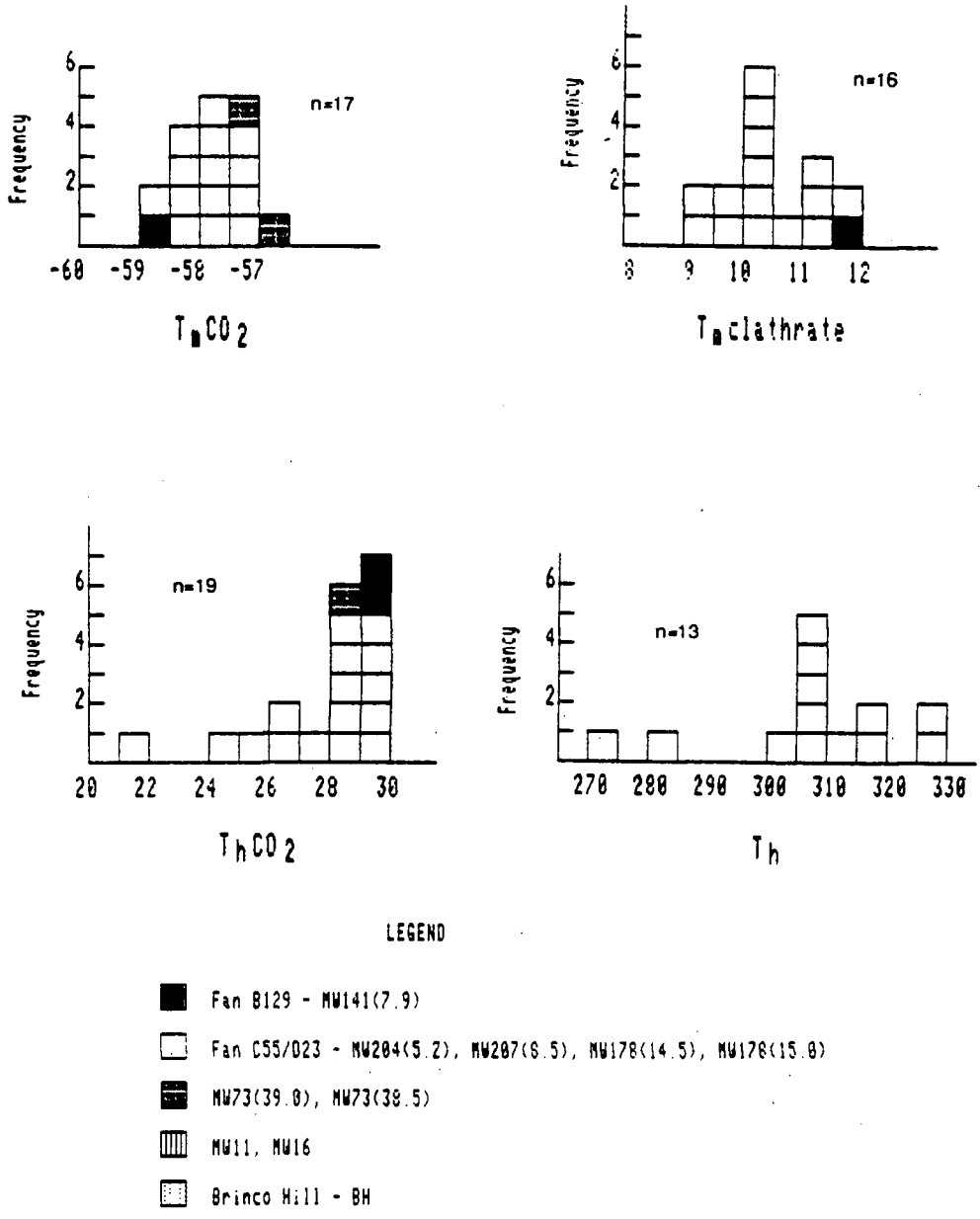

Figure 4-49: Histograms of data, type 2 inclusions. Legend gives sample locations (cf. Figure 4-47).

percent NaCl equivalent). First (eutectic) melting, where observable, commonly occurred at temperatures as low as -40°C, well below the -21°C eutectic of the H_2O-NaCl system. This indicates that $CaCl_2$ is probably an important electrolyte in the liquid phase (Roedder, 1984). Because CO_2 melting temperatures are on average slightly higher than in type 1 inclusions, and clathrate melting temperatures are on average lower, CH_4 content of type 2 inclusions is less than that of type 1 inclusions.

The CO_2 phases mostly homogenize to vapour near 28.5°C, although Th_{CO_2} as low as 21°C was observed. In some cases, the CO_2 phases homogenized to either vapour or liquid in different inclusions within the same group. Liquid to vapour ratios in the immiscible CO_2 rich phase vary widely, as do CO_2 rich to H_2O rich phase ratios. Calculated densities of the CO_2 rich phase within a single group (sample 207 (8.5)) range from 0.26 to 0.6 grams/cubic centimetre, using the method of Burruss (1981). Homogenization temperatures span roughly the same range as type 1 inclusions, with a mode of 307.5°C (Figure 4-49). This is probably artificial, however, as only homogenization temperatures for inclusions with fairly consistent CO_2 rich to H_2O rich phase ratios were recorded. The implications of these data are discussed in section 4.6.5. Type 2 inclusions commonly decrepitate in the 350-400°C range, whereas type 1 inclusions often have decrepitation temperatures in excess of 450°C.

Type 3 (liquid rich, H_2O-CO_2-NaCl) inclusions (Table 4-3, Figure 4-50) are subdivided into two subtypes: type 3a, high temperature (T_h > 265°C), and type 3b, moderate temperature (T_h < 220°C). Type 3a inclusions occur as primaries and secondaries. Type 3a primaries occur mainly with associated type 1 and/or type 2 inclusions, while type 3a secondaries generally do not occur with other inclusion types. In mixed groups, visibly necked inclusions are common. Type 3b inclusions occur as secondaries only. Homogenization by critical phase change was observed in one group of type 3a inclusions.

Since type 3a inclusions occur as both primaries and secondaries they span a temporal range encompassing both quartz deposition and early microfracturing episodes. CO_2 melting temperatures are significantly higher than those recorded for type 1 and 2 inclusions, clustering near -56.6°C. Clathrate melting temperatures are less than 10°C, with a mode of 6.75°C. These two observations indicate that CH_4 is not a significant phase in type 3a inclusions. The clathrate melting temperatures indicate salinities of about 7 weight percent NaCl equivalent. Homogenization temperatures span a range from 267 to 330°C (mode of 292.5°C), with a few higher temperatures recorded in groups with more variable liquid to vapour ratios. The largest cluster of temperatures occurs in the 290-310°C range, overlapping with

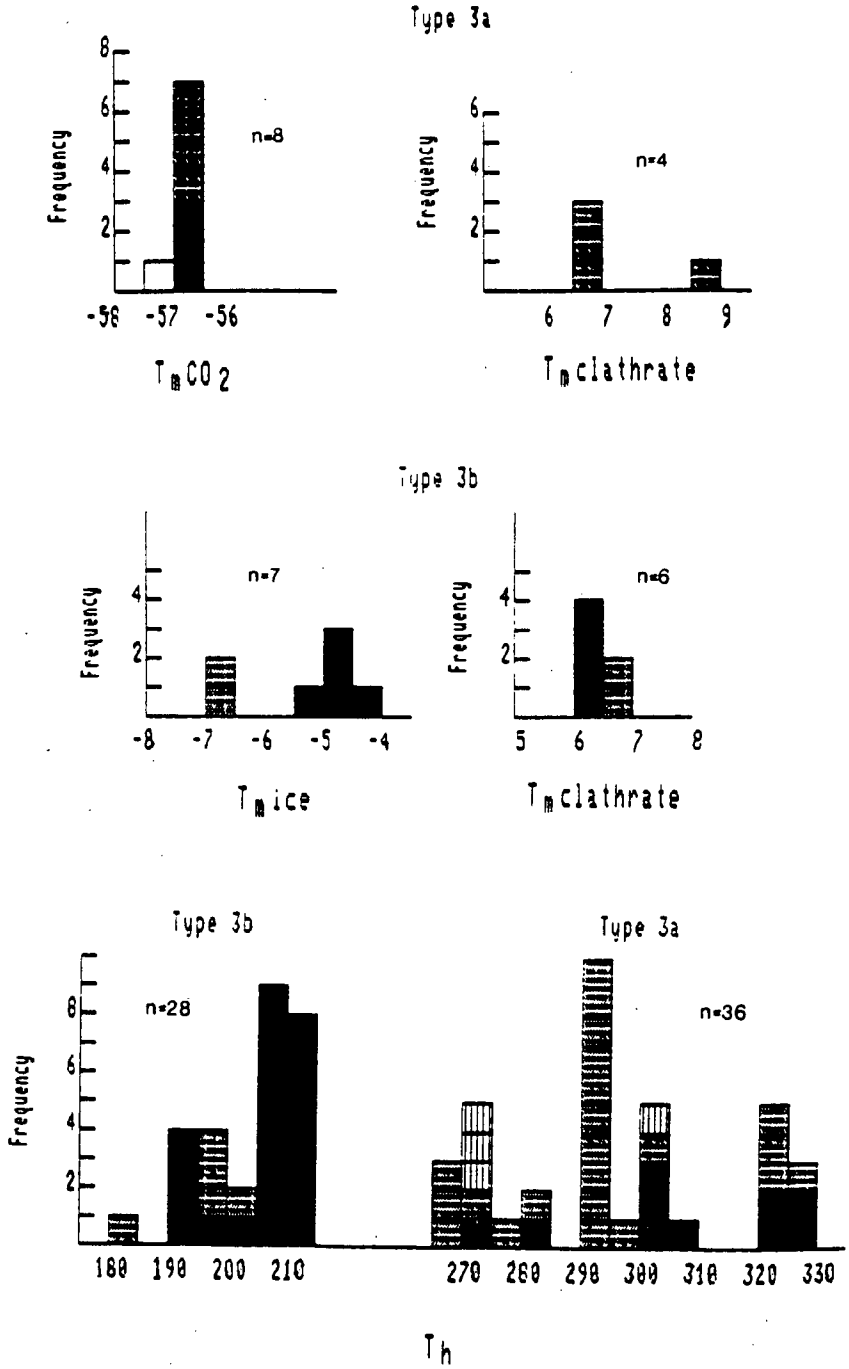

Figure 4-50: Histograms of data, type 3a and 3b inclusions. Legend is in Figure 4-49.

type 1 inclusions (Figure 4-50).

One sample (141 (7.9)) contained inclusions with larger vapour bubbles than those typical of type 3a. These inclusions also exhibited atypical melting and homogenization behaviour. In two of the three groups in which these inclusions occurred, homogenization occurred to the liquid phase (i.e. type 3a), whereas in one of the groups homogenization to the vapour phase (type 1) occurred. In both cases, decrepitation occurred immediately upon homogenization. CO_2 melting occurred at -56.6°C, indicating that no methane was present (a feature typical of type 3a inclusions, but not of type 1 inclusions). Ice melting in the three groups occurred at -14.5, -17.0 and -16.3°C. These uncharacteristically low ice melting temperatures indicate salinities of about 21 weight percent NaCl equivalent. A lower salinity, more consistent with salinities usually observed in type 3 inclusions, would be implied if $CaCl_2$ was the principal electrolyte. It is possible, therefore, that these inclusions record localized carbonate dissolution episodes.

Type 3b inclusions are distinguished from type 3a on the basis of occurrence, homogenization temperature, and freezing behaviour. They occur only as secondary inclusions, homogenize at temperatures less than 215°C (mode of 207.5°C), and locally exhibit ice formation during freezing. CO_2 melting was not

observed, perhaps indicating lower CO_2/H_2O than in type 3a inclusions. The presence of carbon dioxide is indicated by clathrate formation. Clathrate melting occurs at approximately the same temperatures (mode 6.25oC) as in type 3a inclusions, suggesting roughly equivalent salinities. Ice melting occurs in the range of -4 to -7oC (mode -4.75oC). Generally, either ice or clathrate melting is observed; both are rarely seen in the same inclusion, although both can occur in the same group of inclusions. Homogenization of type 3b inclusions occurs between 180 and 215oC, clustering in the upper part of that range (Figure 4-50).

Type 4 (liquid rich, H_2O-NaCl) inclusions (Table 4-3, Figure 4-51) occur only as secondary inclusions. CO_2 content is negligible, as neither clathrate melting nor CO_2 melting were observed. Ice melting temperatures cluster around -7.25oC, indicating salinities of around 10 weight percent NaCl equivalent. This may be somewhat less if dissolved CO_2 is present in unobserved amounts. Homogenization occurs from 122 to 176oC, with a mode of 152.5oC.

Daughter minerals were observed in two inclusions within a group of mixed inclusions, probably secondaries. The daughters dissolved at 149oC, prior to homogenization, and appeared from their cubic outlines to be halite. This implies a salinity of

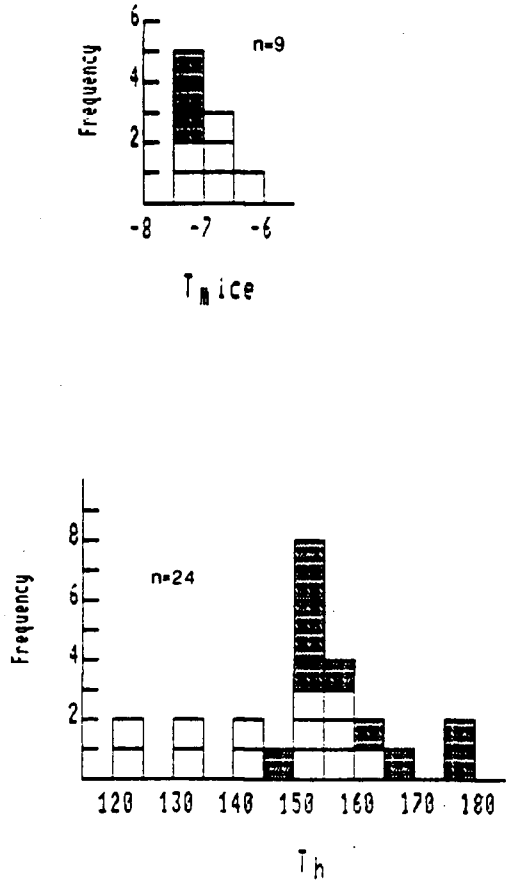

Figure 4-51: Histograms of data, type 4 inclusions. Legend is in Figure 4-49.

about 29 weight percent NaCl equivalent, using the equation of Potter et al. (1977).

One phase "inclusions" are common, but are enigmatic. They include clear inclusions, of variable shape, which do not nucleate a vapour bubble on cooling to -195°C (as CH_4 inclusions would). They might be a fluid other than CH_4, or more likely, they could be solid inclusions such as quartz. Very small (< 3 microns), irregular black inclusions are locally common. These do not undergo phase changes during cooling or heating, and might be organic matter such as bitumins derived from the wallrocks.

4.6.5. Temporal Evolution of Fluids

The data summarized above show a systematic shift in mode of origin of inclusions, temperature and composition. This records part of the temporal evolution of fluids involved in Midway mineralization (Figure 4-52). Fluids which deposited quartz and sulphides were trapped in primary and pseudosecondary inclusions of types 1, 2, and 3a. Later microfracturing episodes trapped secondary inclusions of type 3a, 3b and 4 at progressively lower temperatures.

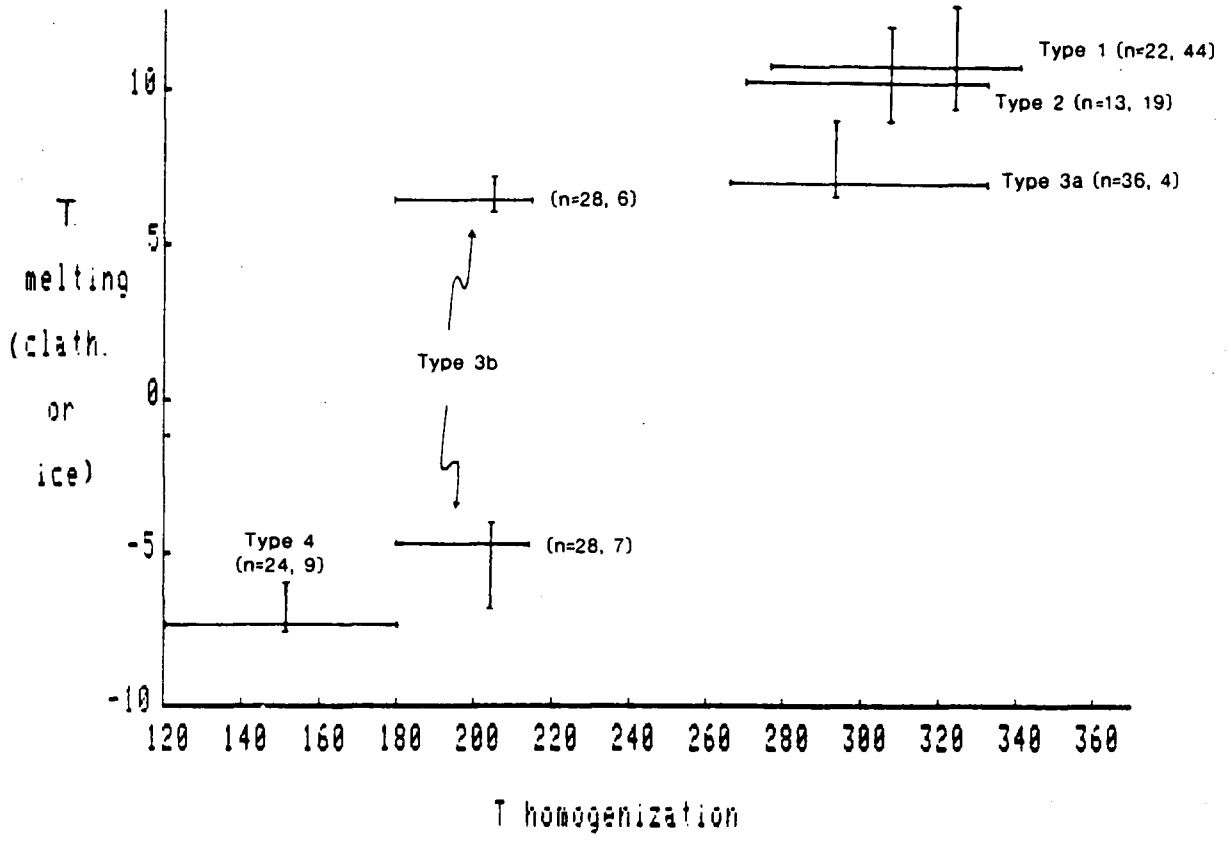

Figure 4-52: Plot of homogenization temperature versus final melting temperature. Positive melting temperatures are clathrate, negative melting temperatures are ice. Temporal evolution of fluids is from upper right (high temperature, immiscible CO_2-CH_4 rich vapour and H_2O-CO_2-NaCl liquid) to lower left (low temperature, aqueous liquid). N = number of measurements, with the first number referring to homogenization measurements and the second to melting measurements.

Co-occurrence of primary and pseudosecondary vapour rich and liquid rich inclusions in quartz cores indicates the presence of immiscible vapour and liquid phases during part of quartz - sulphide deposition. Compositional contrasts between type 1, 2, and 3a inclusions are consistent with this interpretation. (Note that boiling is a special case of immiscibility where the two phases have the same composition; cf. Pichavant et al., 1982). Vapour rich and three phase inclusions contain significant amounts of methane and probably low salinities, whereas liquid rich inclusions have negligible methane and moderate salinities. This suggests the partitioning of methane (and probably carbon dioxide) into an immiscible vapour phase, with electrolytes thereby concentrated in the liquid phase as fluid T - P conditions dropped below the solvus.

The presence of inclusions homogenizing by critical phase change indicates that during part of quartz deposition, the fluid was supercritical; generally the fluid was probably near critical T and P during trapping of most primary and pseudosecondary inclusions. Locally, fluids must have been dominantly of either liquid or vapour phase, producing quartz cores and pseudosecondary planes dominated by inclusions of a single type.

Inclusions also record subsequent evolution of the fluid

system from a two phase (immiscible vapour and liquid), near critical H_2O-CO_2-CH_4-NaCl fluid (types 1, 2 and 3a) to an H_2O-CO_2-NaCl liquid with no methane and lower CO_2 content (type 3b). This compositional change accompanied cooling of the fluid below temperatures in excess of 300°C. The magnitude of this temperature decrease is probably significantly less than the approximately 100°C difference between type 3a and type 3b homogenization temperatures. This is because, on the interpretation above, type 3a inclusions were in equilibrium with an immiscible vapour phase; hence homogenization temperatures for type 1 and type 3a inclusions are equal to temperatures of trapping. Type 3b inclusions are not coeval with type 1 inclusions, and therefore measured homogenization temperatures are a minimum estimate and must be corrected for pressure. For an inferred depth in excess of two kilometres (0.5 kilobars), a pressure correction of about 50°C is not unreasonable (Roedder, 1984).

Salinities of the type 3a and type 3b inclusions remained approximately the same. Lower volatile contents in the fluid resulted from partitioning of CO_2 and CH_4 into the immiscible vapour phase, and from decreasing CO_2 solubilities with decreasing temperature (Takenouchi and Kennedy, 1965).

The final stage of fluid evolution recorded in quartz inclusions is to a low temperature aqueous brine (type 4). Since homogenization temperatures of type 4 and 3b inclusions overlap, the distinction between them is somewhat arbitrary, and in fact, they probably represent a continuum of fluid evolution in both T and X. On this interpretation, since the distinction between type 3b and type 4 is based on observable features such as clathrate melting, the transition represents a small compositional change (decreasing CO_2/H_2O) beyond which clathrate compounds will not nucleate. The apparent shift in salinity from 7 to 10 weight per cent NaCl equivalent is therefore mainly a function of changing from a ternary to a binary phase diagram (i.e. from the H_2O-CO_2-NaCl system to the H_2O-NaCl system; cf. Collins, 1979).

4.6.6. Spatial Variation of Inclusion Populations

Inclusion types are not distributed homogeneously in quartz thoughout the Midway deposit. Although the data set is very limited, certain observations on inclusion population distributions can be made. Samples were studied from two massive sulphide bodies in the Silver Creek deposit, at diamond drill fan C55/D23 and fan B129 (Figure 4-47). Useable inclusions were found in all of the studied sections in fan C55/D23, whereas only one out of four studied sections from B129 contained

inclusions suitable for microthermometric study. All samples from C55/D23 contained abundant type 1 inclusions, which were rare in samples from B129 (Figure 4-48). This suggests that fluid immiscibility did not occur throughout the Midway deposit, but was a more localized phenomenon. Alternatively, this difference could be a function of different timing of mineralization in the two sulphide bodies.

Type 1 inclusions are also abundant in vein quartz from Brinco Hill (Figures 4-1, 4-48). These inclusions are similar in composition to those in Fan C55/D23 and contain significant methane. This similarity is further evidence for the genetic relationship between Midway mineralization and alteration in the Brinco Hill area (cf. section 4.3).

Vapour rich inclusions are rare in the quartz - carbonate - sulphide vein of diamond drill hole MW 73 (Figure 4-48). Methane bearing inclusions are likewise absent. The main inclusion types are 3a secondaries and lower temperature secondaries, which are more abundant here than in the Silver Creek deposit (Figure 4-50).

The highest clathrate melting temperatures obtained were from inclusions in quartz from the Discovery deposit (DDH 16: Figure 4-47). These also had the lowest CO_2 melting

temperatures, indicating that a greater amount of CH_4 was present in comparison with the Silver Creek deposit. The Discovery deposit samples are from intersections 200 metres lower than the Silver Creek samples. Greater abundance of methane at those levels suggests a positive relationship between depth and CH_4 content, although more extensive sampling is required to establish this.

4.6.7. Pressure and Depth of Formation

The presence of at least four main components in the Midway hydrothermal fluid (H_2O, CO_2, CH_4 and NaCl) makes it impossible to obtain quantitative estimates of pressure and depth of formation with current thermodynamic data. However, data are available on phase relations for the binary H_2O-CO_2 and ternary H_2O-CO_2-NaCl systems (e.g. Bowers and Helgeson, 1983). These data provide a limiting case for the quaternary system.

As described above, type 1 and type 3a inclusions were trapped in different fractures as well as in quartz cores containing inclusions of both types. These inclusion types have different compositions, but homogenize in roughly the same temperature range. The occurrence of mixed groups indicates the contemporaneity of the two inclusion types. The presence of greater amounts of CH_4 in the vapour rich inclusions is what one

would expect if the two inclusion types were coeval and evolved from a single phase fluid of intermediate composition.

Type 2 inclusions occur in groups of mixed inclusion types with variable CO_2 rich to H_2O rich phase ratios. This, and the variable densities exhibited by type 2 inclusions in the same group, indicates that type 2 inclusions represent mixtures of varying amounts of liquid and vapour -- another indication of the contemporaneity of the two phases. Type 2 inclusions in groups without type 1 and type 3a inclusions are unknown. This indicates that primary inclusions were never trapped above the solvus in the one phase field; hence the solvus provides an upper limit for pressure of trapping. For an H_2O-CO_2 fluid at 300°C the solvus crest is at P = 600 bars (Figure 4-53). However, addition of NaCl and other electrolytes pushes the solvus crest to much higher pressures (Takenouchi and Kennedy, 1964). In the H_2O - CO_2 - NaCl system with 6 weight percent NaCl, trapping of a fluid above the solvus with an X CO_2 of 0.2 requires a pressure of at least 1000 bars at a trapping temperature of 350°C (Figure 4-54). Addition of CH_4 extends the two phase field to higher pressures still. For H_2O-CO_2-CH_4-NaCl fluids below 400°C, fluid unmixing is the rule; hence, pressures are poorly constrained.

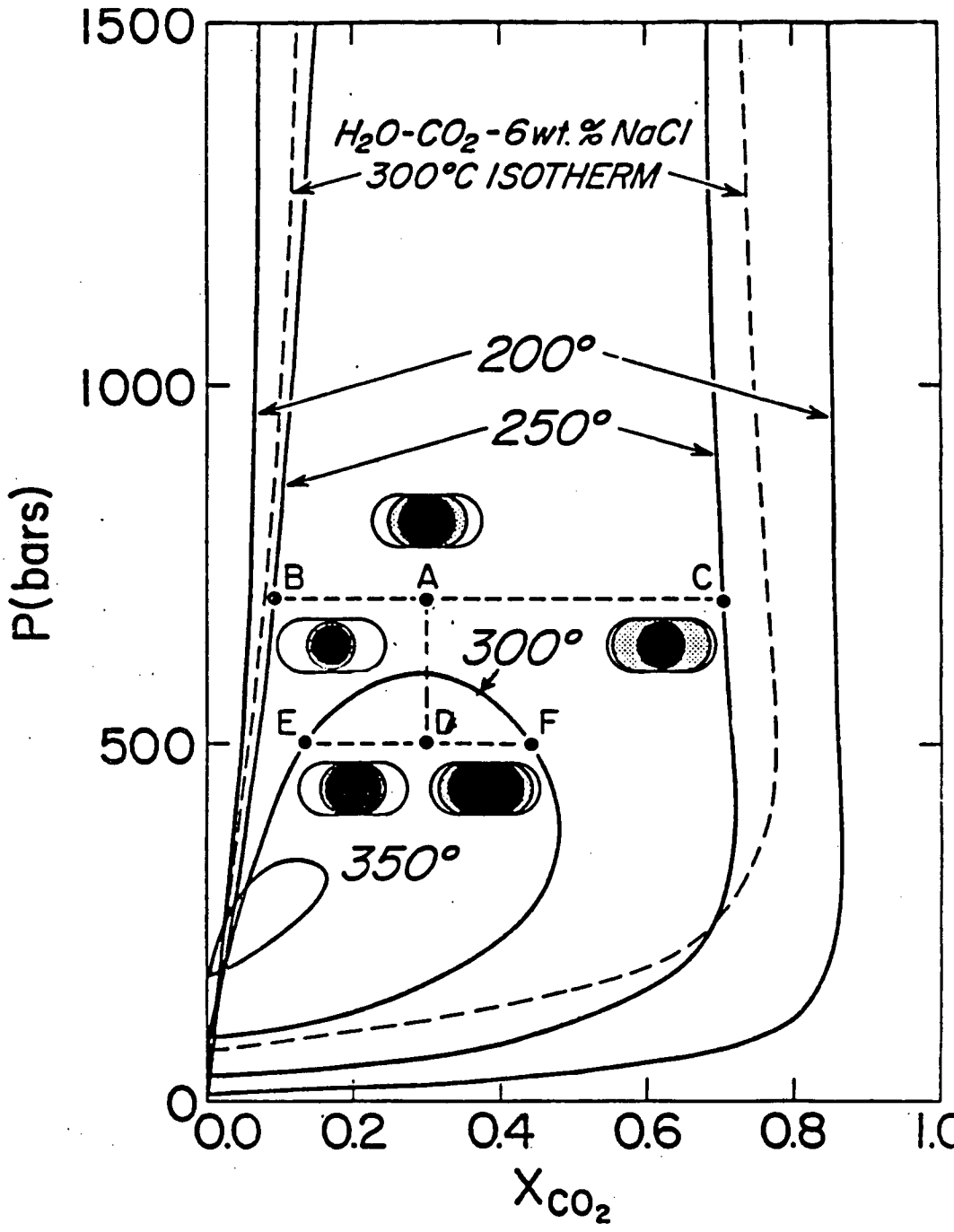

Figure 4-53: Isotherms showing the compositions of coexisting liquid and vapour phases in the system H_2O-CO_2 and H_2O-CO_2-NaCl. Also shown are the 25°C phase relations of H_2O-CO_2 fluid inclusions with a bulk composition of 30 mole % CO_2 trapped at various temperatures and pressures represented by the points A-F (from Bodnar and Kuehn, 1982).

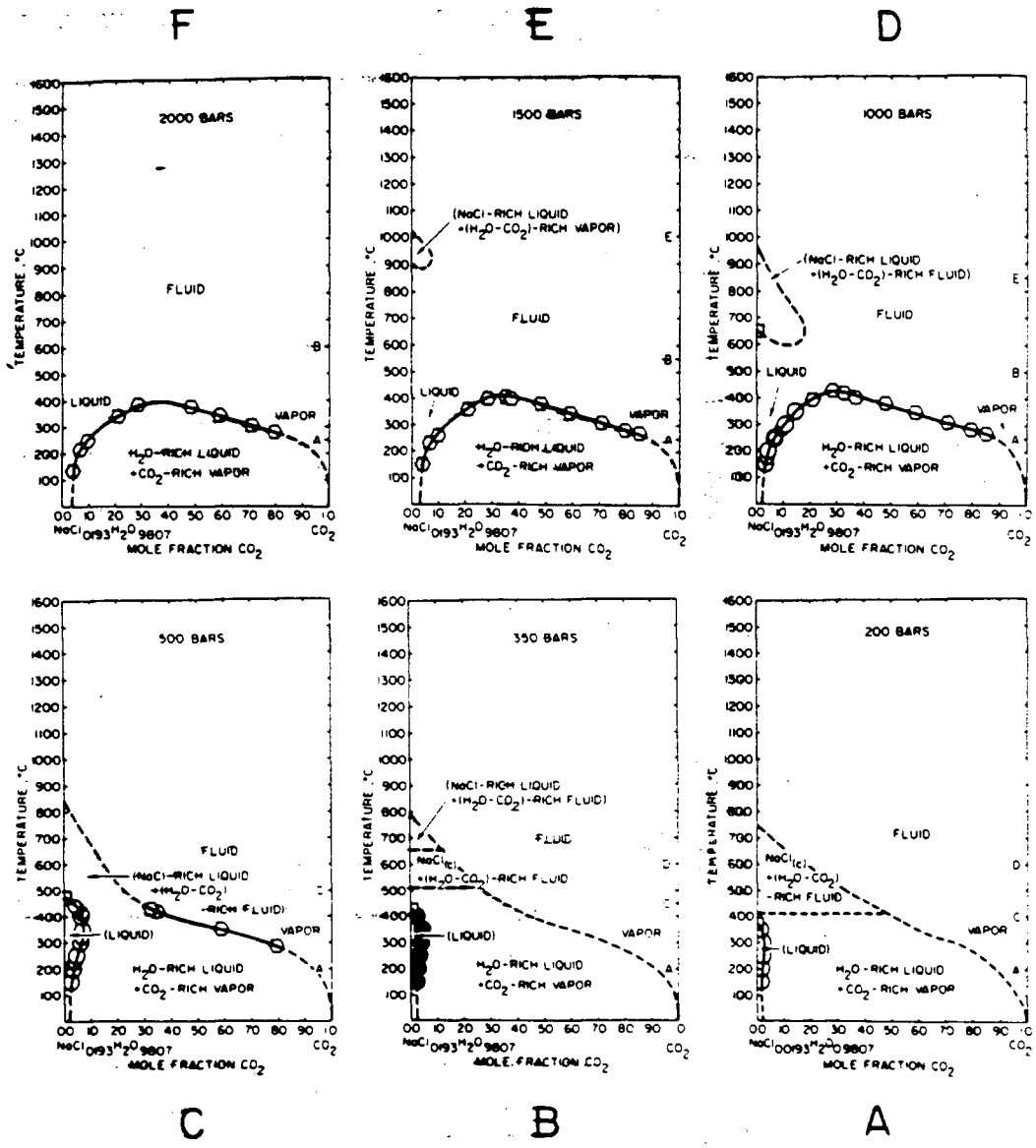

Figure 4-54: T - X diagrams for 6 weight percent NaCl relative to H_2O + NaCl (from Bowers and Helgeson, 1983).

Stratigraphic depth provides a better constraint on depth of formation of the Midway deposit. A reasonable estimate of minimum thickness of the Earn Group in the deposit area is about 650 metres (section 3.3). Earn Group is overlain on Whitehorn Mountain by about 700 metres of the Sylvester allochthon (Figure 4-1, Plate 1). A total minimum thickness of strata overlying the McDame Group in the immediate deposit area is therefore about 1.35 kilometres. Thickness of the Sylvester allochthon in the Midway area in the Late Cretaceous is unknown, but it probably exceeded 1 kilometre, and might have been in excess of 1.5 kilometres, based on mapping in the Blue Dome (104P/12) map area (Harms et al., 1988). A depth of formation of 1.5 to 2 kilometres is therefore consistent with stratigraphic evidence. Depths of 2 kilometres or more are consistent with the presence of 3 phase CO_2 bearing inclusions and wispy secondary inclusion textures (T.J. Reynolds, personal communication, 1987).

Fluid immiscibility, producing type 1 and type 3a inclusions, could be produced by pressure decrease, temperature decrease, or increase of CO_2 derived from wallrock reactions or oxidation of CH_4. If sulphides were deposited in zones of increased porosity in the McDame Group (section 4.4.4), the influence of pressure might have been important. With a depth of formation of 1.5 to 2 kilometres, zones of enhanced porosity were probably water filled and supported under hydrostatic to sublithostatic

pressure (cf. the discussion of the karst model for Nanisivik, Baffin Island: Olson, 1984; Ford, 1986; Olson, 1986). It is possible, therefore, that immiscibility was produced by rapid transitions from near-lithostatic to near-hydrostatic pressure as fluids entered high porosity karst breccia zones from tightly confined fracture systems (cf. Roedder and Bodnar, 1980). This provides a complex mechanism for deposition of metals from solution, involving pressure decrease, loss of CO_2 and possibly temperature decrease through mixing with cooler ambient waters in zones of high porosity.

4.6.8. Comparison With Other Skarn - Manto Systems

Fluid inclusion studies of five skarn - manto deposits were selected from the literature for comparison with Midway. These are: Providencia (Sawkins, 1964; Rye, 1966), Fresnillo (MacDonald et al., 1986), Leadville, Colorado (Thompson et al., 1985), Deer Trail, Utah (Beaty et al., 1986), and Deer Trail, Washington (Fluet et al., 1987). Other inclusion studies of this type of system are not widely available.

At Providencia, inclusions indicate temperatures of sulphide deposition ranging from 205°C to 365°C for latest sphalerite. Salinities range from 5 to 40 weight percent NaCl equivalent, and inclusions with multiple daughter minerals are common.

CO_2 bearing inclusions are present. Vapour rich inclusions occur locally, but appear to be uncommon. Methane was not reported.

At Fresnillo, inclusions are all liquid rich, and no daughter minerals were observed. Homogenization temperatures range from 185°C to 390°C in mantos. Some necked groups were probably used in these measurements, as variable liquid to vapour ratios are reported. Salinities range from <1 to 12 weight percent NaCl equivalent. Minor CO_2 is reported in one zone only.

At Leadville, the maximum homogenization temperature was about 320°C, and salinities ranged up to 5.2 weight percent NaCl equivalent. No evidence of CO_2 was reported, but the authors believed it to be present nonetheless. No evidence of boiling was reported.

At Deer Trail, Utah, the highest homogenization temperatures of 250°C to 300°C and highest salinites of 17 to 22 weight percent NaCl equivalent were measured in sphalerite. Homogenization temperatures of 170°C to 300°C and salinites of 1 to 2 weight percent NaCl equivalent were measured in quartz. Evidence of boiling (not specified) was observed locally in quartz. CO_2 liquid occurred only in sphalerite. Birefringent

daughters, probably carbonate minerals, occurred locally.

At Deer Trail, Washington, CO_2 - H_2O inclusions are common, and clathrate melting temperatures of 6°C to 8°C were reported. Ice melting ranged from -5°C to -0.6°C, for a salinity of 1 to 8 weight percent NaCl equivalent. Homogenization temperatures of 120°C to 250°C were measured.

There are several differences between these studies and data obtained on the Midway deposit. First, occurrences of groups of vapour rich inclusions and evidence of contemporaneity of liquid rich and vapour rich inclusions have not been reported in the literature on manto deposits. Second, the presence of CO_2 is either not noted or not investigated systematically in all of these studies except for the study of the Deer Trail, Washington deposit. Third, the presence of methane was not noted in any of these studies. Homogenization temperatures are broadly comparable, although the upper limit varies from 250 to 390°C.

4.7. Stable Isotopes

4.7.1. Introduction

Stable isotope analyses of sulphides, sulphates, carbonates and wallrock were used to characterize the isotopic geochemistry of the fluids involved in ground preparation and mineralization at Midway. Sulphur isotopes helped to constrain temperatures of sulphide deposition and to assess the relative importance of equilibrium and kinetic depositional processes and possible sulphur sources. Carbon and oxygen isotopes were used to assess the effect of isotopic alteration of McDame Group limestones, and to constrain the isotopic composition and sources of the fluids that interacted with them.

4.7.2. Sample Preparation and Analysis

Mineral separates for sulphur isotope analysis were hand picked from samples crushed to 0.3 to 0.5 millimetres, at which size about 50% liberation was attained. Samples picked were small enough (< 1 cubic centimetre) that liberated minerals originally were in contact or close proximity. Polished section examination indicated that phases sampled showed limited crosscutting or replacement textures. In some cases, more than one distinct phase of pyrite was evident, decreasing the

likelihood of co-deposition of pyrite and other phases. Coexisting mineral pairs or triplets were picked from each sample to allow testing of equilibrium among phases.

Del ^{34}S values determined at the Stable Isotope Laboratory, University of Calgary, were analyzed as follows. Sulphide analyses were performed on SO_2 gas extracted by high temperature combustion of the sample with cupric oxide. Barite was analyzed by direct combustion to SO_2 gas. Gypsum was dissolved in acid and reprecipitated as $BaSO_4$. Mass spectrometric analyses are referenced to the Canyon Diablo standard.

Carbon and oxygen isotope analyses of carbonates were also performed at the Stable Isotope Laboratory, University of Calgary. Finely ground carbonate samples were reacted in vacuo with H_3PO_4 at 75°C, and the liberated CO_2 collected until the reaction was essentially complete. Mass spectrometric analyses of carbon and oxygen isotope compositions of the CO_2 were corrected to KH-2 standard, referenced to Peedee Belemnite (carbon) and Standard Mean Ocean Water (oxygen) (del $^{13}C_{PDB}$ = +1.97 and del $^{18}O_{SMOW}$ = +27.8).

4.7.3. Sulphur Isotopes

Sulphur isotope analyses of 64 mineral separates were provided by the Stable Isotope Laboratory, University of Calgary

Department of Physics, and by the Geological Survey of Canada (W.D. Sinclair, written communication, 1986). Samples were analyzed from the Silver Creek, Discovery and Silvertip areas, and from vein and exhalative mineralization hosted in Earn Group clastic sediments. Results are presented in Table 4-4.

4.7.3.1. Sample Duplicates and Interlaboratory Comparison

Within sample variability was assessed by duplicate analyses. Three samples were picked separately for duplicate analysis at the University of Calgary. The difference in del values for these duplicates was less than 0.2‰. (Table 4-4). Two duplicates in the data from the Geological Survey of Canada (Table 4-4) have differences of 0.1 and 0.6‰.. The latter amounts to 8% of del, which may indicate impurities in the mineral separate.

No systematic differences are apparent in the data sets from the two laboratories. Samples from the same locality were not included in both data sets, but both contain samples from the Discovery deposit and Earn Group hosted mineralization (Figure 4-55; Table 4-5). Pyrite separates from the Discovery deposit have overlapping del ^{34}S values from the two data sets, but the average of the University of Calgary analyses is greater than the Geological Survey of Canada average by about 1‰.. A single

Table 4-4: Sulphur isotope data, Midway area, north-central British Columbia (104O/16).

Location[1]	Mineral[2]	Host Rock/ Deposit[3]	Lab[4]	del 34S[5]	Comments
144(8.5)	Py	Mls/SC	K	7.79	
144(8.5)	Sp	"	"	6.31	
144(8.5)	Gn	"	"	5.57	
143(4.75)	Py	"	"	7.66	
143(4.75)	Sp	"	"	8.27	
143(4.75)	Gn	"	"	6.21	
142(9.8)	Py	"	"	7.30	
142(9.8)	Sp	"	"	7.01	Duplicate
142(9.8)	Sp	"	"	7.17	Duplicate
142(9.8)	Sp	"	"	7.09	Average
142(9.8)	Gn	"	"	5.88	
178(15.0)	Sp	"	"	7.68	
178(15.0)	Gn	"	"	5.67	
204(6.8)	Sp	"	"	7.73	
204(6.8)	Gn	"	"	6.04	Duplicate
204(6.8)	Gn	"	"	5.91	Duplicate
204(6.8)	Gn	"	"	5.98	Average
207(8.0)	Py	"	"	9.05	
207(8.0)	Sp	"	"	7.29	
207(8.0)	Gn	"	"	5.47	
60(109)	Py	"	"	8.47	
60(109)	Gn	"	"	6.36	
60(109)	Gc	"	"	6.39	
77(298)	Sp	"	"	7.16	
77(298)	Gn	"	"	5.70	
77(307)	Sp	"	"	7.82	
77(307)	Gn	"	"	7.84	
84(319)	Sp	"	"	6.76	
84(319)	Gn	"	"	5.78	
97(319)	Sp	"	"	7.18	
97(319)	Gn	"	"	5.50	
3(114.4)	Py	Mls/Disc	G	5.9	
3(114.4)	Sp	"	"	5.9	
3(114.4)	Gn	"	"	4.7	
3(114.4)	Ba	"	"	5.6	Duplicate
3(114.4)	Ba	"	"	5.7	Duplicate
3(114.4)	Ba	"	"	5.7	Average
8(LZ)	Py	"	"	7.7	
8(LZ)	Gn	"	"	6.5	
89(234.9)	Py	"	K	7.68	
89(234.9)	Sp	"	"	7.77	
11(317.7)	Py	"	"	7.88	
16(385.8)	Po	"	"	6.95	
26(584.2)	Po	"	"	5.81	
4(82.0)	Py	Esln/Exh	"	7.71	Duplicate
4(82.0)	Py	"	"	7.78	Duplicate
4(82.0)	Py	"	"	7.75	Average
4(82.0)	Sp	"	"	7.54	Yellow
4(82.0)	Gn	"	"	6.29	
DZ Trench	Py	"	G	8.4	
DZ Trench	Py	"	"	8.3	Fine grained
DZ Trench	Py	"	"	8.1	Coarse grained
DZ Trench	Sp	"	"	8.2	Yellow
DZ Trench	Sp	"	"	8.1	Brown
DZ Trench	Ba	"	"	7.2	
DZ Trench	Py	"	"	7.98	
DZ Trench	Gn	"	"	4.9	Late vein
DZ Trench	Py	"	"	8.3	
DZ Trench	Py	"	"	6.1	
DZ Trench	Sp	"	"	7.8	Yellow, Dup.
DZ Trench	Sp	"	"	7.2	Duplicate
DZ Trench	Sp	"	"	7.5	Average
DZ Trench	Gn	"	"	6.1	
DZ Trench	Ba	"	"	7.1	
80(133)	Sp	Mls/ST	K	8.32	
80(133)	Gn	"	"	6.13	
40(443.4)	Sp	"	"	8.52	
40(443.4)	Gn	"	"	6.44	
JN5-1	Ba	Esln/Exh	"	22.71	
JN5-8	Ba	"	"	24.66	
JB35-5	Ba	"	"	29.70	
JB12-5	Ba	"	"	21.09	
MWUnd	Ba	Mls/SC	"	21.80	Late, vuggy
MWUnd	Gp	"	"	11.54	Late, vuggy

1. Abbreviations for locations are: 77(298) refers to diamond drill hole number and metreage; JN and JB are sample location prefixes from 1987 field season; DZ Trench refers to the Earn Group hosted Discovery zone; MW Und refers to an unknown location in the Midway underground workings.

2. Mineral abbreviations are: Py = pyrite, Sp = sphalerite; Gn = galena, Po = pyrrhotite, Gc = geocronite, Ba = barite, Gp = gypsum.

3. Host rock and deposit abbreviations are: Mls = McDame Group limestone, Esln = Earn Group siltstone, SC = Silver Creek deposit, Disc = Discovery deposit, Exh = Exhalite; ST = Silvertip showing.

4. Laboratory abbreviations are: K = Stable Isotope Laboratory of H.R. Krouse, Department of Physics, University of Calgary, G = Ian Jonasson, Geological Survey of Canada.

5. Del ^{34}S values are referenced to Canyon Diablo troilite standard (CDT).

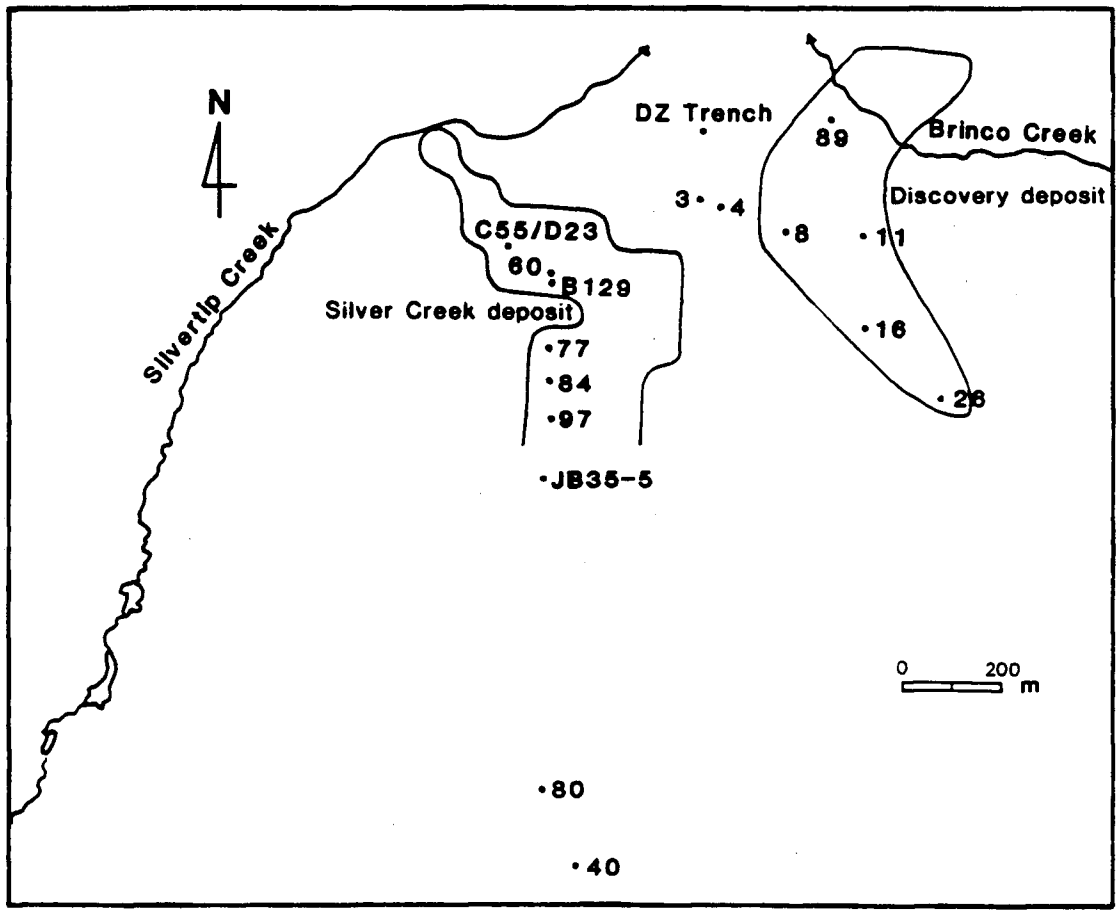

Figure 4-55: Location of sulphur isotope samples from the Midway area. C55/D23 and B129 are underground drill stations (Figures 4-10 and 4-11), JB35-5 is a traverse station; the other numbers refer to surface diamond drill holes (for metreage of sample see Table 4-4).

Table 4-5: Interlaboratory comparison of sulphur isotope data, Midway area, north-central British Columbia. Py = pyrite; Sp = sphalerite; S.D. = standard deviation; n = number of analyses. Data are from Table 4-4.

Deposit	Laboratory[1]	$\overline{del\ ^{34}S}$ Py	S.D.	$\overline{del\ ^{34}S}$ Sp	S.D.	$\overline{del\ ^{34}S}$ Gn	S.D.
Discovery	Calgary	7.78	0.1 n=2	7.77	- n=1	-	-
Discovery	G.S.C.	6.8	1.3 n=2	5.9	- n=1	5.6	1.3 n=2
Exhalite	Calgary	7.75	- n=1	7.54	- n=1	6.29	- n=1
Exhalite	G.S.C.	7.86	0.9 n=5	7.85	0.5 n=3	5.5	0.8 n=2

1. Calgary - Stable Isotope Laboratory, Department of Physics, University of Calgary.
   G.S.C. - Ian Jonasson, Geological Survey of Canada, Ottawa. Data is courtesy of W.D. Sinclair.

Discovery deposit sphalerite from the Calgary data has a higher del value than the Geological Survey of Canada sphalerite average as well (Table 4-5). Of the Earn Group samples, pyrite and sphalerite analyzed at the University of Calgary had lower del ^{34}S than the Geological Survey of Canada averages, whereas the galena value was higher. There is therefore no systematic disparity between the data sets; but the evidence is not based on the same samples, so is not conclusive.

4.7.3.2. Results

Analytical results of the sulphur isotope study are in Table 4-4, with average values for the three main sulphides presented by deposit in Table 4-6 and Figure 4-56. Overall, del ^{34}S values for sulphides are tightly constrained between 4.7 and 9.05‰., a range of 4.35‰.. The sixteen pyrites have del values between 5.9 and 9.05‰., averaging 7.8‰. (0.8 standard deviation). Seventeen sphalerites have a similar range of 5.9 to 8.52‰., with a slightly lower average of 7.5‰. (0.7 standard deviation). Eighteen galena analyses span a range from 4.7 to 7.84‰., averaging 5.9‰. (0.7 standard deviation). Two pyrrhotite separates have an average del value of 6.4‰.. One geocronite separate has a del value of 6.39‰., which is essentially the same as coexisting galena. Separation of galena and geocronite by hand picking was based on the lack of cubic cleavage in the

Table 4-6: Average del ^{34}S by mineral and deposit, Midway area, north-central British Columbia. Abbreviations are as in Table 4-5. Data are from Table 4-4.

Host Rock	Deposit	del ^{34}S Py	S.D.	del ^{34}S Sp	S.D.	del ^{34}S Gn	S.D.
McDame limestone	Silver Creek	8.05	0.6 n=5	7.33	0.5 n=10	6.00	0.6 n=11
McDame limestone	Discovery	7.29	0.9 n=4	6.84	1.3 n=2	5.6	1.3 n=2
McDame limestone	Silvertip	-	-	8.42	0.1 n=2	6.29	0.2 n=2
Earn siltstone	Exhalite	7.84	0.8 n=6	7.84	0.4 n=4	5.76	0.8 n=3

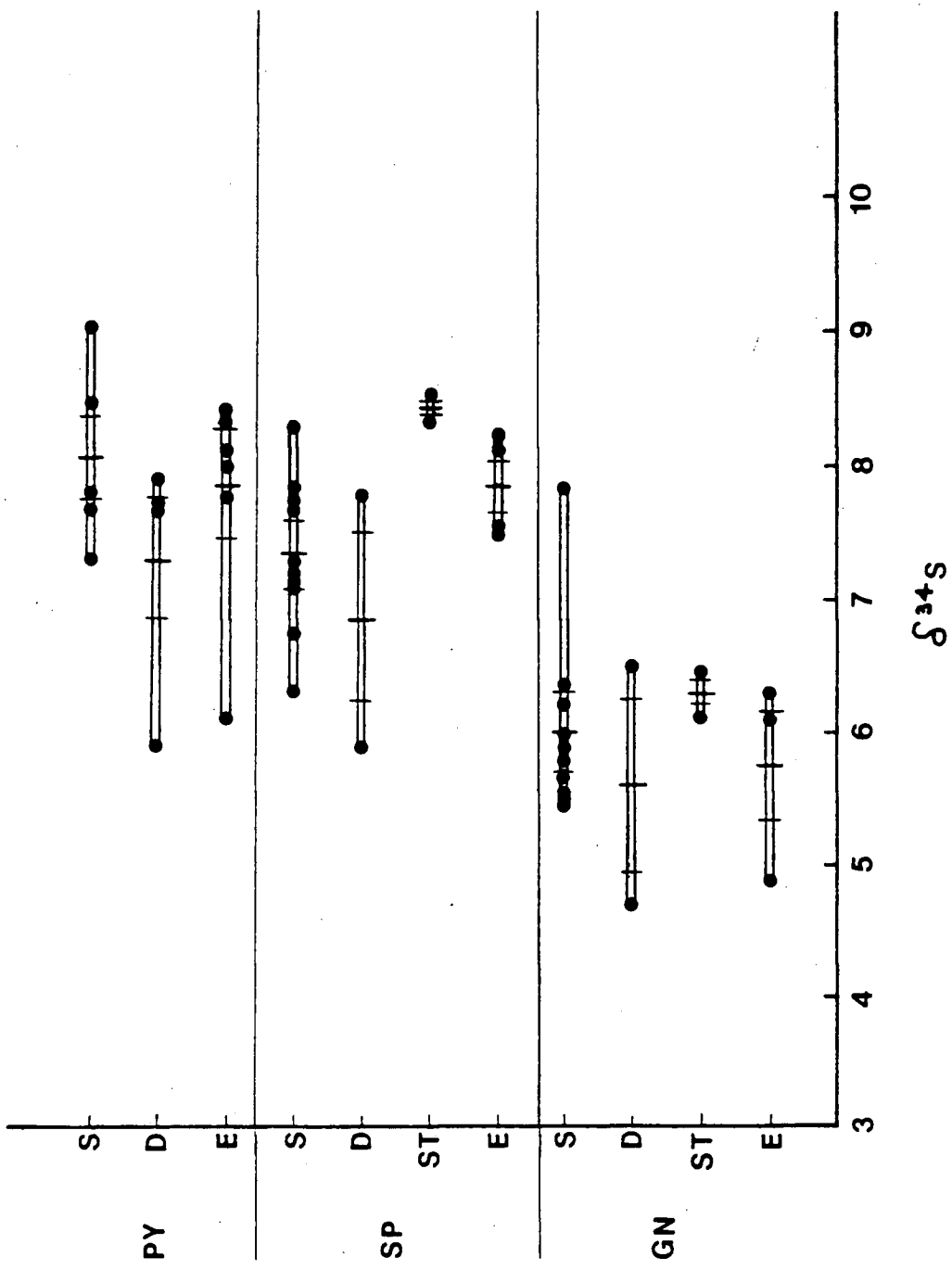

Figure 4-56: Range and means of sulphur isotope compositions by deposit and mineral. Abbreviations are: Py - pyrite, Sp - sphalerite, Gn - galena, S - Silver Creek deposit, D - Discovery deposit, ST - Silvertip showing, E - Earn Group hosted.

latter. The similar isotopic compositions suggest that fine intergrowths of galena and geocronite would not significantly affect del ^{34}S values of galena.

Comparison of results from the different deposits (Table 4-6, Figure 4-56) shows that average del ^{34}S values increase from the Discovery deposit, to the Silver Creek deposit, to the Silvertip showing. The differences are statistically significant for Silvertip and Discovery galenas and sphalerites, for Silvertip and Silver Creek sphalerites, and for Silver Creek and Discovery pyrites. Standard deviations about means for these groups show little or no overlap (Figure 4-56). The comparisons are limited because most of the Discovery deposit analyses are Geological Survey of Canada data. The evidence for small between deposit differences in sulphur isotope compositions is therefore permissive, but not conclusive. No other spatial zoning is evident in the data.

Order of enrichment of del ^{34}S of the main sulphide phases is generally pyrite > sphalerite > galena, in accordance with the equilibrium fractionation factors of Ohmoto and Rye (1979). This indicates attainment of partial isotopic equilibrium for samples with this enrichment order, assuming that the phases are coeval. Complicated multi - episodic mineral paragenesis may be a factor in the departures from this order, since codeposition

cannot be proven, but is assumed in the absence of textural evidence to the contrary. Pyrrhotite del ^{34}S values are substantially less than the average for sphalerite, although equilibrium fractionation factors indicate that they should be similar. This could be a function of the different location of the pyrrhotite samples, which were from sulphide intersections farther to the south (and probably closer to the intrusive heat source) than the Discovery deposit sphalerite samples.

4.7.3.3. Mineral Pairs and Equilibrium

Differences in del ^{34}S for various mineral pairs are presented in Table 4-7, along with calculated temperatures of deposition based on equilibrium fractionation factors. The calculated temperatures span a wide range for all three mineral pairs. Pyrite - sphalerite and pyrite - galena temperatures are almost all geologically unrealistic and in conflict with fluid inclusion data, which indicate depositional temperatures of 300 to 330°C. This might be due to a combination of two factors. First, due to the complexity of pyrite paragenesis, some of these pairs may violate the assumption of codeposition. This reflects the fact that pyrite deposition requires oxidation - reduction reactions whereas galena and sphalerite deposition is independent of oxidation state (Ohmoto, 1986). Second, pyrite generally equilibrates at a slower rate than the other phases;

Table 4-7: Del ^{34}S and calculated temperatures of deposition for mineral pairs, Midway area, north-central British Columbia. Abbreviations are as in Table 4-5. The dash indicates that one or both of the minerals were not analyzed. Data are from Table 4-4.

Sample	Δ Py-Sp	(TOC)	Δ Py-Gn	(TOC)	Δ Sp-Gn	(TOC)
144(8.5)	1.48	177	2.22	434	0.74	700
143(4.75)	-	-	1.45	598	2.06	310
142(9.8)	0.21	922	1.42	607	1.21	488
204(6.8)	-	-	-	-	1.75	359
178(15.0)	-	-	-	-	2.01	317
207(8.0)	1.76	140	3.58	281	1.82	347
60(109)	-	-	2.11	449	-	-
77(298)	-	-	-	-	1.46	419
84(319)	-	-	-	-	0.98	572
97(319)	-	-	-	-	1.68	372
4(82.0)	0.21	922	1.46	595	1.25	475
3(114.4)	-	-	1.2	684	1.2	491
8(LZ)	-	-	1.2	684	-	-
80(133)	-	-	-	-	2.19	292
40(443.4)	-	-	-	-	2.08	307
Average	0.92	540	1.83	542	1.50	419
S.D.	0.82	441	0.81	141	0.46	122
n	4		8		13	

1. Fractionation factors are:
^{34}S Py-Sp = 0.3 (106/ T2), ^{34}S Py-Gn = 1.1 (106/ T2), (Kajiwara and Krouse, 1971); and ^{34}S Sp-Gn = 0.7 (106/ T2), (Czamanske and Rye, 1974).

hence the unrealistic temperatures might reflect kinetic fractionation rather than equilibrium (Ohmoto, 1986). The dendritic or bladed textures in pyrite, which are reasonably interpreted as resulting from rapid precipitation, are consistent with kinetically governed fluid - mineral exchange, which would in turn be reflected in nonequilibrium mineral pairs. This problem is discussed from a different perspective in section 4.7.3.6.

Sphalerite - galena pairs on average give much lower calculated temperatures than pairs with pyrite, and 5 out of 13 pairs have temperatures between 292 and 347°C, a range roughly consistent with fluid inclusion temperatures. This is due to the greater likelihood of codeposition for sphalerite and galena, based on paragenetic observations, and to faster reaction rates for these phases relative to pyrite (Sakai, 1976).

4.7.3.4. Del ^{34}S (H_2S) Values

Sulphur isotope compositions of sulphides can be used as tracers for the source of sulphur in the hydrothermal system. The isotopic composition of individual sulphur species in the fluid can be estimated given the composition of mineral phases and temperature of deposition, providing that mineral and fluid sulphur were in equilibrium, and that the relevant fractionation

factor is known. Estimation of the isotopic composition of total fluid sulphur requires some knowledge of sulphur speciation in the fluid, which depends on several mutually interacting factors, including pH, fO_2 (oxygen fugacity), T (temperature), I (ionic strength) and sulphur concentration (Ohmoto, 1972).

Del ^{34}S (H_2S) is estimated here using the fractionation factors in Ohmoto and Rye (1979), and a depositional temperature of 320oC. These estimates are relatively insensitive to temperature. For example, lowering the temperature to 275oC alters del 34S (H_2S) by only about 0.3‰. at del ^{34}S (galena) of 4.7‰.; generally, changes in del values for similar temperature differences are less than this. At 320oC, del ^{34}S (H_2S) in equilibrium with pyrite ranges from 4.76 to 7.91‰., with an average value of 6.66‰. (Table 4-8). For sphalerite, del ^{34}S (H_2S) ranges from 5.62 to 8.24‰., with an average of 7.22‰., and for galena it ranges from 6.49 to 9.63‰., averaging 7.69‰.. Since pyrite is quantitatively the most significant sulphide in the deposit, del ^{34}S (H_2S) for the total fluid system probably averaged about 7.0‰.(i.e. the value for a fluid in equilibrium with an assemblage of 60% pyrite, 20% galena and 20% sphalerite, using the average del ^{34}S values above).

This value assumes mineral - fluid sulphur equilibrium. As discussed in section 4.7.3.3., however, temperatures calculated

Table 4-8: Del ^{34}S (H_2S) for fluid in equilibrium at various temperatures with pyrite, sphalerite and galena Data are from Table 4-4.

Mineral	del ^{34}S	del ^{34}S (H_2S)[1] at T = 275	320	350 oC
Pyrite	low 5.9	4.59	4.76	4.87
	high 9.05	7.74	7.91	8.02
	avg. 7.8	6.49	6.66	6.76
Sphalerite	low 5.9	5.57	5.62	5.64
	high 8.52	8.19	8.24	8.26
	avg. 7.5	7.17	7.22	7.24
Galena	low 4.7	6.79	6.49	6.32
	high 7.84	9.94	9.63	9.46
	avg. 5.9	8.00	7.69	7.52

1. Mineral - H_2S fractionation factors are from Ohmoto and Rye (1979).

from pyrite - sphalerite and pyrite - galena pairs appear to indicate a lack of equilibrium. However, the small diferences between calculated del ^{34}S (H_2S) for the three phases argues that the estimates of that value are reasonable. To see why, consider for example, that if pyrite - galena temperatures were closer to geologically reasonable values, delta del ^{34}S (pyrite - galena) would be greater, which in turn implies either higher del ^{34}S (pyrite) or lower del ^{34}S (galena) or both. Either change would bring del ^{34}S (H_2S) calculted from pyrite and galena closer together, between 6.66 and 7.69‰..

4.7.3.5. Hydrothermal Environment and Sulphur Sources

Sakai (1968) and Ohmoto (1972) showed that the isotopic composition of fluid sulphur depends on sulphur speciation -- which in turn is a function of fO_2, pH, T and I -- and on fractionation factors among sulphur species. Constraints on some of these parameters can be derived from mineral assemblages which interacted with the fluids.

Pervasive alteration of Earn Group sediments is believed to be related to the hydrothermal system that deposited Midway sulphides (section 4.3). The alteration assemblage sericite - pyrite - quartz implies acid conditions, with an upper limit of about pH 4.5 for muscovite + quartz stability at T = 350°C and

I = 1.0 (Figure 4-57). Slightly lower pH is required to produce this assemblage at lower temperature (e.g. pH 4.3 at 250°C). These acid fluids interacted with cover rocks above the intrusive centre, and must have equilibrated with McDame Group carbonates during sulphide deposition. This caused an increase in pH, which enabled calcite deposition during the late carbonate - dominant paragenetic stage. At T = 250°C, a pH of about 7.3 is compatible with calcite deposition; pH would increase slightly with decreasing temperature (So et al., 1983). These considerations give rough constraints on pH during sulphide deposition, as well as a general evolutionary trend from low to moderate pH. This trend is illustrated in Figure 4-57.

The parameter fO_2, which is proportional to the ratio of oxidized and reduced sulphur species in the fluid, can be constrained by mineral assemblages and sulphur isotopes. A large variation in del ^{34}S values for sulphide phases suggests either wide temperature fluctuations, or (more likely) that the oxidation state of the fluid was in the vicinity of the SO_2/H_2S stability field boundary (Ohmoto and Rye, 1979). This would create significant fractionations between coexisting sulphate and sulphide species. Conversely, if sulphide sulphur isotope compositions are tightly grouped, temperature and oxidation state must have remained relatively constant and well below the

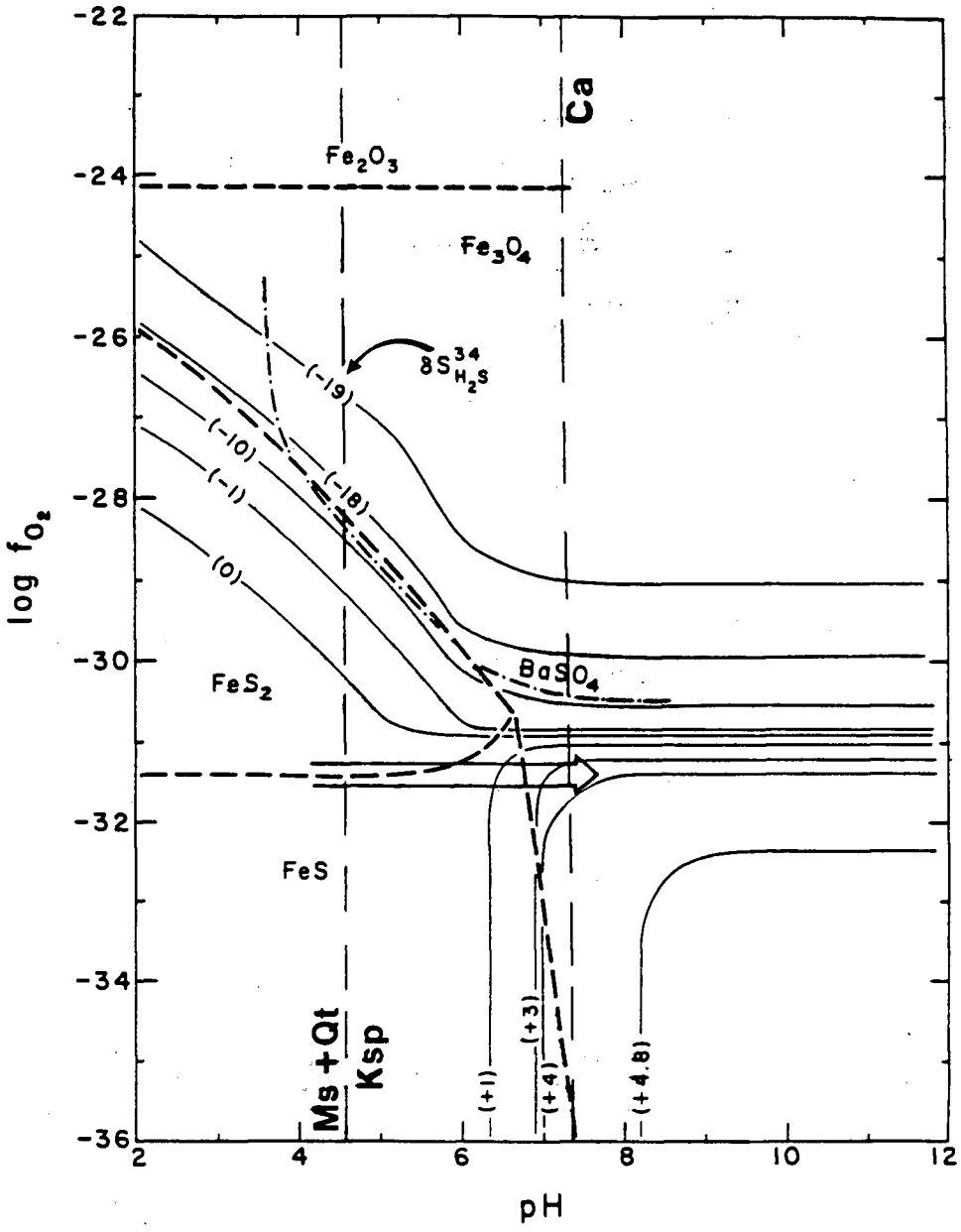

Figure 4-57: Comparison of the positions of del ^{34}S contours with the stability fields of Fe-S-O minerals at T=350°C and I=1.0. Thick dashed lines are Fe-S-O mineral boundaries at m S_T = 0.01 moles/kilogram H_2O. Solid lines are del ^{34}S contours. Values in brackets are for H_2S at del $^{34}S_{ES}$ = 0‰.. Barite solubility boundary is at $m_{Ba^{2+}} \times m_S = 10^{-3}$. Thin dashed lines marking muscovite + quartz = K-feldspar reaction and calcite solubility boundary are from So et al., 1983. K = 0.1 molal. Arrow shows a fluid evolution path for a fluid initially in equilibrium with pyrite, pyrrhotite and muscovite, and which re-equilibrates with carbonate wallrocks (Ohmoto, 1972).

SO_2/H_2S boundary.

Abundance of pyrrhotite in parts of the Midway deposit and lack of hypogene sulphate and oxide phases during main stage sulphide deposition implies low fO_2, in the vicinity of the pyrite - pyrrhotite stability field boundary (Figure 4-57). Pyrrhotite is common in the southern part of the Silver Creek deposit and in much of the Discovery deposit (section 4.4.7). Paragenetic relations do not show a consistent temporal relationship between the two minerals, suggesting fO_2 and/or pH fluctuations near the pyrite - pyrrhotite boundary. In those parts of the deposit which do not contain pyrrhotite, the fluid may have been slightly more oxidized, with a higher sulphate/sulphide ratio.

The actual value of fO_2 depends on a number of other parameters. For example, at m S_T = 0.01 (molality of total fluid sulphur, in moles/kilogram H_2O), if temperature is decreased from 350 to 250°C, the pyrite - pyrrhotite boundary shifts from log fO_2 = -31.5 to -41.0 (Ohmoto, 1972) (i.e. pyrite stabilizes relative to pyrrhotite at lower oxidation states). Increasing m S_T will decrease the size of the pyrrhotite field, stabilizing pyrite at lower fO_2. Using values of T = 320°C and m S_T = 0.01, the pyrite - pyrrhotite boundary lies at log fO_2 = -34.3 (Ohmoto, 1972, using a linear interpolation). Changing m S_T by

an order of magnitude changes fO_2 by about two log units either way.

In the temperature and pH range of main stage sulphide deposition, delta del ^{34}S (H_2S-S_T) is negligible at oxidation states near the pyrite - pyrrhotite boundary (Figure 4-57). Therefore, the calculated estimate of average del ^{34}S (H_2S) of about 7.0‰ represents a reasonable value for del ^{34}S (S_T) in the fluid system.

Fluid sulphur with this isotopic composition is compatible with both a magmatic and sedimentary source, or a mixture of the two. Although "magmatic" sulphur is commonly described as having an isotopic composition of 0 $\pm$ 3‰., compositions in the 3 to 7‰. range are also possible, depending on the initial oxidation state of the melt and the subsequent path of fluid derived from it (Ohmoto and Rye, 1979). Fluids derived from relatively oxidized magmas may have del ^{34}S (fluid) as much as 4‰. greater than del ^{34}S (melt). An increased melt oxidation state can occur during late stages of crystallization, resulting in progressively higher del ^{34}S (fluid). This is not likely in the case of Midway, however, because the source intrusion is more likely to be analogous to S-type magmas, which have significantly lower oxidation states than I-type intrusions (Ohmoto, 1986). Alternatively, higher del ^{34}S (melt) can result

from contamination by upper crustal sulphur during emplacement.

Some remobilization of sedimentary pyrite or organic sulphur is also compatible with a del ^{34}S (fluid) of 7.0‰.. Diagenetic pyrite may have a wide range of sulphur isotope compositions, commonly in the 10 to 20‰. range. No data is available for sedimentary sulphur in the Midway area. Possible strata containing sedimentary sulphur include the Lower Cambrian Boya Formation, Ordovician - Silurian Road River Group, Middle Devonian McDame Group, Devono - Mississipian Earn Group, and the lower sedimentary package of the Sylvester allochthon. The Midway ore - forming solutions circulated within the Earn Group and to a lesser extent the Sylvester allochthon (based on alteration haloes), but it is not known whether they interacted with sub - McDame Group strata. The Earn Group contains abundant sedimentary exhalative pyrite and barite, some of which might have been remobilized. Incorporation of H_2S of organic origin from fetid McDame Group limestone is also possible. Some increase of del ^{34}S (fluid) is implied by interaction between the fluid system which deposited manto sulphides, and sulphides of exhalative origin within the Earn Group (cf. section 4.7.3.7).

4.7.3.6. Del versus Delta Del and Equilibrium

The del versus delta del diagram has been used to determine the del ^{34}S (S_T) of fluids which coprecipitated sulphates and sulphides (Field and Gustafson, 1976; Shelton and Rye, 1982). The idea of this graphical technique is that differences in isotopic compositions of coexisting phases which correlate with their isotopic compositions reflect a range of temperatures, which can be extrapolated to the 0 fractionation point (Y intercept) to determine the isotopic composition of the fluid. This requires the assumption of sulphide - sulphate equilibrium; therefore the technique provides another means of analyzing whether equilibrium conditions applied. It can also be used to explicate fluid - mineral relationships in a system under reducing conditions, as at Midway. Under these conditions, it is assumed that fluid sulphur is H_2S dominated, and fractionation between fluid sulphide and sulphate can be ignored. Because the coordinates are not independant, misleading correlations can be induced (Ohmoto, 1986). Since there are various conditions under which correlations can occur, interpretation cannot assume closed system equilibrium conditions; rather the diagrams are more useful for analyzing whether such conditions obtain (Krouse et al, 1988).

Del versus delta del diagrams for sphalerite - galena and pyrite - galena pairs are presented in Figures 4-58 and 4-59. In the sphalerite - galena case, the mineral pairs vary about two

straight lines with positive slopes, which converge at a Y - intercept value of about 5.5‰.. In the pyrite - galena case, the data vary widely about lines which meet at a Y - intercept value of 6.3‰.. The galena data has a negative slope, in contrast to the sphalerite - galena diagram.

Under an equilibrium interpretation of the diagrams, del ^{34}S (fluid) is constant and the variation in delta del values is a function of temperature only. The point of convergence (Y - intercept) represents a fractionation factor of zero (T = very high), and therefore indicates the isotopic composition of fluid sulphur. Del ^{34}S (fluid) values obtained in this way are just 1.2 and 0.4‰. less than values obtained from geochemical considerations in section 4.7.3.4. However, the range of temperatures implied (up to 700°C) is clearly unrealistic and does not support an equilibrium interpretation.

Alternatively, the pairs with low delta del ^{34}S values could represent precipitation under disequilibrium conditions, in which isotopic compositions are controlled by reaction kinetics. For example, during a unidirectional reaction:

$$PbCl_2 + H_2S \rightarrow PbS + 2H^+ + 2Cl^-$$

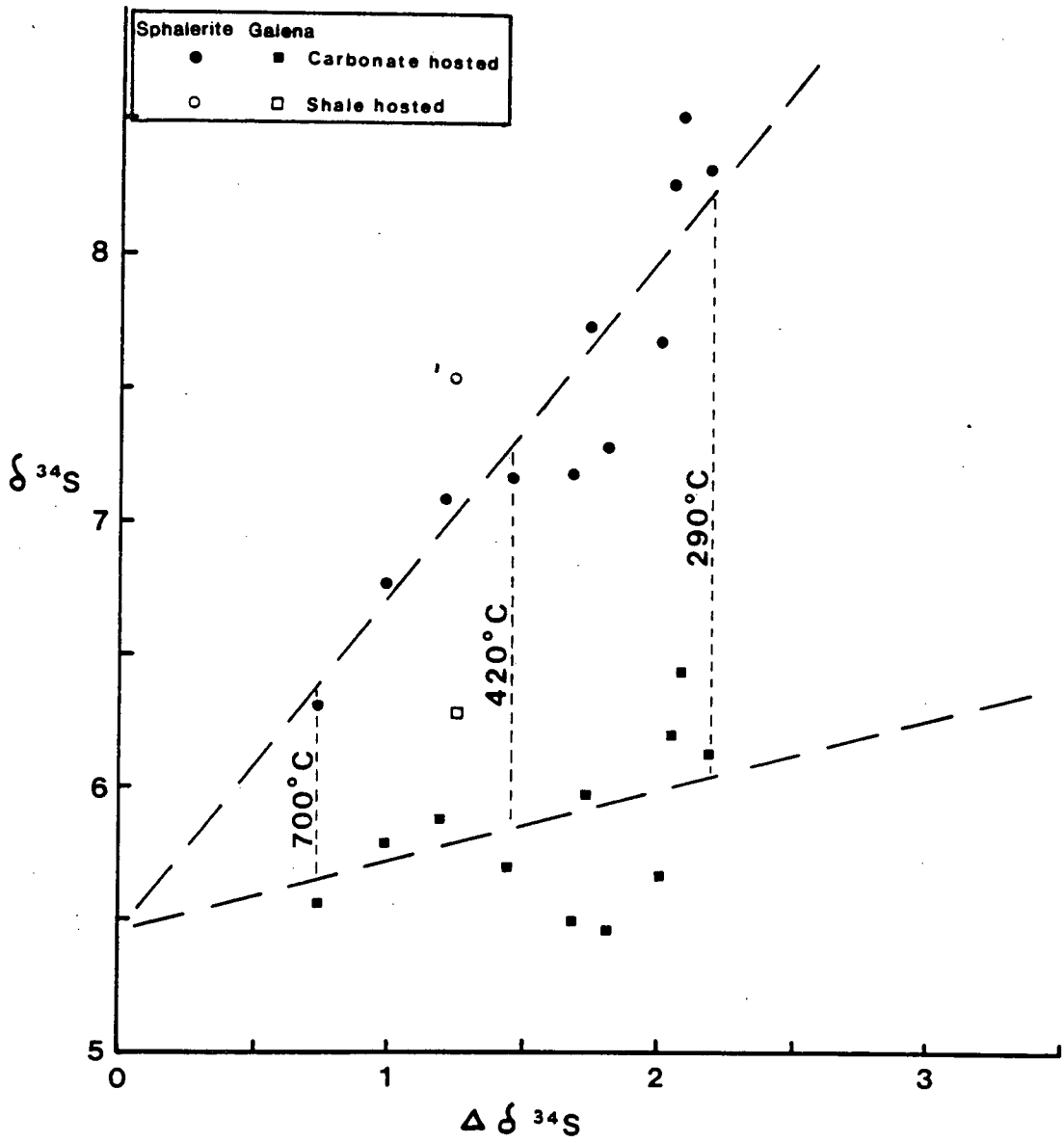

Figure 4-58: Del versus delta del diagram for sphalerite - galena pairs. Data is from Table 4-4.

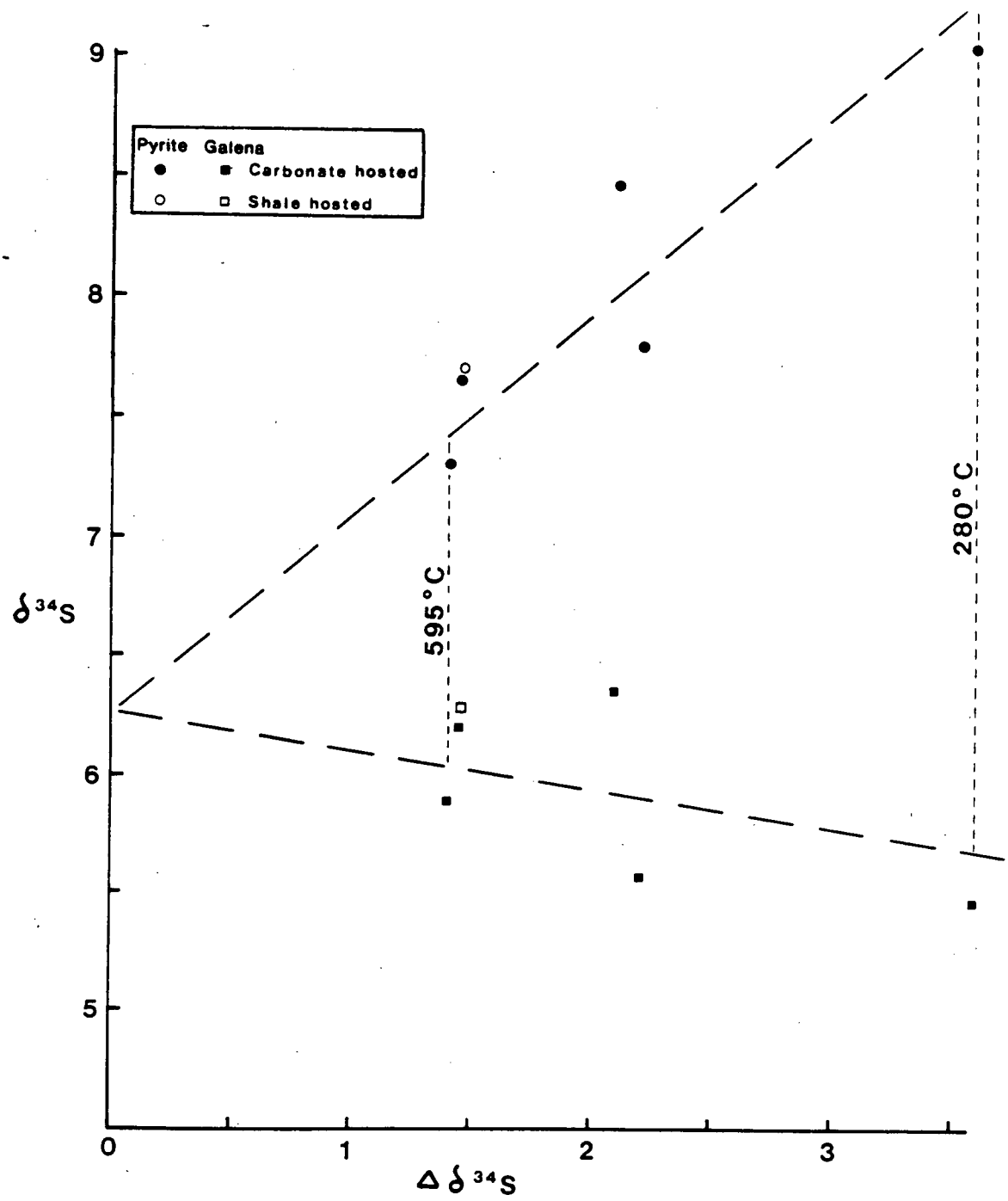

Figure 4-59: Del versus delta del diagram for pyrite - galena pairs. Data is from Table 4-4.

the lighter isotope will react faster and be removed at a higher rate by precipitation of sulphide. This causes a general increase in del ^{34}S (fluid) as the reaction continues (assuming that precipitation rate exceeds fluid influx), with the reaction proceeding toward equilibrium as sulphide is removed.

Positive slopes for both galena and sphalerite are indicators of disequilibrium, since kinetically governed reactions evolve toward heavier isotopic compositions (Krouse et al., 1988). Alternatively, in the equilibrium interpretation, two positive slopes imply the presence of a more ^{34}S - depleted phase or species, such as H_2S. Since, as we have seen (section 4.7.3.5), del ^{34}S (H_2S) = del ^{34}S (fluid) under the oxidation conditions of the Midway system, this is a further argument against the equilibrium interpretation.

Assuming disequilibrium, the Y -intercept value represents a lower limit for del ^{34}S (fluid), which evolved toward somewhat higher values as sulphide precipitation reactions proceeded toward equilibrium. Temperatures near the low end of the range therefore represent approximations of equilibrium values or true temperatures of sulphide deposition (about 290oC). These are consistent with fluid inclusion temperatures. The higher average values for del ^{34}S (fluid) of 6.7 to 7.0‰. derived in section 4.7.3.4 are consistent with this interpretation.

4.7.3.7. Clastic Hosted Sulphide and Sulphate

So - called exhalative sulphide mineralization in Devono - Mississipian Earn Group clastic sediments in the Midway area (section 4.2.1.3) has essentially the same del ^{34}S signature as the carbonate hosted mantos (Table 4-6). Pyrite and sphalerite have average del ^{34}S values of 7.84‰., whereas galena averages 5.76‰.. These values are within 0.5‰ of averages for the Silver Creek deposit. The range of values is similar as well.

Both the range and mean for Earn Group hosted sulphides are distinctly different from typical values for most sedimentary exhalative deposits elsewhere in the northern Cordillera. For example, at the Devonian (Frasnian) Jason deposit in the MacMillan Pass camp, Yukon Territory, del ^{34}S values of sulphides range from 8.5 to 22.5‰., averaging 15.5‰. (Gardner and Hutcheon, 1985). Sedex sulphides have a much wider range of isotopic compositions (e.g. 14.0 and 20.7‰. at the Jason and nearby Tom (Large, 1980) deposits, respectively, versus 3.6‰ for Midway clastic hosted sulphides). This is probably due to substantial and variable fractionation during reduction of seawater sulphate, which did not occur in the more reducing, sulphide - dominant system at Midway.

The similarity of isotopic signatures of manto and clastic hosted mineralization at Midway, and the lack of typical exhalative isotopic characteristics of the clastic hosted sulphides suggests either that they were deposited from the same solutions as the manto deposits or that they re-equilibrated with those solutions. Galena within the stratiform horizons is commonly fracture controlled and is texturally compatible with an epigenetic origin. In addition, galena lead isotope data is incompatible with a syngenetic origin for galena within the Earn Group (section 2). However, finely laminated sphalerite and quartz occurring in these horizons (Figure 4-6) is hard to reconcile with an epigenetic model. Pyrite is commonly coarse grained and associated with sericite, suggesting recrystallization and alteration. The textural and isotopic evidence therefore suggests that most galena is epigenetic, whereas silica, sphalerite and pyrite are mainly syngenetic, but interacted with the high temperature, reducing Late Cretaceous fluids. In so doing, the syngenetic sulphides underwent isotopic exchange reactions with fluid sulphur. This overprinting episode must have been pervasive, with fluids penetrating not only fractures, but also laminae and grain boundaries. Exchange reactions would have caused preferential diffusion of ^{34}S into the fluid, depleting sulphide phases of heavy sulphur, and increasing <u>del</u> ^{34}S (fluid).

That these horizons in the Earn Group are exhalative is clear at a larger scale, as shown by analyses of stratiform barite horizons, which are lateral stratigraphic equivalents to the sulphide rich exhalites near Midway. The closest sample to the DZ Trench sulphide samples (Table 4-4) is JB35-5, about 500 metres to the southwest (Figure 4-55). Del ^{34}S values for these barites range from 21.09 to 29.70‰. averaging 24.54‰. (Table 4-4). These are typical values for Devono - Mississipian exhalative barite in the Selwyn Basin and Kechika Trough (Gardner and Hutcheon, 1985). In comparison, barite from the Jason deposit has del ^{34}S ranging from 22.86 to 26.79‰., and barite from the Tom deposit ranges from 18.5 to 31.9‰. (Gardner and Hutcheon, 1985; Large, 1980), consistent with a seawater sulphate source. Barite in the sulphide rich overprinted clastic hosted horizons has a strikingly different isotopic composition of about 7.2‰. (Table 4-4), which is clearly incompatible with a seawater sulphate source.

Two late sulphate samples from the manto deposits were also analyzed (samples MW Und, Table 4-4). Coarsely crystalline barite intergrown with late sulphide has a del ^{34}S value of 21.80‰.. Coarse gypsum in vugs has a lower del ^{34}S value of 11.54‰.. The high del value for barite indicates that it is probably a hypogene phase, with sulphur derived from ^{34}S - enhanced fluid sulphate at relatively high temperatures as the

system became progressively more oxidized in the late stages of sulphide deposition. The lower gypsum del ^{34}S value indicates that its sulphur is derived from oxidation of ^{34}S - depleted minerals under supergene, near surface, non - equilibrium conditions (cf. Field and Fifarek, 1987).

4.7.3.8. Comparison With Other Skarn - Manto Systems

Sulphur isotope data from five well documented Ag-Pb-Zn skarn - manto systems are in Table 4-9. Of these, three have sulphide sulphur isotopic compositions averaging near 0‰. (Deer Trail, Utah; Leadville, Colorado; Darwin, California), with a clearly implied igneous sulphur source. Sulphide sulphur with negative del ^{34}S values at Fresnillo, Mexico (MacDonald et al., 1986) is also compatible with an igneous source. At the Deer Trail, Washington mine, del ^{34}S values range from +4.5 to +11.9 (Fluet et al., 1987). The low end of this range is compatible with an igneous source but the predominance of high values indicates that remobilization of wallrock sedimentary sulphur is likely. The Midway data lies between the clearly igneous source deposits and the Deer Trail, Washington values. The high end of the Midway range (> +9‰) indicates that sedimentary sulphur, perhaps host rock derived H_2S, is probably a significant component.

Table 4-9: Sulphur isotope data for Midway, British Columbia, and other North American skarn - manto systems.

Deposit	Range	Average del ^{34}S Pyrite	Average del ^{34}S Sphalerite	Average del ^{34}S Galena	Sulphur Source[1]
Midway, B.C.[2]	+4.7-+9.05	+7.76	+7.51	+5.95	I, S
Deer Trail, Utah[3]	-2.4-+4.0	+4.0	+0.6	-1.1	I
Leadville, Colorado[4]	-1.9-+0.3	-	-	-0.7	n.i.
Fresnillo, Mexico[5]	-6.0--3.5	-	-	-	I
Darwin, California[6]	-5.7-+4.4	-	-	-	n.i.
Defiance	-	+3.27	+2.50	+0.29	
Thompson	-	+2.36	+1.77	-0.17	
Deer Trail, Washington[7]	+4.5-+11.6	-	+10.6	+6.2	S

1. I = igneous; S = sedimentary; n.i. = not indicated in cited source.

2. Table 4-4.

3. Beaty et al., 1986.

4. Thompson et al., 1984.

5. MacDonald et al., 1986.

6. Rye et al., 1974. Defiance and Thompson are different workings in the Darwin deposit area.

7. Fluet et al., 1987.

4.7.4. Carbon and Oxygen Isotopes of Carbonates

Carbon and oxygen isotope analyses of 20 calcite and altered and unaltered limestone samples are in Table 4-10.

4.7.4.1. Results

The carbonate isotopic analyses group clearly into three clusters, corresponding to unaltered limestone, altered limestone, and calcite. Mean isotopic compositions for each group are in Table 4-11, and data are plotted in Figure 4-60. The separation of groups reflects oxygen isotope compositions alone, since carbon isotope compositions of the three groups overlap significantly.

The "unaltered limestone" group includes two dolomitic samples (JB13-3 and MW 207 (8.3)), both of which have del ^{18}O greater than 23‰. The non-dolomitic limestones have oxygen isotope compositions ranging from 18.89 to 21.47‰. Carbon isotope compositions range from -3.19 to -0.18‰. These values are comparable to reported ranges for Devonian limestones (del ^{18}O = +19 to 27 and del ^{13}C = -5 to +3 ‰.: Veizer and Hoefs, 1976).

Table 4-10: Oxygen and carbon isotope data, Midway area, north-central British Columbia.[1]

Sample[2]	Type[3]	del ^{13}C (PDB)	del ^{18}O (SMOW)	Comment[3]
JB13-3	Unaltered ls	-2.81	24.43	Silvertip Hill, laminated dolomitic ls
JB5-6	Unaltered ls	-3.19	18.86	Smoke Mountain
90(218)	Unaltered ls	-0.23	19.97	Tour Ridge
178(1.53)	Unaltered ls	-0.18	20.37	5 m from orebody
193(22.0)	Unaltered ls	-0.55	21.47	1 m from orebody, slightly bleached
207(8.3)	Unaltered ls	-0.18	23.14	adjacent to orebody, bleached, dolomitic ls
MW Portal	Altered ls	-0.40	12.55	200 m from orebody
143(45.0)	Altered ls	-0.29	10.13	35 m from orebody
178(11.7)	Altered ls	-3.93	11.83	adjacent to orebody, moderately bleached
178(11.75)	Altered ls	-7.38	11.40	white recrystallized ls, replaced by Py, Gn
143(11.95)	Altered ls	-1.29	10.54	adjacent to orebody, strongly bleached
142(4.65)	Altered ls	-1.42	10.87	adjacent to orebody, bleached
B84	Altered ls	-0.42	11.34	ls clasts in calcite spar matrix breccia
B84	Spar	-3.21	1.24	matrix of ls breccia
207(8.0)	Spar	-3.33	0.18	white spar, replaced by Gn, Sp
146(2.0)	Spar	-2.82	-1.68	grey-white spar with stylolitic Py
B88	Spar	-2.79	1.95	vuggy spar, replaced by sulphides
143(27.25)	Vug filling	-3.03	0.95	late spar
143(3.7)	Calcarenite	-3.90	1.31	carbonate clastic fill and mixed shale fragments
143(45.0)	Vein	-2.69	0.94	calcite veinlet in limestone

1. Samples were analyzed at the Stable Isotope Laboratory of H.R. Krouse, Department of Physics, University of Calgary, using KH-2 standard.

2. Sample location designations: 77(298) refers to diamond drill hole number and metreage; B84 refers to underground heading and metreage from the beginning of the heading; JB13-3 refers to traverse stations from the 1987 field season.

3. Abbreviations: ls = limestone; Py = pyrite; Sp = sphalerite; Gn = galena.

Table 4-11: Average carbon and oxygen isotope compositions of unaltered and altered limestone and calcite, Midway area, north-central British Columbia.

Material analyzed	$\delta^{13}C$ (PDB)[1]	S.D.[2]	$\delta^{18}O$ (SMOW)[3]	S.D.[2]
Unaltered limestone (n=6)	-1.19	1.41	21.37	2.09
Altered limestone (n=7)	-2.16	2.62	11.24	0.81
Calcite, others (n=7)	-3.11	0.42	0.70	1.17

1. PDB = Pee Dee Belemnite (Craig, 1957).

2. S.D. = standard deviation.

3. SMOW = Standard Mean Ocean Water (Baertschi, 1976).

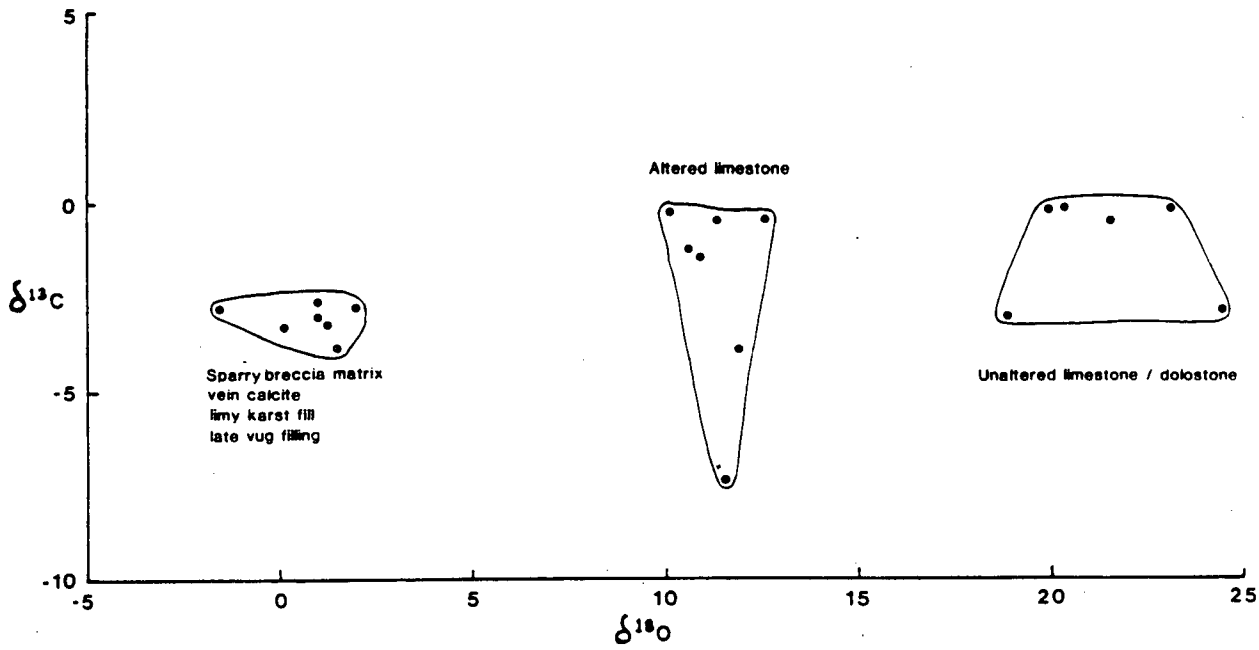

Figure 4-60: Oxygen and carbon isotope compositions of carbonates from the Midway area.

The "altered limestone" group has del ^{18}O values ranging from 10.54 to 12.55‰. (Table 4-10), averaging 11.24‰.. (Table 4-11). Average ^{18}O depletion in altered limestone, relative to a mean unaltered del ^{18}O of +21.37‰. (Table 4-11), is 10.13‰.. In contrast, carbon isotope compositions are very similar in the two groups. The average ^{18}O depletion amounts to almost 50% of the average unaltered del ^{18}O value. Also significant is the tight clustering of the two groups, and lack of intermediate del ^{18}O values (Figure 4-60).

All limestones from both groups are thoroughly recrystallized. Although several of the samples in the altered group are strongly bleached, samples MW Portal and B84 are not visibly altered. As well, two of the unaltered group of samples are visibly bleached (MW 193 (22.0) and MW 207 (8.3)). Therefore, the isotopic alteration is "cryptic", and not predictable on the basis of visible alteration. The bleached effect might be due to oxidation of organic carbon during fluid - rock exchange, releasing CO_2 into the fluid. The lack of a strong correlation between oxygen and carbon isotope depletions means that fluid - rock exchange, and not decarbonation, is the principle mechanism involved (Valley, 1986). However, the most intensely bleached and recrystallized sample (MW 178 (11.75)) is also strongly depleted in ^{13}C, probably a result of

decarbonation.

The data set includes McDame Group samples taken at distances from the Midway sulphide bodies ranging from adjacent to seven kilometres (JB5-6). The three samples from distances of over 500 metres (JB13-3, MW 90 (218) and JB5-6) are in the unaltered group. One of the altered samples (MW Portal) was about 200 metres from the nearest known massive sulphide; all other altered samples were located 35 metres or less from orebodies. Three of the unaltered samples were from locations less than 5 metres from massive sulphide. This suggests that if there is a spatial relationship between the isotopic depletions and the sulphide bodies, it is irregular and variable. A large number of analyses would be needed to display such a relationship conclusively.

The third group of samples includes several types of calcite, which have del ^{18}O values from -1.68 to +1.95‰.. (Table 4-10). Del ^{13}C ranges from -3.90 to -2.69‰.. Three of the calcites are partly replaced by sulphide and therefore are premineral (MW 207 (8.0), MW 146 (2.0) and B88). Sample B84 is from the sparry matrix of a limestone breccia with angular rotated clasts of unbleached altered limestone. Sample MW 143 (3.7) consists of pale grey, granular calcite containing abundant shale fragments. Both of these calcites might be

related to premineral brecciation and matrix infilling. Samples MW 143 (27.25), from a white sparry calcite vug filling, and MW 143 (45.0), from a white calcite vein, could be either premineral or late stage carbonate from the mineralizing system.

4.7.4.2. Interpretation

Isotopic alteration of limestones in mineralized districts has been a well-known phenomenon since the study of the Leadville limestone in Colorado by Engel et al.(1958). The ^{18}O depletions in limestones at Midway are among the largest recorded in the mineral deposit literature (cf. Engel et al., 1958; Lovering et al., 1963; Hall and Friedman, 1969; Pinckney and Rye, 1972). Isotopic depletions are usually of smaller magnitude and wider range, and in some skarn - manto districts are not found at all (e.g. Providencia, Mexico; cf. Pinckney and Rye, 1972). The depletions offer clear evidence of extensive fluid - rock interaction, and almost certainly indicate a meteoric water component. Since meteoric waters generally become increasingly depleted in ^{18}O with higher latitudes, the large magnitude of the depletions at Midway could be, in part, a function of its northerly location.

Similarly, the del ^{18}O values of calcite are among the lowest reported in the literature; in fact, the only similar

compositions (averaging about 0‰.) are from the Bluebell Mine, British Columbia (Ohmoto and Rye, 1972). The calcites could only have been deposited from isotopically depleted (i.e. meteoric) waters.

An examination of four of the calcite samples failed to discover useable fluid inclusions. Inclusions observed were very small (less than 5 microns) and contained tiny, rapidly moving bubbles, indicating low homogenization temperatures (probably less than 150°C). These inclusions could have been primaries or secondaries. However, the oxygen isotope compositions of Midway calcites would be difficult to reconcile with nonmeteoric waters at almost any reasonable temperature. Using the calcite - water fractionation equation of Friedman and O'Neil, 1977:

$$\text{delta (calcite-water)} = 2.78\ (10^6 / T^2) - 3.39$$

water in equilibrium with calcite of del ^{18}O of 0.70‰. will have del ^{18}O of -17.7‰. at T = 100°C. Such values are only likely to occur in meteoric waters. The normal range of magmatic waters is 5-9‰., and ocean water is 0‰. by definition (Taylor, 1979).

Timing of the fluid - rock interaction responsible for the isotopic depletions is not constrained by the data available. There is no evidence to link the depletions directly to the

mineralizing system, even if they were spatially zoned about the sulphide bodies. The McDame Group in the Midway area has undergone a complex history of fluid circulation, including Middle Devonian diagenesis (ocean water), Late Devonian uplift, erosion and karsting (meteoric water), Late Devonian subsidence and basin sedimentation (ocean water), Cretaceous intrusion and hydrothermal activity (meteoric $\pm$ magmatic water), and recent erosion and groundwater flow (meteoric water). Untangling the relative effects of these different episodes on the isotopic composition of the limestones is impossible with present data.

4.8. Deposit Model

The observations and data presented above provide the framework for a model of the genesis of the Midway deposit. A Late Cretaceous intrusion - driven hydrothermal cell deposited massive sulphides in relatively permeable karsted limestone horizons beneath a Late Devonian unconformity. Low pH, high temperature, moderately saline reducing solutions rose upward and outward from a buried felsic stock, guided by high angle fault conduits and a shale capping horizon. Sulphides were deposited in porous brecciated zones along the flanks of an antiformal structural trap, and replaced carbonate breccia matrix and wallrock outward from these zones.

This sketch of a genetic model for the Midway deposit is discussed below in terms of: (1) stratigraphic and structural controls, (2) origin of fluids and ore components, (3) sulphide deposition, and (4) fluid evolution.

4.8.1. Stratigraphic and Structural Controls

The most obvious control on localization of sulphide bodies is the favourable stratigraphic horizon, fetid limestones of the upper McDame Group. Physical and chemical characteristics of this horizon were favourable to fluid flow and sulphide

deposition.

Significant physical characteristics are the enhanced permeability and porosity of brecciated limestones (section 4.2.1.2) and the permeability contrast provided by overlying Earn Group silt shales (section 4.2.1.3). Late Devonian uplift and exposure of the carbonate shelf produced an unconformity that cuts across over 100 metres of stratigraphy (section 4.2.1.2). Infiltration of meteoric waters and limestone dissolution produced vug to cavern scale porosity and induced the formation of limestone collapse breccias. Subsequent submergence of the platform followed by deposition of anoxic basinal shales caused further solution collapse and mixing of shale and limestone fragments (section 4.4.3). These breccias were later partially healed by carbonate mud infilling and calcite deposition and recrystallization. Preservation of significant porosity and permeability in the McDame Group is a key part of the model. Infilling of early calcite breccia matrix and possible filling of remaining cavities by water could have provided the support to maintain porosity during Earn Group deposition and later compressional tectonic events.

In contrast to the vuggy, brecciated and generally well jointed McDame Group, overlying lowermost Earn Group represents a horizon of low permeability which guided fluid migration.

Locally this cap was absent or was breached, permitting significant fluid migration upward into the Earn Group, especially above the buried stock. This caused intense alteration of the clastic sediments (section 4.3). Sulphide veins and stockwork zones in the shale cap were produced where it was fractured above massive sulphide bodies.

The most important chemical characteristic of the upper McDame Group is its reactivity with infiltrating acid hydrothermal solutions. This was a probable contributing mechanism to sulphide deposition, especially deposition of sphalerite and galena. The mechanism enabling maintenance of low pH at some distance from the intrusion is unclear. Large quartz vein intersections in the Silvertip Hill area and silicified zones around sulphide bodies suggest that silicification of conduits in the limestone might have moderated carbonate - fluid reactions, enabling fluids to maintain low pH levels at increasing distances into the limestones.

Important structural controls on fluid migration were developed during both Jurassic and Late Cretaceous deformation. Northeasterly directed Jurassic compression produced an antiformal structural trap which probably localized fluid migration into the Silver Creek - Discovery area (section 4.2.2). The southeasterly plunge of structures in the Silvertip

Mountain area caused ascending hydrothermal solutions to migrate northwesterly away from the intrusive heat source beneath Brinco Hill. High angle faulting during the Late Cretaceous generated crushed gouge zones which guided fluid flow mainly between the Camp Creek and Brinco Creek faults. The Camp Creek fault and related splays could have acted as feeders to both Silver Creek and Silvertip mineralization. Specifically, convergence of faults to the north could have forced fluids into a tight structural trap as they migrated in a northwesterly direction.

4.8.2. Origin of Fluids and Ore Components

The origin of the mineralizing waters can only be speculated on in the absence of isotopic analyses of inclusion fluids. Oxygen isotope data on carbonates clearly shows that significant interaction occurred between wallrock and depleted meteoric waters, and that carbonate breccia matrix was deposited from meteoric solutions. Timing of the meteoric water interaction is unknown, although a combination of Late Devonian karsting, Late Cretaceous mineralization and recent groundwater flow is possible.

Fluid characteristics can be defined on the basis of fluid inclusion data. Coexisting immiscible liquid and vapour phases indicate temperatures in the 300 - 340^{o}C range for main stage

sulphide deposition (section 4.6.5). Textural evidence and the presence of CO_2 liquid in three phase inclusions are consistent with stratigraphic evidence indicating depths of 1.5 to 2 kilometres or more (section 4.6.7). Salinities of 7 to 10 weight percent NaCl equivalent were observed, with anomalous salinities of up to 21 weight percent. The anomalous salinities could be due to locally enhanced $CaCl_2$ /(NaCl + $CaCl_2$) ratios, which would depress the eutectic ice melting temperature without requiring substantially increased total solute contents. Fluids during main stage sulphide deposition were H_2O - CO_2 - CH_4 mixtures, with an estimated 0.2 mole fraction CO_2, and small amounts of methane (section 4.6.4). Pressure and/or temperature reduction near the site of deposition caused the separation of immiscible liquid and vapour phases, with CO_2 and CH_4 partitioning into the vapour phase and electrolytes partitioning into the liquid phase. Liquid - vapour mixtures were locally trapped, producing three phase inclusions of variable density (section 4.6.4).

Fluids were initially acidic, with a pH of 4.5 to 5.0, as indicated by sericitic alteration assemblages in the Earn Group (section 4.7.3.5). This enabled significant carbonate dissolution and replacement by quartz and sulphides. Carbon isotope compositions of altered McDame Group underwent only small changes, suggesting that del ^{13}C of fluid carbonate

species was about the same as that of the wallrock. Therefore, most carbonate in solution was probably derived from wallrock dissolution.

Sulphide assemblages (section 4.4.6), the narrow range of sulphur isotope compositions (section 4.7.3.2), the lack of hypogene oxide and sulphate phases and the presence of CH_4 (section 4.6.4) all imply reducing fluids, in the vicinity of the pyrite - pyrrhotite buffer. Transition from pyrrhotitic to pyritic assemblages with decreasing depth might reflect an increasing fluid oxidation state, perhaps due to mixing with more oxygenated groundwater. Other factors such as an increase in total sulphur content could also be involved. Control of redox reactions by carbonaceous shales at the unconformity cannot be documented, but bleaching of limestones near sulphide bodies suggests that oxidation of organic carbon might have occurred at some stage. Such reactions coupled with reduction of fluid sulphur might have locally precipitated iron sulphide phases.

The relatively homogeneous sulphide sulphur isotope compositions indicate a well mixed source and low sulphate/sulphide ratio (section 4.7.3.4). Calculated $\underline{del}\ ^{34}S$ (H_2S) compositions are compatible with a relatively oxidized magmatic sulphur source, although the upper end of the range of

values suggests significant incorporation of sedimentary sulphur.

Fluid salinities in the 7 to 10 weight percent range permit transport of most of the silver, lead, zinc and copper in solution as chloride complexes.

Lead isotopes show that Midway lead is among the least radiogenic of Rancheria district epigenetic deposits, but is still broadly upper crustal in nature. Lead isotope signatures of mid-Cretaceous to Eocene epigenetic deposits of the Rancheria district define a linear array with a slope compatible with mixing between two distinct lead sources. The radiogenic end member of the mixing system can be approximated by lead evolution from a source of 2.0 Ga in an environment with mu equal to about 12.78 (section 2.5). The less radiogenic end member is uranium poor but thorium enriched relative to typical mantle sources, and therefore might be lower crustal in origin. In general, base metals in the deposit were likely derived from a combination of igneous and sedimentary sources.

4.8.3. Sulphide Deposition

A number of mechanisms of sulphide deposition are compatible with the evidence. Initiation of deposition in massive sulphide

zones might have occurred as a result of rapid transition from lithostatic to sub-lithostatic pressures as fluids encountered karst cavities. If these zones were water filled, significant temperature decreases by groundwater mixing might have been important as well. Widespread fine feathery or dendritic pyrite textures (section 4.4.6) suggest a rapid crystallization mechanism, which implies rapid P and/or T fluctuations. Over time, fluids must have equilibrated with carbonate wallrock, causing an increase in pH, and precipitating sulphides through replacement. Lower wallrock reactivity due to silicification could have enabled an acidity front to progressively infiltrate the limestones, causing replacement on a large scale. Immiscible vapour phase loss through wallrock microfractures in permeable zones probably increased solute concentrations, causing precipitation. Oxidation of methane in the fluid and organic carbon in wallrocks, coupled with reduction of fluid sulphur species probably enabled deposition of iron sulphide phases.

4.8.4. Fluid Evolution

Sulphur isotopes (section 4.7.3.5), the tin sulphide signature (section 4.4.6) and fluorine alteration haloes aound the inferred intrusive centre (section 4.3) suggest that late stage igneous fluids were released from the buried stock and mixed with convecting groundwater. Alteration of country rock by

acid, chloride - fluoride solutions caused widespread sericitization, pyrite deposition and substitution of fluorine for hydroxyl groups in secondary micas. Dissolution of limestone and oxidation of organic carbon caused an increase in dissolved carbon dioxide, which might have been coupled with reduction of fluid sulphur. Deeper level skarnification of carbonate country rocks also might have contributed significant CO_2 to the fluid system.

The acidic fluids silicified carbonate wallrocks along fault and joint conduits, and replaced carbonate with sulphide outward from permeable karst breccia zones. Liquid - vapour immiscibility occurred, perhaps as a result of transition to sublithostatic pressure in these zones, causing release of CO_2 and CH_4 along fractures. Convective heat loss, probably coupled with mixing with cooler groundwater, caused a decrease in fluid temperature as migration took place up and outward from the heat source. Lower temperature fluids with low CO_2 and no CH_4 evolved to an aqueous saline solution with negligible dissolved carbon dioxide, which was trapped in microfractures in previously deposited minerals.

Late stage to post-mineral, oxygenated carbonate and sulphate rich meteoric waters deposited barite, calcite and gypsum in remaining vugs and breccia cavities, and altered

pyrrhotite to marcasite along fractures. With uplift and erosion, renewed karsting and groundwater flow reopened karst cavities and locally overprinted sulphides with a supergene hydroxide - carbonate - sulphate assemblage.

5. The Manto Deposit Model and Exploration

The Midway deposit as described in previous chapters is a classic manto deposit with several features of broader exploration significance. Manto deposits are similar to skarns in being genetically related to intrusions, but occur in a more distal environment in unskarned carbonate host rocks. Historically they have been a significant source of both base (zinc, lead and copper) and precious (silver and gold) metals, and currently represent attractive exploration targets.

Lead isotope data for the Midway deposit, in the broader regional context of the Rancheria silver district (section 2.5.2.1.), indicate a dominantly upper crustal source of metals with minor lower crustal input in a two component mixing system. Cassiar Terrane sediments could supply upper crustal lead, with a lower crustal contribution from an intrusive source modelled as a lower crustal melt. Mixing of the two end members could be accomplished by contamination of a small batch lower crustal melt by upper crustal sediments, or by hydrothermal fluid circulation within the intrusion and country rock at the site of intrusive emplacement. In the northern Cordillera, the distinctively radiogenic lead isotope signature of Cretaceous - Tertiary intrusion related deposits, including skarns, veins and mantos, can help distinguish these targets from older,

relatively precious metal poor deposits (section 2.5.1).

Regionally, manto deposits are important targets in the miogeoclinal sediments in Cassiar Terrane and along the North American margin east of the Tintina - Northern Rocky Mountain Trench transcurrent fault (section 2.2). Lower Cambrian (Rosella Formation: section 3.2.1.) and Middle Devonian (McDame Group: section 3.2.5.) limestones are particularly significant stratigraphic horizons, containing carbonate sections with thicknesses in excess of 200 metres. In the case of the McDame Group, the unconformable contact with overlying black shales of the Earn Group played an important role at Midway in guiding hydrothermal fluid flow and thereby localizing some of the massive sulphide bodies along the contact. Similar horizons of contrasting permeability in carbonate sections could be of considerable exploration utility.

Several Cretaceous - Tertiary granitic intrusive suites are related to skarn - manto systems in the northern Cordillera (sections 3.5. and 4.3). All intrusions emplaced in the thickened continental crust of the northern Omineca Belt and North American margin have high initial strontium ratios indicative of their crustal origin (Armstrong, 1988; Anderson, 1988). Both S-type and A-type analogues are present (Anderson, 1988). Manto deposits are commonly related to unexposed

intrusions because of their more distal nature, as in the case of Midway. Nevertheless, geophysical anomalies, widespread sericitic alteration, quartz veining, pyritization and hornfelsing are common indicators of buried intrusions related to skarn - manto systems. Exploration geochemistry in this environment would focus on granophile elements such as W, Sn, Mo, F, U and REE's, as well as on the more standard As, Sb, Pb, Zn, Cu and Ag (section 4.3).

High level emplacement of highly evolved small batch melts in thickened continental crust is more likely in an extensional environment; therefore, high angle normal fault systems are likely to occur in significant skarn - manto districts, as at Midway (sections 3.7.3. and 4.2.2). Doming and radial fault patterns above buried intrusions are also highly prospective structural features. The relationship between these high angle fault systems and Cretaceous - Tertiary transcurrent faults is inadequately known at present (section 3.7.3), but extensional zones along major transcurrent faults (e.g. at fault bends) are possible focal points for emplacement of small granitic stocks.

Fluid trapping structures such as domes and antiforms could also become significant target areas, especially when a relationship between a mineralized horizon and an unconformity or other fluid flow guide is established (section 4.2.2).

Hydrothermal fluids tend to migrate updip or up-plunge along such horizons, with pooling of fluids occurring in domes or along the apex of antiforms, analogously to the migration of brines in oil fields.

Host rock porosity is another geological feature of potential exploration importance. The link between karsted carbonate horizons and mineralization is well established in some "Mississipi Valley type" deposit districts (e.g. Nanisivik and Pine Point, N.W.T.) and might apply in manto districts as well, as shown at Midway (section 4.4.3. and 4.4.4). In this context, oxygen isotopes represent an unused exploration tool, which is especially applicable in the northern Cordillera where meteoric water is very low in ^{18}O (section 4.7.4). Even in cases where the timing of meteoric water interaction is equivocal, intense ^{18}O depletions in carbonates might signal karsted horizons of enhanced porosity or hydrothermal activity.

Fluid inclusion data indicates that the fluid that deposited quartz and sulphides at Midway was a high temperature (300°C or greater), CO_2 and CH_4 bearing brine with a salinity of 7-10 weight % NaCl equivalent. Fluid temperatures distinguish skarn - manto systems from lower temperature carbonate hosted deposits related to basin dewatering. The loss of carbonic components over time is recorded in sets of lower temperature secondary

inclusions, and could be due to partitioning into an immiscible vapour phase as well as to declining CO_2 solubilities in H_2O as temperatures decrease.

The narrow range of sulphur isotope values of sulphides at Midway is typical of high temperature skarn - manto systems (section 4.7.3.8) and distinguishes them from "sedex" and "Mississippi Valley type" deposits which commonly have a range of values of 20‰. or more. The calculated del ^{34}S value of 7‰. for total fluid sulphur is compatible with a mixture of both magmatic and sedimentary sulphur sources (section 4.7.3.5).

Iron sulphide mineralogy and zoning suggests fluid oxidation states near the pyrite - pyrrhotite buffer, with a possible transition to more oxidized levels (pyrite - dominated assemblages) as fluids move away from the intrusive centre. Since the pyrite stability field expands with decreasing temperature relative to pyrrhotite, this zoning relationship (section 4.4.7) is probably due mainly to decreasing fluid temperature. The establishment of mineral and metal ratio zoning patterns is a fundamental exploration tool in skarn - manto districts, where copper - iron sulphide (gold, bismuth) skarn cores commonly grade into lead - silver sulphosalt rich assemblages in the more distal, higher level manto environment.

6. References

Abbott, J.G. (1984): Silver - Bearing Veins and Replacement Deposits of the Rancheria District. Yukon Exploration and Geology 1983, Exploration and Geological Services Division, Indian and Northern Affairs Canada, 34-44.

Anderson, R.G. (1988): An Overview of Some Mezozoic and Tertiary Plutonic Suites and their Associated Mineralization in the Northern Canadian Cordillera. In Taylor, R.P. and Strong, D.F., eds., Recent Advances in the Geology of Granite-Related Mineral Deposits, Special Volume 39, The Canadian Institute of Mining and Metallurgy.

Andrew, A, Godwin, C.I. and Sinclair, A.J. (1984): Mixing Line Isochrons: A New Interpretation of Galena Lead Isotope Data from Southeastern British Columbia. Economic Geology, 79, 919-932.

Archambault, M. (1985): Geology and Mineralography of the Silver Creek Deposit, Midway Property, North - Central British Columbia. Unpublished M.Sc. Report, University of British Columbia, 96 pages.

Armstrong, R.L. (1988): Mesozoic and Early Cenozoic Magmatic Evolution of the Canadian Cordillera. Rogers Symposium Volume, Geological Society of America Special Paper 218.

Baertschi, P. (1976): Absolute ^{18}O content of Standard Mean Ocean Water. Earth and Planetary Science Letters, 31, 341.

Beaty, D.W., Cunningham, C.G., Rye, R.O., Steven, T.A., and Gonzalez - Urien, E. (1986): Geology and Geochemistry of the Deer Trail Pb-Zn-Ag-Au-Cu Manto Deposits, Marysvale District, West - Central Utah. Economic Geology, 81, 1932 - 1952.

Birnie, R.W., and Petersen, U. (1977): The Paragenetic Association and Compositional Zoning of Lead Sulphosalts at Huachacolpa, Peru. Economic Geology, 72, 983-992.

Bodnar, R.J., Reynolds, T.J. and Kuehn, C.A. (1985): Fluid - Inclusion Systematics in Epithermal Systems. In Berger, B.R. and Bethke, P.M. (eds.) Geology and Geochemistry of Epithermal Systems; Reviews in Economic Geology, 2.

Bowers, T.S. and Helgeson, H.C. (1983): Calculation of the Thermodynamic and Geochemical Consequences of Nonideal mixing in the System H_2O-CO_2-NaCl on Phase Relations in Geologic Systems: Equations of State for H_2O-CO_2-NaCl Fluids at High Pressures and Temperatures. Geochimiica et Cosmochimica Acta, 47, 1247-1275.

Bradford, J.A. and Godwin, C.I. (1988): Midway Silver - Lead - Zinc Manto Deposit, Northern British Columbia (1040/16). B.C. Ministry of Energy, Mines and Petroleum Resources, Geological Fieldwork, 1987, Paper 1988-1, 353-360.

Brown, P.E. and Lamb, W.H. (1986): Mixing of H_2O-CO_2 in Fluid Inclusions; Geobarometry and Archean Gold Deposits. Geochimica et Cosmochimica Acta, 50, 847-852.

Brundland, E.(1958): Report on Silver Tip Option 1958. Noranda - Canex - Bralorne Joint Venture, unpublished private report, British Columbia Ministry of Energy, Mines and Petroleum Resources Property File.

Burruss, R.C. (1981): Analysis of Phase Equilibria in C-O-H-S Fluid Inclusions. In Hollister, L.S. and Crawford, M.L., eds., Fluid Inclusions: Applications to Petrology; Mineralogical Association of Canada Short Course, 6, 39-74.

Carne, R.C. and Cathro, R.J. (197): Sedimentary Exhalative (Sedex) Zinc - Lead - Silver Deposits, Northern Canadian Cordillera. Canadian Institute of Mining and Metallurgy Bulletin, 75, 66-81.

Christopher, P.A., White, W.H., and Harakal, J.E. (1972): Age of Molybdenum and Tungsten Mineralization in Northern British Columbia. Canadian Journal of Earth Sciences, 9, 1727-1734.

Collins, P.L.F. (1979): Gas Hydrates in CO_2 - Bearing Fluid Inclusions and the Use and Misuse of Freezing Data for Estimation of Salinity. Economic Geology, 74, 1435-1444.

Collins, W.J., Beams, S.D., White, A.J.R., and Chappell, B.W. (1982): Nature and Origin of A - Type granites with Particular Reference to Southeastern Australia. Contributions to Mineralogy and Petrology, 80, 189-200.

Cooke, B.J., and Godwin, C.I. (1984): Geology, Mineral Equilibria, and Isotopic Studies of the McDame Tungsten Skarn Prospect, North-Central British Columbia. Economic Geology, 79, 826-847.

Cordilleran Engineering (1981): Geological and Geochemical Report on Way 1-23, Bull 1-5, Climax 1-11, Post 1 and Macc Mineral Claims, Liard Mining Division. British Columbia Ministry of Energy, Mines and Petroleum Resources, Assessment Report 9,912.

Cordilleran Engineering Ltd. (1982): Geological, Geochemical, Geophysical and Drilling Report on Way 1-33, Bull 1-6, Climax 1-11, Post 1-10 and Macc Claims, Liard Mining Division, B.C. British Columbia Ministry of Energy, Mines and Petroleum Resources, Assessment Report 11,020.

Cordilleran Engineering (1983): Diamond Drilling Report on Way 1-35, Bull 1-27, Climax 1-16, Post 1-16, Beth 1-4, Star 2-3, Renee 1 and Toots 4 Claims, Liard Mining Division, B.C. British Columbia Ministry of Energy, Mines and Petroleum Resources, Assessment Report 11,799.

Cordilleran Engineering (1984): Diamond Drilling and Physical Report, Way 1-35, Bull 1-27, Climax 1-16, Post 1-16, Beth 1-4, Star 2-3, Renee 1 and Toots 4 Claims, Liard Mining Division, B.C. British Columbia Ministry of Energy, Mines and Petroleum Resources, Assessment Report 13,259.

Cordilleran Engineering (1985): Physical and Diamond Drilling Report on the Bull 16, 23 and 25FR Claims. British Columbia Ministry of Energy, Mines and Petroleum Resources, Assessment Report 14,104.

Craig, H. (1957): Isotopic standards for carbon and oxygen and correction factors for mass - spectrometric analysis of carbon dioxide. Geochica et Cosmochimica Acta, 12, 133-149.

Dawson, K.M., Godwin, C.I. and Gabites, J. (1985): Lead Isotope Analyses from Silver - Rich Deposits in the Cassiar, Midway and Ketza River Areas of the Northern Cordillera. Geological Association of Canada, Cordilleran Section, Abstract and Program, "Silver '85" Symposium, 6-8.

Diakow, L.J. and Panteleyev, A. (1982): Cassiar Gold Deposits, McDame Map Area (104P/4,5). British Columbia Ministry of Energy, Mines and Petroleum Resources, Geological Fieldwork, 1981, Paper 1982-1, 156-161.

Doe, B.R. and Zartman, R.E. (1979): Plumbotectonics, the Phanerozoic. In Barnes, H.L., ed. Geochemistry of Hydrothermal Ore Deposits, Second Edition; Wiley and Sons, New York, 22-70.

Engel, A.E.J., Clayton, R.N. and Epstein, S. (1958): Variations in Isotopic Composition of Oxygen and Carbon in Leadville Limestone (Mississipian, Colorado) and In Its Hydrothermal and Metamorphic Phases. Journal of Geology, 66, 374-393.

Erdmer, P. and Baadsgaard, H. (1987): 2.2 Ga Age of Zircons in Three Occurrences of Upper Proterozoic Clastic Rocks of the Northern Cassiar Terrane, Yukon and British Columbia. Canadian Journal of Earth Sciences, 24, 1919-1924.

Evans, A.M. (1959): A Tin - Bearing Ore from the Coal River Area, Yukon Territory. The Canadian Mineralogist, 6, 119-127.

Farley, A.L. (1979): Atlas of British Columbia. The University of British Columbia Press, 136 pp.

Field, C.W. and Fifarek, R.H. (1987): Light Stable Isotope Systematics in the Epithermal Environment. In Berger, B.R., and Bethke, P.M., ed. Geology and Geochemistry of Epithermal Systems; Reviews in Economic Geology, 2, 99-128.

Field, C.W., and Gustafson, L.B. (1976): Sulfur Isotopes in the Porphyry Copper Deposit at El Salvador, Chile. Economic Geology, 71, 1533-1548.

Fluet, D.W., Changakoti, A., Morton, R.D., Gray, J., and Krouse, H.R. (1987): The Genesis of the Deer Trail Zn-Pb-Ag Vein Deposits, Northeast Washington, U.S.A.: Evidence from Fluid Inclusion and Stable Isotope Studies. Canadian Journal of Earth Sciences, 24, 1715-1726.

Ford, D.C. (1986): Genesis of Paleokarst and Strata-Bound Zinc-Lead Sulphide Deposits in a Proterozoic Dolostone, Northern Baffin Island, Canada - A Discussion. Economic Geology, 1562-3.

Friedman, I. and O'Neil, J. (1977): Compilation of Stable Isotope Fractionation Factors of Geochemical Interest. in Fleischer, M. (ed.), Data of Geochemistry, Sixth Edition, United States Geological Survey Professional Paper 440-KK, KK1-KK12.

Fritz, W.H. (1980): Two New Formations in the Lower Cambrian Atan Group, Cassiar Mountains, North - Central British Columbia. Current Research, Part B, Geological Survey of Canada, Paper 80-1B, 217-225.

Fritz, W.H. (1985): The Basal Contact of the Road River Group - a Proposal for Its Location in the Type Area and in Other Selected Areas in the Northern Canadian Cordillera. Current Research, Part B, Geological Survey of Canada, Paper 85-1B, 205-215.

Gabrielse, H. (1963): McDame Map Area, British Columbia. Geological Survey of Canada, Memoir 319, 138 p.

Gabrielse, H. (1969): Geology of Jennings River Map Area, British Columbia (104-O). Geological SUrvey of Canada, Paper 68-55, 37 p.

Gabrielse, H. (1981): Stratigraphy and Structure of Road River and Associated Strata in Ware (West Half) Map Area, Northern Rocky Mountains, British Columbia. Current Research, Part A, Geological Survey of Canada, Paper 80-1A, 201-207.

Gabrielse, H. (1985): Major Dextral Transcurrent Displacements Along the Northern Rocky Mountain Trench and Related

Lineaments in North - Central British Columbia. Geological Society of America, Bulletin, 96, 1-14.

Gabrielse, H., and Mansy, J.L. (1980): Structural Style in Northeastern Cry Lake Map Area, North - Central British Columbia. Current Research, Part A, Geological Survey of Canada, Paper 80-1A, 33-35.

Gardner, H.D. and Hutcheon, I. (1985): Geochemistry, Mineralogy, and Geology of the Jason Pb-Zn Deposits, MacMillan Pass , Yukon, Canada. Economic Geology, 80, 1257-1276.

Godwin, C.I., Armstrong, R.L.A. and Thompson, K.M. (1980): K-Ar and Rb-Sr Dating and the Genesis of Tungsten at the Clea Tungsten Skarn Property, Selwyn Mountains, Yukon Territory. C.I.M. Bulletin, 73, no. 821, 90-93.

Godwin, C.I., Gabites, J. and Andrew, A. (1988): LEADTABLE: A Galena Lead Isotope Data Base For the Canadian Cordillera, With a Guide to its Use by Explorationists, British Columbia Ministry of Energy, Mines and Petroleum Resources, Paper 1988-4.

Godwin, C.I. and Sinclair, A.J. (1982): Average Lead Isotope Growth Curves for Shale - Hosted Zinc - Lead Deposits: Canadian Cordillera. Economic Geology, 77, 675-690.

Godwin, C.I., Sinclair, A.J. and Ryan, B.D. (1982): Lead Isotope Models for the Genesis of Carbonate - Hosted Zn-Pb, Shale - Hosted Ba-Zn-Pb, and Silver - Rich Deposits in the Northern Canadian Cordillera. Economic Geology, 77, 82-94.

Gordey, S.P., Abbott, J.G., and Orchard, M.J. (1982): Devono - Mississipian (Earn Group) and Younger Strata in East - Central Yukon. in Current Research, Part B, Geological Survey of Canada, Paper 82-1B, 93-100.

Gordey, S.P., Abbott, J.G., Tempelman - Kluit, D.J., and Gabrielse, H. (1986): "Antler" Clastics in the Canadian Cordillera. Geology, 15, 103-107.

Goutier, F. (1986): Galena Lead Isotope Study of Mineral Deposits in the Eagle Bay Formation, Southeastern British Columbia. Unpublished M.Sc. Thesis, University of British Columbia, 153 pages.

Hall, W.E. and Friedman, I. (1969): Oxygen and Carbon Isotope Compositions of Ore and Host Rock of Selected Mississipi Valley Deposits. in Geological Survey Research, 1969, United States Geological Survey Professional Paper 650-C, C140-C148.

Hall, W.E., and MacKevett, E.M., Jr. (1958): Economic Geology of the Darwin Quadrangle, Inyo County, California. United States Geological Survey Professional Paper 368, 87 pages.

Harms, T.A. (1984): Structural Style of the Sylvester Allochthon, Northeastern Cry Lake Map Area, British Columbia. Current Research, Part A, Geological Survey of Canada, Paper 84-1A, 109-112.

Harms, T.A. (1985a): Pre-emplacement Thrust Faulting in the Sylvester Allochthon, Northeast Cry Lake Map Area, British Columbia. Current Research, Part A, Geological Survey of Canada, Paper 85-1A, 301-304.

Harms, T.A. (1985b): Cross Sections Through Sylvester Allochthon and Underlying Cassiar Platform, Northern British Columbia. Current Research, Part B, Geological Survey of Canada, Paper 85-1B, 341-346.

Harms, T.A. (1986): Structural and Tectonic Analysis of the Sylvester Allochthon, Northern British Columbia: Implications For Paleogeography and Accretion. Unpublished PhD. Thesis, University of Arizona.

Harms, T.A., Nelson, J. and Bradford, J. (1988): Geological Transect Across the Sylvester Allochthon North of the Blue River, Northern British Columbia (104P/12). British Columbia Ministry of Energy, Mines and Petroleum Resources, Geological Fieldwork, 1987, Paper 1988-1, 245-8.

Holland, S.S. (1968): Silvertip, Liard Mining Division. British Columbia Department of Mines and Petroleum Resources, Annual Report 1968, 24-33.

Kajiwara, Y. and Krouse, H.R. (1979): On the Rate of Sulfur Isotope Homogenization in Some Metallic Sulfide Systems. Annual Report of the Institute of Geoscience, University Tsukuka, 5, 58-61.

Krouse, H.R., Ueda, A., and Campbell, F.A. (1988): Sulphur Isotope Abundances in Coexisting Sulphate and Sulphide; Kinetic Effects Versus Exchange Phenomena. in H.K. Herbert, ed., Special Publication, Geological Society of Australia.

Large, D.E. (1980): On the Geology, Geochemistry and Genesis of the Tom Pb-Zn-Barite Deposit, Yukon Territory, Canada. Unpublished PhD Thesis, Braunschweig, West Germany, Institute Geology Paleontology, 153 pages.

Lefebure, D. (1987): Northwestern District. British Columbia Ministry of Energy, Mines and Petroleum Resources, Exploration in British Columbia, 1986, A39-A49.

Lovering, T.S., McCarthy, J.H. and Friedman, I. (1963): Significance of $^{18}O/^{16}O$ and $^{13}C/^{12}C$ Ratios in Hydrothermally Dolomitized Limestones and Manganese Carbonate Replacement Ores of the Drum Mountains, Juab County, Utah. in Short Papers in Geology and Hydrology, United States Geological Survey Professional Paper 475-B, B1-B9.

Lovering T.S., Tweto, O., and Lovering, T.G., (1978): Ore Deposits of the Gilman District, Eagle County, Colorado. United States Geological Survey Professional Paper 1017, 90 pages.

Lowey, G.W. and Lowey, J.F. (1986): Geology of Spencer Creek (105B1) and Daughney Lake (105B2) Map Areas, Rancheria District, Southeast Yukon. Indian and Northern Affairs Canada, Yukon Region, Open File 1986-1.

MacDonald, A.J., Kreczmer, M.J., and Kesler, S.E. (1986): Vein , Manto and Chimney Mineralization at the Fresnillo Silver - Lead - Zinc Mine, Mexico. Canadian Journal of Earth Sciences, 23, 1603-1614.

MacIntyre, D.M. (1982): Midway Occurrence. British Columbia Ministry of Energy, Mines and Petroleum Resources, Geological Fieldwork, 1981, Paper 1982-1, 162-166.

MacIntyre, D.M. (1983): A Comparison of the Geological Setting of Stratiform Massive Sulphide Deposits of the Gataga District with the Midway and Windy - Craggy Deposits, Northern British Columbia (94F, L; 104O/16; 114P/12). British Columbia Ministry of Energy, Mines and Petroleum Resources, Geological Fieldwork, 1982, Paper 1983-1, 149-170.

Mato, G., Ditson, G. and Godwin, C.I. (1983): Geology and Geochronometry of Tin Mineralization Associated With the Seagull Batholith, South-Central Yukon Territory. C.I.M. Bulletin, 76, no. 854, 43-49.

McClay, K.R. and Insley, M.W. (1986): Structure and Stratigraphy of the Gataga Fold and Thrust Belt, Northeastern British Columbia. Current Research, Part A, Geological Survey of Canada, Paper 86-1A, 259-264.

Monger,J.W.H. and Berg, H.C. (1984): Lithotectonic Terrane Map of Western Canada and Southeastern Alaska, in Siberling, N.J. and Jones, D.L., ed., Lithotectonic Terrane Maps of the Northern Cordillera, United States Geological Survey, Open File Report 84-523, B1-B31.

Mortenson, J.K. (1979): Stratigraphic, Structural ans Tectonic

Setting of an Upper Devonian - Mississipian Volcanic - Sedimentary Sequence and Associated Base Metal Deposits in the Pelly Mountains, Southeastern Yukon Territory. M.Sc. Thesis, The University of British Columbia, 122 pages.

Mortenson, J.K. (1981): Geological Setting and Tectonic Significance of Mississipian Felsic Metavolcanics in the Pelly Mounatains, Southeastern Yukon Territory, Canadian Journal of Earth Sciences, 19, 8-22.

Mortenson, J.K. and Jilson, G.A. (1985): Evolution of the Yukon - Tanana Terrane: Evidence from Southeastern Yukon Territory. Geology, 13, 806-810.

Mulligan, R.H. (1975): Geology of Canadian Tin Occurrences. Geological Survey of Canada, Economic Geology Report, Number 28, 155 pp.

Mundy, D.J.C. (1984): Report on the McDame Limestone at Midway. Regional Resources Ltd., Private Report.

Murphy, D.C. (1988): Geology of Gravel Creek (105B/10) and Irvine Lake (105B/11) Map - Areas, Southeastern Yukon. Indian and Northern Affairs Canada, Yukon Region, Open File 1988-1, 61 pages.

Nelson, J.L. and Bradford, J.A. (1987a): Geology of the Area Around the Midway Deposit, Northern British Columbia (104O/16). British Columbia Ministry of Energy, Mines and Petroleum Resources, Geological Fieldwork, 1986, Paper 1987-1, 181-192.

Nelson, J.L. and Bradford, J.A. (1987b): Tootsee Lake Map Area (104O/16). British Columbia Ministry of Energy, Mines and Petroleum Resources, Open File 1987-5.

Nelson, J.L., Bradford, J.A., Green, K., and Marsden, H. (1988): Geology and Patterns of Mineralization, Blue Dome Map Area (104P/12). British Columbia Ministry of Energy, Mines and Petroleum Resources, Geological Fieldwork, 1987, Paper 1988-1,

Nelson,J., Bradford, J.A. and Marsden, H. (1988): Geochemical and Assay Results, Jennings River Map Area (104O/16). British Columbia Ministry of Energy, Mines and Petroleum Resources, Geological Fieldwork, 1987, Paper 1988-1, 525-528.

Nelson, R.A. (1985): Geologic Analysis of Naturally Fractured Reservoirs. Houston: Gulf Publishing Co.

Ohmoto, H. (1972): Systematics of Sulphur and Carbon Isotopes in

Hydrothermal Ore Deposits. Economic Geology, 67, 551-578.

Ohmoto, H. (1986): Stable Isotope Geochemistry of Ore Deposits. in Valley, J.W., Taylor, H.P., and O'Neil, J.R., eds. Stable Isotopes in High Temperature Geological Processes; Reviews in Mineralogy, 16, 491-559.

Ohmoto, H. and Rye, R.O. (1970): The Bluebell Mine, British Columbia. I. Mineralogy, Paragenesis, Fluid Inclusions, and the Isotopes of Hydrogen, Oxygen and Carbon. Economic Geology, 48, 417-437.

Ohmoto, H. and Rye, R.O. (1979): Isotopes of Sulfur and Carbon. in Barnes, H.L., eds. Geochemistry of Hydothermal Ore Deposits: New York, Wiley, 507-567.

Olson, R.A. (1984): Genesis of Paleokarst and Strata-Bound Zinc-Lead Sulphide Deposits in a Proterozoic Dolostone, Northern Baffin Island, Canada. Economic Geology, 79, 1056-1103.

Olson, R.A. (1986): Genesis of Paleokarst and Strata-Bound Zinc-Lead Sulphide Deposits in a Proterozoic Dolostone, Northern Baffin Island, Canada - A Reply. Economic Geology, 81, 1563-6.

Orchard, M.J. and Irwin, S. (1988): Conodont Biostratigraphy, Midway Property, Northern British Columbia (104O/16). British Columbia Ministry of Energy, Mines and Petroleum Resources, Geological Fieldwork, 1987, Paper 1988-1,

Panteleyev, A. (1980): Cassiar Map - Area (104P). British Columbia Ministry of Energy, Mines and Petroleum Resources, Geological Fieldwork, 1979, Paper 1980-1, 80-88.

Panteleyev, A. (1985): Cassiar Map - Area (104P/4, 5). British Columbia Ministry of Energy, Mines and Petroleum Resources, Geology in British Columbia 1977-1981, 188-190.

Pell, J (1987): Alkaline Ultrabasic Rocks in British Columbia: Carbonatites, Nepheline Syenites, Kimberlites, Ultamafic Lamprophyres and Related Rocks. British Columbia Ministry of Energy, Mines and Petroleum Resources, Open File 1987-17, 109 pages.

Pichavant, M., Ramboz, C. and Weisbrod, A. (1982): Fluid Immiscibility in Natural Processes: Use and Misuse of Fluid Inclusion Data. I. Phase Equilibria Analysis - A Theoretical and Geometrical Approach. Chemical Geology, 37, 1-27.

Pinckney, D.M. and Rye, R.O. (1972): Variation of $^{18}O/^{16}O$, $^{13}C/^{12}C$, Texture, and Mineralogy in Altered Limestone in the

Hill Mine, Cave-in -Rock District, Illinois. Economic Geology, 67, 1-18.

Poole, W.H. (1956): Geology of the Cassiar Mountains in the Vicinity of the Yukon - British Columbia Boundary. Unpublished PhD Thesis, Princeton University.

Potter, R.W., Babcock, R.S. and Brown, D.L. (1977): A New Method for Determining the Solubility of Salts in Aqueous Solutions at Elevated Temperatures. United States Geological Survey, Journal of Research, 5, 389-395.

Ramboz, C., Schnapper, D, and Dubessy, J. (1985): The P-V-T-X-fO_2 Evolution of H_2O-CO_2-CH_4-Bearing Fluid in a Wolframite Vein: Reconstruction From Fluid Inclusion Studies, Geochimica et Cosmochimica Acta, 49, 205-219.

Roddick, J.A. (1964): The Tintina Trench, Journal of Geology, 75, 23-33.

Roedder, E. (1984). Fluid Inclusions. Mineralogical Society of America, Reviews in Mineralogy, volume 12.

Roedder, E. and Bodnar, R.J. (1980): Geologic Pressure Determinations From Fluid Inclusion Studies, Annual Review of Earth and Planetary Science, 8, 263-301.

Rye, R.O. (1966): The Carbon, Hydrogen and Oxygen Isotopic Composition of the Hydrothermal Fluids Responsible for the Lead - Zinc Deposits at Providencia, Zacatecas, Mexico. Economic Geology, 61, 1399-1427.

Sawkins, F.J. (1964): Lead - Zinc Ore Deposition in the Light of Fluid Inclusion Studies, Providencia Mine, Zacatecas, Mexico. Economic Geology, 59, 883-919.

Sakai, H. (1986): Isotopic Properties of Sulphur Compounds in Hydrothermal Processes. Geochemical Journal, 2, 29-49.

Shelton, K.L., and Rye, D.M. (1982): Sulfur Isotopic Compositions of Ores from Mines Gaspe, Quebec: and Example of Sulfate - Sulfide Disequilibrium in Ore - Forming Fluids With Applications to Other Porphyry - Type Deposits. Economic Geology, 77, 1688-1709.

Simons, F.S., and Mapes, E. (1956): Geology and Ore Deposits of the Zimapan Mining District, State of Hidalgo, Mexico. United States Geological Survey Professional Paper 284, 128 pages.

Sinclair, W.D. (1986a): Molybdenum,Tungsten, and Tin Deposits and Associated Granitoid Intrusions in the Northern Canadian Cordillera and Adjacent Parts of Alaska. In Morin, J.L.,

ed., Mineral Deposits of the Canadian Cordillera ; Special Volume 37, Canadian Institute oif Mining and Metallurgy, 216-223.

Sinclair, W.D. (1986b): Early Tertiary Topaz Rhyolites and Associated Mineral Deposits in the Northern Canadian Cordillera: Products of Anorogenic Magmatism. Geological Association of Canada - Mineralogical Association of Canada, Program with Abstracts, 11, 127-128.

Sketchley, D.A., Sinclair, A.J. and Godwin, C.I. (1986): Early Cretaceous Gold - Silver Mineralization in the Sylvester Allochthon, Near Cassiar, North Central British Columbia. Canadian Journal of Earth Sciences, 23, 1455-1458.

So, C.S., Rye, D.M. and Shelton, K.L. (1983): Carbon, Hydrogen, Oxygen and Sulfur Isotope and Fluid Inclusion Study of the Weolag Tungsten - Molybdenum Deposit, Republic of Korea: Fluid Histories of Metamorphic and Ore - Forming Events. Economic Geology, 77, 1688-1709.

Sorenson, J. (1985): The Long Road to Midway. Canadian Mining Journal, 106, number 4, 20-27.

Stacey, J.S. and Kramers, J.D. (1975): Approximation of Terrestrial Lead Isotope Evolution By a Two - Stage Model. Earth and Planetary Science Letters, 26, 207-221.

Stilwell, F.L. and Edwards. A.B. (1943): Mineral Composition of the Tin Ores at Renison Bell, Tasmania. Australian Institute of Mining and Metallurgy, Proceedings, 131-132, 173-186.

Takenouchi, S. and Kennedy, G.C. (1964): The Binary System H_2O-NaCl At Elevated Temperatures and Pressures. American Journal of Science, 260, 487-509.

Taylor, B.E. (1987): Stable Isotope Chemistry of Ore - Forming Fluids. in Kyser, T.K., ed. Stable Isotope Geochemistry of Low Temperature Fluids; Mineralogical Association of Canada Short Course, 13, 337-445.

Taylor, H.P. (1979): Oxygen and Hydrogen Isotope Relationships in Hydrothermal Mineral Deposits. in Barnes, H.L., ed., Geochemistry of Hydrothermal Ore Deposits; New York, Wiley, 235-277.

Tempelman - Kluit, D.J. (1979): Transported Cataclasite, Ophiolite and Granodiorite in Yukon: Evidence of Arc - Continent Collision. Geological Survey of Canada, Paper 79-14, 27 pages.

Thompson, T.B., Arehardt, G.B., Johansing, R.J., Osborne, L.W.

and Landis, G.P. (1983): Geology and Geochemistry of the Leadville District, Colorado. in The Genesis of Rocky Mountain Ore Deposits: Changes With Time and Tectonics; Proceedings of the Denver Region Exploration Geologists Society.

Valley, J.W. (1986): Stable Isotope Geochemistry of Metamorphic Rocks. in Valley, J.W., Taylor, H. and O'Neil, J., eds., Stable Isotopes in High Temperature Geological Processes, Reviews in Mineralogy, 16, 445-490.

Veizer, J. and Hoefs, J. (1976): The Nature of $^{18}O/^{16}O$ and $^{13}C/^{12}C$ Secular Trends in Sedimentary Carbonate Rocks. Geochimica et Cosmochimica Acta, 40, 1387-1394.

Whalen, J.B., Currie, K.L. and Chappell, B.W. (1987): A - Type Granites: Geochemical Characteristics, Discrimination and Petrogenesis. Contributions to Mineralogy and Petrology, 95, 407-419.

Wheeler, J.O., Brookfield, A.J., Gabrielse, H., Monger, J.W.H., Tipper, H.W. and Woodsworth, G.J. (1987): Terrane Map of the Canadian Cordillera, unpublished.

APPENDIX A: LEAD ISOTOPE DEPOSIT AND SAMPLE DESCRIPTIONS, RANCHERIA, SEAGULL AND CASSIAR DISTRICTS, NORTHERN BRITISH COLUMBIA AND SOUTHERN YUKON TERRITORY

A. RANCHERIA DISTRICT

Map Area 104O/16

Amy (Marbaco): Ag-Pb-Zn replacement in Lower Cambrian carbonates.
30552-001 - no details available
30552-002 - 86JB25-16; trench 100 metres east-southeast of upper adit; massive galena - tetrahedrite
30552-003 - lower adit dump
30552-004 - same as -002

Midway: Ag-Zn-Pb massive sulphide mantos in Middle Devonian limestone (coded M), and galena bearing veins in Lower Mississipian clastics (E).
30460-001 - MW81-3 (114.18 m); M
30460-002$ - MW81-3 (69.76 m); E
30460-004 - Trench 81-8; E
30460-005 - MW82-10 (256.5 m); M
30460-006 - MW83-24 (60.2 m); E
30460-007A - MW81-3 (71.8 m); E
30460-007PA - same as -007A
30460-008A - Discovery trench; E
30460-009R - MW81-3 (44.7 m); E
30460-010 - MW82-8 (207.1 m); M
30460-011 - Silvertip showing trench; M
30460-012A - same as -011
30460-013 - MW82-8; M
30460-501 - Silvertip showing; M
30460-502 - Discovery zone; E
30460-503A - Discovery zone; E
30460-504 - M
30460-505 - Discovery zone; E
30460-506 - Discovery zone; E
30460-507 - Silvertip showing; M
30460-508 - Silvertip showing; M
30460-509 - Upper zone; E
30460-510 - O zone; E
30460-511 - M

Silverknife: Ag-Zn-Pb replacement in Lower Cambrian carbonates.
30876-101 - R85-4 (80.24 m); 0.2 metres of massive galena in brecciated marble, with siderite - quartz
30876-002 - R85-27 (21.0 m); galena in fractures in marble
30876-003 - R85-27 (142 m); pink dolostone with 5% sphalerite - pyrite, trace galena, quartz veins
30876-004 - R85-24A (91.4 m)

Lucky: galena bearing quartz veins in Cassiar batholith.
30680-001 - KG28-07; massive galena - tetrahedrite vein 8 cm wide

Tootsee Star: silicified shear zone in Sylvester allochthon chert - argillite, with sphalerite - galena.
30888-001D - JB24-15; partly oxidized galena - plumbojarosite.

Gum Mountain: quartz veins with pyrite and minor galena associated with Late Cretaceous porphyry dykes intruding Sylvester allochthon phyllite.
30970-001 - JN30-10; pyrite - galena blebs in quartz veins

Map Area 105B/1

Lola (Dale): Ag-Pb-Zn bearing quartz vein associated with north trending steep fault in Cassiar batholith.
10168-001A - no details available
10168-002 - no details available
10168-003 - no details available
10168-501 - galena - sphalerite - chalcopyrite - pyrite

Fiddler: Wolframite - cassiterite veins in Lower Cambrian phyllite - limestone, and scheelite bearing quartz - phyllite breccia.
10177-101 - no details available
10177-102 - no details available

YP (Butler Mountain, Lord): quartz veins, pyrrotite rich lenses and metasediment - sulphide breccias in Lower Cambrian carbonate and phyllite.
10166-501 - DDH 85-1 (557 feet)
10166-502 - DDH 85-502 (560 feet); lower contact with limestone is at 563 feet
10166-503 - DDH 85-5 (387 feet); mixed quartz feldspar porphyry and limestone breccia
10166-504 - DDH 85-1 (485 feet); quartz - feldspar - muscovite porphyry
10166-505 - DDH 84-8 (600 feet); vein in quartz feldspar porphyry
10166-506 - no details available

Meister (MR) - oxidized Zn-Pb-Ag mineralization along contact between Lower Cambrian? marble and phyllite
10154-002A - host is sericitic phyllite

Map Area 105B/2

Alan (Black Rock) - silver bearing limonitic patches in Cassiar batholith.
10145-001A - no details available

Map Area 105B/7

Silver Hart (CMC, Mid): Ag-Pb-Zn veins, replacements along Lower Cambrian schist - marble contacts adjacent to Cassiar batholith.
10186-001 - Meteorite zone
10186-101 - Meteorite zone
10186-102 - Breccia zone

Map Area 105B/9

Wolf: lenses and laminated sphalerite - galena - pyrite in Lower Cambrian and older schist, calcareous phyllite, and pyrite - chalcopyrite - galena in breccia with scheelite clasts.
10155-001D - no details available

B. SEAGULL DISTRICT

Map Area 105B/4

Logtung (Darva, Logjam): Ag-Pb-Zn veins associated with Seagull batholith.
10102-001 - galena - arsenopyrite - sphalerite in vein; Pure Silver adit, 1.2 km northeast of Logtung W-Mo stockwork

MC: cassiterite bearing sulphide veins and layers in hornfelsed argillite - tuff - limestone 1.5 kilometres southwest of Seagull batholith.
10134-001A - DDH K-3 (182.9 m); pyrrhotite - sphalerite - galena in diopside - calcite - axinite skarn
10134-002 - DDH K-1 (157 m); pyrrhotite - sphalerite - galena vein 4 cm wide

C. CASSIAR DISTRICT

Map Area 104O/8

Cottonwood: stratabound carbonate hosted Pb-Zn.
30744-501 - no details available

Map Area 104P/3

Bill (Carlick): Pb-Ba in Lower Cambrian limestone.
30873-101 - barite - siderite - galena - sphalerite - pyrite
30873-102 - galena - barite - siderite veins in 4 metre wide feldspar porphyry dyke and replacing limestone

Map Area 104P/4

Needlepoint: Ag-Pb-Zn veins associated with Late Cretaceous Needlepoint Mountain stock.
30872-101 - massive galena vein 1 metre wide, 10 metres long

Lang Creek - volcanogenic massive sulphide lens in Sylvester allochthon.
30742-501 - no details available

Erickson (Maura - Allison): Au-quartz veins in Sylvester allochthon.
30436-501 - no details available
30436-502 - no details available

Erickson (Vollaug): Shallowly dipping ribbon Au-quartz vein in Sylvester allochthon.
30436-002 - no details available
30436-503 - no details available
30436-504 - no details available

Erickson (Cusac): Au-quartz veins in Sylvester allochthon
30400-501 - no details available
30400-502 - no details available

Map Area 104P/5

Marble Basin (Magno, Silver Queen) - Ag-Pb-Zn replacement with manganiferous magnetite in Lower Cambrian limestone.
30383-002A - no details available
30383-004 - no details available
30383-101 - Magno West Zone, 2.8 metres wide, from dump of upper adit; massive magnetite - pyrite - pyrrhotite - sphalerite - galena
30385-102A - 1.5 metre wide structuiral contact zone; massive pyrite - pyrrhotite - sphalerite - galena - arsenopyrite - magnetite

Map Area 104P/6

Mount Haskin: Ag-Zn-Pb skarn in Lower Cambrian marble, associated with Eocene stock.
30682-101A - 4 metre wide skarn, with pyrite - pyrrhotite - chalcopyrite - arsenopyrite - sphalerite - galena in pyroxene - grossular - actinolite skarn, 1500 metres southeast of stock
30682-102 - pyrite - sphalerite - galena in pyroxene - grossular - actinolite skarn, 300 metres from stock
30682-001A - top of Mt. Haskin, thin bedded marble with magnetite - pyrrhotite - galena - sphalerite pods and

accessory fluorite.
30682-003 - skarn body on road low on northwest ridge with pyrrhotite - pyrite - chalcopyrite - galena - sphalerite

McDame Belle: Ag-Pb-Zn replacement with minor scheelite in Lower Cambrian limestone.
30743-501 - no details available

Map Area 104P/12

Axe: galena veins and galena - sphalerite - chalcopyrite in breccias in Lower Cambrian limestone.
30022-001 - galena vein about 8 centimetres wide

Blue: oxidized Zn-Pb bearing horizons in Lower Mississipian clastic sediments.
30461-001A - no details available

Reggie: en echelon galena bearing quartz filled tension gashes in Lower Mississipian clastic sediments.
30223-001A - partly oxidized galena in quartz

APPENDIX B: SULPHIDE MINERALOGRAPHY

Abbreviations: Py=pyrite; Qt=quartz; Sp=sphalerite; Gn=galena; Gc=geocronite; Tt=tetrahedrite; Fr=franckeite; St=stannite; Cp=chalcopyrite; Ca=calcite; Mc=marcasite; As=arsenopyrite; Po=pyrrhotite
(Note: the number in parentheses following the mineral abbreviation is the mode for the polished section. "M" denotes amounts less than 1%).

(A) Fan C55/D23

MW 178 (14.5 m)

Py (30)	----- --------	Feathery texture (early); subhedral inclusions in Sp, Qt (late).
Qt (25)	----------	Later euhedral Qt overgrows some Sp, Py.
Sp (25)	--------	Interstitial to early Py.
Gn (10)	-------	Interstitial to late Qt.
Gc (5)	-------	Intergrown with Gn.
Tt (5)	---	Intergrown with Gn, Sp.

MW 178 (15.0 m)

Qt (20)	--------	Euhedral.
Py (25)	---------	Subhedral, fine to coarse grained, intergrown with Sp.
Sp (40)	---------	
Gn (10)	-------	Fracture filling and replacing Sp, Py in part.
Gc (5)	-------	With Gn.
Tt (M)	---	

MW 204 (5.2 m)

Qt (40)	---------	Subhedral - euhedral.
Py (20)	-------- - - -	Mutual boundaries with Sp.
Sp (30)	--------	
St (M)	----	Intergrown with Sp.
Gn (4)	-------	Locally veins Py, Sp.
Gc (4)	-------	Intergrown with Gn.
Tt (2)	---	Intergrown with Gn.

MW 204 (6.8 m)

Qt (30)	---------	Euhedral with interstitial late sulphide.
Py (10)	----------	Intergrown with Sp, Gn, Gc.
Sp (20)	----------	
Cp (2)	-----	Inclusions in Sp.
St (M)	-----	Inclusions in Sp.
Tt (5)	------	Intergrown with Sp, Gn; replaces Py.
Gn (28)	---------	Locally overgrows and relaces Py, Sp; interstitial to Qt.
Gc (5)	---------	Same as Gn.

MW 207 (8.5 m)

Py (20)	----- ------	Early growth zoned.
Qt (55)	----------	
Sp (M)	------	
Gn (10)	------	Overgrows early Py; interstitial to Qt.
Gc (8)	------	Intergrown with Gn.
Tt (2)	---	Irregular blebs in Gn, Gc.
Ca (5)	---	Fracture, void filling.

MW 207 (10.6 m)

Py (30)	----- ----------	Early euhedral, growth zoned; later intergrown with Sp.
Qt (40)	---------	Euhedral.
Sp (20)	----------	Mutual boundaries with Py; Py inclusions.
St (M)	------	Inclusions in Sp.
Gn (6)	--------	Interstitial to Qt; replaces some Sp, Py.
Gc (4)	--------	Intergrown with Gn.
Tt (M)	--------	Inclusions in Gn, Sp, Py.
Fr (M)	--------	Inclusions in Gc.

MW 178 (20.9 m)

Qt (70)	------ ----	Spongey intergrowths; euhedral vug linings.
Py (20)	-------	Alternating layers with Qt; fine grained inclusions in Sp.
Sp (5)	-----	Void filling in Qt.
Mc (5)	----	Replaces Py.

(B) Fan B129

MW 139 (2.9 m)

Py (60)	-------	Breccia; angular clasts.
Qt (20)	-------	Same as Py.
Sp (M)	-----	Inclusions in Py.
Gn (M)	-----	Same as Sp.
Ca (20)	------	Breccia matrix.

MW 141 (7.9 m)

Py (40)	---------	
Qt (15)	-----	Subhedral intergrowths with interstitial sulphide; Py, Sp inclusions.
Sp (10)	---------	
Gn (8)	----------	
St (5)	------	Inclusions in Sp, Gn, Gc.
Gc (5)	----------	
Fr (2)	----	Inclusions in Gc.
Tt (M)	----	Inclusions in Gn, Gc.
Ca (15)	--- ---	Early, replaced by Qt, sulphides; late vug filling.

MW 142 (9.8)

Py (25)	----------	Subhedral - euhedral, overgrown by Sp, Gn; inclusions in Sp.
Sp (40)	----------	Abundant Py, Cp inclusions.
St (5)	------	Common adjacent to Sp, Cp.
Gn (15)	--------	
Cp (10)	------	Inclusions in Sp, Gn.
Ca (5)	-----	Late veins and vug fillings.

MW 143 (2.3 m)

Py (20)	----- ----	Feathery, with interstitial sulphides; inclusions in Sp.
Qt (20)	-----	Euhedral.
Sp (20)	------	Inclusions in Py; interstitial to early Py; fracture filling in later Py.
As (M)	----	
St (M)	----	
Gn (10)	----	
Gc (10)	----	Intergrown with Gn.
Tt (5)	----	Inclusions in Sp, Gn.
Fr (5)	----	Inclusions in Gn, Gc, Tt.
Ca (10)	----	Void filling.

MW 143 (4.75 m)

Py (35)	----- ----	Early coarse grained, euhedral; later intergrown with Sp.
Qt (10)	----------	Overlaps early Py; inclusions in Sp.
Sp (30)	-------	
As (M)	----	Overgrown by Gn, Gc.
St (M)	----	Inclusions in Sp.
Gn (10)	-------	
Gc (5)	-------	Lamellar inclusions in Gn.
Tt (M)	---	Inclusions in Gn, Gc.
Fr (M)	---	Same as Tt.
Ca (10)	---	

MW 144 (8.5 m)

Py (50)	----- ------	Coarse grained, brecciated; fine grained inclusions in Sp.
Qt (5)	--------	Some overgrows Py; Py, Sp inclusions.
Sp (30)	------	Intergrown with Py.
Gn (10)	------	
Tt (M)	----	Inclusions in Gn.
Ca (5)	----	Breccia matrix.

(C) Other Silver Creek deposit locations

B199

Qt (80)	--------	
Py (10)	---------	
Sp (5)	-------	Irregular intergrowths with Py.
Gn (3)	-------	Same as Sp.
Cp (1)	-----	Inclusions in Sp.
St (1)	-----	Same as Cp.

B187

Py (40)	-------	Coarse grained, subhedral - euhedral, alternating with Qt.
Qt (15)	----------	Layers 1-2 mm thick, with Py; also filling interstices in Py.
Sp (5)	----	
Mc (40)	------	Very fine grained, porous; after Py.

MW 73 (38.5 m)

Ca (40)	-----	
Qt (50)	-------	Interlayered with Ca (replacement).
Sp (5)	-------	Blebs with Py, St inclusions.
Py (5)	--------	Euhedral inclusions; subhedral, overgrowing Sp.
St (M)	----	Inclusions in Sp.

(D) Discovery deposit

MW 26 (584.2 m)

Ca (40)	-----	
Qt (20)	-----	
Po (30)	------	Anhedral; locally included in Qt.
Py (10)	------	Mutual boundaries with Po.
Sp (M)	----	
Cp (M)	----	
Gn (M)	-- - -	

MW 16 (385.8)

Py (15)	-------	Irregular mutual boundaries with Sp; has Sp inclusions.
Po (5)	-------	Mutual boundaries with Py.
Qt (5)	-------	Euhedral inclusions in Sp, Py.
? (5)	----	Unknown silicate; bladed texture.
Sp (70)	-------	
Cp (M)	-----	Inclusions in Sp.

(E) Silvertip showing

MW 40 (443.4 m)

Qt (6)	--------	Subhedral - euhedral inclusions in Gn; corroded against Py, noncorroded against Gn.
Py (60)	-------	Subhedral, coarse grained.
Sp (4)	-------	
Gn (20)	---------	Inclusions in Py; replaces Py.
Cp (M)		Inclusions in Sp.
Ca (10)	-----	

(F) Exhalites

Discovery zone trench

Sp (40)	
Qt (45)	Subhedral - euhedral, laminated with Sp.
Py (15)	Scattered small, subhedral - euhedral grains; larger anhedral grains; small cubes, pyritohedrons.
Cp (M)	Small rounded blebs in patches in Sp.
Gn (M)	Very small inclusions in Sp.

APPENDIX C: FLUID INCLUSION DATA

Abbreviations:

Th-l (-v, -c) - temperature of homogenization to liquid phase (to vapour, by critical disappearance of phase boundary)
Tm-CO2 - temperature of melting of CO2 rich phase
Tm-i - temperature of ice melting
Tm-c - temperature of clathrate melting
Th-CO2 - temperature of homogenization of CO2 rich phases
Tf - temperature of freezing of one or more phases

MW 141 (7.9)

Descriptive: Three main varieties of quartz: (A) subhedral, 300-1000 micron diameter, whitish, cloudy, with subparallel wispy streaks; (B) finer grained (60 - 180 microns) intergrowths with triangular interstices, porous looking, greyish with some clear areas, more intergrown opaques 50-200 microns; boundary between A and B quartz is gradational, marked by size change, (C) clear quartz adjacent to pyrite clusters, about 300 microns, sparser inclusions, few planar secondaries.

Inclusions: A quartz - (1) closely packed secondaries <1 - 3 microns, very irregular shapes, variable liquid to vapour ratios (L/V) where discernable, follow planes with variable orientations.

(2) groups of 5 - 15 inclusions with 3 - 25 micron diameters within 150 micron diameter area, not on single plane but scattered variably within section, irregular to equant shapes, variable L/V (but not extreme), generally L rich; type 3a, 3b, or 4.

(3) planes of secondaries <1 - 10 microns, subequant to slightly irregular, some with small bouncing bubbles, consistent L/V, generally in fairly clear areas, may be elongate; type 3b or 4.

(4) highly variable, very irregular to subequant, 3 - 35 microns, obvious necking textures, L rich to V rich, in irregular nonplanar clusters.

(5) secondaries on planes and grain boundaries, dark and dense - looking, very irregular, ragged shapes, not clearly fluid.

(6) elongate, planar secondaries, L - filled or solid, 1 - 4 microns.

(7) three phase inclusions (H2O, CO2 liquid, CO2 vapour) in mixed groups, to 20 microns; type 2.

B - quartz - (1) very small (<<1 - 2 microns) irregularly scattered throughout grains with fine dusting of opaques, some contain discernable bouncing bubbles.

Data:
(a) type 3b inclusions, elongate subequant secondaries 1 - 10 microns long, long dimension parallel to strike of microfracture, some bubble movement.
Th-l: 16 measured (211.2, 211.2, 211.5, 212.6, 212.6, 210.2, 210.2, 210.2, 209.4, 209.4, 207.8, 208.1, 208.5, 207.8, 211.5, 209.7); avg. 210.1.
Tm-c: 6 measured (+6.2, 6.1, 6.4, 6.0, 6.1, 6.3); avg. 6.2.
Tf: 2 measured (-35.9, -35.1).

(b) type 3b inclusions, 5 - 20 microns, slightly inconsistent L/V, subequant, L rich.
Th-l: 4 measured (198.5, 205.5, 206.1, 202.5); avg. 203.2.
Tm-i: 5 measured (-4.3, -4.7, -4.6, -5.3, -4.9); avg. -4.8.
Tf: 4 measured (-46.5, -47.5, -48.2, -47.2).

(c) type 3b? secondaries, subequant, 3 microns, consistent L/V. No freezing attempted due to size.
Th-l: 4 measured (194.6, 193.8, 191.1, 190.7); avg. 192.6.

(d) single large equant type 2 primary? Dimensions 21x 30 microns (hexagonal), inner bubble at 25 C 12 micron diameter, outer bubble 17 microns; type 2.
Tf: -28.5, -40, -98.5.
Tm-CO2: -58.7.
Tm-c: 11.6
Th-CO2: 29.2.

(e) 2 inclusions with irregular shapes, 16 microns, containing clear daughter mineral, in group of type 3a and 2 inclusions.
Tm-d: 148, 149. Tm-d before Th.

(f) in subhedral quartz grain 350 microns intergrown with pyrite, 3 - 9 micron inclusions, type 4, subequant.
Th-l: 4 measured (157.8, 159.5, 160.7, 161.4); avg. 159.9.
Tm-i: 4 measured (-6.4, -6.7, -6.8,-6.7); avg. -6.6.
Tf: 3 measured (-46.9, -44.7, -44.6).

(g) equant secondaries, L rich, 3 - 9 microns, fairly consistent L/V; type 3a.
Th-l: 6 measured (283, 304, 302, 270, 307, 304); avg. 287.
Tf: 4 measured (-74, -71, -73, -70).

(h) large (up to 24 microns), irregular to subequant type 1? inclusions scattered in clear quartz, not on single plane.
Degree of filling: 50% vapour, much less than usual for type 1.
Th-v: vapour bubble expands and inclusion decrepitates between 320-340.
Tm-CO2: 3 measured (-56.8, -56.8, -56.6); avg. -56.7.
Tm-i: 3 measured (-14.4, -14.4, -14.7); avg -14.5.
Tf: 3 measured (-65, -97.9; -64.5, -97.0; -63.8, -95.3).

(i) subhedral quartz grain 400 microns across, with 10-30 micron pyrite inclusions. Abundant secondary planes with subequant type 3 and fewer type 2 inclusion 1-40 microns. Inconsistent L/V.
Th: decrepitation begins at 260.
Tm-i: 3 measured (-16.9, -17.4, -16.8); avg. -17.0.
Tm-CO2: 1 observed, -56.6.

(j) relatively clear quartz grain with group of subequant to equant type 3? inclusions 5-20 microns, with dark vapour bubbles, somewhat variable L/V.
Th: variable, some to liquid and some to vapour between 380 and 420. Decrepitated rapidly after homogenization.
Tm-i: 6 measured (-16.2, -16.2, -16.6, -16.1, -16.3, -16.4); avg. -16.3.

MW 204 (5.6)

Descriptive: Gangue consists mainly of quartz, 200 - 400 microns, intergrown with sphalerite and pyrite. Dominant feature of inclusions is dense swarms of mainly V rich, some in hexagonal cores or other zones overgrown by clear quartz - primaries and pseudosecondaries. Also small (<1 micron) dark inclusions outline crystallographic growth zones.

Data:
(a) anhedral quartz grain 400 x 750 microns, fairly clear, intergrown with sphalerite. Group of type 1 and type 2 inclusions, <1 - 18 microns, largest toward core of grain, decreasing in size toward edges, probably primary, mainly equant, elongate, with consistent L/V.
Th-v: 8 measured, accuracy ± 5-10 C, 2 around 330, 4 between 335 - 340 2 about 345. Avg. 340.
Tm-CO2: 8 measured (-58.1, -58.0, -57.6, -58.5, -58.1, - 58.2, -58.5, -57.1); avg. -58.0.
Tm-c: 8 measured (9.8, 10.7, 10.9, 11.2, 11.0, 9.8, 9.9, 9.9,); avg. 10.4.
Th-CO2: 6 measured (31.2, 20.8, 22.7, 24.1, 26.1); avg. 22.3.
Tf: 8 measured (-24.7, -96.2; -25.7, -97.4; -96.7; -24.6, -97.4; -25, -96.7; -24.5, -96.2; -97.6; -26, -96.3).
No decrepitation of type 1 up to 480 C.

(b) Quartz grain 130 x 180 microns, anhedral, with pyrite. Several types of inclusions: (1) subequant type 1 with rare type 3a, consistent L/V (data following); (2) type 3a and 2, variable L/V, 2 - 10 microns; (3) very irregular dark dendritic blobs on growth zones and microfractures. Type 2 and 3a inclusions commonly as clots, locally coring grains, with less inclusion rich quartz overgrowing.
Th: difficult to see, several in range of 295 - 315 C.
Tm-CO2: 3 measured (-58.3, -58.0, -58.2); avg. -58.2.
Tm-c: 4 measured (11.0, 11.0, 11.0, 10.9); avg 11.0.

Tf: 4 measured (-97.7, -98.4, -97.6, -97.4).

(c) plane of type 1 and type 2, subequant, diamond shaped pseudos, consistent L/V, similar size (5 - 7 microns).
Th-c: 6 measured (289, 283, 284, 289, 293, 279); avg 286.
Accuracy good for type 1 (± 2 - 3 C) because phase boundary stays away from inclusion wall during critical disappearance.
Tm-CO2: 3 measured (-57.8, -57.8, -57.4); avg -57.7.
Tm-c: 3 measured (10.6, 11.6, 11.7); avg. 11.3.

(d) subhedral quartz grain 600 x 400 microns in layer of quartz between sphalerite and pyrite - quartz layers. Contains secondary planes with variable L/V, elongate parallel to strike of microfracture, minute inclusions defining "picket fence" grain boundary, and type 1 inclusions with glossy black bubbles in rhombic, hexagonal, and triangular shape, fairly consistent L/V along measured plane, but some type 3a present probably by necking. Inclusions show size gradation across grain (smaller toward edge; probably pseudos), measured ones 9 microns.
Th-c: 320 - 325. Several measured in this range; others Th unclear.
Tm-CO2: 3 measured (-58.2, -57.6, -58.4); avg. -58.1.
Tm-c: 3 measured (10.8, 10.8, 10.7); avg. 10.8.
Tf: 3 measured (-97.7, -97.0, -98.0).
No decrepitation up to 450 C.

(e) plane of type 1 pseudos, 10 - 25 microns, subequant.
Th-v: 4 measured (314, 326, 320, 322); avg. 321.
Tm-CO2: 4 measured (-58.0, -57.8, -57.9, -58.1); avg. -58.0.
Tm-c: 3 measured (11.7, 11.5, 11.1); avg. 11.4.

(f) Clear quartz grain 500 x 300 microns surrounded by sphalerite, pyrite. Type 4 inclusions, equant (small) to irregular (big), most <4 microns, a few > 10 microns (largest 20 microns), secondaries, no V rich.
Th-l: 7 measured (122, 123, 134, 135, 151, 155, 154); avg. 145.
Tm-i: 2 measured (two largest - ice melting visible) (-7.1, -7.1); avg. -7.1.

MW 73 (39.0)

Descriptive: Quartz contains abundant planes of secondaries with variable L/V, some showing obvious necking textures, variable size (<<1 - >20), including "L filled", type 1, and type 2, but mainly type 3 and 4, crisscrossing microfractures with variable orientations. Also some very elongate, needle - like inclusions. Growth zoning in places.

Data:
(a) Type 4 secondaries along microfracture, slightly variable L/V, 2 - 9 microns long, subequant.

Th-1: 9 measured (152.8, 152.5, 155.3, 155.5, 142.5, 145.1, 144.8, 154.7, 152.5); avg. 150.6.

(b) Subhedral quartz grain 1000 microns, with scattered irregular (large) to equant (small) type 3b and 4 inclusions, no crosscutting secondary planes. Small inclusions 3 - 6 microns, large inclusions 10 - 30 microns. Some bouncing bubbles in small ones.
Th-1: 7 measured (196, 197, 196, 184, 168, 196, 205); avg. 188.
Tm-i: 7 measured (large: -7.1, -7.4, -7.1; small: -5.8, -5.6, -6.7, -6.7); avg. -6.7.
Tm-c: 2 measured (both small: 6.8, 6.8); avg. 6.8.
Tf: 8 measured (-34.8, -36.4, -36.9, -35.7, -35.7, -36.0, -37.8, -38.0).

(c) Growth zoned quartz grain 350 microns, with inclusion rich core containing mainly equant type 3a primaries, 3 - 10 microns. No type 1.
Th-1: 10 measured (292, 294, 295, 295, 296, 293, 294, 302, 292, 293); avg. 295.
No visible freezing effects.

(d) quartz grain 700 x 1300 microns, fairly clear, with some scraggly opaque material and inclusions in core. Plane of type 3a secondaries with consistent L/V, 3 - 6 microns, subequant, with some type 2, 12 - 14 microns.
Th-c: 7 measured (334, 331, 328, 329, 320, 320, 325); avg. 329.
Tm-CO2: 6 measured (-56.6, -56.7, -57.0, -56.6, -56.8, -56,6); avg. -56.7. Negligible CH4.
Tf: 4 measured (-39.4, -54, -97; -28.9, -34.7, -95.6; -39.9, -97.2; -39.8, -55.8, -97.6).
No reliable melting data obtained.

MW 73 (38 5)

Descriptive: Similar to MW 73 (39.0).

Data:
(a) Elongate, angular quartz grain 450 x 1500 microns, surrounded by calcite (quartz relacing early spar?), clear, cut by several microfractures with small type 3a inclusions. One plane with very elongate, needle shaped inclusions and some larger, more equant inclusions, consistent L/V.
Th-1: 7 measurements (277, 275, 283, 267, 269, 268, 270); avg. 273.
Tm-c: 3 measurements (6.9, 7.0, 7.0); avg. 7.0.
Tf: 3 measurements (-28.5, -41.7; -33.7, -41.8; -31.8, -40.6).

MW 207 (8.5)

Data:
(a) Quartz grain 1000 microns across, with associated pyrite grains 100 - 200 microns, cut by microfractures (secondaries and pseudos) with 90% type 1, 5% type 3a, and 5% type 2 inclusions <1 - 20 microns.
Th: widely variable, >275 C.
Tm-CO2: 9 measured (-58.4, -58.0, -57.8, -58.1, -59.1, -58.7, -58.3, -58.2, -58.6); avg. -58.4.
Tm-c: 6 measured (10.5, 10.6, 10.3, 10.4, 10.5, 10.6); avg. 10.5.
Tf: 6 measured (-98.3, -97.8, -97.8, -97.6, -97.5, -98.5).

(b) Subhedral quartz grain 250 microns, surrounded by pyrite, with plane of equant type 1 inclusions 3 - 10 microns, most showing 100% V phase, but some with visible L phase, also 2% clear inclusions. Type 1 inclusions have typical almond shapes. Probably pseudos.
Th-c: 4 measured (296, 298, 299, 308); avg. 300.
Tm-CO2: 4 measured (-57.8, -57.2, -57.6, -57.7); avg. -57.6.
Tm-c: 4 measured (10.9, 10.3, 10.8, 10.5); avg. 10.7.
No decrepitation to 370 C. Critical fading very clear in two inclusions, somewhat clear in two others. Phase change not observable in most because of low L filling.

(c) Quartz grain 800 x 1500 microns, anhedral, with subparallel stringers of secondaries and pseudos, type 1 and abundant type 2 , lesser type 3a, some equant, others irregular. Data on subequant to equant type 2, 6 - 16 microns.
Th-v: 9 measured (274, 328, 281, 314, 302, 307, 308, 306, 317) avg. 309.
Tm-CO2: 6 measured (-57.6, -57.1, -57.5, -57.6, -57.6, -57.6) avg. -57.5.
Tm-c: 6 measured (11.2, 10.2, 9.2, 10.4, 10.5, 10.3) avg. 10.3.
Th-CO2-v: 6 measured (29.0, 28.4, 29.0, 29.2, 29.3, 29.1); avg. 29.0.

MW 178 (14.5)

Data:
(a) quartz grain 200 x 500 microns, intergrown with sphalerite, pyrite, galena, sulphosalt assemblage. Equant, mixed inclusions (L rich > V rich), 5 - 15 microns, dispersed, possibly primaries, but necking renders homogenization data suspect. Data on type 1 inclusions.
Th-v: Most between 320 and 340, some between 350 and 370. Accuracy poor.
Tm-CO2: 5 measured (-59.0, -59.1, -57.6, -58.8, -58.3); avg. -58.6.
Tm-c: 2 measured (10.0, 9.9); avg. 10.0.

(b) type 1 pseudos, 3-12 microns, one type 2, 20 microns; consistent L/V.

Th-v: 2 measured (318.6, 323.6); avg, 321.1.
Tm-CO2: 5 measured (-58.2, -58.3, -57.5, -57.5, -57.4); avg. -57.8.
Tm-c: 5 measured (11.0, 10.7, 11.0, 11.2, 10.7); avg. 10.9.
Th-CO2: 1 measured (26.4).
Tf: 5 measured (-97.2, -95.2, -98.6, -97.3, -94.9).

MW 178 (15.0)

Descriptive: Fine grained, locally growth zoned sphalerite, some densely intergrown with fine grained pyrite, and fine to coarse grained quartz. Subparallel planes of L - rich secondaries (type 3b?) are common. Abundant, randomly scattered zones of type 1 inclusions. Obvious necking is common, many groups of mixed inclusions with variable L/V ratios. Some quartz cores with closely packed, small, equant type 1 inclusions with rare type 3 or 2.

Data: type 1 primaries in quartz core, equant to elongate, <1-8 microns, 80-100% V filled.
Th-v: not clear in most, 320-330 in few in which V filling was observable.
Tm-CO2: 3 measured (-57.4, -57.5, -57.6); avg. -57.5.
Tm-c: 4 measured (11.0, 10.6, 10.7, 10.8); avg. 10.8.
Tf: 3 measured (-98, -98, -98.6).

MW 144 (8.5)

Descriptive: Quartz grains 300 - 500 microns, intergrown with pyrite > sphalerite, and containing sulphide inclusions 5 -30 microns. Also calcite grains 150 - 200 microns, with unclear paragenetic relation ship to others. Scattered microfractures with very small, very irregular, dark inclusions in quartz; these may be non-fluid (organics?). Locally very irregular light inclusions exist in same plane. Some dark inclusions have rodlike shapes. Sphalerite shows growth zoning. No useful inclusions for microthermometry.

MW 143 (4.75)

Descriptive: Subhedral quartz grains have small included pyrite and sphalerite grains, and scattered very small (1 micron or less) secondaries. Rare euhedral quartz has no inclusions. Some quartz shows corroded margins where overgrown by calcite. Locally minute dark inclusions along microfractures. One quartz grain with abundant pyrite inclusions has sphalerite pseudomorph shape. Rare inclusion surfaces along growth zones in quartz, too small for microthermometry. Microfractures with small inclusions apparently perpendicular to C axis of quartz with triangular crystal termination.

Calcite is late, overgrowing sphalerite, pyrite, filling vugs. Calcite contains abundant dark and light squiggly

inclusions along fracture and cleavage planes, no obvious vapour bubbles.

Sphalerite has scattered clusters of minute (<< 1 micron) inclusions. Some sphalerite shows red - brown cores and orange rims. Sphalerite contains abundant very small (10 microns) pyrite inclusions.

MW 16 (385.8)

Descriptive: Texturally different from most Silver Creek quartz in having a dense wispy fabric, with few areas of clear quartz.

Data:
(a) anhedral quartz grain 900 by 1000 microns, in quartz - pyrite assemblage, generally coarse grained, with euhedral quartz and pyrite. Quartz mainly wispy textured. This grain fairly clear, with two subparallel curviplanar pseudosecondary planes with equant type 1 inclusions <1-7 microns.
Tm-c: 5 measured (11.5, 11.2, 11.5, 11.8, 12.2); avg. 11.6.
Tm-CO2: 2 measured (-59.2, -59.0); avg. -59.1.
Th: too difficult to determine.

(b) anhedral quartz grain 250 by 250 microns, surrounded by pyrite, with abundant primary? inclusions not associated with planar microfractures, equant, type 1, <3-12 microns.
Tm-c: 2 measured (12.6, 11.5); avg. 12.1.
Tm-CO2: 1 measured (-61.8).

MW 11 (317.65)

Descriptive: Similar to MW 16.

Data:
(a) Quartz grain 800 by 400 microns, with less of a wispy texture than most, surrounded by pyrite, contains small sphalerite inclusions. Scattered equant type 3a inclusions, not related to secondary planes, 2-5 microns, fairly consistent L/V.
Th: 7 measured (303, 275, 270, 272, 290, 271, 291); avg. 282.
No freezing data.

BH:

Descriptive: Quartz vein 2 centimetres in width, cutting Earn Group coarse grained sandstone (unit 3D). Has clear, non-wispy quartz, mainly 500 microne to 1 millimetre. Contains planes of irregular to equant, 3-15 micron type 1 inclusions, commonly with a few type 3 necked off. Also planes of type 3a inclusions, with about 40-50% vapour filling. Type 2 inclusions occur locally, especially in groups containing mainly type 1 inclusions.

Data:
(a) type 1 secondaries or pseudos, 3-19 microns, mainly about 5 microns, with rare type 2.
Th: not readily observable, but greater than 320.
Tm-CO2: 4 measured (-57.2, -57.2, -57.3, -57.3); avg. -57.3.
Tm-c: 6 measured (10.9, 10.9, 10.5, 10.5, 10.7, 10.8); avg. 10.7.
Tf: 2 measured (-28.2, -44.7, -96.8; -26.7, -97.5)

(b) type 1 secondaries, 10-25 microns, fairly equant.
Tm-CO2: 3 measured (-57.2, -57.5, -57.7); avg. -57.5.
Tm-c: 5 measured (11.3, 11.3, 11.5, 10.7, 10.9); avg. 11.1.